N-Heterocyclic Olefins: Applications in Catalysis and Low-Coordinate Element Stabilization

by

Ian C. Watson

A thesis submitted in partial fulfillment of the requirements for the degree of

Doctor of Philosophy

Department of Chemistry
University of Alberta

Abstract

The work in this Thesis outlines the use of *N*-heterocyclic olefins (NHOs) as organocatalysts, as supporting ligands in palladium-catalyzed cross-coupling, and the development of anionic NHOs as ligands for main group element and transition metal centers.

N-Heterocyclic olefin-hydridodiborane complexes were synthesized with the aim of performing the catalytic hydroboration of ketones and aldehydes with pinacolborane. These NHO-hydridodiborane complexes were not active catalysts, but the precursor NHOs were the catalyst in the hydroboration of ketones and aldehydes.

New NHOs were synthesized and explored as supporting ligands in Buchwald-Hartwig aminations. Through a combination of imaging, poisoning, and kinetic experiments, it was determined that a well-defined NHO-supported Pd^0 complex was not the active catalyst, but palladium nanoparticles formed *in situ*.

NHO-AlR_3 Lewis acid-base adducts were shown to catalyze the polymerization of acrylic Michael-type monomers via a frustrated Lewis pair mechanism.

A two-coordinate zinc(II) complex supported by anionic *N*-heterocyclic olefin (aNHO) ligands was synthesized and was shown to undergo transmetallation with main group element halides and hydrides. Group 4 and Group 8 metal centers were also stabilized by aNHO ligands.

Preface

Portions of the work discussed in this Thesis were completed in collaboration with researchers within the Rivard group, other researchers within the Department of Chemistry at the University of Alberta, and with researchers external to the University of Alberta.

All single-crystal X-ray crystallographic studies described herein were performed by Dr. Robert McDonald, Dr. Michael J. Ferguson, or Dr. Yuqiao Zhou at the University of Alberta, including the mounting of crystals, diffractometer operation, structure refinement, and the preparation of crystallographic data tables. Elemental analyses and Karl-Fisher titrations were performed by the Analytical Instrument Laboratory at the University of Alberta.

The computational studies in this Thesis were made possible by the facilities of the Shared Hierarchical Academic Computing Network (SHARCNET: www.sharcnet.ca), Westgrid (www.westgrid.ca), and Compute Canada (www.computecanada.ca). The work in this Thesis was supported by the Natural Sciences and Engineering Research Council of Canada (NSERC), the Canadian Foundation for Innovation, the Faculty of Science at the University of Alberta, the American Chemical Society Petroleum Research Fund, and the Alberta/Technical University of Munich International Graduate School for Hybrid Functional Material (NSERC CREATE grant).

In Chapter 2, the initial syntheses of [IPr–CH(BH$_2$)$_2$(μ–H)] and [IPr–CH(BH$_2$){BH(OTf)}(μ–H)], DFT studies, and 50 % of the substrate scope were completed by Dr. C. Hering-Junghans (a previous post-doctoral fellow in the Rivard group).

In Chapter 3, the initial syntheses of the NHOs reported therein (except for SIPrCH$_2$), and the initial syntheses of NHO-palladium complexes (except for [(^{Me}IPrCHCHCH$_2$)PdCl$_2$(3-Cl-pyr)]) were completed by Dr. Christian Hering-Junghans (during his post-doctoral fellowship in the Rivard group). PMe$_3$ poisoning experiments were performed, and the isolated yields of the cross-coupled products as part of the substrate scope were obtained by Dr. André Schumann at the Leibniz Institute for Catalysis (LIKAT). SEM and TEM imaging experiments were performed by Dr. Haoyang Yu at the University of Alberta. Valuable input and assistance in preparing the manuscript were provided by Dr. Emma. C. Davy and Dr. Christian Hering-Junghans. Sean Liew and Kate Powers performed early synthetic work on the project.

In Chapter 4, Moritz Kränzlein (Technical University of Munich) performed gel permeation chromatography (GPC) on p(DMAA) and analyzed the data. Alvaro Omaña and Dr. Bruno Luppi (University of Alberta) collected GPC data on p(MA) and p(2VP), and analyzed the data.

In accordance with the policy within our research group, each Chapter of this Thesis is essentially self-contained and prepared in the form of a paper that is intended

for publication in peer-reviewed journals. Portions of this Thesis have been published elsewhere, these publications are listed below:

Chapter 2: Hering-Junghans, C.; Watson, I. C.; Ferguson, M. J.; McDonald, R.; Rivard, E. *Dalton Trans.* **2017**, *46*, 7150-7153.

Chapter 3: Watson, I. C.; Schumann, A.; Yu, H.; Davy, E. C.; McDonald, R.; Ferguson, M. J.; Hering-Junghans, C.; Rivard, E. *Chem. Eur. J.* **2019**, *25*, 9678-9690.

Chapter 4: Watson, I. C.; Zhou, Y.; Ferguson, M. J.; Kränzlein, M.; Rieger, B.; Rivard, E. *Z. Anorg. Allg. Chem.* **2020**, *646,* 547-551.

Chapter 5: Watson, I. C.; Ferguson, M. J.; Rivard, E. *Inorg. Chem.* **2021**, *60*, 18347-18359.

Dedicated to my family and friends

"[…] Nine tenths of alchemy was chemistry. And nine tenths of chemistry was waiting." *The Slow Regard of Silent Things* by Patrick Rothfuss

Acknowledgements

First and foremost, I offer my sincerest thanks to my supervisor Prof. Eric Rivard. Without his continued support and mentorship, my success in this program would not have been possible. I have learned a tremendous amount from him and will be eternally grateful for his guidance.

Next, I would like to thank my examining committee members: Prof. Paul Hayes, Prof. Dennis Hall, Prof. Rylan Lundgren, and Prof. Arthur Mar. I thank Prof. Josef Takats for his role as non-examining chair. Their support and input into this Thesis is greatly appreciated.

The professional and personal support of my colleagues has been central to my experience at the U of A. I would like to thank all Rivard group members past and present, with specific attention to Christian Hering-Junghans, Manu Hupf, Eike Dornsiepen, Paul Lummis, Sarah Parke, Matthew Roy, Jocelyn Sinclair, Bruno Luppi, Alvaro Omaña, Sam Baird, Brandon Frenette, William Medroa del Pino, Abhishek Muralidharan, Dominic Lavergne, Gunwant Matharu, Eva Dugbenu, and Linkun Miao. The Rivard group has been host to students from research groups around the world, and I would be remiss not to thank them as well: Shiori Fujimori, Yuki Tsuchiya, Felix Kaiser, Yohei Minami, Susumu Tanaka, Avik Bhattacharjee, and Matthias Ackermann.

I would also like to extend my thanks to the Rieger group who hosted me in Munich for a research exchange, particularly Prof. Rieger, Marc Kloberg, Matthi Nobis, Tom Pehl, and Moritz Kränzlein.

Thank you to my brother Sean for his (mostly virtual) company throughout my degree, and for holding down the fort at home while I have been gone. I am grateful for the support of my parents, Sally Watson and Oreste Papageorgiou, my step-mother Wafa Manuel, and my many aunts, uncles, and cousins.

My friends from the University of Guelph have been supportive of each other as we have made our way through grad school at our separate institutions and moved into the workplace. I am proud to count Kate Marczenko, Andrew Rinald, Marina Childs, Devita Charron, and Bruce Courtin among my closest friends and thank them for their support.

The technical staff at the University of Alberta are second-to-none and have been instrumental to my research. Thank you to Dr. Michael Ferguson, Dr. Bob McDonald, Mark Miskolzie, Wayne Moffatt, Jennifer Jones, Ryan Lewis, Mike Barteski, and all the staff in the machine shop.

Lastly, thank you to Jocelyn. You are the best dinner buddy that a guy could ask for, and your support throughout the PhD process has made a world of difference. This adventure would have looked radically different without you, and I wouldn't have changed it for the world.

Table of Contents

Chapter 1: Introduction

Chapter 2: Organocatalytic Hydroboration Promoted by *N*-Heterocyclic Olefins

Chapter 3: *N*-Heterocyclic Olefin-Ligated Palladium(II) Complexes as Pre-Catalysts for Buchwald-Hartwig Aminations

Chapter 4: Trialkylaluminum *N*-Heterocyclic Olefin (NHO) Adducts as Catalysts for the Polymerization of Michael-Type Monomers

Chapter 5: Zinc-Mediated Transmetallation as a Route to Anionic *N*-Heterocyclic Olefin Complexes in the p-Block

Chapter 6: Group 4 and 8 Transition Metal Complexes with Anionic *N*-Heterocyclic Olefin Ligands

Chapter 7: Summary and Future Work

List of Figures

List of Tables

List of Schemes

List of Charts

List of Symbols, Nomenclature, and Abbreviations

$\{^nX\}$	Decoupled nucleus ^nX
$\%V_{burr}$	Percent buried volume
2VP	2-Vinylpyridine
Å	Angstrom
acac	Acetylacetonate
Ad	Adamantyl
AIM	Atoms-in-molecules
aNHO	Anionic *N*-heterocyclic olefin
aNHC	Abnormal carbene
Anth	Anthracenyl
Ar	Aryl
Ar^F	$3,5\text{-}(F_3C)_2C_6H_3$
Ar^{Me6}	$2,6\text{-}Mes_2C_6H_3$
avg	Average
BHT	Butylated hydroxytoluene, $4\text{-}Me\text{-}2,6\text{-}^tBu_2C_6H_2O$
BIAN	Bis(acenaphthene)
BINAP	2,2′-Bis(diphenylphosphino)-1,1′-binaphthyl
bipy	2,2′-Bipyridine
Bn	Benzyl
BrettPhos	2-(Dicyclohexylphosphino)3,6-dimethoxy-2′,4′,6′-triisopropyl-1,1′-biphenyl
HBpin	Pinacolborane
°C	Degrees Celsius
ca.	Circa; approximately
cf.	Confer; compare
CAAC	Cyclic(alkyl)amino carbenes

.cif	Crystallographic information file
^{Cl}IPr	(ClCNDipp)$_2$C:
cm^{-1}	Wavenumber
Cp	Cyclopentadienyl, C$_5$H$_5$
Cp*	Pentamethylcyclopentadienyl η^5-C$_5$Me$_5$
Cy	Cyclohexyl
dba	Dibenzylideneacetone
DBU	1,8-Diazabicyclo[5.4.0]undec-7-ene
dec.	Decomposed
Dep	Diethylphenyl, 2,6-Et$_2$C$_6$H$_3$
°	Degree
DEVP	Diethylvinylphopshonate
DFT	Density functional theory
DIBAL-H	Diisobutylaluminum hydride
Dipp	Diisopropylphenyl, 2,6-^{i}Pr$_2$C$_6$H$_3$
DMAA	Dimethylacrylamide
DMAP	4-Dimethylaminopyridine
DMSO	Dimethyl sulfoxide
DP	Degree of polymerization
dppf	1,1´-Bis(diphenylphosphino)ferrocene
EDX	Energy dispersive X-ray
element. anal.	Elemental analysis
EPR	Electron paramagnetic resonance
eq	Equivalent
ESI-MS	Electrospray ionization mass spectrometry
Et	Ethyl
Et$_2$O	Diethyl ether

eV	Electron volt
EWG	Electron-withdrawing group
Fc	Ferrocenyl, $(C_5H_5)Fe(C_5H_4)$
FLP	Frustrated Lewis pair
g	Gram
GPC	Gel permeation chromatography
h	Hour
HAADF	High Angle Annular Dark Field
HBcat	Catecholborane
HOMO	Highest occupied molecular orbital
HSAB	Hard-soft acid-base
IAd	$(HCNAd)_2C:$
I^{tBu}	$(HCNI^tBu)_2C:$
IMes	$(HCNMes)_2C:$
$ImMe_2$	$(HCNMe)_2C:$
$ImMe_4$	$(MeCNMe)_2C:$
ImMeEt	$(HCNMe)(HCNEt)C:$
$ImMe_2Ph_2$	$(PhCNMe)_2C:$
IPh	$(HCNPh)_2C:$
IPr	$(HCNDipp)_2C:$
^iPr	Isopropyl
I*	Initiator Efficiency
KHMDS	Potassium bis(trimethylsilyl)amide
k_{obs}	Observed rate constant
kcal	Kilocalorie
kJ	Kilojoule
LALS	Low angle light scattering

LPP	Lewis pair polymerization
LUMO	Lowest unoccupied molecular orbital
MA	Methyl acrylate
M	Moles/liter
Me	Methyl
^{Me}IPr	(MeCNDipp)$_2$C:
Mes	Mesityl, 2,4,6-Me$_3$C$_6$H$_2$
MIC	Mesoionic carbene
min	Minute
MMA	Methyl methacrylate
M_n	Number average molecular weight
MO	Molecular orbital
mol	Mole
mol%	Mole percent
MorDalphos	Di(1-adamantyl)-2-morpholinophenylphosphine
mNHO	Mesoionic *N*-heterocyclic olefins
mp	Melting point
MTS^{iPr}	1-triisopropylsiloxy-1-methoxy-2-methyl-1-propene
M_w	Weight average molecular weight
^{n}Bu	*n*-Butyl
NBO	Natural bond orbital
NHC	*N*-Heterocyclic carbene
NHI	*N*-Heterocyclic imine
NHO	*N*-Heterocyclic olefin
NHOP	*N*-Heterocyclic olefin-phosphine
NICS	Nucleus-independent chemical shift
nm	Nanometer

NMR	Nuclear magnetic resonance
NPA	Natural population analysis
^{n}Pr	n-Propyl
Nu	Nucleophile
OAc	Acetate
OTs	Tosylate, $SO_3C_6H_4Me$
PA	Proton affinity
PdAd-Dalphos	1,3,5,7-Tetramethyl-8-(2-di-o-tolylphosphinophenyl)-2,4,6-trioxa-8-phosphaadamantane
PDI	Polydispersity index
PEO	Poly(ethylene oxide)
PEPPSI	Pyridine enhanced pre-catalyst preparation and stabilization
Ph	Phenyl
PPO	Poly(propylene oxide)
ppm	Parts per million
PNP	1,8-bis(phosphino)-3,6-di-$tert$-butyl-9H-carbazole
PTFE	Polytetrafluoroethylene
pyr	Pyridine
Q_{NPA}	Natural charges
RALS	Right angle light scattering
RI	Refractive index
ROMP	Ring-opening metathesis polymerization
RT	Room temperature
Samb$V$ca	Salerno molecular buried volume calculator
SImMe$_2$	$(H_2CNMe)_2C$:
SIPr	$(H_2CNDipp)_2C$:
SQUID	Superconducting quantum interference device

S$_N$Ar	Nucleophilic aromatic substitution
STEM	Scanning Transmission Electron Microscopy
TBAB	Tetrabutylammonium bromide
^{t}Bu	t-Butyl
TD-DFT	Time-dependent density functional theory
TEP	Tolman electronic parameter
Tf	Triflate, O$_3$SCF$_3$
THF	Tetrahydrofuran
TEM	Transmission electron microscopy
TMEDA	Tetramethylethylenediamine, Me$_2$NCH$_2$CH$_2$NMe$_2$
TOF	Turnover frequency
Trip	Triisopropylphenyl, 2,4,6-^{i}PrC$_6$H$_2$
UV-vis	Ultraviolet-visible spectroscopy
Xantphos	4,5-Bis(diphenylphosphino)-9,9-dimethylxanthene
XPhos	2-Dicyclohexylphosphino-2′,4′,6′-triisopropylbiphenyl
xs	Excess
Xyl	Xylyl, 2,6-Me$_2$C$_6$H$_3$
WBI	Wiberg bond indices
δ	Partial charge or chemical shift in ppm
ΔE	HOMO-LUMO gap
λ$_{max}$	Wavelength of maximum absorbance
η	Hapticity
μ	Micro

Chapter 1: Introduction

1.1 *N*-Heterocyclic Carbenes

N-Heterocyclic carbenes (NHCs) are a class of ligand featuring an intraring two-coordinate carbon atom in a divalent state. NHCs adopt a singlet electronic ground state ($R_2C:$) whereby one carbon atom contains an sp^2-hybridized lone pair as well as a formally vacant orbital of p-character. The adjacent nitrogen atoms to the carbenoid carbon in NHCs lower the energy of the lone pair via induction, while the empty p-orbital of the carbenoid carbon interacts with the lone pairs of the adjacent nitrogen atoms, lending stability to the low-valent carbon center via N–C–N π-bonding (Figure 1.1).[1,2]
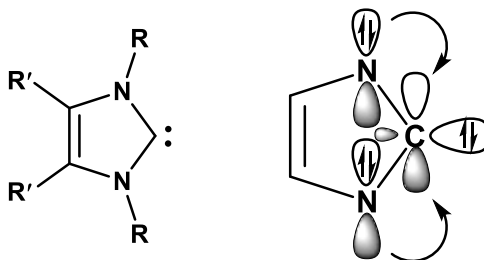
Figure 1.1. A generic Arduengo-type NHC (left) and electronic stabilization of an Arduengo-type NHC (right).

Reactions have been performed with NHCs since the 1960s, when Wanzlick observed that this class of ligand exists in equilibrium with the tetraaminoethene [$(HCNPh)_2C=C(PhNCH)_2$] (**1**), a so-called Wanzlick pair. As shown in Scheme 1.1,

the reactivity of the resulting free NHC was investigated with a variety of small

molecules.[3]
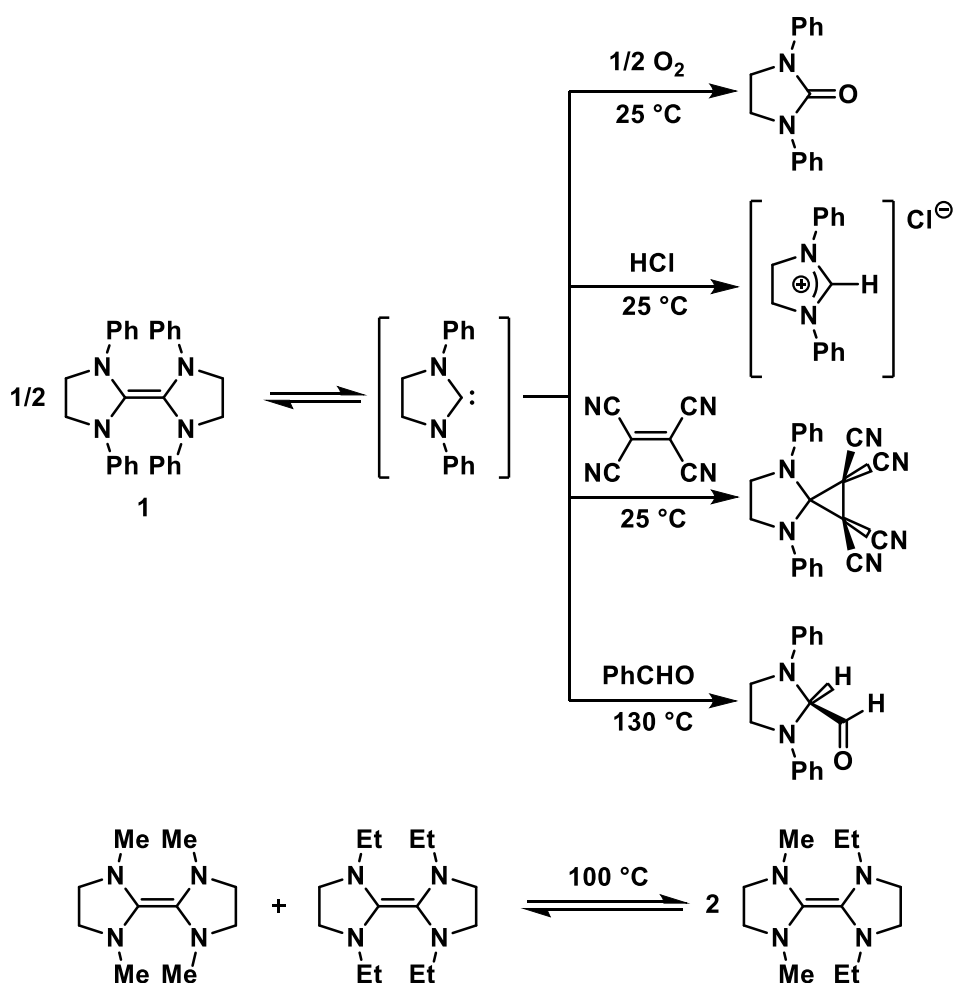
Scheme 1.1. Initial reactivity studies by Wanzlick with an NHC generated from Wanzlick pairs (top) and a cross-over experiment supporting the existence of the Wanzlick equilibrium (bottom).

A Wanzlick pair forms when *N*-heterocyclic carbenes lack steric bulk

surrounding the carbenoid carbon. This occurs particularly readily when the backbone

of the NHC is saturated, as an unsaturated backbone leads to increased stability of the

carbene monomer through resonance.[4] As mentioned, a Wanzlick pair exists in an equilibrium with its free monomeric carbene, called the Wanzlick equilibrium, as confirmed by cross-over experiments using two distinct carbene dimers (Scheme 1.1, bottom).[5] As such, small NHCs are often not isolable. However, it is possible to generate an NHC *in situ* by deprotonation of the corresponding imidazolium salt. This strategy was utilized by the groups of Wanzlick and Öfele to access the first NHC-transition metal complexes: $[(IPh)_2Hg][ClO_4]_2$ (**2**) $[IPh = (HCNPh)_2C:]$ and $ImMe_2 \cdot Cr(CO)_5$ (**3**) $[ImMe_2 = (HCNMe)_2C:]$, respectively (Scheme 1.2).[6] It is worth noting that utilizing this strategy of generating small carbenes *in situ* for reaction with metal or metalloid centers is still used in contemporary research.[7] NHC-transition metal complexes are also accessible via ligand exchange of a Wanzlick pair with metal-phosphine complexes, as shown by notable examples from Lappert, *e.g.,* formation of the stable complex **4** (Scheme 1.2).[8]
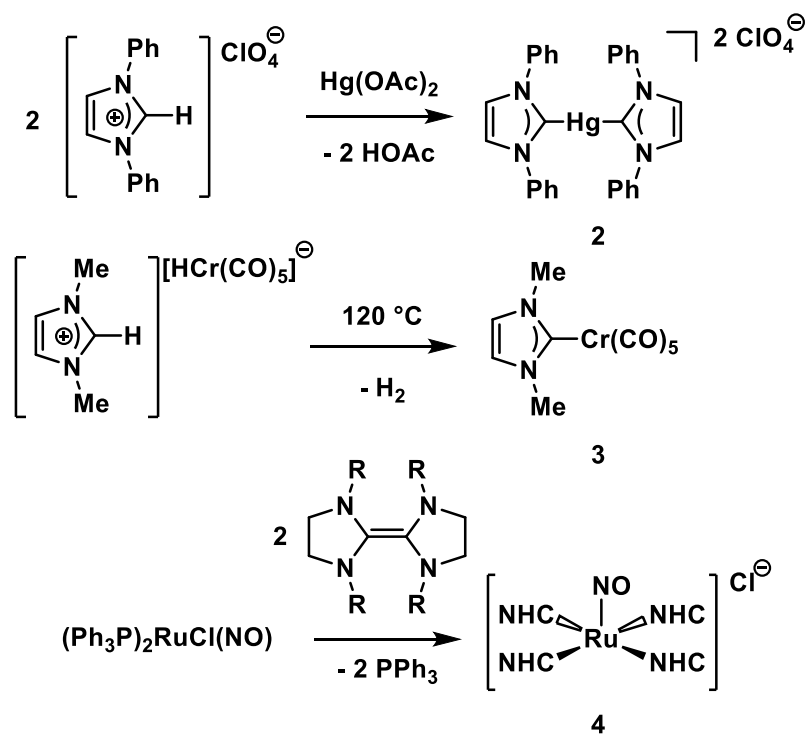
Scheme 1.2. Early examples of NHC-transition metal complexes.

While *N*-heterocyclic carbenes have been known since the 1960s, examples of singlet carbenes could not be isolated as stable solids until 1988, when Bertrand and coworkers prepared the stable phosphinosilylcarbene (**5**) (Chart 1.1, left).[9] Shortly thereafter, Arduengo and coworkers synthesized the first "bottleable" NHC, IAd (1,3-di-1-adamantylimidazol-2-ylidene) (**6**) (Chart 1.1, right).[10] IAd is thermally stable, although it is both air- and water-sensitive. A key to Arduengo's successful synthesis of an isolable NHC is placement of bulky substituents (*e.g.,* adamantyl) on the nitrogen centers of the heterocycle to prevent carbene dimerization.
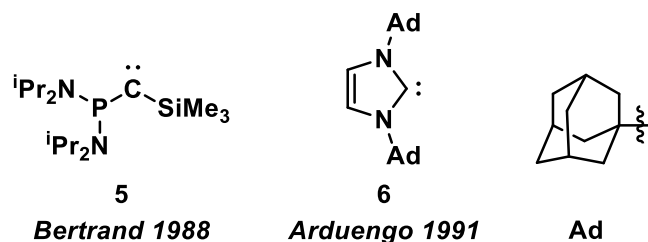
Chart 1.1. The first isolable carbene (left) and the *N*-heterocyclic carbene (right); Ad = adamantyl.

The accessibility, stability, and ease of structural tunabilility of *N*-heterocyclic carbenes makes the study of these ligands convenient; moreover, their high nucleophilicity makes them excellent donor ligands, often outperforming traditional phosphine ligands in this regard. The insights provided by the work by Bertrand and Arduengo proved revolutionary, leading to the synthesis of a tremendous number of carbenes that have found use in coordination chemistry,[11] metal-mediated catalysis,[12] materials chemistry,[13] and as organocatalysis.[14]

1.1.1. Donor Properties of *N*-Heterocyclic Carbenes

The ability of *N*-heterocyclic carbenes (NHCs) to act as strong electron-donating ligands has been a major reason for their widespread use in organometallic and main group chemistry.[11] While the ability of these carbenes to act as electron donors (Lewis base) and nucleophiles is intuitive, and was apparent from the preparation of the first NHC complexes,[4] the degree of π-bonding (*i.e.,* metal-to-carbene π-backbonding) that occurs upon the binding of an NHC to a metal center was not immediately apparent. Initially, it was believed that NHCs solely interacted with a

metal center via a σ-bonding interaction, as the lone pairs on the nitrogen atoms of the NHC can donate π-electron density into the empty p-orbital of the carbenoid carbon (Figure 1.1). However, examination of the NHC-copper complex (**7**, Chart 1.2) showed that the Cu-NHC bond was significantly shorter than would be expected for a system where only a σ-interaction was present.[15] Computational studies performed by Meyer and Frenking revealed significant π-interactions (M(d) → C(p)) between late transition metals and NHCs, with approximately 20 % of the interaction between a Group 11 metal and an NHC due to π-backbonding (for example, in the model complex **8** in Chart 1.2).[16,17]
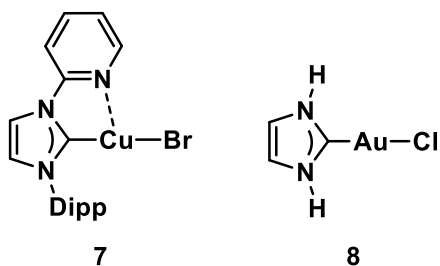
Chart 1.2. Transition metal-NHC complexes that exhibit metal-to-ligand π-backbonding interactions through crystallographic (left) and computational (right) studies; Dipp = 2,6-^{i}Pr$_2$C$_6$H$_3$.

While *N*-heterocyclic carbenes have become commonplace in synthetic chemistry and are by far the most studied class of carbene, cyclic(alkyl)amino carbenes (CAACs) have become the focus of intense study. First reported by Bertrand and coworkers in 2005, CAACs are similar to NHCs in that they have a singlet carbene

electronic ground state based on an *N*-heterocyclic framework, but with one of the amine substituents (N–R) in the ring replaced by a methylene (CR$_2$) group.[18] This structural change has a dramatic effect on the donor properties of the resulting carbene, making CAACs stronger σ-donors and also better π-acceptors than NHCs. This is due to the HOMO of the CAAC being higher in energy and the LUMO being lower in energy, resulting in a smaller HOMO-LUMO gap (193 kJ/mol *vs.* 285.1 kJ/mol, Chart 1.3).[19]
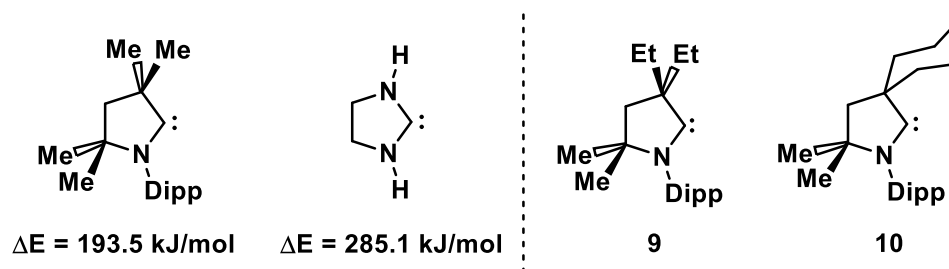
Chart 1.3. The HOMO-LUMO gap (ΔE) of a CAAC (left) and a model NHC (center left) computed at the B3LYP/6-311g** level of theory,[19] and CAACs with alkyl (center right, **9**) and cyclohexyl (right, **10**) substituents.

Another consequence of having a quaternary carbon adjacent to the carbenoid carbon of the CAAC, instead of a second amino substituent as in an NHC, is that the steric profile of the ligand changes. The alkyl groups attached to this quaternary carbon allow for steric bulk to be introduced above and below the plane of the *N*-heterocycle, and depending on the alkyl substituents chosen, different levels of steric congestion and flexibility can be obtained. For example, alkyl chains such as the ethyl

7

groups bound to this quaternary carbon in the CAAC **9** can rotate around in solution providing flexible bulk, while having a cyclohexyl group (**10**) adjacent to the carbene locks the steric bulk into position providing a rigid wall to protect the carbene donor site.[20]

Traditional *N*-heterocyclic carbene ligands have the carbene moiety (R_2C:) localized on the C2 carbon of the imidazole ring, but it is also possible to have the carbene lone pair localized on the C4 or C5 carbon atoms (Scheme 1.3, top). A result of having the carbene located at the C4 or C5 position is that a canonical resonance form cannot be drawn without formal charges on the imidazole ring.[21] These ligands are known commonly by two names: abnormal *N*-heterocyclic carbenes (aNHCs) or mesoionic carbenes (MICs). The first example of an aNHC was reported in 1993 by Araki and coworkers, where 1,3,4,5-tetraazolium salts were designed as ligand precursors that would result in an aNHC bound to either mercury or palladium (**11**) (Scheme 1.3, middle).[22] Further exploration into aNHCs would not be made until 2001 when Crabtree and coworkers reacted an imidazolium salt with a pendant pyridine group with $IrH_5(PPh_3)_2$ to yield a complex where the imidazole unit was bound to the iridium center through a backbone (C4) position (**12**) (Scheme 1.3, bottom).[23]
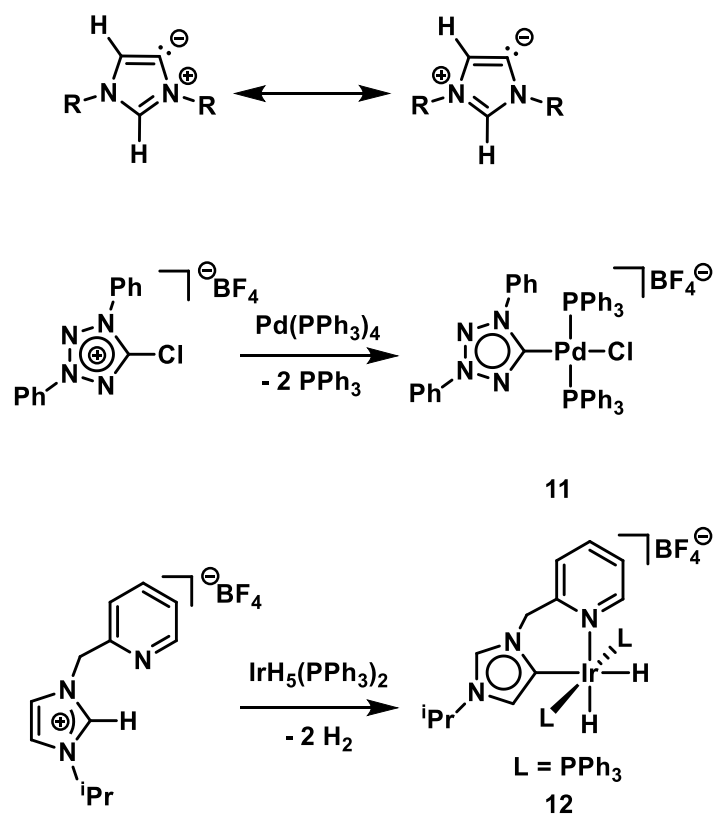
Scheme 1.3. Canonical resonance forms for abnormal *N*-heterocyclic carbenes (top) and the first aNHC complexes by Araki (middle, **11**) and Crabtree (bottom, **12**).

Much like with *N*-heterocyclic carbenes, aNHCs were first identified as ligands bound to transition metals, but were later functionalized such that a free aNHC could be isolated. Specifically, Bertrand and coworkers were able to deprotonate the C5 position of an imidazolium unit by first blocking the C2 position with a phenyl group, leading to the first isolable aNHC (**13**) (Scheme 1.4, top).[24a] The same group later used click reactions to access aNHC precursors, allowing for easy access to stable aNHCs (**14**) (Scheme 1.4, bottom).[24b]
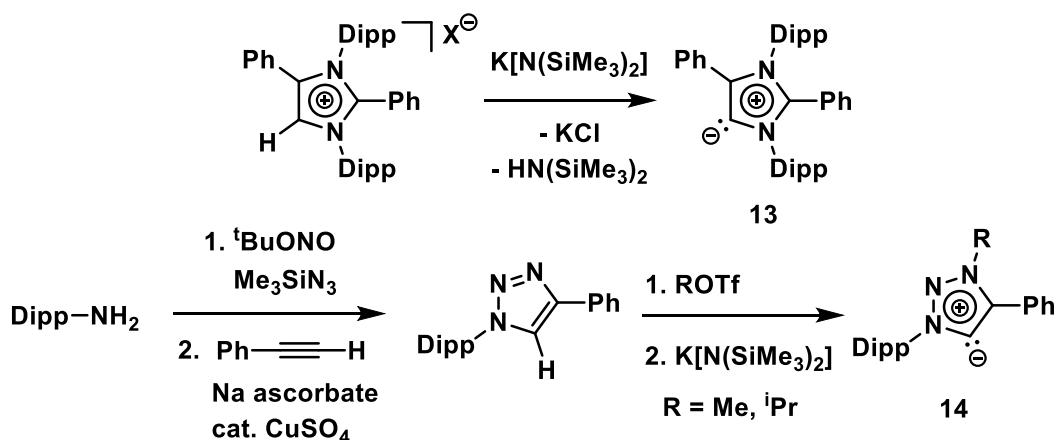
Scheme 1.4. The first isolable aNHC ligand (top) and a notable aNHC formed by a click reaction (bottom).

According to a comprehensive computational study by Gusev, aNHCs are stronger σ-donors than most NHCs.[25] Another property of aNHCs is their inability to form Wanzlick pairs via dimerization (*vide supra*), allowing for the preparation of less bulky ligands when compared to NHCs.[21] Notably, the pK$_a$ of a proton appended to the C2 carbon of an imidazolium ring (24.9) was computed by Yates and Magill to be significantly lower than that in the C4 position (33.0),[26] implying that there are considerable kinetic contributions associated with the formation of an aNHC instead over a normal NHC. Indeed, this is corroborated by computations from Bertrand and colleagues who have shown that the HOMO of the aNHC **13** lies at –4.40 eV, while that of its NHC isomer **15** (Chart 1.4) has a HOMO that is significantly lower in energy at –5.00 eV.[24a]
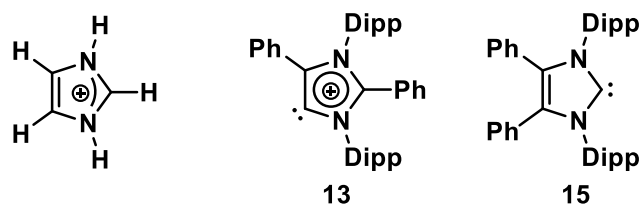
Chart 1.4. Imidazolium on which pK_a values were computed by Yates (left) and the isolable aNHC **13** and its NHC isomer **15**.

1.2 *N*-Heterocyclic Olefins

N-Heterocyclic olefins (NHOs) represent a compound class that contain an alkylidene unit (CH_2 or CR_2) appended to an *N*-heterocyclic carbene (NHC) framework (Chart 1.5). The terminal alkylidene units in NHOs feature highly polarized C=C π-bonds, leading to a significant degree of ylidic character, allowing these olefins to act as neutral 2-electron donors to main group and transition metal species.[27] This accumulation of charge on the exocyclic carbon also allows NHOs to act as efficient Brønsted bases and strong nucleophiles.[27] Much like NHCs, NHOs have multiple sites for functionalization (R, R′, R″, Chart 1.5), allowing for the tuning of their steric and electronic properties.
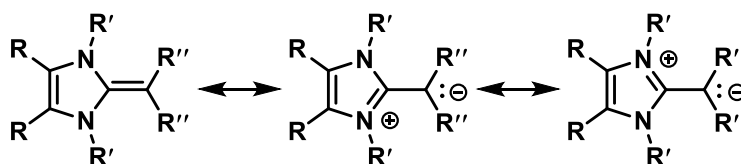
Chart 1.5. Dominant canonical forms of *N*-heterocyclic olefins (NHOs), demonstrating the ylidic nature of the C=C bond, and the multiple sites available for structural modification.

1.2.1 Properties of *N*-Heterocyclic Olefin Ligands

NHOs are softer carbon-based donors when compared to their parent NHCs due to increased levels of p-orbital character at the terminal olefinic carbon atom that is used for ligation. To evaluate the relative electron donor strengths of NHOs and NHCs, the Tolman electronic parameters (TEP) of both ligands were compared.[28] In 2016, the Rivard Group prepared the Rh(I) complexes IPr•RhCl(CO)$_2$ (**16**) and IPrCH$_2$•RhCl(CO)$_2$ (**17**) (IPr = (HCNDipp)$_2$C:, IPrCH$_2$ = (HCNDipp)$_2$C=CH$_2$, Dipp = 2,6-^{i}Pr$_2$C$_6$H$_3$) (Scheme 1.5), and used the average IR ν(CO) stretching frequencies of the resulting complexes to show that IPrCH$_2$ was more electron-donating.[29] Specifically, a stronger electron-donating ligand will provide more electron density to the metal center, which in turn weakens the C–O bonding in the CO ligands via increased Rh(d)−CO(π*) backbonding. As such, a lower average carbonyl stretching frequency leads to a lower TEP value and is indicative of a more electron-donating ligand.
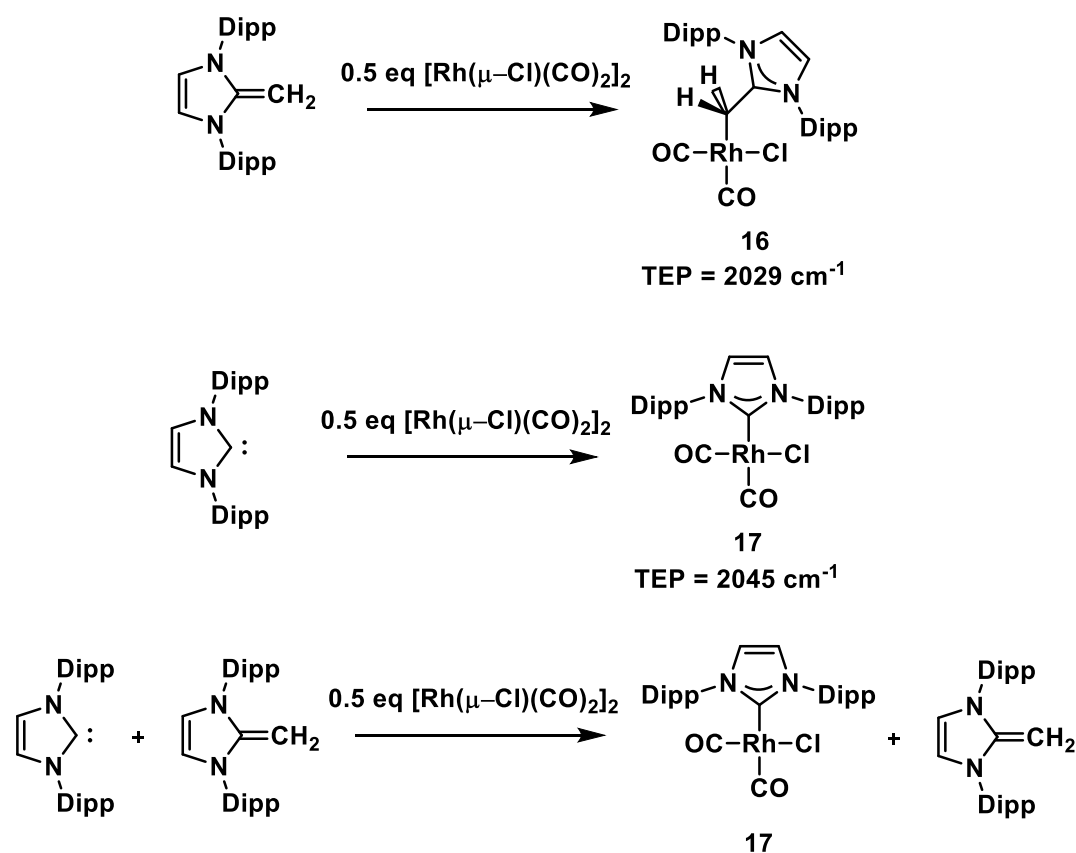
Scheme 1.5. Synthesis of IPr·RhCl(CO)₂ (**16**) (top) and IPrCH₂·RhCl(CO)₂ (**17**) (middle), and a competition study showing that NHCs bind preferentially to rhodium (bottom).

The TEP obtained from measuring the IR spectrum of the NHO complex IPrCH₂·RhCl(CO)₂ (**16**) (2029 cm⁻¹) is smaller than the value of 2045 cm⁻¹ for the carbene-bound congener IPr·RhCl(CO)₂ (**17**), implying that NHOs are stronger electron donors than NHCs.[29] These results mirror the observations by Fürstner, who noted that coordination of the NHO ImMe₂CH₂ (ImMe₂CH₂ = (HCNMe)₂C=CH₂) to a RhCl(CO)₂ moiety resulted in a lower average ν(CO) stretching frequency in relation to the corresponding NHC·RhCl(CO)₂ complexes.[30] However, when a 1:1 mixture of

IPr and IPrCH$_2$ was combined with [Rh(μ-Cl)(CO)$_2$]$_2$, the NHC adduct IPr•RhCl(CO)$_2$ (**17**) was formed exclusively, showing that NHOs are weaker Lewis bases than their parent NHCs (Scheme 1.5). It was determined via computational studies that this observation is due to NHOs having minimal π-accepting ability, whereas NHCs act as weakly π-accepting ligands.[29] As such, the higher TEP of NHC-metal carbonyl complexes compared to their corresponding NHO complexes can be rationalized by electron density being removed from the metal center via (M $\rightarrow$ C) π-backdonation in the case of the NHC-Rh complex (**17**).

The steric bulk of a ligand can be evaluated by computing the percent buried volume (%V$_{burr}$), as proposed by Nolan and Cavallo.[31] The percent buried volume quantifies the percentage of the first coordination sphere of a metal that is occupied by a ligand (Figure 1.2).[32] A putative metal atom with a radius of 3.5 Å is often chosen as the sphere that the ligand is bound to, as this radius is a good approximation of the first coordination sphere of many metals. Values of a given ligand's %V$_{burr}$ can be obtained using the Samb$V$ca (Salerno molecular buried volume calculator) software, a tool developed by Cavallo and colleagues, which uses the crystallographic structural information obtained from a .cif (crystallographic information file) to calculate the percent buried volume.[33] The Samb$V$ca software was initially developed to evaluate the steric congestion around a metal center resulting from the coordination of an NHC ligand, but has since been used to compute the %V$_{burr}$ of a wide variety of ligands.[34] Gandon and coworkers compared the %V$_{burr}$ of ImMe$_2$ (ImMe$_2$ = (HCNMe)$_2$C:) with that of the *N*-heterocyclic olefin ImMe$_2$CH$_2$, and found values of 26 % and 19 %,

respectively.[35] Powers compared the structures of IPr·AuCl and IPrCH$_2$·AuCl and found that IPr covered 45 % of the gold atom, while IPrCH$_2$ only covered 35 % (Figure 1.2).[36] This percent buried volume trend is intuitive, as the key difference between an NHC and NHO ligand is the presence of an added alkylidene (CR$_2$) unit between the metal center and the *N*-heterocyclic ring of the ligand in an NHO, which decreases the steric bulk around the metal center.
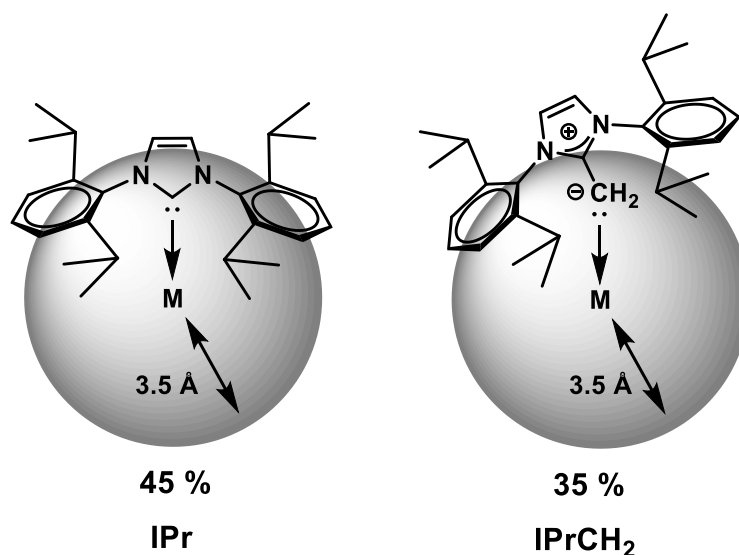
Figure 1.2. Comparison of the percent buried volume (%V$_{burr}$) of IPr and IPrCH$_2$.

Recently, several experimental and computational studies have been undertaken to examine the proton affinities, Brønsted basicity, and nucleophilicity of *N*-heterocyclic olefins. Given that NHOs have multiple sites available for structural modification (Chart 1.6), there is significant interest in examining the influence of varying functional groups at these positions. Studies by Naumann and coworkers showed that the proton affinity (PA) of an NHO increases when alkyl groups are

installed on the exocyclic carbon (Chart 1.6).[37] The same study revealed that electron-withdrawing groups (*e.g.,* Cl) on the backbone reduce the proton affinity of the resulting NHO. Overall NHOs are potent Brønsted bases, reaching the upper end of the superbasicity scale (*e.g.,* absolute proton affinities > 245.3 kcal/mol).[38] Notably, NHOs have higher proton affinities than structurally related NHCs, where $ImMe_4CH_2$ [$ImMe_4CH_2$ = $(MeCNMe)_2C=CH_2$] has a PA of 273.9 kcal/mol, while the *N*-heterocyclic carbene ImMeEt [(HCNMe)(HCNEt)C:] has a PA of 251.3 kcal/mol (Chart 1.6).[39]

ImMe₄=CH₂
PA = 273.9 kcal/mol

ImMe₄=CHMe
PA = 279.5 kcal/mol

ImMe₄=CMe₂
PA = 283.6 kcal/mol

ImCl₂Me₂=CH₂
PA = 261.6 kcal/mol

ImMeEt
PA = 251.3 kcal/mol
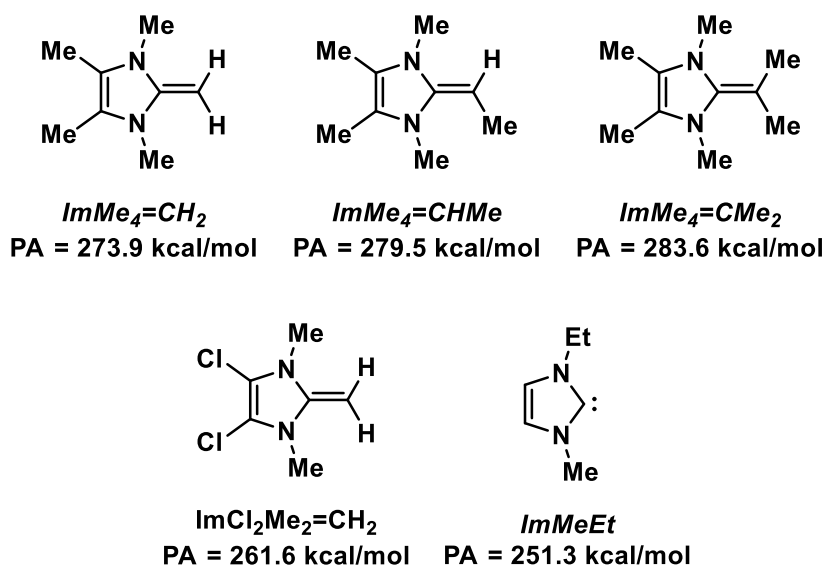
Chart 1.6. The effect of NHO functionalization on the proton affinity (PA) of NHOs, and the proton affinity of the NHC ImMeEt.

While proton affinities can be correlated to Brønsted basicity, chemists often describe the Brønsted basicity of a molecule in terms of pK_{aH}, the pK_a of its conjugate acid. Ji and coworkers computed the pK_{aH} for a wide range of NHOs in

DMSO that included examples with varying heteroatoms in the 1-position of the heterocycle, different heterocycle ring sizes, and flanking N-substituents (Chart 1.7).[40] Ji also showed that there is a linear correlation of the pK_{aH} in DMSO to the Gibbs free energy of reaction associated with an NHO reacting with CO_2, suggesting NHOs with higher Brønsted basicities form stronger NHO-CO_2 adducts, allowing for a straightforward computational method to estimate the potential Lewis basicity of *N*-heterocyclic olefins.[40] A notable observation from this study is that there is a dramatic difference in pK_{aH} values for imidazole and imidazoline-based NHOs (*e.g.,* heterocycles with unsaturated *vs.* saturated backbones, respectively). Imidazole-based NHOs have pK_{aH} values between 5 and 6 units higher than their imidazoline counterparts (Chart 1.8). This can be rationalized by an increase in aromaticity of the NHO unit upon protonation (to form NHC–CR_2H^+) in the case of imidazole-based NHOs, whereas the imidazoline-based NHOs do not gain the same degrees of aromatic character upon protonation, as evidenced by nucleus-independent chemical shift (NICS) computations.[40]

$pK_{aH} = 19.2$ $pK_{aH} = 24.6$ $pK_{aH} = 22.1$ $pK_{aH} = 14.9$
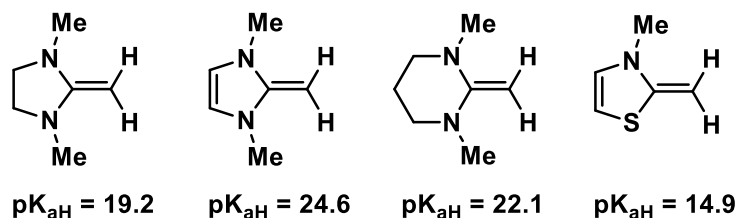
Chart 1.7. The computed pK_{aH} values of NHOs with different structural properties.

The first investigation into the Brønsted basicity of NHOs was performed by Heuschmann in 1987, where pK_{aH} values were determined for protonated NHOs by potentiometric titration, revealing values of 21.6 to 28.2 in acetonitrile, depending on how the NHO unit was functionalized.[41] An experimental study by Ji and coworkers investigated the Brønsted basicity of a variety of NHOs, indicating that NHOs can have Brønsted basicities that range from 17.0 to 24.1 pk_{aH} units (Chart 1.8).[42]

$$pK_{aH} = 17.0 \qquad pK_{aH} = 24.1 \qquad pK_{aH} = 20.0$$
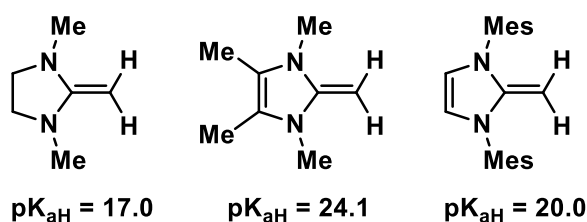
Chart 1.8. Experimentally measured pK_{aH} values for NHOs determined by Ji.

Ji measured the nucleophilicities of several NHOs using a method originally pioneered by Mayer and coworkers,[43] by reacting the NHOs with a series of different *p*-quinone methides as reference electrophiles (Chart 1.9) and following the kinetics of the reactions via UV-Vis spectroscopy.[42] The authors used a ten-fold excess of NHO to achieve pseudo-first order conditions, then the time-dependant absorbance (as determined by UV-Vis spectroscopy) was fitted to Equation 1.1 to obtain the first order rate constant k_{obs}.

$$A = A_0 \exp(-k_{obs}t) + C \qquad (1.1)$$

Then, k_{obs} could be plotted against the concentration of the NHO, revealing a linear correlation between the two values. The slope of this resulting line corresponds to the second order rate constant k_2. This rate constant k_2 was determined with all reference electrophiles, and the logarithms of k_2 were then plotted to form a line (see Equation 1.2 for the equation of the line), where E is a solvent-independent electrophilicity parameter, N is a solvent-dependent characteristic of nucleophilicity, and s_N is a sensitivity parameter of the nucleophile that indicates how dependent N is on the reference electrophiles. For example, varying degrees of steric bulk around two different nucleophiles can result in different s_N values.

$$\log_{10}k_2(20\ °C) = s_N(N+E) \qquad (1.2)$$
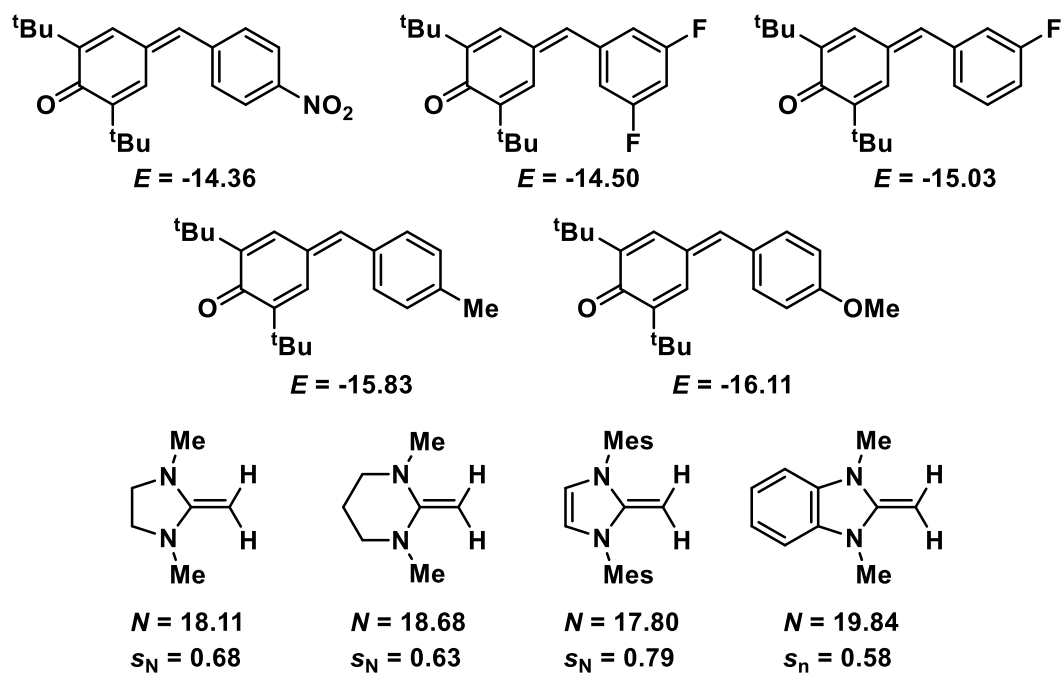
Chart 1.9. The reference electrophiles (top) used to determine the nucleophilicity of NHOs (listed at the bottom).

The nucleophilicity (N) of four different NHOs is summarized in Chart 1.9. The nucleophilicity of IMesCH$_2$ (IMesCH$_2$ = (HCNMes)$_2$C=CH$_2$; Mes = 2,4,6-Me$_3$C$_6$H$_2$) was compared to its parent carbene IMes (IMes = (HCNMes)$_2$C:), which revealed that the NHC is more nucleophilic than the NHO (N = 21.72 *vs.* N = 17.80, respectively). However, the authors advise caution when comparing the nucleophilicity of NHOs and NHCs because these measurements are highly sensitive (*e.g.,* have high s_N values) to the steric bulk of the electrophiles used to measure the value (Chart 1.9, bottom).[42] While it appears that NHOs are less nucleophilic than their corresponding NHCs, the weakest nucleophile of the NHO series evaluated (IMesCH$_2$) is more nucleophilic than both 4-dimethylaminopyridine (DMAP) and triphenylphosphine (PPh$_3$) (N = 17.80 *vs.* N = 15.90 and N = 13.59, respectively).[43]

1.2.2 Examples of *N*-Heterocyclic Olefin in Coordination Chemistry

The first reported synthesis of an *N*-heterocyclic olefin (NHO) and its subsequent reaction with a transition metal was reported by Kaska in 1979, where SImMe$_2$CH$_2$ (SImMe$_2$CH$_2$ = (H$_2$CNMe)$_2$C=CH$_2$) was combined with Zeise's dimer [(η^2-H$_2$CCH$_2$)PtCl$_2$]$_2$ to give the dimeric complex [(SIMe$_2$CH$_2$)PtCl(μ-Cl)]$_2$ (Chart 1.10).[44] In this example, the NHO exhibited two binding modes: one where the alkylidene unit binds to the platinum center in an η^2-fashion, and another mode where η^1-coordination is observed (**18a** and **18b**, respectively). It is worth noting that η^2-

binding of the exocyclic alkylidene unit of an NHO to a metal center is rare; the vast majority of NHO complexes involve end-on (η^1) coordination of the NHO. Heuschmann expanded the library of available NHOs, providing a general route to functionalize the *N*-heterocyclic backbone, the nitrogen atoms of the imidazole unit, and the terminal alkylidene positions, highlighting the tunability of this class of ligand.[41] Pioneering work done by Kuhn and coworkers provided more examples of NHO-transition metal complexation, with initial examples involving adducts with molybdenum and tungsten pentacarbonyls (**19**, Chart 1.10).[45] Soon after, Kuhn reported NHO complexes of the rare earth metals lanthanum and yttrium, as well as the transition metal niobium.[46] NHO chemistry would largely lie dormant for more than a decade, until 2010 when Beller developed an NHO-phosphine salt, [IPr–CH$_2$– PCy$_2$]I, which was used as a supporting ligand for palladium-catalyzed cross-coupling reactions (**20**, Chart 1.10).[47]
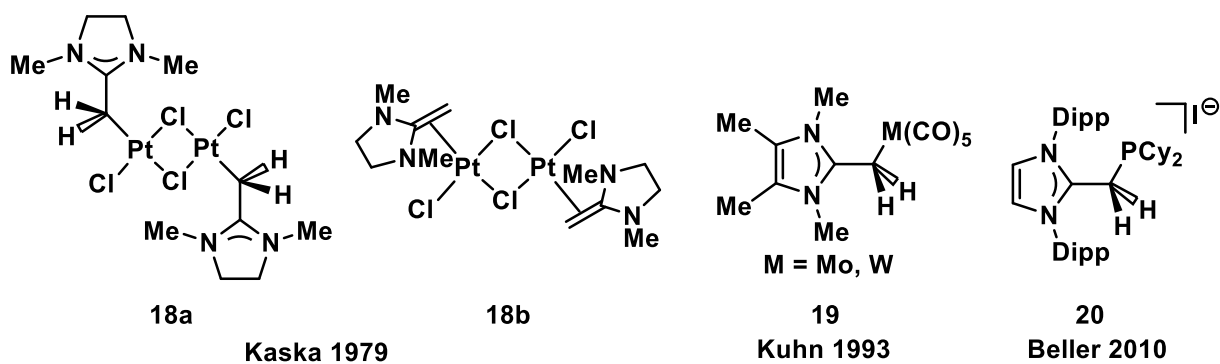
Chart 1.10. Early examples of NHO complexes.

Over the past decade, many more examples of NHO complexes have appeared in the literature. Notable examples of NHO-supported main group complexes include: NHO-stabilized EH_2 complexes $IPrCH_2 \cdot EH_2 \cdot W(CO)_5$ [E = Ge (**21**), Sn (**22**)][48] (Chart 1.11) and the inorganic ethylene complex $IPrCH_2 \cdot H_2GeGeH_2 \cdot W(CO)_5$ (**23**)[49] from the Rivard Group, and mono- and di-cationic hydridoboron compounds $[(IPrCH_2 \cdot BH_2)_2(\mu\text{-H})][NTf_2]$ and $[(IPrCH_2 \cdot BH)_2(\mu\text{-H})_2][NTf_2]_2$ (**24a** and **24b**, Chart 1.11) from the Ghadwal Group $[NTf_2 = N(SO_2CF_3)_2]$.[50] Other examples of NHO-bound transition metal complexes include: an NHO-gold(I) complex $[ImMe_2CH_2 \bullet Au(PPh_3)][SbF_6]$,[30] a rhodium complex wherein the exocyclic carbon of the NHO donor is functionalized (*e.g.,* **25**, Chart 1.11),[51] and an NHO-tungsten olefin metathesis catalyst (**26**, Chart 1.11).[52] Interestingly, Fogg and coworkers have identified that olefin metathesis catalysts bearing a methylidene ligand (*e.g.,* $(Cy_3P)_2Cl_2Ru=CH_2$) can decompose upon addition of the small NHC, $ImMe_4$, yielding the *N*-heterocyclic olefin $ImMe_4CH_2$ as a product (Equation 1.3).[53]
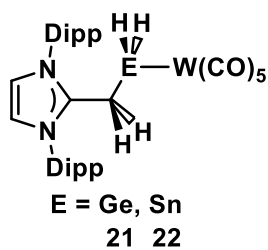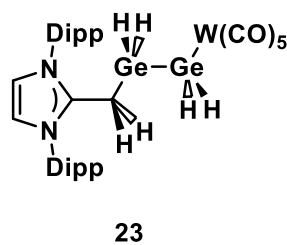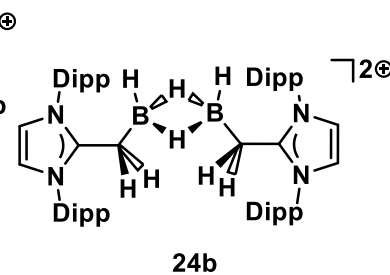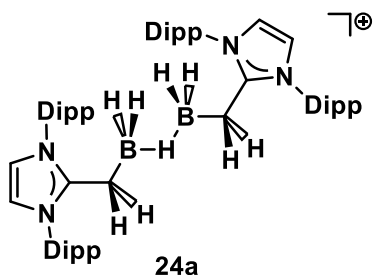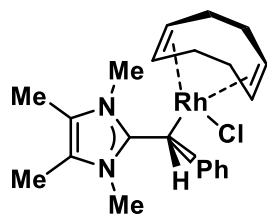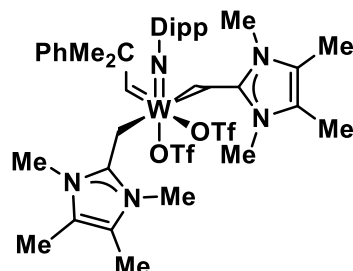
Chart 1.11. Examples of NHO-main group and NHO-transition metal complexes.

(1.3)
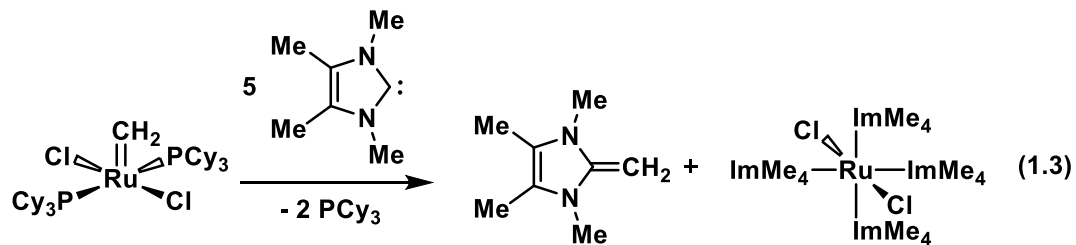
1.2.3. Synthesis of *N*-Heterocyclic Olefins

There are multiple routes available to access NHOs. The earliest route by Kaska involved combining 2-chloro-1,3-dimethylimidazolinium chloride ([SImMe$_2$Cl]Cl) with two equivalents of methyl lithium in diethyl ether (Scheme 1.6, top).[32] Methane and lithium chloride are the only by-products formed, both of which are easily separated from the desired NHO product. This route likely involves the formation of the imidazolinium salt [SImMe$_2$–CH$_3$]Cl followed by deprotonation by a second equivalent of MeLi to give SImMeCH$_2$. Heuschmann presented a general route to access backbone saturated NHOs of the form (H$_2$CNR)$_2$C=CR′H, where an imidazolidium salt is reacted with sodium hydride, deprotonating the salt to access the NHO (Scheme 1.6, middle).[30] It is worth noting that Heuschmann and coworkers were able to access 22 different NHOs in this manner. Strategies similar to those of Heuschmann are often employed in the synthesis of small, less bulky NHOs, especially when functionalization of the exocyclic carbon of the NHO is desired. Kuhn's route to synthesize ImMe$_4$CH$_2$ involved the combination of [ImMe$_4$–CH$_3$]I with *tert*-butyllithium followed by vacuum thermolysis of the resulting NHO-LiI adduct (Scheme 1.6, bottom).[33]
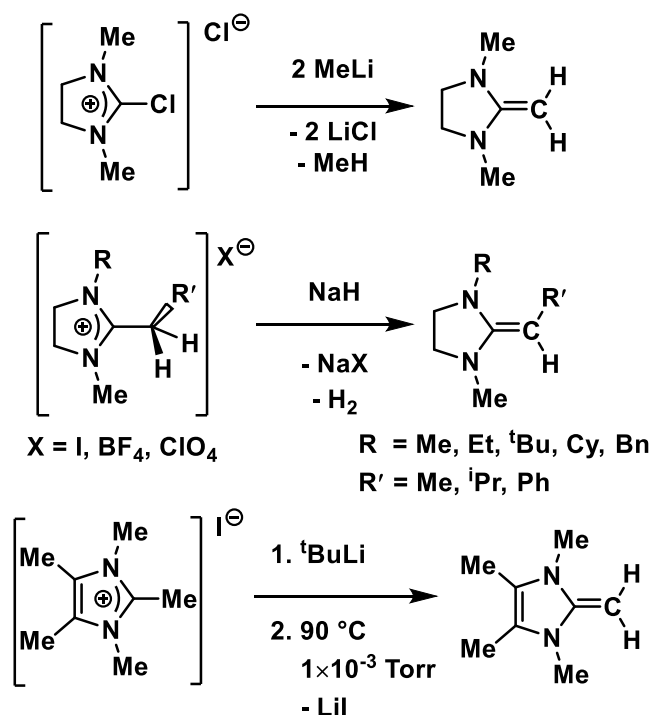
Scheme 1.6. The first reported routes to access NHOs by Kaska (top), Heuschmann (middle), and Kuhn (bottom).

Contemporary NHO syntheses involve generation of the NHO from its parent NHC. For example, IPrCH₂ can be made via combination of IPr with methyl iodide, followed by deprotonation of the resulting imidazolium salt [IPr–CH$_3$]I with a base, such as *n*-butyllithium or potassium *tert*-butoxide (Scheme 1.7, top).[29,47] This route takes inspiration from Kuhn's NHO synthesis (*vide supra*). Ideally, a base is chosen such that the by-products can be easily separated from the desired NHO (*e.g.,* by filtration or by vacuum distillation). To this end, the Rivard Group has developed a novel multigram synthesis to access IPrCH₂ where ClCH$_2$SiMe$_3$ is used as a methylating agent (Scheme 1.7);[29] this procedure gives IPrCH₂ in a 79 % isolated

yield and the volatile Me$_3$SiCl by-product can be removed via evaporation. A third noteworthy strategy to access NHOs was developed by Robinson and coworkers, where the reaction of IPr with ^{n}BuLi first yields the anionic carbene salt (LiCNDipp)(HCNDipp)C:, followed by the addition of methyl iodide to give IPrCH$_2$ (Scheme 1.7).[54]
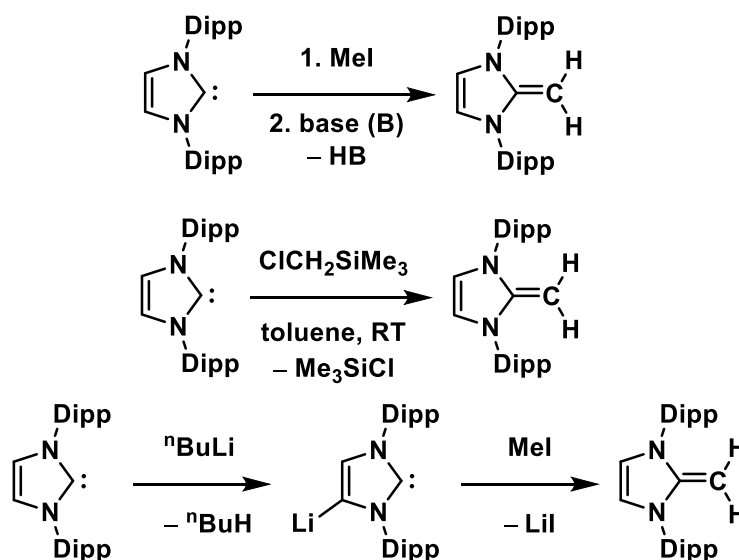
Scheme 1.7. A general pathway (top), Rivard's pathway (middle), and Robinson's pathway to access the bulky NHO IPrCH$_2$.

While imidazole-based NHOs are becoming common, triazole-derived NHOs are significantly rarer. The earliest example of this class of NHO was reported by Enders and coworkers, where Enders' carbene [PhCN(NPh)$_2$)C:, Scheme 1.8] was combined with ethylfumarate to give the NHO (PhCN(NPh)$_2$)C=C(CO$_2$Me)(CH$_2$CO$_2$Me) (**27**, Scheme 1.8).[55] Another example of a triazole-based NHO was reported by Matsuoka and coworkers, who combined

Enders' carbene with methyl methacrylate (MMA) to give $(PhCN(NPh)_2)C=CH(CHMeCO_2Me)$ (**28**, Scheme 1.8).[56]
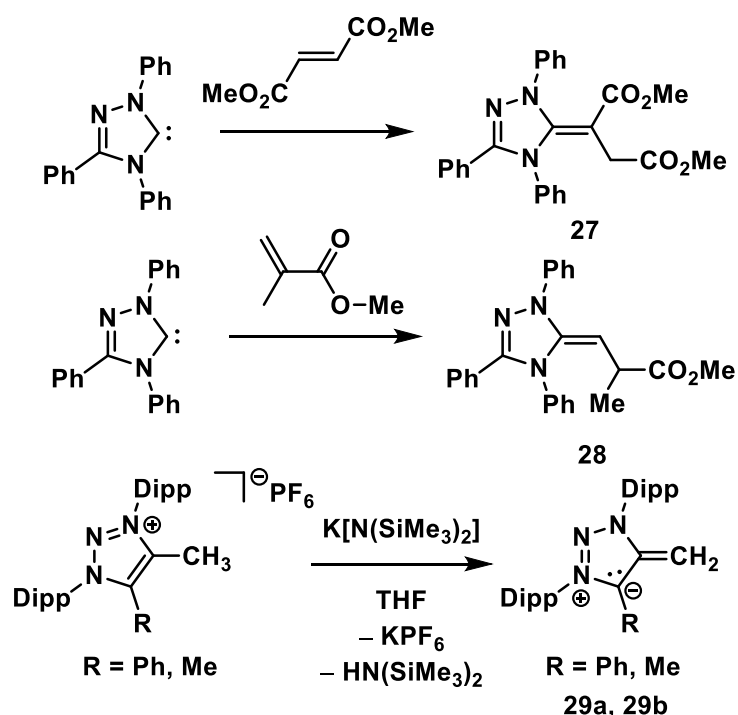
Scheme 1.8. Synthesis of triazole- and mesoionic-based NHOs.

Recently, Hansmann and coworkers reported the synthesis of mesoionic NHOs (mNHOs).[57] Much like their NHC analogues, mesoionic NHOs cannot be represented without formal positive and negative charges in their canonical Lewis structures. The synthesis of mNHOs is straightforward, as the triazolium salt precursor (Scheme 1.8, bottom) can be obtained from commercially available precursors in two steps.[57] With the triazolium salt in hand, deprotonation with potassium bis(trimethylsilyl)amide (KHMDS) yields the corresponding mNHO in 63 and 69 % yields, respectively (**29a** and **29b**, Scheme 1.8).

1.2.4. Anionic *N*-Heterocyclic Olefins (aNHOs)

While neutral NHOs act as 2σ-electron donors, it is possible to generate deprotonated analogues, called anionic NHOs (aNHOs), which are formally 2σ, 2π-electron donors (Scheme 1.9). These anionic ligands are highly electron-releasing and have proven to be exceedingly valuable in stabilizing coordinatively unsaturated main group centers.

The earliest examples of aNHOs were obtained by mixing the NHCs with the triphosphabenzene $(PC^tBu)_3$ or the phosphaalkyne $^iPr_2NC\equiv P$, as reported by Nixon and Hahn, respectively (**30** and **31**, Scheme 1.9).[58,59] Another salient example of aNHO complex formation was reported by Kuhn and coworkers in 2002, where the previously reported salt $[ImMe_4\text{-}CH_2PPh_2]Cl$ was deprotonated by either one equivalent of $ImMe_4$ or $ImMe_4CH_2$ to yield the aNHO- substituted phosphine $ImMe_4CH\text{–}PPh_2$ (**32**, Scheme 1.9).[60]
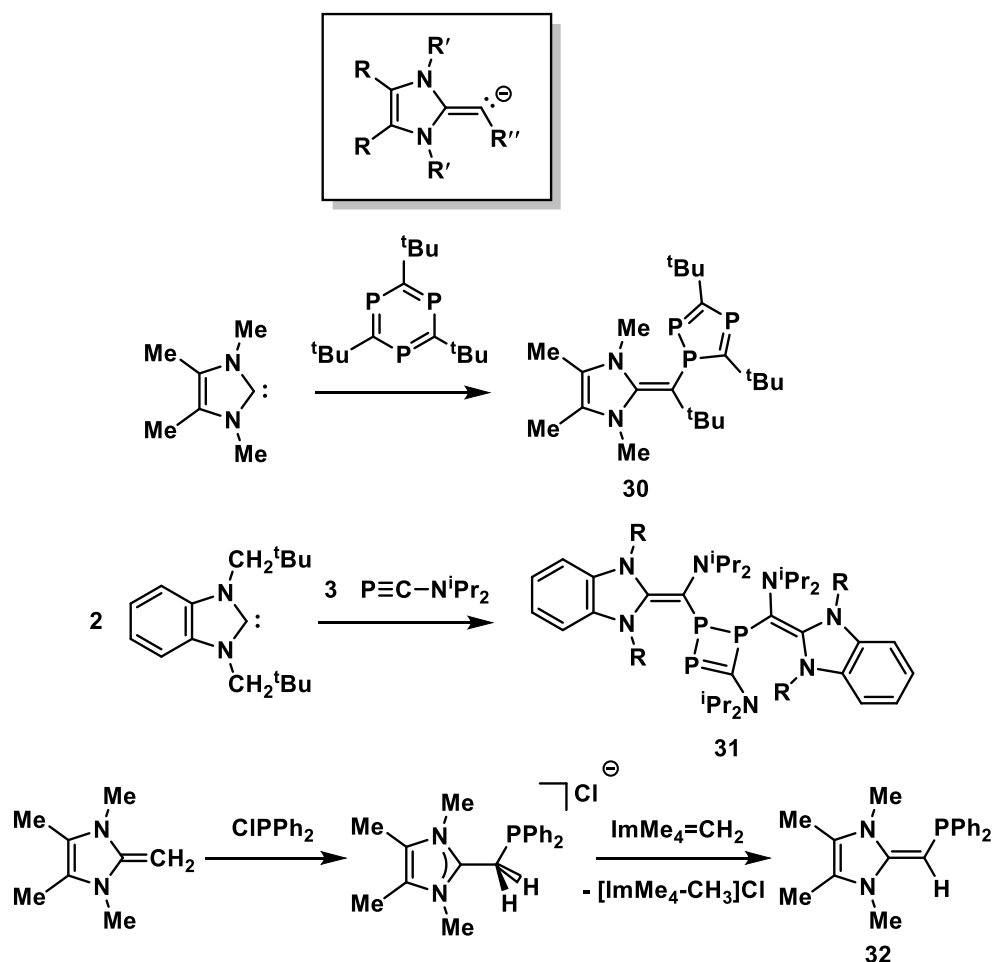
Scheme 1.9. Generic structure of an aNHO (top) and early examples of aNHO complexes.

In 2011, Rivard and coworkers reported the reaction between the cyclic phosphazene $(Cl_2PN)_3$ and IPrCH$_2$, which resulted in the formation of the aNHO-phosphazene $[(IPr=CH)P(Cl)N(PCl_2N)_2]$ (**33**) and $[IPr–CH_3]Cl$ (Scheme 1.10).[61] The authors postulated a reaction mechanism involving initial coordination of the NHO to a phosphorus atom in the phosphazene ring followed by the deprotonation of the coordinated IPrCH$_2$ unit by a second equivalent of NHO acting as a Brønsted base.
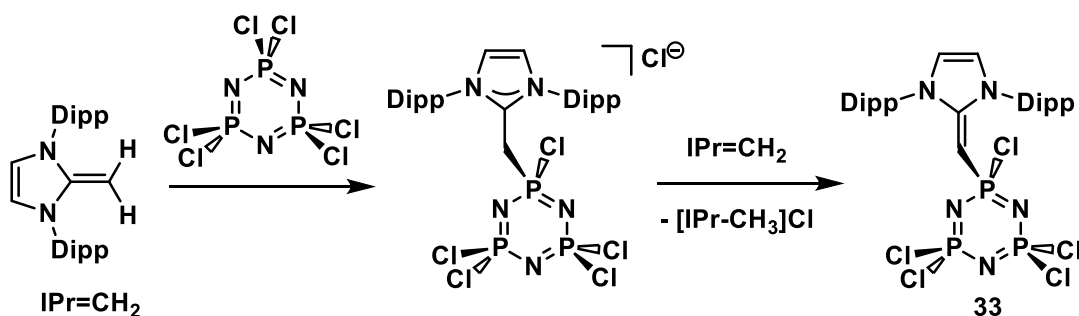
Scheme 1.10. Synthesis of an aNHO-phosphazene complex.

Later, Rivard and coworkers reported syntheses for (IPr=CH)PR$_2$ [R = Ph (**34**), ^{i}Pr (**35**)] by combining two equivalents of IPrCH$_2$ with ClPR$_2$ (R = ^{i}Pr or Ph). As above, one equivalent of IPrCH$_2$ reacts with ClPR$_2$ to form an intermediate [IPr–CH$_2$–PR$_2$]Cl salt, while the second equivalent of IPrCH$_2$ acts as a Brønsted base (Scheme 1.11).[62] In the same study, an anionic NHO functionalized with a dimethylamino substituent IPr=CH–NMe$_2$ (**37**) was accessed by reacting two equivalents of IPr with Eschenmoser's salt, [H$_2$C=NMe$_2$]I, where again one equivalent of IPr acts as a Brønsted base (Scheme 1.11). The resulting IPr=CH–ER$_2$ (E = N, P) ligands show the ability to bind Lewis acids and transition metals in different positions. For example, IPr=CH–PPh$_2$ (**34**) preferentially binds AuCl (**37**, Scheme 1.11), BH$_3$, and Pd(cinnamyl)Cl through a phosphorus atom donor site. Conversely, IPr=CH–NMe$_2$ binds AuCl through the exocyclic carbon atom of the ligand (**38**). A later study showed that it is possible to engage both donor sites of IPr=CH–PPh$_2$, as demonstrated by combining IPr=CH–PPh$_2$(AuCl) (**37**) with Me$_2$S•AuCl, resulting in

binding of a second gold center through the exocyclic carbon atom to give **39**
(Scheme 1.11).[63]
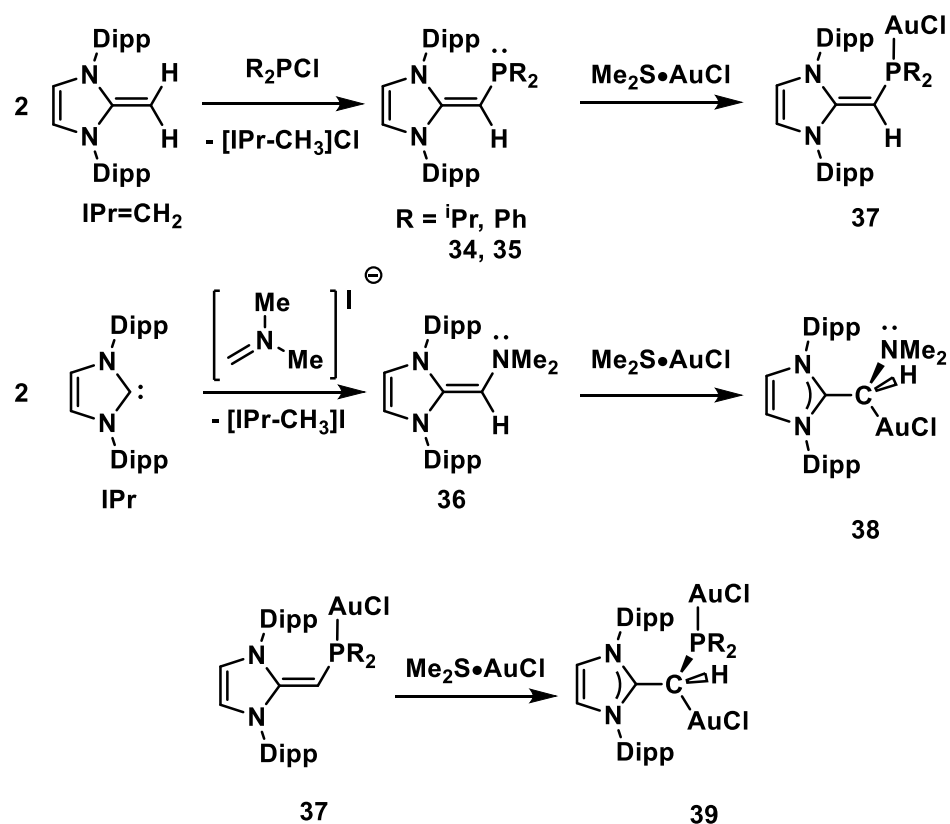
Scheme 1.11. Synthesis of IPr=CH–ER$_2$ (E = N, P) compounds and their reactivity with Me$_2$S•AuCl.

In 2017, the Rivard Group provided another strategy to obtain anionic NHOs, where instead of deprotonating a pre-coordinated NHO, an anionic NHO transfer agent (^{Me}IPr=CH)SiMe$_3$ was used (**40**, Scheme 1.12) (^{Me}IPr = (MeCNDipp)$_2$C:).[64] For example (^{Me}IPr=CH)SiMe$_3$ (**40**) was combined with GeCl$_4$ to give (^{Me}IPr=CH)GeCl$_3$ (**41**, Scheme 1.12), which upon reduction with KC$_8$ yielded the deep-red acyclic

divinylgermylene (^{Me}IPrCH)$_2$Ge (**42**, Scheme 1.12),[64] illustrating the ability of anionic

NHOs to stabilize low-valent main group centers. In 2019, Severin and coworkers

showed that the reaction between NHOs and N$_2$O gas can result in the formation of

diazenes (**43**, Scheme 1.12).[65]
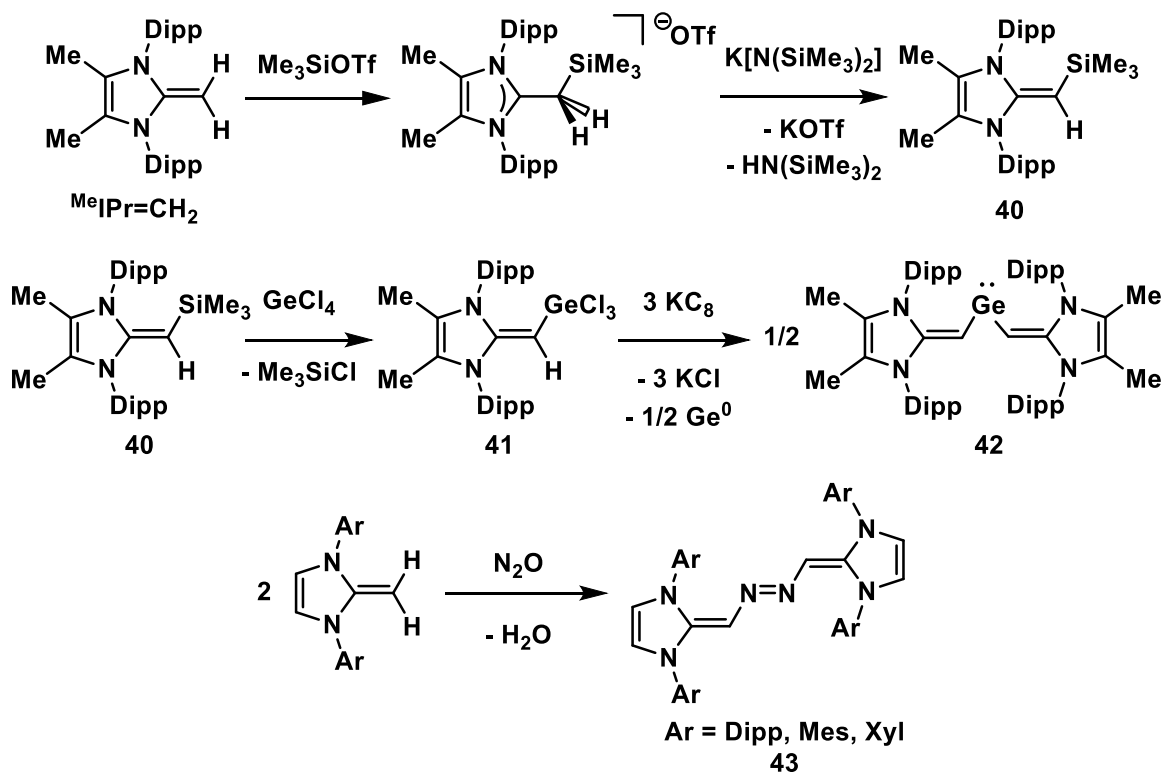
Scheme 1.12. Examples of anionic NHOs from the Rivard and Severin Groups (Xyl = 2,6-Me$_2$C$_6$H$_3$).

While (^{Me}IPr=CH)SiMe$_3$ (**40**) proved effective in the synthesis of the

germylene **42**, this reagent was not able to facilitate the formation of the

corresponding silylene, stannylene, or plumbylene, due to a lack of reactivity with the

respective main group halides. As such, a one-pot synthesis of the lithiated NHO

dimer [(^{Me}IPrCH)Li]$_2$ (**45**) was developed to drive reactions with element halides

through salt metathesis. This lithiated reagent can be accessed in a three-step synthesis starting from ^{Me}IPrCH$_2$ (^{Me}IPrCH$_2$ = (MeCNDipp)$_2$C=CH$_2$) (Scheme 1.13). The first step involves combining ^{Me}IPrCH$_2$ with iodine followed by deprotonation of the intermediate imidazolium salt [^{Me}IPr–CH$_2$–I]I with K[N(SiMe$_3$)$_2$] to yield the iodinated NHO ^{Me}IPr=CH(I) (**44**, Scheme 1.13). ^{Me}IPr=CH(I) (**44**) is then combined with one equivalent of ^{n}BuLi to yield the target lithiated NHO [(^{Me}IPrCH)Li]$_2$ (**45**), which crystallizes as a centrosymmetric dimer.[66] Note that protection of the NHO backbone with methyl groups is necessary, as it has been shown by Harder and coworkers that the backbone-positioned C–H groups in some unsaturated NHOs are prone to lithiation by ^{n}BuLi.[67]
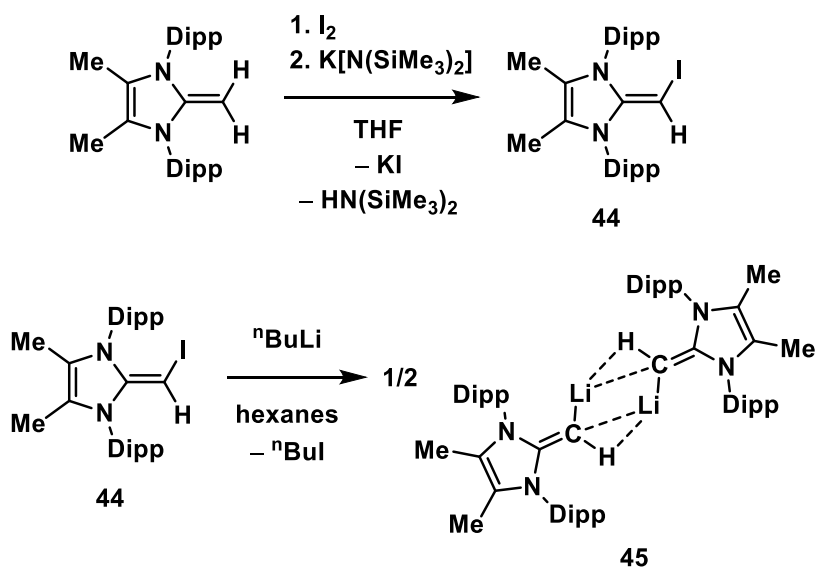
Scheme 1.13. Synthesis of the [^{Me}IPrCH]$^-$ transfer agent [(^{Me}IPrCH)Li]$_2$ (**45**).

1.2.5. *N*-Heterocyclic Olefins as Organocatalysts

NHO-like structures have a long history in the field of organocatalysis.[68,69] When proposing a mechanism for thiamine-catalyzed benzoin condensations, Prof. Ronald Breslow proposed an intermediate where the reactivity of a substrate (*e.g.,* aldehyde) changes from being predominantly electrophilic to nucleophilic after coordination to a carbene (Scheme 1.14).[70,71] A subsequent proton transfer event yields a species that is commonly known as a Breslow intermediate, which bears close resemblance to *N*-heterocyclic olefins.[27a,69] This resemblance is so close that NHOs are sometimes referred to as deoxy-Breslow intermediates. It is worth noting that a classic Breslow intermediate was first isolated in the solid state by Berkessel and coworkers in 2018.[70]
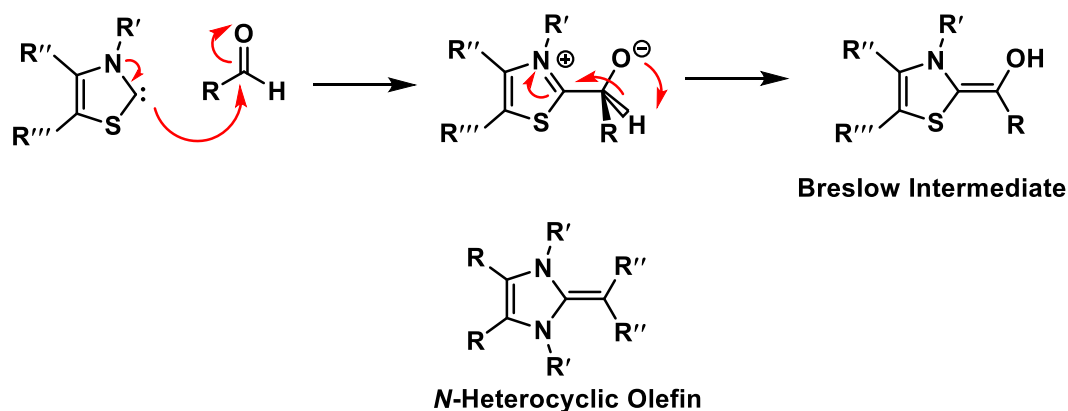
Scheme 1.14. Formation of a carbene-aldehyde adduct and its rearrangement into a Breslow intermediate, as proposed by Breslow (top); general structure of an NHO (bottom).

Isolable NHOs would not be used directly in organocatalysis until about a decade ago. Seminal work by Lu and coworkers in 2013 showed a key difference

between NHOs and NHCs in their reactivity with CO_2.[71] While both molecules readily form CO_2 adducts, the carbene-based NHC-CO_2 adducts are more stable than their NHO-CO_2 counterparts (Scheme 1.15, Reaction A). This difference in stability was important as NHC-CO_2 adducts are too stable to take part in most catalytic cycles, while NHO-CO_2 adducts are labile enough to allow a catalytic annulation reaction between CO_2 and propargyl alcohols to occur.[71] Another NHO-catalyzed reaction involving CO_2 is the insertion of CO_2 into aziridines, as reported by Bhanage and coworkers (Scheme 1.15, Reaction B).[72]

Nyugen and Enders have shown that *in situ* generated NHOs can catalyze the dehydrogenative silylation of alcohols in the presence of silanes at 50 °C (Scheme 1.15, Reaction C).[73] *In situ* NMR studies of this NHO-catalyzed silylation reaction show that the NHO deprotonates the alcohol, facilitating subsequent Si-O bond formation with turnover frequencies (TOFs) as high as 0.33 h^{-1}. The same group showed that NHOs can catalyze transesterifications, with the conversion of dimethyl terephthalate into bis(2-hydroxylethyl) terephthalate occurring at room temperature with TOFs up to 12 h^{-1}.[74] Branco and coworkers used NHOs to catalyze the room temperature ring-opening and subsequent reaction of bicyclic amidines (*e.g.,* DBU = 1,8-diazabicyclo[5.4.0]undec-7-ene) with aldehydes to yield ε-caprolactam- and γ-lactam-derived imines with TOFs of up to 1.6 h^{-1} (Scheme 1.15, Reaction D).[75]
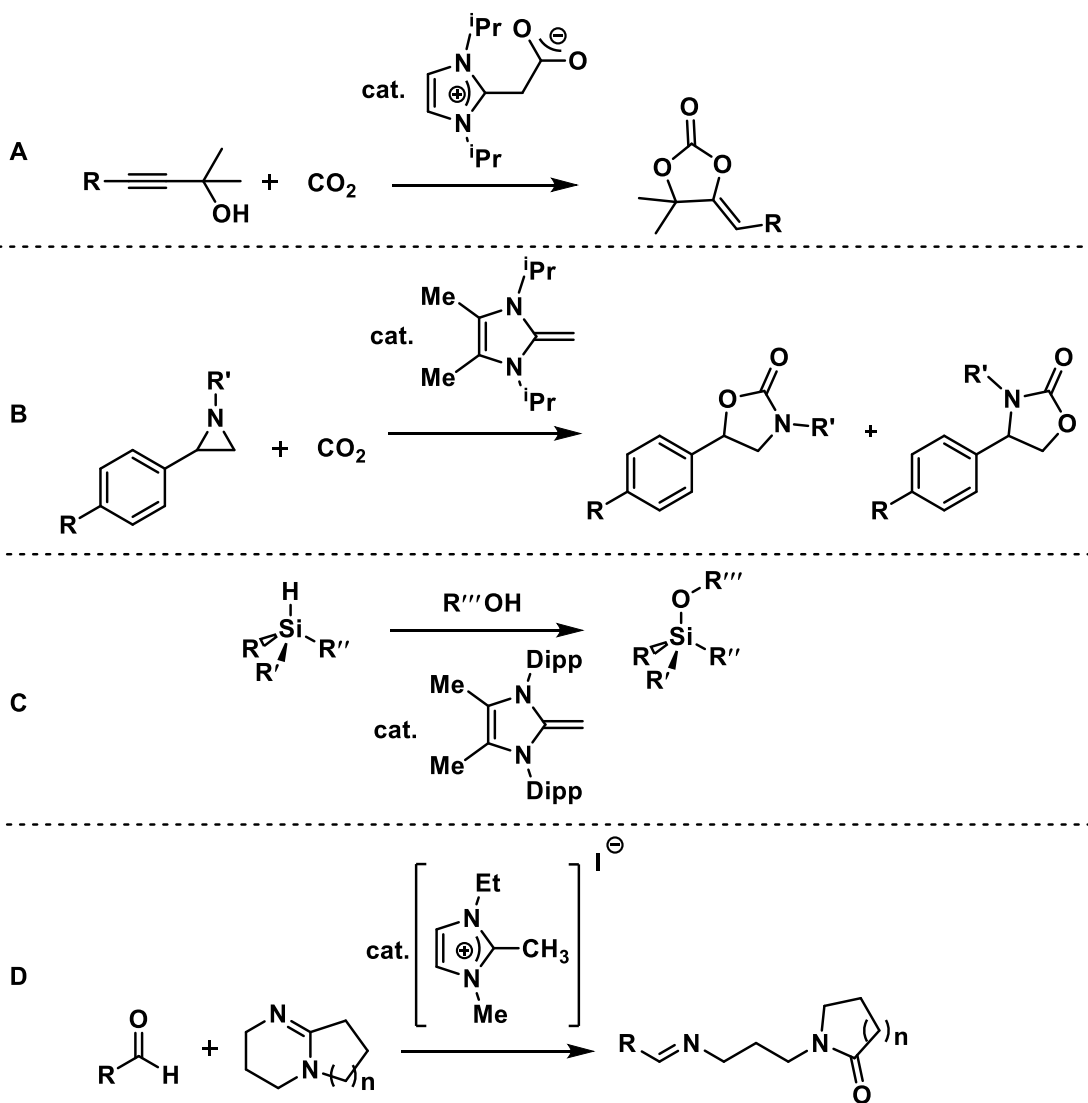
Scheme 1.15. Examples of organocatalysis promoted by NHOs.

1.2.6. *N*-Heterocyclic Olefins as Polymerization Catalysts

In 2010, Chen and coworkers showed that frustrated Lewis pairs (FLPs) can be used to polymerize polar monomers, such as acrylates and lactones, in a process called Lewis pair polymerization (LPP).[76] These polar monomers can be activated by the Lewis acid coordinating to the carbonyl of the acrylate or lactone, followed by a

nucleophilic attack on the monomer (*e.g.,* methyl methacrylate, MMA) by the Lewis base (Scheme 1.16). This method of polymerization works with both FLPs and classical Lewis acid-base adducts, so long as the Lewis acid-base pair can dissociate in solution (*e.g.,* 2,6-lutidine and $B(C_6F_5)_3$).[76] The zwitterionic species derived from FLP activation of a monomer then reacts with another monomer that is coordinated by a Lewis acid, thus growing the polymer chain. Examples of suitable Lewis acids for LPP include: $B(C_6F_5)_3$, $Al(C_6F_5)_3$, $Mg[N(SiMe_3)_2]_2$, and $ZnCl_2$. Examples of NHOs used as effective Lewis bases in LPP include: $ImMe_4=CH_2$, $ImMe_2Ph_2CMe_2$ $(ImMe_2Ph_2)C=CMe_2 = (PhCNMe)_2C=CMe_2)$, $IPrCH_2$, and $IMesCH_2$ (Chart 1.12).[77]
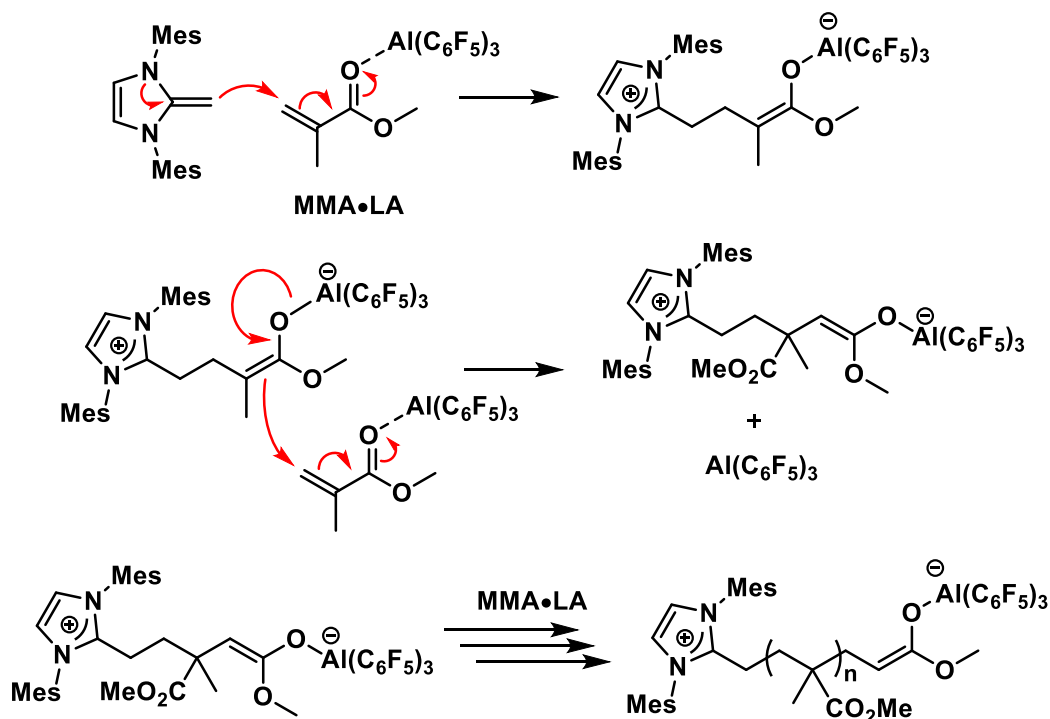
Scheme 1.16. Methyl methacrylate (MMA) polymerization promoted by an NHO and $Al(C_6F_5)_3$.
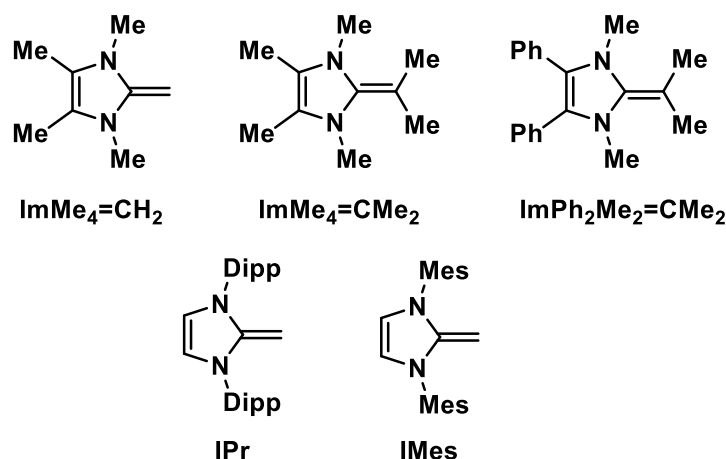
Chart 1.12. Examples of NHOs used in Lewis pair polymerizations.

The Lu Group also showed that NHOs act as efficient Lewis bases in the Lewis pair polymerization (LPP) of acrylates. By employing Lewis basic NHOs, such as IMesCH$_2$, in conjunction with Al(C$_6$F$_5$)$_3$ as a Lewis acid, acrylates and acrylamides were polymerized.[78] In 2018, the groups of Chen and Zhang reported the living polymerization of methyl methacrylate promoted by ImPh$_2$Me$_2$=CMe$_2$ and MeAl(BHT)$_2$ (BHT = 4-Me-2,6-^{t}Bu$_2$-C$_6$H$_2$O).[79] The same year, the Chen Group also reported the NHO-based LPP of methyl crotonate, a monomer that is known to be particularly challenging to polymerize.[80] A key discovery that made this polymerization possible was that functionalizing the exocyclic carbon of the NHO with methyl groups prevented premature chain termination.

Naumann and coworkers utilized an NHO-based FLP to form high molecular weight poly(propylene oxide).[81] The authors found that a catalyst mixture of Mg[(N(SiMe$_3$)$_2$] and ImMe$_4$CH$_2$ was able to polymerize propylene oxide to give high

number-average molecular weight polymers (M_n = 61 000 g/mol, PDI = 1.47; PDI = polydispersity index). This polymerization reaction occurred quickly at room temperature with quantitative consumption of the monomer after 5 minutes when the catalyst loading was 0.1 mol%.

It is possible to use NHOs as polymerization catalysts without a Lewis acid co-activator present. For example, Dove and coworkers used $ImMe_4=CMe_2$ (Chart 1.12) as an organocatalyst for the solvent- and metal-free polymerization of poly(propylene oxide), using benzyl alcohol as an initiator.[82] This work highlights the advantages of NHOs over NHCs in organocatalysis: NHCs have been proposed to have two mechanisms of polymerization, a Brønsted basic and nucleophilic pathway (Scheme 1.17), leading to a bimodal polymer distribution and thus a high polydispersity. However, using an NHO catalyst increases the basicity (*vide supra*) and decreases the nucleophilicity, thereby supressing the nucleophilic pathway and achieving a narrow PDI.
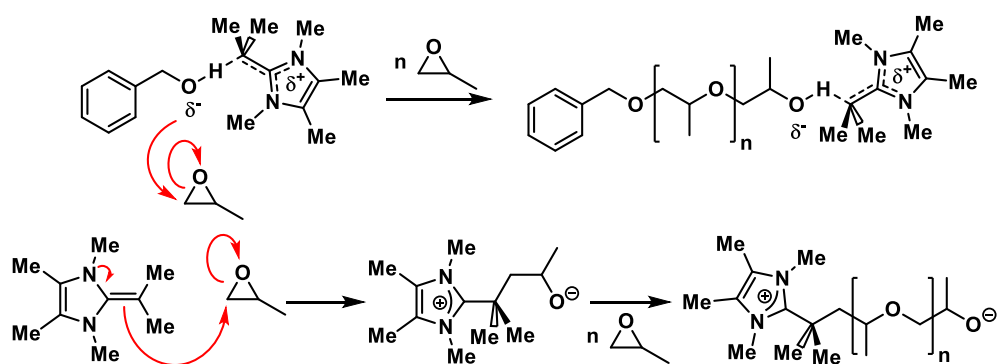
Scheme 1.17. Brønsted basic (top) and nucleophilic (bottom) polymerization pathways available for the polymerization of propylene oxide.

NHO-catalyzed polymerizations can be highly controlled, allowing for the formation of block copolymers, as demonstrated by Naumann and coworkers' use of catalytic $ImMe_4=CMe_2$ (Chart 1.15) to make a poly(propylene oxide)-poly(ethylene oxide)-poly(propylene oxide) (PPO-PEO-PPO) triblock copolymer.[83] These triblock copolymers undergo solvent evaporation-induced self-assembly in the presence of cross-linking agents (phenolic resins and formaldehyde), allowing for the tailoring of mesoporous carbon pore size once the self-assembled polymer is carbonized by heating to 700 °C.[83]

L-lactide   δ-valerolactone   dimethylacrylamide

$ImMe_4=CH_2$ $ImMe_4=CMe_2$ $SImMe_2=CMe_2$
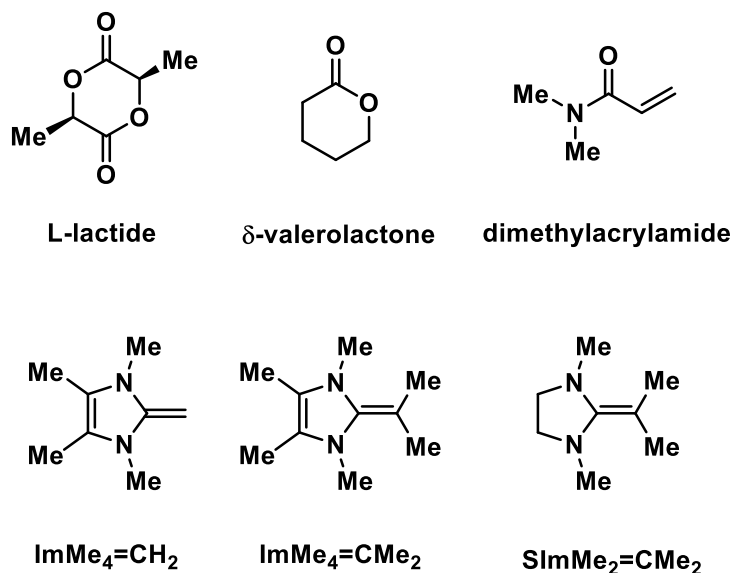
Chart 1.13. Examples of polar monomers that can be polymerized directly by NHOs (top), and representative NHOs that have been used as organocatalysts (bottom).

In a study focusing on the polymerization of lactones, Dove and coworkers utilized the structural tunability of NHOs to prepare well-defined polylactones with

narrow polydispersities.[84] They first explored $ImMe_4CH_2$ (Chart 1.13) as an organocatalyst, but found that lactone polymerization was deactivated by the NHO binding too strongly to the monomer. To circumvent this issue, they increased the steric bulk around the exocyclic carbon of the NHO by installing methyl groups, to yield $ImMe_4=CMe_2$. While $ImMe_4=CMe_2$ was an effective organocatalyst, the NHO was so active that it led to reduced control over the polymer molecular weight (PDI = 1.78). As such, they utilized the less basic $SImMe_2=CMe_2$, which allowed the authors to access polymers with a PDI as low as 1.19.

While *N*-heterocyclic olefins have been shown to be effective catalysts for the polymerization of lactones and propylene oxide, they are less effective when polymerizing acrylic monomers. The Naumann Group have shown that $ImMe_4=CH_2$ can polymerize dimethylacrylamide (DMAA); however the rate of polymerization is slow when the polymerization was performed with a 5 mol% catalyst loading, at –36 °C in toluene, with the authors observing only 37 % monomer conversion after 3 days (M_n = 18 000 g/mol).[85] The addition of a five-fold excess of LiCl had a dramatic effect on the rate of polymerization, leading to high molecular weight polymers (M_n = 118 000 g/mol after only 2 minutes). The authors believe that the presence of Li^+ in solution has a stabilizing effect on the enolate anion resulting from nucleophilic attack of the NHO on the substrate.

1.3. Transmetallation

Transmetallation is a fundamental reaction in organometallic chemistry, with Edward Frankland's historic study of alkylzinc reagents signifying the birth of the field.[86] Frankland prepared diethylzinc and dimethylzinc by combining zinc metal with ethyl iodide or methyl iodide, respectively (Scheme 1.18).[86,87] With these ZnR_2 compounds in hand, Frankland then showed that the alkyl ligands could be exchanged for halides of a different metal salt, providing the first clear example of transmetallation: an organometallic reaction where organic or main group (R_3Sn, R_3Si, etc.) ligands are transferred from one element center to another. This includes organic groups being exchanged for halides via metathesis (*vide supra*) as well as the transfer of ligands from an organometallic species to a neutral, elemental metal, as first shown by the transfer of the alkyl groups from dimethylmercury to zinc metal, resulting in the formation of dimethylzinc (Scheme 1.18).[88]

$$3 \ \ R-I \ \ \xrightarrow{\text{3 Zn}_{(s)}} \ \ ZnR_2 \ + \ R\text{-}Zn-I \ + \ ZnI_2$$

R = Me, Et

$$HgR_2 \ \ \xrightarrow{\text{Zn}_{(s)}} \ \ ZnR_2 \ + \ Hg_{(l)}$$

R = Me, Et
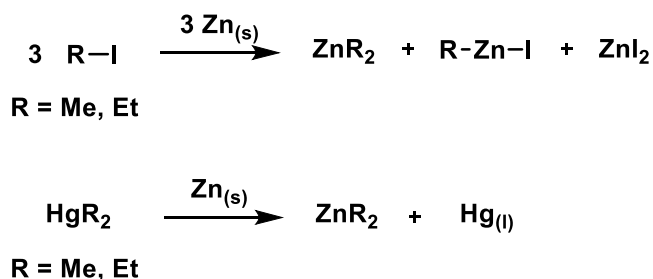
Scheme 1.18. Early routes to organometallic ZnR_2 reagents.

The thermodynamic driving force behind transmetallation is the stability of the metal-ligand bond that is formed compared to the metal-ligand bond that is broken.[89]

One can view these reactions through the lens of the Hard-Soft Acid-Base (HSAB) principle, which categorizes Lewis acids and bases as "hard" (smaller, less polarizable) or "soft" (larger, more polarizable).[89,90] The HSAB principle states that hard Lewis acids prefer to bind with hard Lewis bases and *vice versa*. For example, combining $ZnEt_2$ (a hard metal with a soft ligand) with $SnCl_2$ (a soft metal with a hard ligand) will result in in the transfer of the soft ethyl ligands to the soft tin center and the formation of $ZnCl_2$, a hard-hard Lewis acid-base pair.

The functionalization of transition metal and main group centers via transmetallation has not been relegated to the time of Frankland (the 1860s), as this strategy continues to be used in contemporary research. For example, Warren Piers and his team have used $Zn(C_6F_5)_2$ as a reagent to functionalize boron centers. This was exemplified in early reports where $Zn(C_6F_5)_2$ was shown to transfer C_6F_5– units to a boron center, releasing $ZnCl_2$ as a by-product.[91] Unfortunately, when BCl_3 is used as a reactant, transmetallation with $Zn(C_6F_5)_2$ is poorly controlled, leading to a mixture of $Cl_2B(C_6F_5)$, $ClB(C_6F_5)_2$, and $B(C_6F_5)_3$ (Scheme 1.19). Later, the groups of Piers and Marder used the same diorganozinc reagent to produce the highly Lewis acidic *ortho*-phenylene-bridged perfluorodiborane $1,2-C_6H_4(B(C_6F_5)_2)_2$ (**46**) (Scheme 1.19).[92] Related zinc-element transmetallation reactions are possible between zincocene-type complexes (*e.g.,* $Cp*_2Zn$ and $Cp*ZnZnCp*$; $Cp* = \eta^5-C_5Me_5$) and transition metals, as demonstrated by Carmona and others.[93]
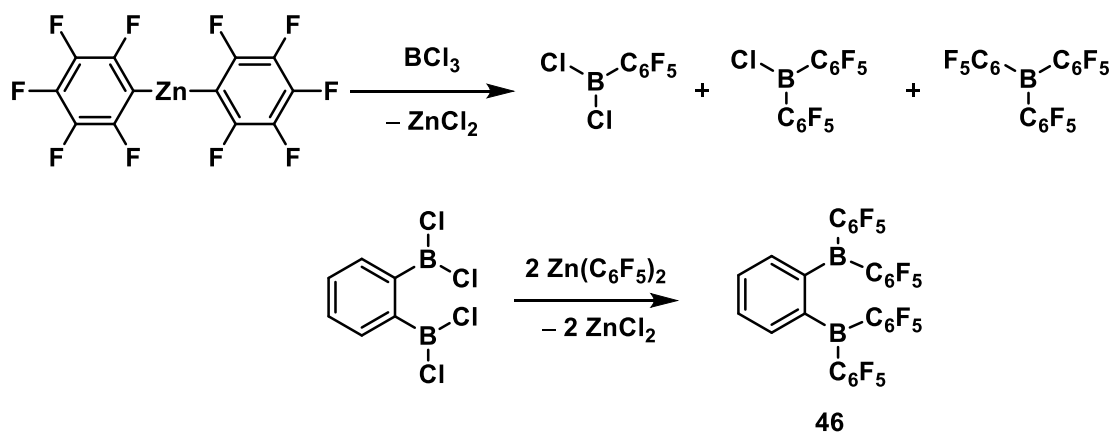
Scheme 1.19. Functionalization of boron centers with C_6F_5 groups via transmetallation.

Transmetallation reactions also provide a convenient route to access main group heterocycles via the Fagan-Nugent reaction (Scheme 1.20).[94] This reaction involves the transmetallation of Cp_2Zr-containing heterocycles ($Cp = \eta^5$-C_5H_5) with a wide variety of main group halides (Ga, Ge, Sn, Pb, P, As, Sb, Bi, S, Se, and Te), eliminating Cp_2ZrCl_2 in the process.[95]
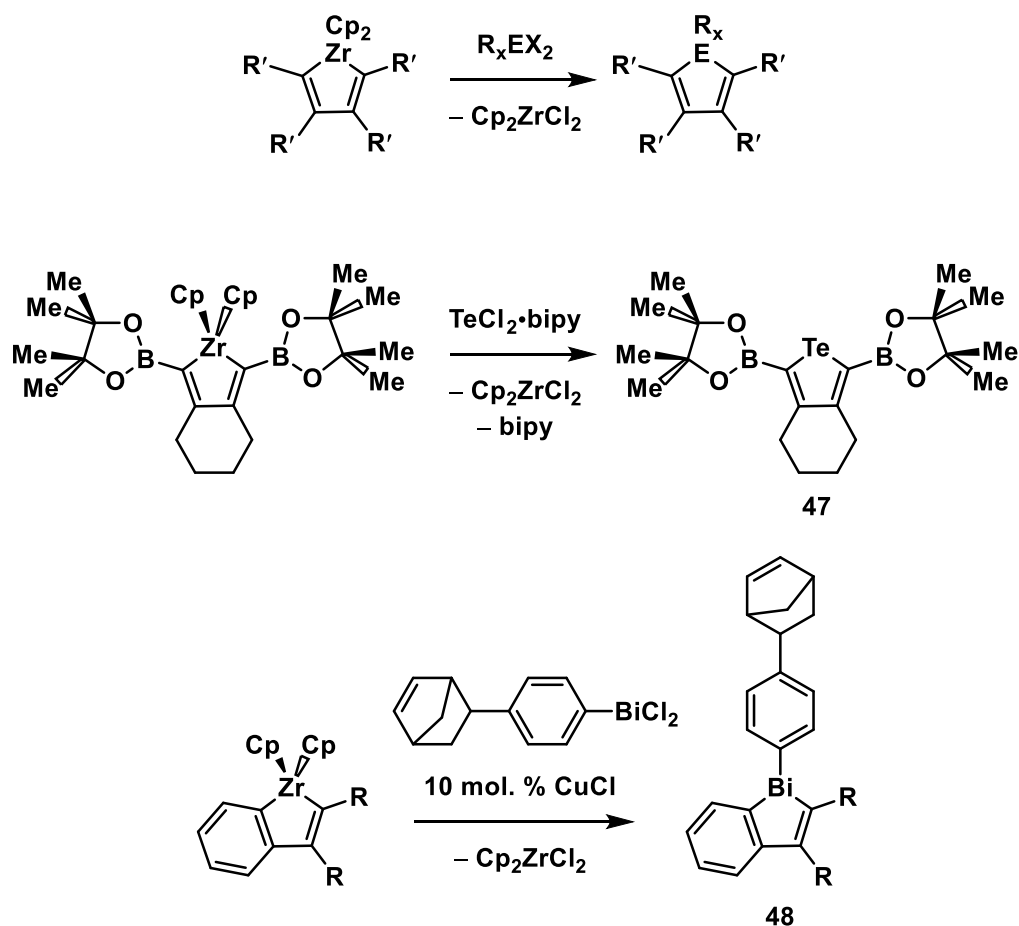
Scheme 1.20. General scheme for the Fagan-Nugent reaction and preparation of polymerizable monomers by the Rivard Group; bipy = 2,2′-bipyridine.

More recently, the Rivard Group has used the Fagan-Nugent reaction to make a variety of luminescent heterocycles including tellurophenes, bismoles, and germoles.[96] Notably, these heterocycles can be functionalized such that polymerization is possible either by Suzuki-Miyaura coupling involving pinacolborane (Bpin) functional groups in **47** or ring-opening metathesis polymerization (ROMP) **48**, (Scheme 1.20).[97]

The most utilized reactions containing a transmetallation step are palladium-catalyzed cross-couplings. These reactions have become ubiquitous in chemical synthesis, providing convenient routes for C–C bond formation under mild conditions. For many of these C–C bond forming reactions, an aryl halide (Ar–X) is combined with a palladium complex, a base, and a coupling partner. The nature of this coupling partner will vary depending on the type of cross-coupling used: Stille coupling uses organotin reagents, Suzuki-Miyaura coupling uses organoboranes, Negishi coupling uses zinc reagents, while Kumada coupling is based on organomagnesium reagents.[98] In the transmetallation step of these cross-coupling reactions, a L_xPd-X unit (X = Cl, Br, I; L = ligand) often undergoes transmetallation with the coupling partner (R′-SnR$_3$, R′-B(OR)$_2$, R′-ZnX, or R′-MgX) to install the organic R group onto the palladium center (Equation 1.4). A subsequent reductive elimination step from an L_xPd(Ar)R′ intermediate completes cross-coupling and forms the Ar-R product.

$$L_xPd\diagdown\substack{X \\ Ar} \xrightarrow[- E-X]{R'-E} L_xPd\diagdown\substack{R' \\ Ar} \quad (1.4)$$

$$E = SnR_3, ZnX, MgX$$
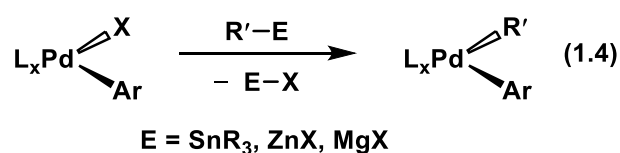
In Suzuki-Miyaura coupling, a base is generally required for the formation of an ArPd(L_x)OR intermediate that precedes the transmetallation step (Scheme 1.21).[99,100] In addition, there is an intermediate Pd–O–B linkage that is formed prior to transmetallation when OH$^-$ is the base, as observed by Denmark (Scheme 1.21).[101]
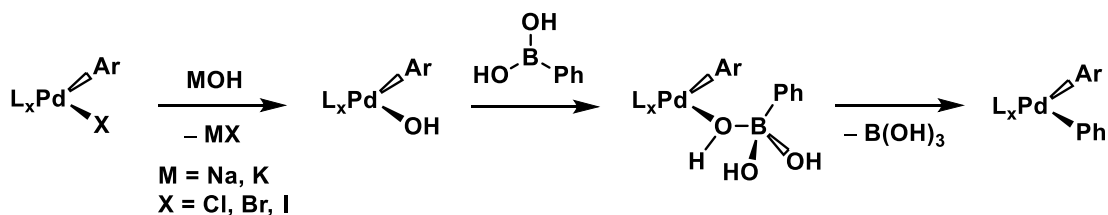
Scheme 1.21. The role of hydroxide base in Suzuki-Miyaura cross-coupling.

The transmetallation step in Negishi coupling is likewise more complicated than Equation 1.4 outlines. Kinetic studies performed by Lei and coworkers revealed that two transmetallation steps can occur, instead of the expected single transmetallation event (as summarized in Scheme 1.22).[102] The first transmetallation occurs as expected, wherein the organic portion of the organozinc reagent (Ar^2–Zn–I) is transferred to the palladium center via nucleophilic substitution involving a Pd–X bond. A second, possibly deleterious, transmetallation event sometimes occurs between a second equivalent of the organozinc reagent (Ar^2–Zn–I) and the intermediate ($L_xPd(Ar^1)Ar^2$), to yield a homocoupled Ar^2–Ar^2 product upon reductive elimination. Lei and coworkers determined that using a less sterically hindered Ar^1 group in conjunction with an Ar^2 group that is functionalized in the *ortho* position (to increase steric bulk about the metal center) significantly disfavors the homocoupling pathway.

47
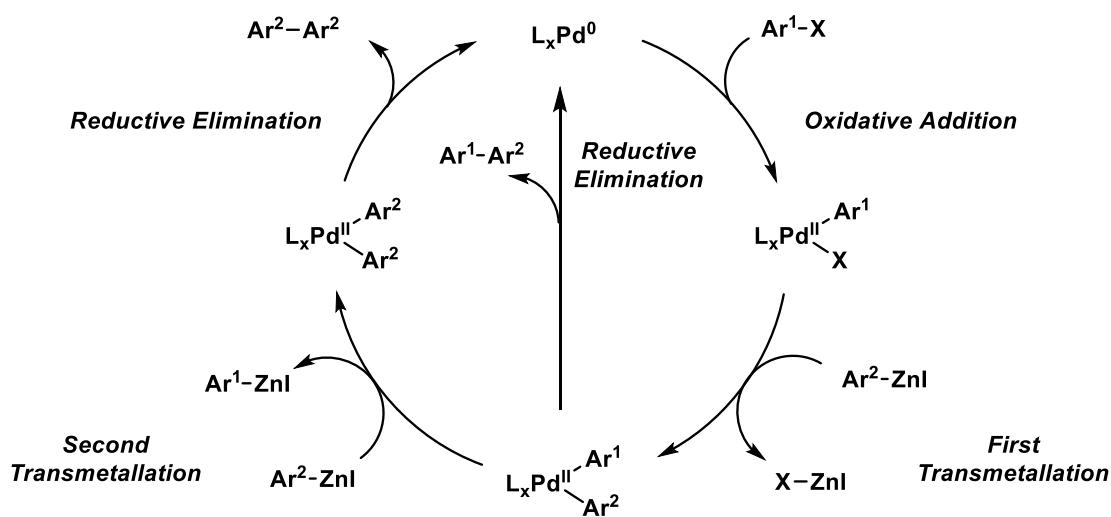
Scheme 1.22. A general depiction of the mechanism of Negishi coupling, including a second transmetallation step that leads to a homocoupled side product.

1.4. Buchwald-Hartwig Aminations

C–N Bond forming reactions are of great value for the preparation of new agrochemicals and pharmaceuticals, and in materials science (*e.g.,* in the syntheses of field-effect transistors and organic pigments for dye-sensitized solar cells).[103] Traditionally, C-N bonds were formed via metal-free nucleophilic aromatic substitution (S_NAr) or via copper-assisted Ullman-Goldberg coupling (Scheme 1.23).[104] While S_NAr reactions do not require transition metal catalysts, the scope of available substrates is limited as the presence of an electron-withdrawing group is required to activate the aryl ring for nucleophilic attack.[105] Alternatively, Ullman-Goldberg couplings require harsh conditions such as high temperatures, toxic solvents (*e.g., N*-methylpyrollidone, nitrobenzene, and dimethylformamide), and high copper

loadings (as high as 20 mol% in modern syntheses) for reactions to proceed.[106] These conditions lower functional group tolerance, making late-stage functionalization of complex molecules difficult, although modern ligand design has lessened these problems to some extent.[106]
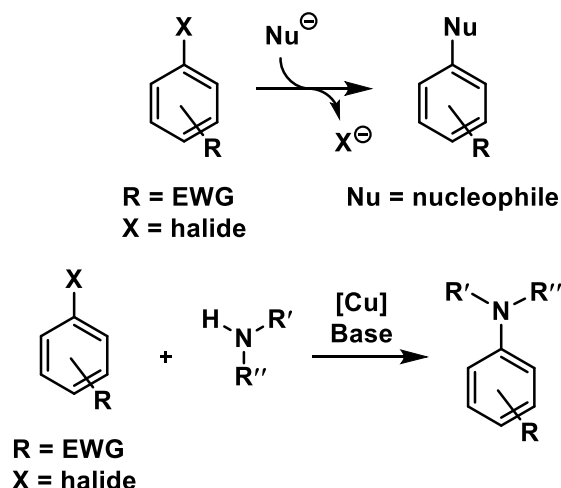
Scheme 1.23. Generic S_NAr and Ullman-Goldberg reactions; EWG = electron-withdrawing group. Examples of [Cu] include copper metal, CuI, and CuOAc.

The earliest example of a Pd-catalyzed C–N bond forming reaction was by Migita and coworkers in 1983, where the aminostannane $Et_2N–Sn^nBu_3$ was coupled to bromobenzene in the presence of 10 mol% $Cl_2Pd[P(o\text{-tolyl})_3]_2$ to form *N,N′*-diethylaniline (Scheme 1.24).[107] However, the use of this aminostannane was undesirable as it is toxic and expensive, hindering the widespread adoption of this technique. Boger and Panek reported the palladium-mediated intramolecular C–N coupling between an aryl halide and aniline, however, attempts to render this reaction catalytic failed due to the lack of a base in the reaction, since a base is required to

deprotonate the intermediate neutral palladium-amine complex and remove the halide

as a salt (Scheme 1.24).[108,109]
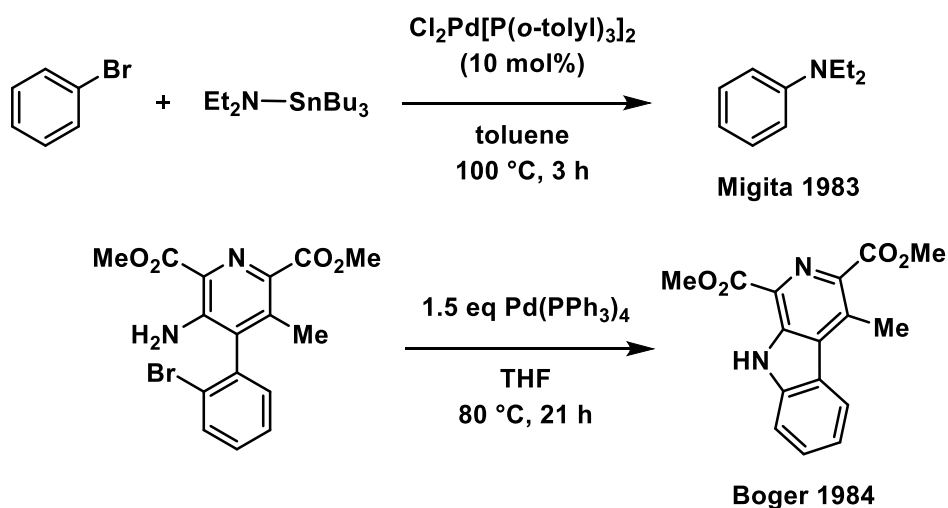
Scheme 1.24. Early examples of palladium-catalyzed C–N bond forming reactions.

The class of C–N bond forming reaction known now as Buchwald-Hartwig

coupling was reported independently by the groups of Buchwald and Hartwig in 1995,

wherein an amine is coupled to an arylbromide by a palladium catalyst in the presence

of a strong base (Scheme 1.24).[110,111] Since these initial reports, tremendous progress

has been made in expanding the utility of this reaction, largely due to advances in

ligand design. The first Buchwald-Hartwig aminations used P(*o*-tolyl)$_3$ as a ligand

(Chart 1.14).
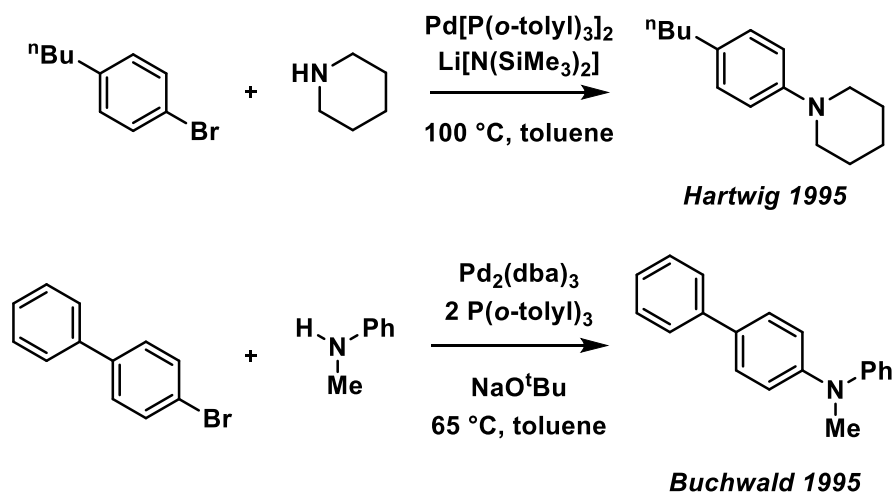
Scheme 1.25. Landmark reactions by the Buchwald and Hartwig Groups; dba = dibenzylideneacetone.
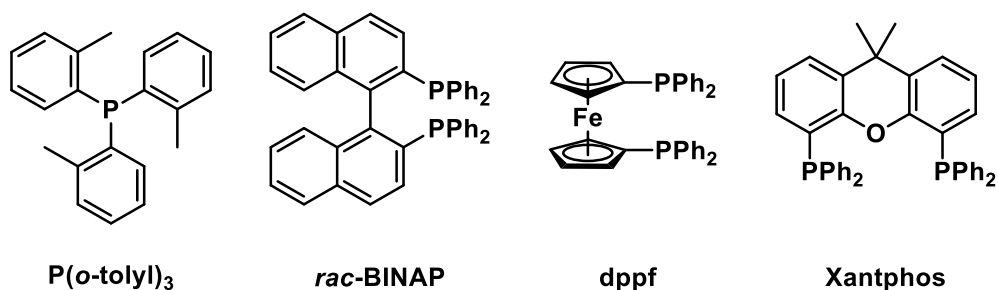
Chart 1.14. Phosphine ligands discussed in this section.

Through a series of experiments by Buchwald, Hartwig, and Blackmond in the 2000's, the mechanism for Buchwald-Hartwig aminations was elucidated (Scheme 1.25).[112] Catalysis begins with oxidative addition of an aryl halide or aryl pseudohalide (*e.g.,* Ar–OTf, Ar–OTs; OTf = O_3SCF_3, OTs = $O_3SC_6H_4Me$) onto a palladium(0) center (L_xPd^0), resulting in a palladium(II) intermediate [$L_xPd(Ar)X$]. Next, nucleophilic substitution transpires involving an amine followed by deprotonation of the bound amine by a base. The resulting palladium(II) complex

[$L_xPd(Ar)NR^1R^2$] then undergoes reductive elimination to form a C–N bond within an arylamine, and the catalytic cycle begins anew. The rate-determining step of this reaction is dependant on the nature of the ligand and substrates used. For example, when P(*o*-tolyl)$_3$ is used as a ligand, reductive elimination is the rate-determining step.[114] However, later studies using *rac*-BINAP as a ligand (Chart 1.14) revealed oxidative addition as the rate-determining step.[113c] Recently, methods of studying the kinetics based on electrospray ionization mass spectrometry (ESI-MS),[115] intramolecular ^{13}C kinetic isotope effects,[116] and *in silico* experiments[117] have been used to investigate further how the rate-determining step changes upon alteration of experimental conditions. A possible β-hydride elimination pathway can occur, yielding an imine and an Ar–H product instead of the desired cross-coupling (Scheme 1.24).[112] This side reaction is more likely to occur when monodentate aryl phosphines are used as ligands, thus bidentate ligands are now often used to supresses this deleterious pathway.
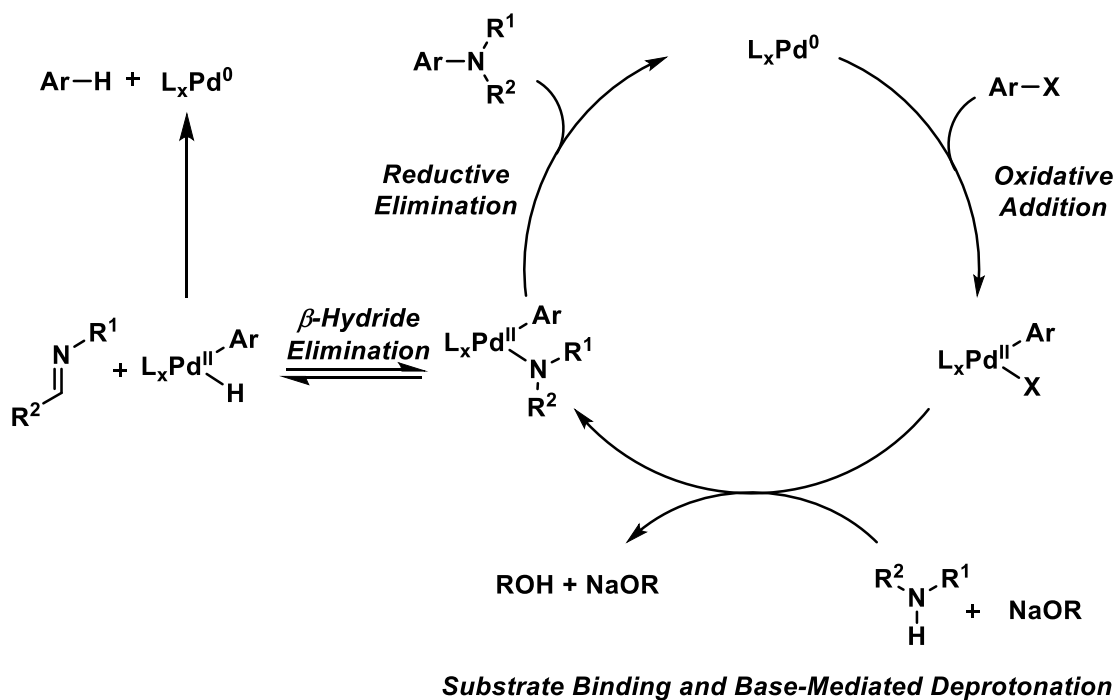
Scheme 1.26. General catalytic cycle for Buchwald-Hartwig aminations and a deleterious β-hydride elimination pathway.

The use of chelating bidentate phosphine ligands, such as BINAP (2,2′-bis(diphenylphosphino)-1,1′-binaphthyl) and dppf (1,1′-bis(diphenylphosphino)ferrocene), improved the efficiency of Buchwald-Hartwig coupling even further. It is worth noting that BINAP can be isolated in (R) and (S) enantiomers, allowing for its use in enantioselective catalysis.[103a] These chelating ligands supress β-hydride elimination, allowing for the coupling of primary amines[118] and other N–H containing functional groups, such as azoles, imines, lactams, and sulfoximines with aryl halides.[119] Additional studies have shown that use of a bidentate ligand with a wide bite angle further supresses β-hydride elimination,[120] as

well as facilitates the reductive elimination of Ar–NR$_2$ products from palladium during catalysis.[121] Hartwig and coworkers investigated the role of ancillary phosphine ligands in the reductive elimination of *N*-aryl amides from palladium.[122] In this study, arylpalladium amidate complexes featuring monodentate and bidentate phosphine ligands were prepared and the rates of reductive elimination of the *N,N*-diarylamide were measured (Scheme 1.26). Bidentate ligands such as Xantphos and dppf (as seen in complexes **49** and **50**, Scheme 1.26) were able to prevent the amidate moiety from binding in a κ^2-fashion, as opposed to the κ^2-binding of the amidate in the related monophosphine FcP^{t}Bu$_2$ palladium amidate complex **51** [Fc = (C$_5$H$_5$)Fe(C$_5$H$_4$)]. The authors found that the rate of reductive elimination was greater when a bidentate ligand was used in place of a monodentate ligand, implying that κ^2 coordination of the amidate hinders reductive elimination. Moreover, the authors found that use of Xantphos as a ligand promoted a greater rate of reductive elimination than dppf, which was attributed to the larger bite angle of Xantphos. It is worth noting that **49** and **50** have the phosphorus atoms of the ligands bound in a *trans* conformation, as revealed by single-crystal X-ray crystallography and ^{31}P NMR studies, respectively, and that the Pd center in **49** is perturbed from an ideal square planar geometry.[122]
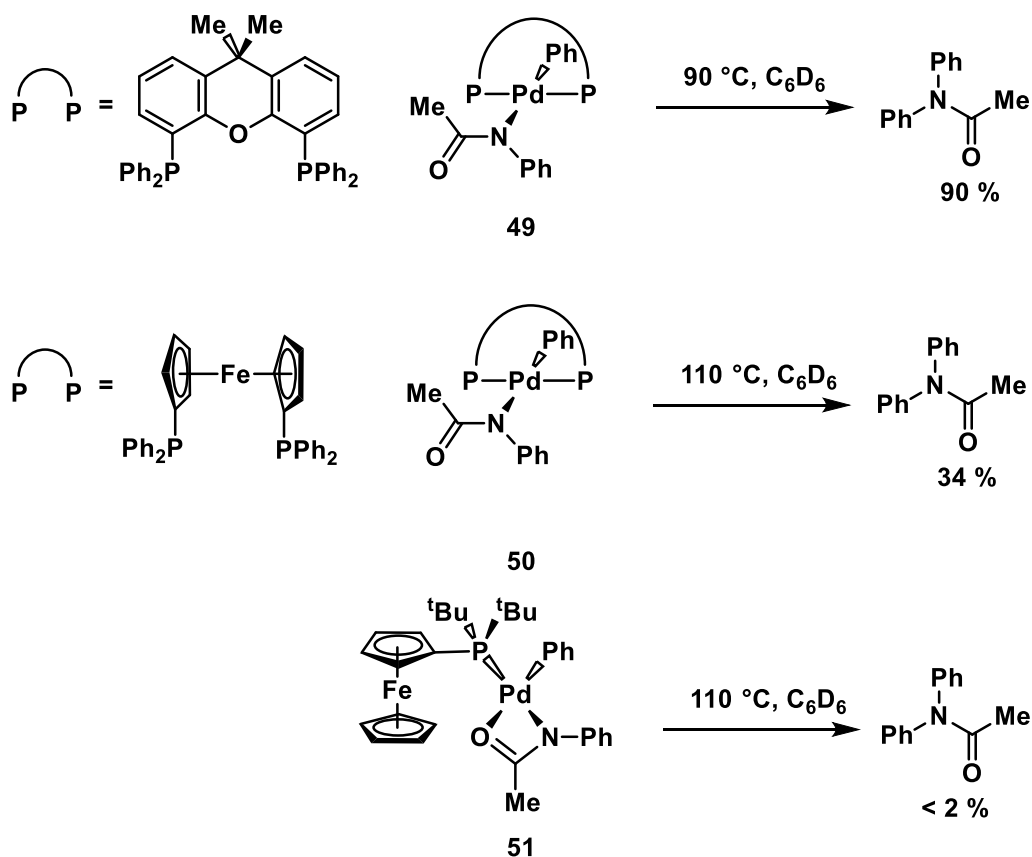
Scheme 1.27. Reductive elimination of *N,N*-diphenylacetamide from the arylpalladium amidate complexes **49**, **50**, and **51**.

Other notable ligands for Buchwald-Hartwig cross-coupling reactions are bulky dialkylbiarylphosphines and the Dalphos family of ligands. Dialkylbiarylphosphine ligands, such as BrettPhos and XPhos (Chart 1.15), are very effective ligands used extensively in the pharmaceutical industry for C–N bond forming reactions.[123] These ligands are resistant to oxidation at phosphorus as the steric bulk from the alkyl groups on the phosphorus atom encourage a geometry where the lone pair on the phosphorus atom points towards the pendant aryl group.[124] These

alkyl groups promote reductive elimination by introducing steric bulk around the palladium center and also promote oxidative addition of substrates to the L_xPd^0 catalyst by providing increased electron density on the Pd atom. Importantly, the pendant aryl group can interact with the active Pd^0 species in an η^6-fashion, providing added stabilization. The Dalphos family of ligands consist of *ortho*-phenylene P,N- or P,P- chelates and are comparatively inexpensive and can be tuned to act as electron-rich (*e.g.,* MorDalphos, Chart 1.15)[125] or electron-poor (*e.g.,* PdAd-Dalphos, Chart 1.15)[126] donors to suit a wide variety of C–N bond forming transformations. In particular, MorDalphos (Chart 1.15) has been shown to be selective for the monoarylation of ammonia and hydrazine using aryl chlorides and tosylates as coupling partners.[125]
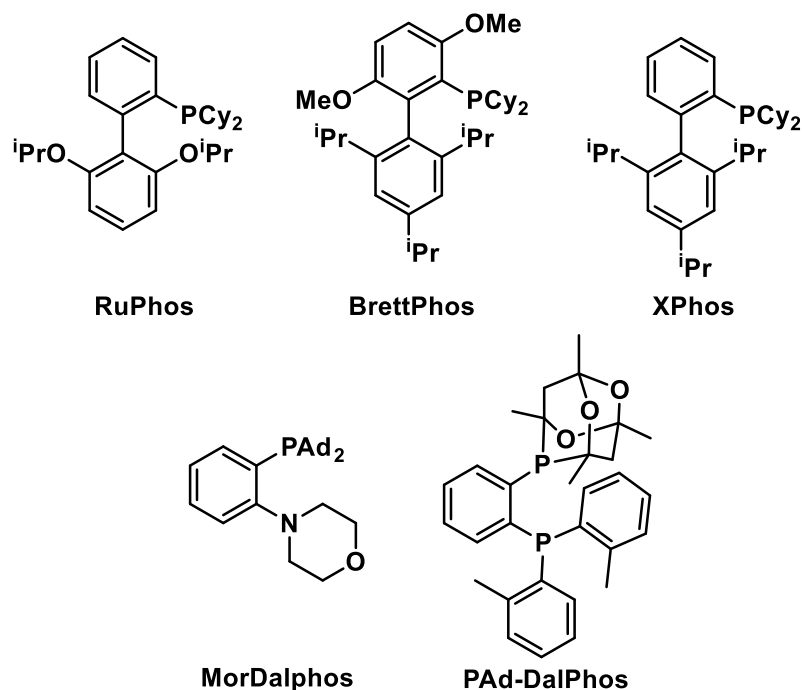
Chart 1.15. Structures of RuPhos, BrettPhos, XPhos, MorDalphos, and PAd-DalPhos; Cy = cyclohexyl; Ad = adamantyl.

Tremendous effort has been put into overcoming challenges in Buchwald-Hartwig aminations. Originally aryl bromides were preferred as reagents over other aryl halides, as aryl chlorides are less likely to undergo oxidative addition to Pd^0 catalysts, and an aryl iodide oxidative addition product could exist in equilibrium between the monomeric $L_xPd(Ar)I$ complex and the iodide bridged dimer $[L_xPd(Ar)(\mu–I)]_2$, leading to slower reaction rates.[112] Moreover, I^- in solution that is generated from deprotonation of the bound amine (Scheme 1.25) can inhibit cross-coupling. While the exact mechanism of inhibition is not known, Buchwald and coworkers postulate that I^- can bind to a palladium(II) intermediate to form a palladate, although choosing a solvent where the iodide salt is not soluble can circumvent this issue.[127] Advances in ligand design have made aryl chlorides and iodides available as substrates, as more electron-rich ligands at Pd facilitate the oxidative addition of aryl chlorides, while bidentate ligands prevent dimerization of the oxidative addition product derived from aryl iodides.[128] Secondary amines have proven to be difficult substrates to couple due to their steric bulk, but ligands with flexible bulk around the palladium center (*e.g.,* RuPhos) have helped overcome this difficulty, as the R_2N^- substrate can still efficiently access the metal center.[129] Nitrogen-rich substrates (and products) can act as ligands and deactivate the Pd catalyst.[130] While this continues to be a problem in catalytic Buchwald-Hartwig aminations, the Buchwald Group has reported a method of isolating the oxidative addition product $[L_xPd(Ar)X]$ and using it as a substrate to couple with amines,

allowing for coupling of complex drug precursors in situations where coupling is not possible under standard catalytic conditions.[131]

1.4.1. *N*-Heterocyclic Carbenes as Ligands in Buchwald-Hartwig Aminations

NHCs were first employed as ligands in Buchwald-Hartwig aminations by Steven Nolan, where an NHC-bearing palladium catalyst (IPr-Pd^0) was generated *in situ* by the deprotonation of the imidazolium salt [IPrH]Cl to form the carbene ligand IPr in the presence of the Pd^0 source Pd$_2$(dba)$_3$ (dba = dibenzylidineacetone).[132] This system was able to catalyze the amination of several aryl chlorides, which are known to be more challenging to couple than aryl bromides. Later work by Hartwig showed that using the saturated backbone NHC, SIPr (SIPr = (H$_2$CNDipp)$_2$C:), generated *in situ* (*vide supra*) led to a more effective catalyst system when combined with Pd$_2$(dba)$_3$.[133] While this approach is effective, much of the progress in this area has been due to the synthesis and use of NHC-bearing pre-catalysts that can be activated *in situ* to generate the active catalyst. This approach ensures strict control of ligand stoichiometry at the palladium center. The first NHC-containing pre-catalyst for Buchwald-Hartwig aminations was (IPr)Pd(allyl)Cl, which is easily generated by the introduction of two equivalents of an NHC to the chloro-bridged palladium dimer [(allyl)Pd(μ–Cl)]$_2$ (Chart 1.16).[134] (IPr)Pd(allyl)Cl has the advantage of being stable in air, making it easy-to-handle and allowing for the use of technical grade solvents during catalysis. It is worth noting that the Nolan Group later reported a cinnamyl-

functionalized derivative of the above pre-catalyst [(IPr)Pd(cinnamyl)Cl, Chart 1.16] providing a dramatic increase in catalytic activity compared to (IPr)Pd(allyl)Cl.[135] Another useful pre-catalyst from the Nolan Group, (IPr)Pd(acac)Cl, is synthesized by refluxing Pd(acac)$_2$ in the presence of the imidazolium salt [IPrH]Cl (Chart 1.16).[136] (IPr)Pd(acac)Cl is an active catalyst for the coupling of aryl bromides with aniline substrates, but struggles in coupling aryl chlorides. However, (IPr)Pd(cinnamyl)Cl is an effective catalyst for coupling both aryl chlorides and aryl bromides, and as such, is used more often.[135,136]

(IPr)Pd(allyl)Cl   **(IPr)Pd(cinnamyl)Cl**   **(IPr)Pd(acac)Cl**   **IPr-PEPPSI**
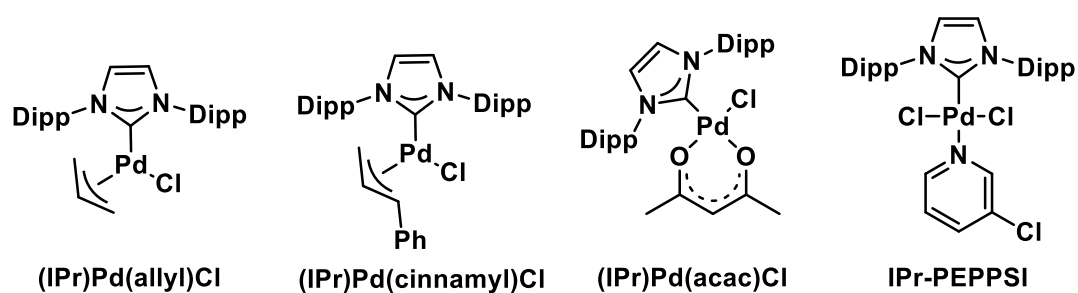
Chart 1.16. NHC-bearing palladium pre-catalysts.

These (NHC)Pd(R-allyl)Cl (R = H or Ph) pre-catalysts are generally activated by nucleophilic attack on the allyl group by a *tert*-butoxide base. This results in reduction of the palladium center, yielding an active Pd^0 catalyst and the elimination of KCl and the ether co-products (Scheme 1.28).[135]
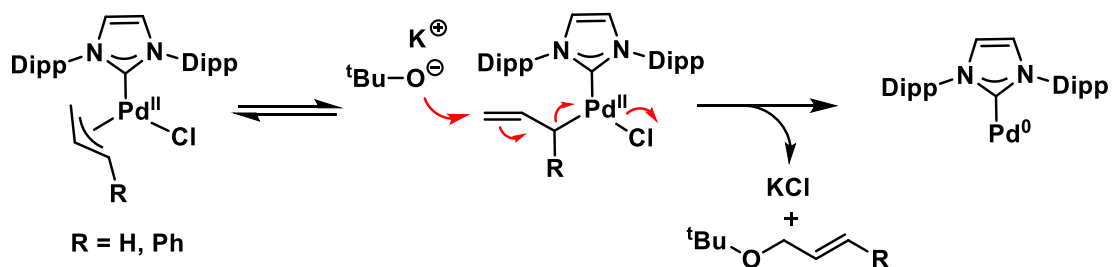
Scheme 1.28. Mechanism for the activation of (NHC)Pd(R-allyl)Cl pre-catalysts.

Efforts to make a more active palladium pre-catalyst were undertaken by the Organ Group, resulting in the PEPPSI class of complexes (PEPPSI = pyridine enhanced pre-catalyst preparation and stabilization) (Chart 1.16).[137] These complexes feature an *N*-heterocyclic carbene bound to a palladium(II) center and have been proven to be active pre-catalysts for Buchwald-Hartwig aminations, Suzuki-Miyaura couplings, Negishi couplings, Stille couplings, and C–S bond forming reactions.[138] The first PEPPSI catalyst developed by the Organ Group was IPr-PEPPSI (**52**), where the NHC IPr is bound to a square planar Pd center with 3-chloropyridine in the *trans* position with respect to the carbene donor (Chart 1.16). A major advantage of this pre-catalyst is that it can be synthesized in air, simply by heating a mixture [IPrH]Cl and K$_2$CO$_3$ in neat 3-chloropyridine (Scheme 1.27).[137a] While IPr-PEPPSI is traditionally made in a one-pot reaction, Nolan and coworkers have shown that a similar reaction goes through a palladate dimer (**53**) before the imidazolium salt is deprotonated (Scheme 1.29).[139] First generation PEPPSI pre-catalysts feature 3-chloropyridine as a "throwaway ligand", a ligand designed to dissociate from the palladium center with ease. While there has been significant effort made to understand how PEPPSI

catalysts are activated [*e.g.,* reduction from Pd(II) to Pd(0)],[140] the exact mechanism of this process is not known in Buchwald-Hartwig aminations.
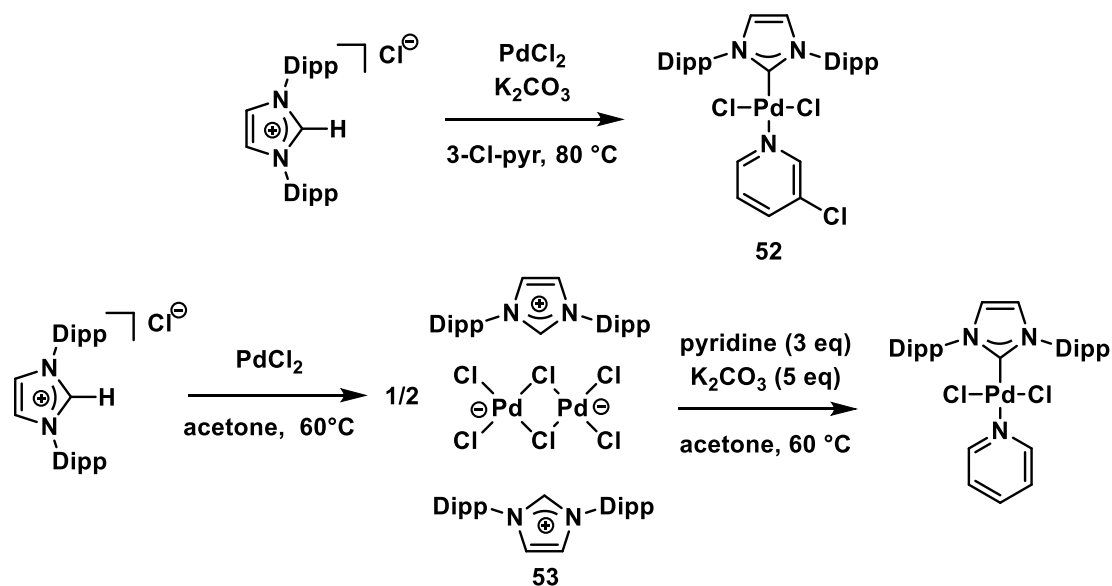
Scheme 1.29. One-pot synthesis of IPr-PEPPSI in 3-chloropyridine (top) and the stepwise synthesis of an IPr-PEPPSI analogue.

A notable feature of both Nolan's (NHC)Pd(allyl)Cl and Organ's NHC-PEPPSI complexes is that both the NHCs and "throwaway ligands" (allyl and pyridine-based ligands, respectively) can be tuned to increase catalyst performance. Nolan and coworkers observed sluggish activation of (IPr)Pd(allyl)Cl, postulating that this is due to the stability of the Pd-allyl interaction. By functionalizing the allyl substituent (*e.g.,* the cinnamyl analogue in Chart 1.16), the Pd-allyl interaction is weakened due to increased interligand repulsion, allowing pre-catalyst activation at room temperature to occur.[135] Modification could likewise be made to the pyridine unit of PEPPSI pre-catalysts to affect their performance, where increasing the steric

bulk of the "throwaway ligand" enables pre-catalyst activation at room temperature. For example, using *o*-picoline in the place of 3-chloropyridine (Chart 1.17), the PEPPSI pre-catalyst can be activated at room temperature due to a weakened Pd-N interaction (*vide supra*).[141]

Much like in Hartwig's work, Nolan found that using SIPr-based pre-catalysts for Buchwald-Hartwig aminations led to a marked increase in catalytic activity versus complexes bearing NHCs with unsaturated backbones.[142] Organ's PEPPSI system has undergone carbene-ligand modifications, with changes of the *N*-aryl groups of the NHC to increase the steric bulk around the palladium center (*e.g.,* 2,6,-isopentylphenyl[143] or 2,6-isoheptylphenyl,[144] Chart 1.17) or by using chlorinated carbene backbones (Chart 1.17) to affect the electronic properties of the NHC. These modifications showcase the structural tunability of NHCs and how these modifications can be leveraged to increase catalytic activity of NHC-ligated catalysts.
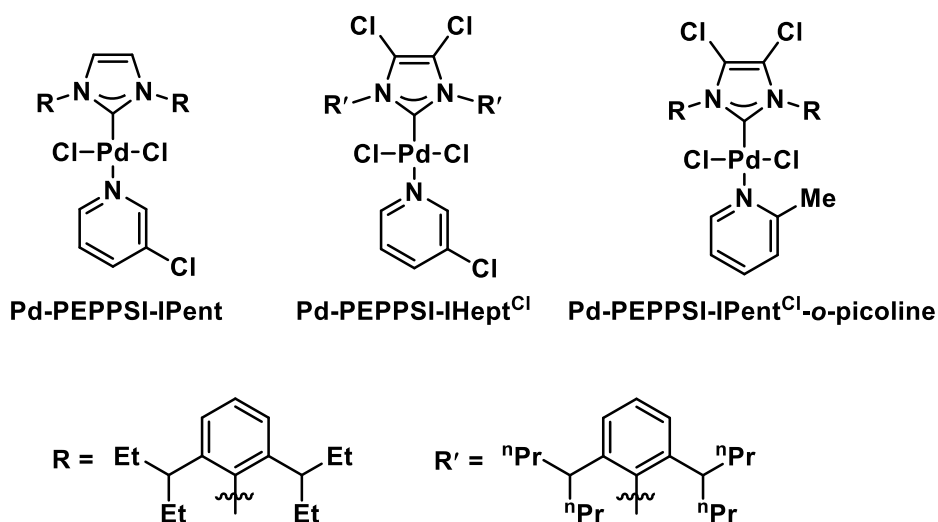
Chart 1.17. Examples of PEPPSI-class pre-catalysts with modifications to the *N*-aryl substituents and backbone of the NHC, and modification of the pyridine unit.

1.5 Thesis Objectives and Goals

A major part of this Thesis aims to expand the body of work surrounding *N*-heterocyclic olefins in catalysis, and discusses metal-free NHO-catalyzed hydroboration, palladium-catalyzed cross-coupling with NHOs as ligands, and the polymerization of Michael-type monomers by NHO-trialkylaluminum adducts. In addition, an anionic NHO-supported zinc compound will be discussed, and its ability to undergo transmetallation reactions to access new main group bonding environments. While NHOs have been used as organocatalysts in a variety of reactions,[68,71-75] these molecules have yet to be used as catalysts in hydroboration reactions. In Chapter 2, an aNHO functionalized with a $[B_2H_5]^+$ unit was synthesized and its efficacy as a hydroboration catalyst was evaluated. Serendipitously, it was found that free IPrCH$_2$ was found to be the active catalyst for these transformations and this NHO organocatalyst was used to promote the hydroboration of ketones and aldehydes. NHO-supported transition metal complexes have been known for decades,[29,44,45,51,52] but there are few examples of using *N*-heterocyclic olefins as supporting ligands in transition metal-mediated catalysis. In efforts to explore this area, new NHOs were prepared and were used as ligands in Buchwald-Hartwig aminations in Chapter 3. It was hoped that by functionalizing the exocyclic carbon of these NHO ligands, a stable molecular catalyst could be formed. It was confirmed with poisoning, imaging, and kinetic studies that the active catalyst was not a well-defined NHO-Pd^0 molecular species, but palladium nanoparticles. Work by Chen and others have shown that NHOs are potent Lewis bases in Lewis pair polymerization

reactions when introduced to polar monomers in the presence of a Lewis acid.[76-80] In efforts to introduce a single reagent to perform these polymerizations (instead of a separate Lewis acid and base), several NHO-trialkylaluminum adducts were prepared in Chapter 4. These adducts were used to polymerize Michael-type monomers, yielding polyacrylates and polyacrylamides. It was found that the NHO-aluminum adduct separated into its free Lewis base (NHO) and Lewis acid (AlR_3) when dissolved in THF, suggesting that the polymerization occurs through a frustrated Lewis pair mediated polymerization mechanism. According to a thorough literature search, there are no known examples of aNHO-supported transition metal complexes. Endeavoring to explore this class of compound, the aNHO transfer reagent ([Me]IPrCH)Li[66] was combined with transition metal halides to afford aNHO-metal complexes. In Chapter 5, an aNHO-zinc complex was prepared as an aNHO transfer agent via transmetallation. This complex was able to undergo transmetallation with various main group halides and hydrides to yield aNHO-main group complexes. In addition to an aNHO-supported zinc complex, Group 4 and Group 8 transition metal complexes were synthesized in Chapter 6.

1.6 References

1. Hopkinson, M. N.; Richter, C.; Schedler, M.; Glorious, F. *Nature* **2014**, *510*, 485-496.

2. Nelson, D. J.; Nolan, S. P. *N*-Heterocyclic Carbenes. In *N-Heterocyclic Carbenes: Effective Tools for Organometallic Synthesis*, 1st ed.; Wiley-VCH Verlag GmbH & Co. KGaA, 2014; pp 1-24.

3. Wanzlick, H. W. *Angew. Chem. Int. Ed. Engl.* **1962**, *1*, 75-80.

4. Hermann, W. A.; Köcher, C. *Angew. Chem. Int. Ed. Engl.* **1997**, *36*, 2162-2187.

5. Denk, M. K.; Hatano, K.; Ma, M. *Tetrahedron Lett.* **1999**, *40*, 2057-2060.

6. a) Wanzlick, H. W.; Schönherr, H. J. *Angew. Chem. Int. Ed. Engl.* **1968**, *7*, 141-142. b) Öfele, K. *J. Organometal. Chem.* **1968**, *12*, 42-43.

7. Sinclair, J.; Dai, G.; McDonald, R.; Ferguson, M. J.; Brown, A.; Rivard, E. *Inorg. Chem.* **2020**, *59*, 10996-11008.

8. Lappert, M. F.; Pye, P. L. *J. Chem. Soc., Dalton Trans.* **1978**, 837-844 and references therein.

9. Igau, A.; Grützmacher, H.; Baceiredo, A.; Bertrand, G. *J. Am. Chem. Soc.* **1988**, *110*, 6463-6466.

10. Arduengo III, A. J.; Harlow, R. L.; Kline, M. *J. Am. Chem. Soc.* **1991**, *113*, 363-365.

11. a) Crudden, C. M.; Allen, D. P. *Coord. Chem. Rev.* **2004**, *248*, 2247-2273. b) Nesterov, V.; Reiter, D.; Bag, P.; Frisch, P.; Holzner, R.; Porzelt, A.; Inoue, S. *Chem. Rev.* **2018**, *118*, 9678-9842.

12. a) Cazin, C. S. J. *N-Heterocyclic Carbenes in Transition Metal Catalysis and Organocatalysis*; Springer, Dordrecht, 2011. b) Peris, E. *Chem. Rev.* **2018**, *118*, 9988-10031.

13. Smith, C. A.; Narouz, M. R.; Lummis, P. A.; Singh, I.; Nazemi, A.; Li, C.-H.; Crudden, C. M. *Chem. Rev.* **2019**, *119*, 4986-5056.

14. Flanigan, D. M.; Romanov-Michailidis, F.; White, N. A.; Rovis, T. *Chem. Rev.* **2015**, *115*, 9307-9387.

15. Tulloch, A. A. D.; Danopoulos, A. A.; Kleinhenz, S.; Light, M. E.; Hursthouse, M. B.; Eastman, G. *Organometallics* **2001**, *20*, 2027-2031.

16. Hu, X.; Tang, Y.; Gantzel, P.; Meyer, K. *Organometallics* **2003**, *22*, 612-614.

17. Nemcsok, D.; Wichmann, K.; Frenking, G. *Organometallics* **2004**, *23*, 3640-3646.

18. a) Lavallo, V.; Canac, Y.; Präsang, C.; Donnadieu, B.; Bertrand, G. *Angew. Chem. Int. Ed.* **2005**, *44*, 5705-5709. b) Melaimi, M.; Jaszzar, R.; Soleilhavoup, M.; Bertrand, G. *Angew. Chem. Int. Ed.* **2017**, *56*, 10046-10068.

19. a) Frey, G. D.; Lavallo, V.; Donnadieu, B.; Schoeller, W. W.; Bertrand, G. *Science* **2007**, *316*, 439-441. b) Lavallo, V.; Canac, Y.; Donnadieu, B.; Schoeller, W. W.; Bertrand, G. *Angew. Chem. Int. Ed.* **2006**, *45*, 3488-3491.

20. Soleilhavoup, M.; Bertrand, G. *Acc. Chem. Res.* **2015**, *48*, 256-266.

21. Crabtree, R. H. *Coord. Chem. Rev.* **2013**, *257*, 755-766.

22. Araki, S.; Wanibe, Y.; Uno, F.; Morikawa, A.; Yamamoto, K.; Chiba, K.; Butsugan, Y. *Chem. Ber.* **1993**, *126*, 1149-1155.

23. Gründemann, S.; Kovacevic, A.; Albrecht, M.; Robert, J. W. F.; Crabtree, R. H. *Chem. Commun.* **2001**, 2274-2275.

24. a) Aldeco-Perez, E.; Rosenthal, A. J.; Parameswaran, P.; Frenking, G.; Bertrand, G. *Science* **2009**, *326*, 556-559. b) Guisado-Barrios, G.; Bouffard, J.; Donnadieu, B.; Bertrand, G. *Angew. Chem. Int. Ed.* **2010**, *49*, 4759-4762.

25. Gusev, D. G. *Organometallics* **2009**, *28*, 6458-6461.

26. Magill, A. M.; Yates, B. F. *Aust. J. Chem.* **2004**, *57*, 1205-1210.

27. a) Roy, M. M. D.; Rivard, E. *Acc. Chem. Res.* **2017**, *50*, 2017-2025. b) Doddi, A.; Peters, M.; Tamm, M. *Chem. Rev.* **2019**, *119*, 6994-7112.

28. a) Tolman, C. A. *Chem. Rev.* **1977**, *77*, 313-336. b) Chianese, A. R.; Li, X.; Janzen, M. C.; Faller, J. W.; Crabtree, R. H. *Organometallics* **2003**, *22*, 1663-1667. c) Kelly III, R. A.; Clavier, H.; Giudice, S.; Scott, N. M.; Stevens, E. D.; Bordner, J.; Samardijev, I.; Hoff, C. D.; Cavallo, L.; Nolan, S. P. *Organomettalics* **2008**, *27*, 202-210. d) Wolf, S.; Plenio, H. *J. Organomet. Chem.* **2009**, *694*, 1487-1492.

29. Powers, K.; Hering-Junghans, C.; McDonald, R.; Ferguson, M. J.; Rivard, E. *Polyhedron* **2016**, *108*, 8-14.

30. Fürstner, A.; Alcarazo, M.; Goddard, R.; Lehmann, C. W. *Angew. Chem. Int. Ed.* **2008**, *47*, 3210-3214.

31. Hillier, A. C.; Sommer, W. J.; Yong, B. S.; Petersen, J. L.; Cavallo, L.; Nolan, S. P. *Organometallics* **2003**, *22*, 4322-4326.

32. Clavier, H.; Nolan, S. P. *Chem. Commun.* **2010**, *46*, 841-861.

33. Poater, A.; Cosenza, B.; Correa, A.; Giudice, S.; Ragone, F.; Scarano, V.; Cavallo, L. *Eur. J. Inorg. Chem.* **2009**, 1759-1766.

34. Falivene, L.; Cao, Z.; Petta, A.; Serra, L.; Poater, A.; Oliva, R.; Scarano, V.; Cavallo, L. *Nat. Chem.* **2019**, *11*, 872-879.

35. El-Hellani, A.; Monot, J.; Guillot, R.; Bour, C.; Gandon, V. *Inorg. Chem.* **2013**, *52*, 506-514.

36. Powers, K. *N-Heterocyclic Olefins: An Investigation into a Developing Class of Ligands.* M.Sc. Dissertation, University of Alberta, Edmonton, AB, 2016.

37. Schuldt, R.; Kästner, J.; Naumann, S. *J. Org. Chem.* **2019**, *84*, 2209-2218.

38. Raczyńska, E. D.; Decouzon, M.; Gal, J.-F.; Maria, P.-C.; Woźniak, K.; Kurg R.; Carins, S. N. *Trends Org. Chem.* **1998**, *7*, 996-103.

39. Chen, H.; Justes, D. R.; Cooks, R. G. *Org. Lett.* **2005**, *7*, 3949-3952.

40. Wang, Z.; Niu, Q.-H.; Xue, X.-S.; Ji, P. *J. Org. Chem.* **2020**, *85*, 13204-13210.

41. Gruseck, U.; Heuschmann, M. *Chem. Ber.* **1987**, *120*, 2053-2064.

42. Li, Z.; Ji, P.; Cheng, J.-P. *J. Org. Chem.* **2021**, *86*, 2974-2985.

43. a) Mayr, H.; Patz, M. *Angew. Chem. Int. Ed. Engl.* **1994**, *33*, 938-957. b) Maji, B.; Breugst, M.; Mayr, H. *Angew. Chem. Int. Ed.* **2011**, *50*, 6915-6919. c) Levens, A.; An, F.; Breugst, M.; Mayr, H. *Org. Lett.* **2016**, *18*, 3566-3569.

44. Ponti, P. P.; Baldwin, J. C.; Kaska, W. C. *Inorg. Chem.* **1979**, *18*, 873-875.

45. a) Kuhn, N.; Bohnen, H.; Bläser, D.; Boese, R. *Chem. Ber*. **1994**, *127*, 1405-1407. b) Kuhn, N.; Bohnen, H.; Kreutzberg, J.; Bläser, D.; Boese, R. *J. Chem. Soc., Chem. Commun*. **1993**, 1136-1137.

46. Schumann, H.; Glanz, M.; Winterfeld, J.; Hemling, H.; Kuhn, N.; Bohnen, H.; Blaser, D.; Boese, R. *J. Organomet. Chem.* **1995**, *493*, C14-C18.

47. Dumrath, A.; Wu, X.-F.; Neumann, H.; Spannenberg, A.; Jackstell, R.; Beller, M. *Angew. Chem. Int. Ed.* **2010**, *49*, 8988-8992.

48. Al-Rafia, S. M. I.; Malcolm, A. C.; Liew, S. K.; Ferguson, M. J.; McDonald, R.; Rivard, E. *Chem. Commun.* **2011**, *47*, 6987-6989.

49. Al-Rafia, S. M. I.; Momeni, M. R.; Ferguson, M. J.; McDonald, R.; Brown, A.; Rivard, E. *Organometallics* **2013**, *32*, 6658-6665.

50. Ghadwal, R. S.; Schürmann, C. J.; Andrada, D. M.; Frenking, G. *Dalton Trans.* **2015**, *44*, 14359-14367.

51. Kronig, S.; Jones, P. G.; Tamm, M. *Eur. J. Inorg. Chem.* **2013**, 2301-2314.

52. Imbrich, D. A.; Frey, W.; Naumann, S.; Buchmeiser, M. R. *Chem. Commun.* **2016**, *52*, 6099-6102.

53. Rufh, S. A.; Goudreault, A. Y.; Foscato, M.; Jensen, V. R.; Fogg, D. E. *ACS Catal.* **2018**, *8*, 11822-11826.

54. Wang, Y. W.; Abraham, M. Y.; Gilliard Jr. R. J.; Sexton, D. R.; Wei, P.; Robinson, G. H. *Organometallics* **2013**, *32*, 6639-6642.

55. Enders, D.; Breuer, K.; Raabe, G.; Runsink, J.; Teles, H.; Melder, J.-P.; Ebel, K.; Brode, S. *Angew. Chem. Int. Ed. Engl.* **1995**, *34*, 1021-1023.

56. Matsuoka, S.; Tochiji, Y.; Takagi, K.; Suzuki, M. *Tetrahedron* **2012**, *68*, 9836-9841.

57. Hansmann, M. M.; Antoni, P. W.; Pesch, H. *Angew. Chem. Int. Ed.* **2020**, *59*, 5782-5787.

58. Clendenning, S. B.; Hitchcock, P. B.; Nixon, J. F.; Nyulászi, L. *Chem. Commun.* **2000**, 1305-1306.

59. Hahn, F. E.; Wittenbecher, L.; Van, D. L.; Frölich, R.; Wibbeling, B. *Angew. Chem. Int. Ed.* **2000**, *39*, 2307-2310.

60. Kuhn, N.; Göhner, M.; Steimann, M. *Z. Anorg. Allg. Chem.* **2002**, *628*, 1108-1115.

61. Al-Rafia, S. M. I.; Ferguson, M. J.; Rivard, E. *Inorg. Chem.* **2011**, *50*, 10543-10545.

62. Paisley, N. R.; Lui, M. W.; McDonald, R.; Ferguson, M. J.; Rivard, E. *Dalton Trans.* **2016**, *45*, 9860-9870.

63. Lui, M. W.; Shynkaruk, O.; Oakley, M. S.; Sinelnikov, R.; McDonald, R.; Ferguson, M. J.; Meldrum, A.; Klobukowski, M.; Rivard, E. *Dalton Trans*. **2017**, *46*, 5946-5954.

64. Hering-Junghans, C.; Andreiuk, P.; Ferguson, M. J.; McDonald, R.; Rivard, E. *Angew. Chem. Int. Ed*. **2017**, *56*, 6272-6275.

65. Eymann, L. Y. M.; Varava, P.; Shved, A. M.; Curchod, B. F. E.; Liu, Y.; Planes, O. M.; Sienkiewicz, A.; Scopelliti, R.; Tirani, F. F.; Severin, K. *J. Am. Chem. Soc.* **2019**, *141*, 17112-17116.

66. Roy, M. M. D.; Baird, S. R.; Dornsiepen, E; Paul, L. A.; Miao, L.; Ferguson, M. J.; Zhou, Y.; Siewert, I.; Rivard, E. *Chem. Eur. J.* **2021**, *27*, 8572-8579.

67. Gentner, T. X.; Ballmann, G.; Pahl, J.; Elsen, H.; Harder, S. *Organometallics* **2018**, *37*, 4473-4480.

68. a) Crocker, R. D.; Nguyen, T. V. *Chem. Eur. J.* **2016**, *22*, 2208-2213. b) Neumann, S. *Chem. Commun.* **2019**, *55*, 11658-11670.

69. Breslow, R. *J. Am. Chem. Soc.* **1958**, *80*, 3719-3726.

70. Paul. M.; Sudkaow, P.; Wessels, A.; Schlörer, N. E.; Neudörfl, J.-M.; Berkessel, A. *Angew. Chem. Int. Ed.* **2018**, *57*, 8310-8315.

71. Wang, Y.-B.; Wang, Y.-M.; Zhang, W.-Z.; Lu, X.-B. *J. Am. Chem. Soc.* **2013**, *135*, 11996-12003.

72. Saptal, V. B.; Bhanage, B. M. *ChemSusChem* **2016**, *9*, 1980-1985.

73. Kaya, U.; Tran, U. P. N.; Enders, D.; Ho, J.; Nguyen, T. V. *Org. Lett.* **2017**, *19*, 1398-1401.

74. Blümel, M.; Noy, J.-M.; Enders, D.; Stenzel, M. H.; Nguyen, T. V. *Org. Lett.* **2016**, *18*, 2208-2211.

75. Peixoto, D.; Malta, G.; Cruz, H.; Barroso, S.; Carvalho, A. L.; Ferreira, L. M.; Branco, P. S. *J. Org. Chem.* **2019**, *84*, 3793-3800.

76. a) Zhang, Y.; Miyake, G. M.; Chen, E. Y.-X. *Angew. Chem. Int. Ed.* **2010**, *49*, 10158-10162. b) Hong, M.; Chen, J.; Chen, E. Y.-X. *Chem. Rev.* **2018**, *118*, 10551-10616.

77. McGraw, M. L.; Chen, E. Y.-X. *Macromolecules* **2020,** *53*, 6102-6122.

78. Jia, Y.-B.; Wang, Y.-B.; Ren, W.-M.; Xu. T.; Wang, J.; Lu, X.-B. *Macromolecules* **2014**, *47*, 1966-1972.

79. Wang, Q.; Zhao, W.; Zhang, S.; He, J.; Zhang, Y.; Chen, E. Y.-X. *ACS Catal.* **2018**, *8*, 3571-3578.

80. McGraw, M.; Chen, E. Y.-X. *ACS Catal.* **2018**, *8*, 9877-9887.

81. Walther, P.; Krauß, A.; Naumann, S. *Angew. Chem. Int. Ed.* **2019**, *58*, 10737-10741.

82. Naumann, S.; Thomas, A. W.; Dove, A. P. *Angew. Chem. Int. Ed.* **2015**, *54*, 9550-9554.

83. Balint, A.; Papendick, M.; Clauss, M.; Müller, C.; Giesselmann, F.; Naumann, S. *Chem. Commun.* **2017**, *54*, 2220-2223.

84. Naumann, S.; Thomas, A. W.; Dove, A. P. *ACS Macro Lett.* **2016**, *5*, 134-138.

85. Naumann, S.; Mundsinger, K.; Cavallo, L.; Falivene, L. *Polym. Chem.* **2017**, *8*, 5803-5812.

86. Frankland, E. *Justus Liebigs Ann. Chem.* **1849**, *71*, 171-213.

87. Frankland, E. *Q. J. Chem. Soc.* **1861**, *13*, 177-235.

88. Frankland, E.; Duppa, B. F. *J. Chem. Soc.* **1864**, *17*, 29-36.

89. Rasmussen, S. C. *ChemTexts* **2021**, *7*, DOI:10.1007/s40828-020-00124-9.

90. Pearson, R. G. *J. Am. Chem. Soc.* **1963**, *85*, 3533-3539.

91. Yimin, S.; Piers, W. E.; Parvez, M. *Can. J. Chem*. **1998**, *76*, 513-517.

92. Williams, V. C.; Piers, W. E.; Clegg, W.; Elsegood, M. R. J.; Collins, S.; Marder, T. B. *J. Am. Chem. Soc.* **1999**, *121*, 3244-3245.

93. a) Esqueda, A. C.; Conejero, S.; Maya, C.; Carmona, E. *Organometallics* **2009**, *28*, 45-47. b) Lee, J.-D.; Han, W.-S.; Kim, T.-J.; Kim, S. H.; Kang, S. O. *Chem. Commun.* **2011**, *47*, 1018-1020. c) Oversby, J. S.; Jayaratne, K. C.; Schoell, N. J.; Hanusa, T. P. *Organometallics* **1999**, *18*, 1663-1668.

94. Fagan, P. J.; Nugent, W. A. *J. Am. Chem. Soc.* **1998**, *110*, 2310-2312.

95. Yan, X.; Xi. C. *Coord. Chem. Rev.* **2017**, *350*, 275-284.

96. Rivard, E. *Chem. Rec.* **2020**, *20*, 640-648.

97. a) He, G.; Kang, L.; Torres Delgado, W.; Shynkaruk, O.; Ferguson, M. J.; McDonald, R.; Rivard, E. *J. Am. Chem. Soc.* **2013**, *135*, 5360-5363. b) Parke, S. M.; Hupf, E.; Matharu, G. K.; de Aguiar, I.; Xu, L.; Yu, H.; Boone, M. P.; de Souza, G. L. C.; McDonald, R.; Ferguson, M. J.; He, G.; Brown, A.; Rivard, E. *Angew. Chem. Int. Ed.* **2018**, *57*, 14841-14846.

98. Johansson, C. C. C.; Kitching, M. O.; Colacot, T. J.; Snieckus, V. *Angew. Chem. Int. Ed.* **2012**, *51*, 5062-5085.

99. Miyaura, N.; Suzuki, A. *Chem. Rev.* **1995**, *95*, 2457-2483.

100. Amatore, C.; Jutland, A.; Le Duc, G. *Chem. Eur. J.* **2011**, *17*, 2492-2503.

101. Thomas, A. A.; Denmark, S. E. *Science* **2016**, *352*, 329-332.

102. a) Liu, Q.; Lan, Y.; Liu, J.; Wu, Y.-D.; Lei, A. *J. Am. Chem. Soc.* **2009**, *131*, 10201-10210. b) Jin. L.; Lei, A. *Org. Biomol. Chem.* **2012**, *10*, 6817-6825.

103. a) Ruiz-Castillo, P.; Buchwald, S. L. *Chem. Rev.* **2016**, *116*, 12564-12649. b) Kawaguchi, K.; Nakano, K.; Nozaki, K. *Org. Lett.* **2008**, *10*, 119-1202. c) Tan, Y.; Liang, M.; Lu, Z.; Zheng, Y.; Tong, X.; Sun, Z.; Xue, S. *Org. Lett.* **2014**, *16*, 3978-3981.

104. Dorel, R.; Grugel, C. P.; Haydl, A. M. *Angew. Chem. Int. Ed.* **2019**, *58*, 17118-17129.

105. Sample, H. C.; Senge, M. O. *Eur. J. Org. Chem.* **2021**, 7-42.

106. a) Sambiago, C.; Marsden, S. P.; Blacker, A. J.; McGowan, P. C. *Chem. Soc. Rev.* **2014**, *43*, 3525-3550. b) Lin, H.; Sun, D. *Org. Prep. Proced. Int.* **2013**, *45*, 341-394.

107. Kosugi, M.; Kameyama, M.; Migita, T. *Chem. Lett.* **1983**, *12*, 927-928.

108. Boger, L. D.; Panek, J. S. *Tetrahedron Lett.* **1984,** *25*, 3175-3178.

109. Sunesson, Y.; Limé, E.; Nilsson Lill, S. O.; Meadows, R. E.; Norrby, P.-O. *J. Org. Chem.* **2014**, *79*, 11961-19969.

110. Guram, A. S.; Rennels, R. A.; Buchwald, S. L. *Angew. Chem. Int. Ed. Engl.* **1995**, *34*, 1348-1350.

111. Louie, J.; Hartwig, J. F. *Tetrahedron Lett.* **1995**, *36*, 3609-3612.

112. Muci, A. R.; Buchwald, S. L. *Practical Palladium Catalysts for C-N and C-O Bond Formation*. In Cross-Coupling Reactions; Topics in Current Chemistry; vol 219. Springer, Berlin, Heidelberg; pp 131-209.

113. a) Alcazar-Roman, L. M.; Hartwig, J. F.; Rheingold, A. L.; Liable-Sands, L. M.; Guzei, I. A. *J. Am. Chem. Soc.* **2000**, *122*, 4618-4630. b) Alcazar-Roman, L. M.; Hartwig, J. F. *J. Am. Chem. Soc.* **2001**, *123*, 12905-12906. c) Singh, U. K.; Strieter, E. R.; Blackmond, D. G.; Buchwald, S. L. *J. Am. Chem. Soc.* **2002**, *124*, 14104-14114. d) Shekhar, S.; Ryberg, P.; Hartwig, J. F.; Mathew, J. S.; Blackmond, D. G. *J. Am. Chem. Soc.* **2006**, *128*, 3584-3591.

114. Louie, J.; Paul, F.; Hartwig, J. F. *Organometallics* **1996**, *15*, 2794-2805.

115. Thomas, G. T.; Janusson, E.; Zijlstra, H. S.; McIndoe, J. S. *Chem. Commun.* **2019**, *55*, 11727-11730.

116. Wambua, V.; Hirschi, J. S.; Vetticatt, M. J. *ACS Catal.* **2021**, *11*, 60-67.

117. Tian, J.; Wang, G.; Qi, Z.-H.; Ma, J. *ACS Omega* **2020**, *5*, 21385-21391.

118. Wolfe, J. P.; Wagaw, S.; Buchwald, S. L. *J. Am. Chem. Soc.* **1996**, *118*, 7215-7216.

119. a) Mann, G.; Hartwig, J. F.; Driver, M. S.; Fernández-Rivas, C. *J. Am. Chem. Soc.* **1998**, *120*, 827-828. b) Wolfe, J. P.; Ahman, J.; Sadigui, J. P.; Singer, R. A.; Buchwald, S. L. *Tetrahedron Lett.* **1997**, *38*, 6367-6370. c) Shakespeare, W. C. *Tetrahedron Lett.* **1999**, *40*, 2035-2038. d) Bolm, C.; Hildebrand, J. P. *Tetrahedron Lett.* **1998**, *39*, 5731-5734.

120. Mole, L.; Spencer, J. L.; Carr, N.; Orpen, A. G. *Organometallics* **1991**, *10*, 49-52.

121. Marcone, J. E.; Moloy, K. G. *J. Am. Chem. Soc.* **1998**, *120*, 8527-8528.

122. Fujita, K.-I.; Yamashita, M.; Puschmann, F.; Alvarez-Falcon, M. M.; Incarvito, C. D.; Hartwig, J. F. *J. Am. Chem. Soc.* **2006**, *128*, 9044-9045.

123. Surry, D. S.; Buchwald, S. L. *Angew. Chem. Int. Ed.* **2008**, *47*, 6338-6361.

124. Barder, T. E.; Buchwald, S. L. *J. Am. Chem. Soc.* **2007**, *129*, 5096-5101.

125. a) Lundgren, R. J.; Peters, B. D.; Alsabeh, P. G.; Stradiotto, M. *Angew. Chem. Int. Ed.* **2010**, 4071-4074. b) Lundgren, R. J.; Stradiotto, M. *Angew. Chem. Int. Ed.* **2010**, *49*, 8686-8690.

126. Lavoie, C. M.; MacQueen, P. M.; Rotta-Loria, N. L.; Sawatzky, R. S.; Borzenko, A.; Chisholm, A. J.; Hargreaves, B. K. V.; McDonald, R.; Ferguson, M. J.; Stradiotto, M. *Nat. Commun.* **2016**, *7*, 11073.

127. Fors, B. P.; Davis, N. D.; Buchwald, S. L. *J. Am. Chem. Soc.* **2009**, *131*, 5766-5768.

128. Surry, D. S.; Buchwald, S. L.; *Chem. Sci.* **2011**, *2*, 27-50.

129. Maiti, D.; Fors, B. P.; Henderson, J. L.; Nakamura, Y.; Buchwald, S. L. *Chem. Sci.* **2011**, *2*, 57-68.

130. Düfert, M. A.; Billingsley, K. L.; Buchwald, S. L. *J. Am. Chem. Soc.* **2013**, *135*, 12877-12885.

131. Ueling, M. R.; King, R. P.; Krska, S. W.; Cernak, T.; Buchwald, S. L. *Science* **2019**, *363*, 405-408.

132. Huang, J.; Grasa, G.; Nolan, S. P. *Org. Lett.* **1999**, *1*, 1307-1309.

133. Stauffer, S. R.; Lee, S. Stambuli, J. P.; Hauck, S. I.; Hartwig, J. F. *Org. Lett.* **2000**, *2*, 1423-1426.

134. Viciu, M. S.; Germaneau, R. F.; Navarro-Fernandez, O.; Stevens, E. D.; Nolan, S. P. *Organometallics* **2002**, *21*, 5470-5472.

135. Marion, N.; Navarro, O.; Mei, J.; Stevens, E. D.; Scott, N. M.; Nolan, S. P. *J. Am. Chem. Soc.* **2006**, *128*, 4101-4111.

136. Marion, N.; Ecarnot, E. C.; Navarro, O.; Amoroso, D.; Bell, A.; Nolan, S. P. *J. Org. Chem.* **2006**, *71*, 3816-3821.

137. a) O'Brien, C. J.; Kantchev, E. A. B.; Valente, C.; Hadei, N.; Chass, G. A.; Lough, A. J.; Hopkinson, A. C.; Organ, M. G. *Chem. Eur. J.* **2006**, *12*, 4743-4748. b) Organ, M. G.; Abdel-Hadi, M.; Avola, S.; Dubovyk, I.; Hadei, N.; Kantchev, E. A. B.; O'Brien, C. J.; Sayah, M.; Valente, C. *Chem. Eur. J.* **2008**, *14*, 2443-2452.

138. Valente, C.; Çalimsiz, S.; Hoi, K. H.; Mallik, D.; Sayah, M.; Organ, M. G. *Angew. Chem. Int. Ed.* **2012**, *51*, 3314-3332.

139. Guillet, S.G.; Voloshkin, V. A.; Saab, M.; Beliš, M.; Van Hecke, K.; Nahra, F.; Nolan, S. P. *Chem. Commun.* **2020**, *56*, 5953-5956.

140. Sayah, M.; Organ, M. G. *Chem. Eur. J.* **2013**, *19*, 16196-16199.

141. Pompeo, M.; Farmer, J. L.; Froese, R. D. J.; Organ, M. G. *Angew. Chem. Int. Ed.* **2014**, *53*, 3223-3226.

142. Fantasia, J.; Petersen, J. L.; Jacobsen, H.; Cavallo, L.; Nolan, S. P. *Organometallics* **2007**, *26*, 5880-5889.

143. Organ, M. G.; Çalimsiz, S.; Sayah, M.; Hoi, K. H.; Lough, A. J. *Angew. Chem. Int. Ed.* **2009**, *48*, 2383-2387.

144. a) Hoi, K. H.; Coggan, J. A.; Organ, M. G. *Chem. Eur. J.* **2012**, *19*, 843-845. b) Atwater, B.; Chandrasoma, N.; Mitchell, D.; Rodriguez, M. J.; Organ, M. G. *Chem. Eur. J.* **2016**, *22*, 14531-14534.

Chapter 2: Organocatalytic Hydroboration Promoted by *N*-Heterocyclic Olefins

2.1 Introduction

The addition of a B–H bond across the double bond of an alkene was first observed in 1956 by H. C. Brown and coworkers, shortly followed by Köster in 1958.[1] Related hydroboration processes now lie at the center of many important synthetic routes, with added technical support provided via the discovery of metal-mediated catalytic B–H bond addition to various unsaturated substrates (including ketones and imines). The hydroboration of ketones and imines provides access to alcohols and amines of industrial relevance under mild conditions.[2] Moreover the installation of easy-to-handle pinacolboronate (BPin; $-B(OCMe_2)_2$) groups onto organic substrates enables further functionalization via Suzuki–Miyaura cross-coupling.[3] Main group element complexes have also been shown to promote the catalytic hydroboration of aldehydes and ketones, with selected examples displayed in Chart 2.1.

Specifically, Jones demonstrated that Ge(II) and Sn(II) centers supported by a bulky amido ligand $[Ar^*N(Si^iPr_3)]^-$ ($Ar^* = C_6H_2\{C(H)Ph_2\}_2{}^iPr\text{-}2,6,4$) (Chart 2.1, **A**) could promote the hydroboration of unhindered aldehydes with extremely high activities (0.05 mol% catalyst, TOF > 13 300 h^{-1} , yields > 99%).[4] In keeping with this theme, Ge or Sn,[5] Mg,[6] P,[7] and Group 13 element-based[8] compounds can also promote hydroboration catalysis with pinacolborane. The Rivard Group has also

shown that Group 12 element hydrides [*e.g.,* [IPr·ZnH(OTf)THF] (Chart 2.1, **C**); IPr = (HCNDipp)$_2$C: Dipp = 2,6-^{i}Pr$_2$C$_6$H$_3$] are competent catalysts for the hydroboration and hydrosilation of more hindered ketonic substrates.[9,10]
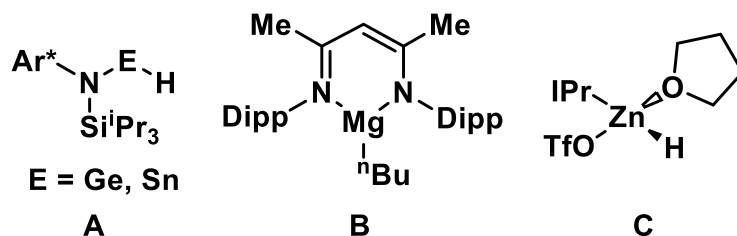
Chart 2.1. Known main group species **A** (E = Ge and Sn; Ar* = C$_6$H$_2$\{C(H)Ph$_2$\}$_2$^{i}Pr-2,6,4), **B** and **C** [IPr = (HCNDipp)$_2$C: Dipp = 2,6-^{i}Pr$_2$C$_6$H$_3$] that are effective hydroboration catalysts.

Recently, the Rivard Group has developed routes to complexes containing highly electron-releasing anionic *N*-heterocyclic olefin units (aNHOs), such as the first base-free divinylgermylene [(IPr=CH)$_2$Ge:].[11] If an aNHO group could be installed onto boron to yield IPr=CH–BR$_2$, then the resulting compounds could contain both Lewis basic (=CH–) and acidic (–BR$_2$) centers in the same molecule; prior work has shown that boron-based intramolecular frustrated Lewis pairs[12] are active catalysts for C–H bond activation[13] and the dehydrogenative coupling of amine–boranes.[14]

In this Chapter, the serendipitous discovery of metal-free hydroboration catalysis based upon readily available[15] *N*-heterocyclic olefins (NHOs), such as IPrCH$_2$ is discussed. This work adds to the growing literature involving the use of

NHOs as organocatalysts, with prior examples of CO_2 fixation, transesterification, and the polymerization of epoxides, acrylates and lactones known.[16]

2.2. Results and Discussion

The known NHO-silane $^{Me}IPr=CH(SiMe_3)$[11,17] (**1**) ($^{Me}IPr = [(MeCNDipp)_2C:]$) was combined with one equivalent of THF·BH_3 with the goal of yielding $^{Me}IPr=CH–BH_2$, or a reactive surrogate of this species. However, incomplete conversion of **1** into a new boron-containing product with a broad ^{11}B NMR resonance at -28.9 ppm in C_6D_6 was noted, consistent with the presence of a four-coordinate boron environment. When **1** was combined with two equivalents of THF·BH_3 in toluene, the same boron-containing product was obtained as a white crystalline solid. Single-crystal X-ray diffraction studies on crystals grown from toluene later identified[18] the product as the hydridodiborane complex $[^{Me}IPr–CH(BH_2)_2(\mu\text{-}H)]$ (**3a**; 40 % yield), which is formally derived from the addition of BH_3 to $^{Me}IPr=CH–BH_2$. Interestingly, the related $[B_2H_5]^+$ complex $[IPr–CH(BH_2)_2(\mu\text{-}H)]$ (**3b**) can also be prepared in high yield by treatment of the known germanium halide $IPr=CH(GeCl_3)$ (**2b**)[11] with 3 equivalents of $Li[BH_4]$ in Et_2O (Scheme 2.1). In addition to starting from compound $^{Me}IPr=CH(SiMe_3)$ **1**, compound **3a** can also be conveniently prepared from $^{Me}IPr=CH(GeCl_3)$ (**2a**)[11a] and $Li[BH_4]$.
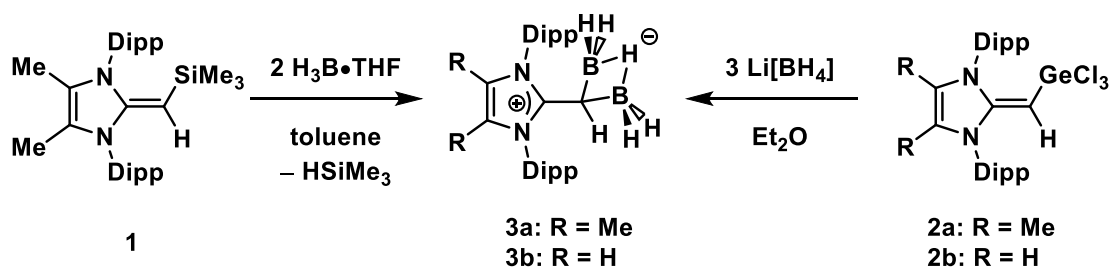
Scheme 2.1. Synthesis of the aNHO-stabilized $[B_2H_5]^+$ complexes $[^{Me}IPr–CH(BH_2)_2(\mu\text{-}H)]$ (**3a**) and $[IPr–CH(BH_2)_2(\mu\text{-}H)]$ (**3b**).

To probe the reactivity of the B_2H_5 unit, compound **3b** was combined with excess MeOTf in fluorobenzene. This afforded the terminally-bound triflato complex $[IPr–CH(BH_2)\{BH(OTf)\}(\mu\text{-}H)]$ (**4**) (Scheme 2.2), which was identified by X-ray crystallography, NMR spectroscopy and elemental analysis.
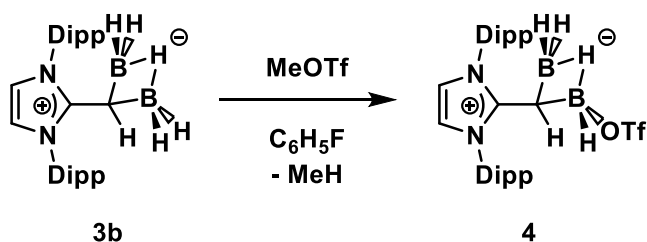
Scheme 2.2. The reaction of $[IPr–CH(BH_2)_2(\mu\text{-}H)]$ **3b** with MeOTf.

The molecular structure of $[IPr–CH(BH_2)_2(\mu\text{-}H)]$ (**3b**)[18] displays an elongated C1–C4 bond [1.434(2) Å] (Figure 2.1) relative to the terminal C=C double bond in IPrCH$_2$ [1.332(4) Å].[15d] However the C1–C4 linkage in **3b** is shorter than the terminal NHO C–C bonds in Ghadwal's IPrCH$_2$-stabilized acyclic $B_2H_5^+$ complex $[(IPrCH_2)BH_2(\mu\text{-}H)BH_2(IPrCH_2)]^+$ [1.467(2) Å].[19] The two C–B bond lengths in **3b** are the same within experimental error [1.611(4) and 1.604(3) Å] and combine to

form a rather acute B1–C4–B2 angle of 72.0(2)°. A B---B bonding interaction can be excluded on the basis of DFT studies (see below) and from atoms-in-molecules (AIM) studies on the related cationic carbodiphosphorane complex [(Ph₃P)₂C(BH₂)₂(μ-H)]⁺ reported by Petz *et al*.[20]
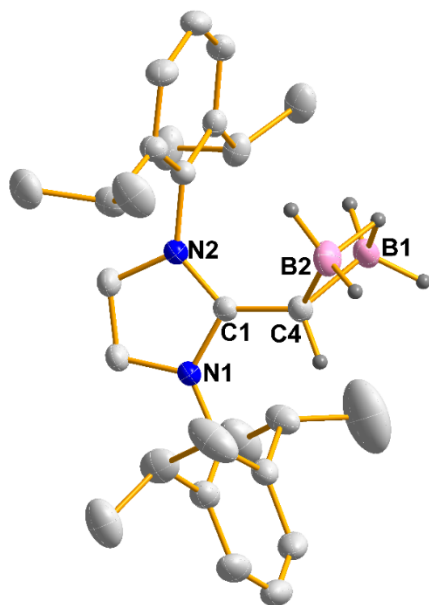
Figure 2.1. Molecular structure of [IPr–CH(BH₂)₂(μ-H)] (**3b**). Ellipsoids are drawn at a 30 % probability level with all hydrogen atoms except those on B1, B2, C4 omitted for clarity. Selected bond lengths (Å) and angles (°): B1–B2 1.889(5), C4–B2 1.611(4), C4–B1 1.604(3), C1–N1 1.357(2), C1–N2 1.361(2), C1–C4 1.434(2); B2–C4–B1 72.0(2).
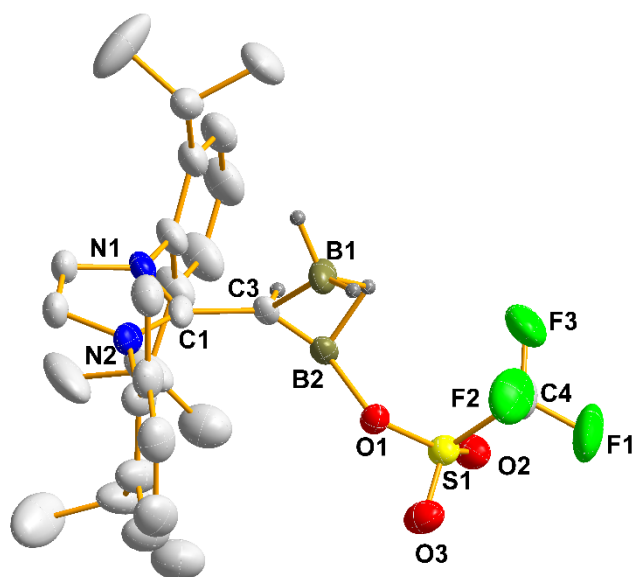
Figure 2.2. Molecular Structure of [IPr–CH(BH$_2$){BH(OTf)}(μ-H)] (**4**). Ellipsoids are drawn at a 30 % probability level with hydrogens except those on C3, B1, and B2 omitted for clarity. Selected bond lengths (Å) and angles (°): C1–C3 1.505(5), C3–B1 1.569(6), C3–B2 1.546(6), B1–B2 1.926(7), O1–B2 1.533(6); B2−C3−B1 76.4(3); C1−C3−B1−B2 117.3(4)

The structural parameters of the B$_2$H$_5$ complexes **3a** and **3b** are also reminiscent of those found in Mézailles' diborane [(SPPh$_2$)$_2$C(BH$_2$)$_2$(μ-H)]Li(OEt$_2$)[21] and underline the notion that the [IPrCH]$^−$ unit in **3b** is acting as a four-electron donor.[22] To gain further insight into the nature of the bonding in **3b**, DFT calculations at the BP86/DEF2SVP level of theory were conducted.[23] Natural population analysis (NPA) revealed an effective charge transfer of 1.27e from [IPrCH]$^−$ to a formal [B$_2$H$_5$]$^+$ unit, indicated by the charge of −0.27e for the [B$_2$H$_5$] moiety in **3b**. As expected, the donor carbon atom [C(4), Figure 2.1] carries a negative NPA charge of −0.77e.

Prior work by Mézailles[21] suggested that the B_2H_5 unit in **3a** and **3b** might act as an activator for ketone and aldehyde hydroboration. However, initial trials involving the use of **3b** as a catalyst (5 mol%) for the hydroboration of Ph_2CO with HBpin showed inconsistent results; in some cases, catalysis was observed, but other times no activity transpired. Upon careful purification of both **3a** and **3b**, it was found that these complexes (as well as **4**) were not active for hydroboration, but rather the NHOs themselves $^{Me}IPrCH_2$ and $IPrCH_2$ were active boration catalysts. This is, to our knowledge, the first example of the catalytic hydroboration of aldehydes and ketones initiated by a carbon-based organocatalyst. Interestingly, it has been shown that CO_2 can be borated with the assistance of an intramolecular P/B based frustrated Lewis pair (FLP).[24]

When Ph_2CO and HBpin were combined with 5 mol% of $IPrCH_2$ as a catalyst in THF (at room temperature), quantitative conversion was observed from the reactants to the borated product, $Ph_2C(H)OBpin$, after 18 h (as determined by ^1H NMR spectroscopy). In the absence of $IPrCH_2$ no reaction transpired, whereas heating the mixture to 60 °C resulted in full conversion after 5 h. This promising result prompted the testing of different substrates. Of note, quantitative HBpin addition to $(4-Cl-C_6H_4)_2CO$ after only 5 min (5 mol% loading of $IPrCH_2$; Table 2.1). Similarly, the bulky aldehyde MesCHO (Mes = $2,4,6-Me_3C_6H_2$) undergoes complete hydroboration with HBpin (5 mol% of $IPrCH_2$) in less than 15 min. Acetophenone was converted into Ph(Me)CHOBpin in a 73% yield after 18 h. In the case of the active substrates $(4-Cl-C_6H_4)_2CO$ and MesCHO the NHO catalyst loading could be

reduced to 1 mol% or 2 mol%, resulting in full conversion within 15 min or 1 h, respectively (Table 2.1). Moreover, the selective boration of an aldehyde unit in 4-acetylbenzaldehyde transpires rapidly (5 min) leaving the ketone residue unaltered during this timeframe (Table 2.1).[25] More challenging aliphatic substrates can also be borated, as evidenced by the reduction of cyclohexanone and cyclohexylaldehyde (Table 2.1). In addition to the above mentioned hydroboration reactions, the hydrosilylation of MesCHO with $PhMeSiH_2$ was screened (with 5 mol% of $IPrCH_2$ catalyst): after 2 h at 60 °C in THF a 28 % conversion of the reactants into the expected silylether $MesCH_2OSiH(Me)Ph$ occurred. Notably, the *N*-heterocyclic carbene, IPr, can also act as a hydroboration catalyst, but only in the case of the more reactive substrates, MesCHO and $(4\text{-}Cl\text{-}C_6H_4)_2CO$ (Table 2.1), and with far inferior activities (*e.g.,* TOF = 0.7 h^{-1} for MesCHO reduction with IPr *vs.* a TOF of 99 h^{-1} with $IPrCH_2$ as an organocatalyst).

Table 2.1. A summary of hydroboration of ketones and aldehydes with HBpin using IPrCH$_2$, ^{Me}IPrCH$_2$, and IPr as organocatalysts.

Cat.	mol%	R/R´	time	yield [%]	TOF [h^{-1}]
IPrCH$_2$	5	Ph/Ph	18 h	99	1.1
IPrCH$_2$	5	Ph/Ph	5 h at 60 °C	>99	4.0
IPrCH$_2$	5	Mes/H	12 min	>99	99
IPrCH$_2$	5	4-MeCO-C$_6$H$_4$/H	6 min	>99	116
IPrCH$_2$	5	Ph/Me	18 h	73	0.8
IPrCH$_2$	1	4-Cl-C$_6$H$_4$/4-Cl-C$_6$H$_4$	15 min	>99	386
IPrCH$_2$	5	4-Cl-C$_6$H$_4$/4-Cl-C$_6$H$_4$	5 min	>99	238
IPrCH$_2$	2	Mes/H	1 h	>99	49.5
IPrCH$_2$	5	Cyclohexanone	18 h	58	0.6
IPrCH$_2$	5	Cy/H	3 h	>99	6.7
^{Me}IPrCH$_2$	5	4-Cl-C$_6$H$_4$/4-Cl-C$_6$H$_4$	5 min	>99	238
IPr	5	Mes/H	24 h	79	0.7
IPr	5	4-Cl-C$_6$H$_4$/4-Cl-C$_6$H$_4$	24 h	9	0.08

To elucidate a mechanism for the NHO-catalyzed hydroborations, IPrCH$_2$ was combined independently with HBpin and Ph$_2$CO in THF. Ph$_2$CO showed no signs of reactivity with IPrCH$_2$, while HBpin does interact slowly (*ca.* 50 % conversion after 30 h) with IPrCH$_2$ to give a mixture of unreacted starting materials and a new NHO-containing product, tentatively assigned as IPrCH$_2$B(H)pin (**A2** in Scheme 2.3). Attempts to isolate this species in pure form by fractional crystallization were not successful. Based on initial DFT studies, two possible pathways for catalysis are

proposed (Scheme 2.3). One path involves the formation of IPrCH$_2$–C(O)R$_2$ (**A**) as an intermediate, and DFT studies show that the oxygen atom in **A** is rendered more nucleophilic, with the negative charge being raised to -0.87e in comparison to a value of -0.53e in Ph$_2$CO. Accordingly, intermediate **A** could attack HBpin to yield intermediate **B**, which later undergoes hydride migration to the borylether pinBOCHR$_2$ and free IPrCH$_2$ (Scheme 2.3, top). Alternatively, slow adduct formation (**A2**) between IPrCH$_2$ and HBpin can transpire (Scheme 2.3, bottom) followed by hydride delivery to R$_2$CO via intermediate **C**, with subsequent Bpin transfer to oxygen and H-migration to regenerate adduct **A2** and liberate pinBOCHR$_2$.
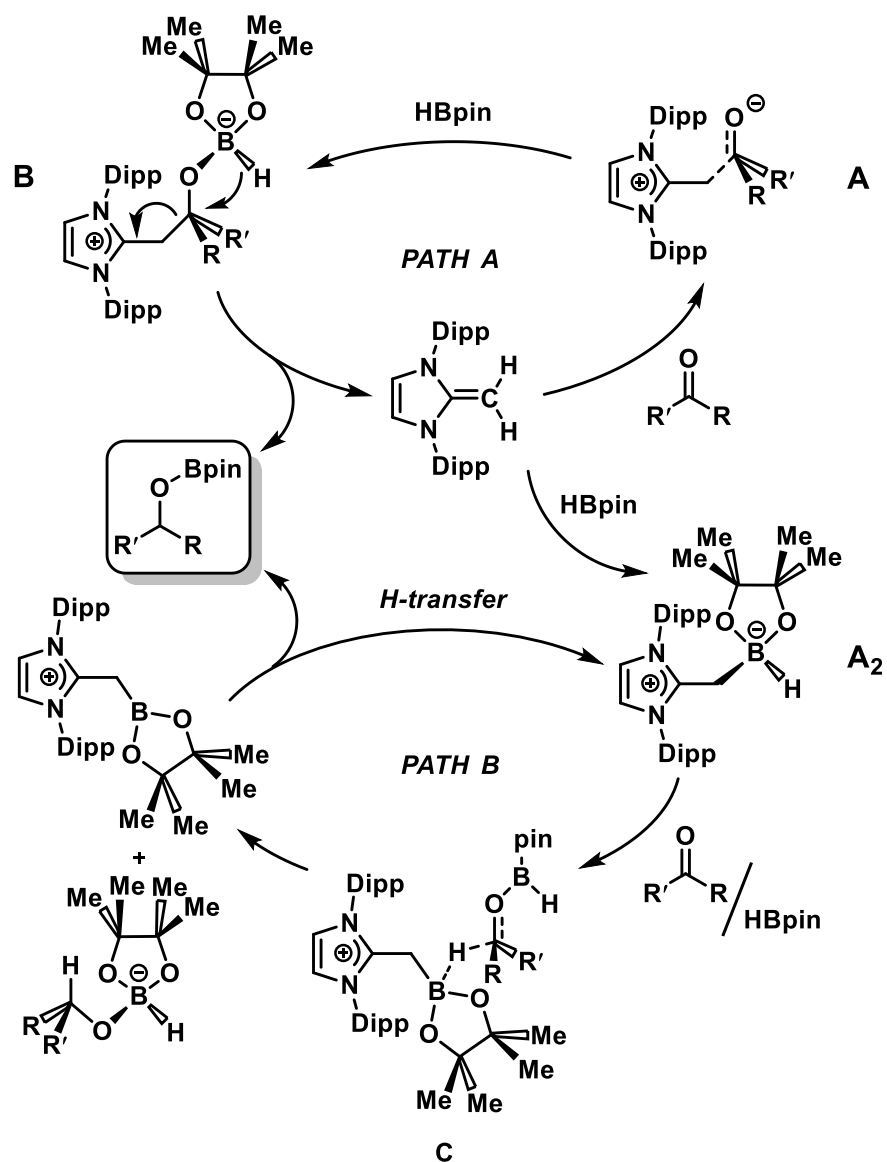
Scheme 2.3. Proposed catalytic cycles for the hydroboration of ketones and aldehydes promoted by NHOs.

2.3. Conclusion

In conclusion, studies on $B_2H_5^+$ complexation led to the discovery that *N*-heterocyclic olefins (NHOs), such as $IPrCH_2$, are efficient organocatalysts for the hydroboration of ketones and aldehydes. This work reveals the untapped potential of NHOs as organocatalysts in a variety of transformations, and future investigations will involve using the library of known NHOs,[15b,d] to expand the substrate scope amenable to mild catalytic hydroboration.

2.4 Experimental Section

2.4.1 Materials and Instrumentation

All reactions were performed using standard Schlenk line techniques under an atmosphere of nitrogen or in an inert atmosphere glovebox (Innovative Technologies, Inc.). Solvents were dried using a Grubbs-type solvent purification system manufactured by Innovative Technologies, Inc., degassed (freeze−pump−thaw method), and stored under an atmosphere of nitrogen prior to use. HBpin, MeOTf, Li[BH₄], THF•BH₃ (1.0 M solution in THF), Ph_2CO, $(4-ClC_6H_4)_2CO$, MeCO(Ph), ^tBuCOMe, $4-CH_3CO-C_6H_4-CHO$ and MesCHO were purchased from MilliporeSigma and used as received. $IPrCH_2$,[15d] $^{Me}IPrCH_2$,[15d] $IPr=CH(GeCl_3)$,[11a] $^{Me}IPr=CH(GeCl_3)$,[11a] and $^{Me}IPr=CH(SiMe_3)$[11a] were prepared according to literature procedures. ^1H, $^{11}B\{^1H\}$, $^{13}C\{^1H\}$ and $^{19}F\{^1H\}$ NMR spectra were recorded on a Varian VNMRS-500 spectrometer and referenced externally to $SiMe_4$ (^1H, $^{13}C\{^1H\}$), $F_3B•OEt_2$ (^{11}B), or

CFCl$_3$ (^{19}F{^{1}H}). Elemental analyses were performed by the Analytical and Instrumentation Laboratory at the University of Alberta. Melting points were measured in sealed glass capillaries under nitrogen using a MelTemp apparatus and are uncorrected.

2.4.2 X-ray Crystallography

Crystals of appropriate quality for X-ray diffraction studies were removed from either a Schlenk flask under a stream of nitrogen, or from a vial (glove box) and immediately covered with a thin layer of hydrocarbon oil (Paratone-N). A suitable crystal was then selected, attached to a glass fiber, and quickly placed in a low-temperature stream of nitrogen. All data were collected using a Bruker APEX II CCD detector/D8 diffractometer using Mo$_{K\alpha}$ or Cu$_{K\alpha}$ radiation, with the crystal cooled to $-100\,°C$ or $-80\,°C$, respectively. The data were corrected for absorption through Gaussian integration from indexing of the crystal faces. Structures were solved using the direct methods programs SHELXT-2014,[26] and refinements were completed using the program SHELXL-2014.[27] Hydrogen atoms were assigned positions based on the sp^2- or sp^3-hybridization geometries of their attached carbon atoms and were given thermal parameters 20 % greater than those of their parent atoms.

2.4.3 Computational Methods

Computational work for this Chapter was performed by Dr. Christian Hering-Junghans. Density Functional theory (DFT) calculations (full geometry optimization) were carried out on [^{Me}IPr–CH(BH$_2$)$_2$(μ-H)] (**3a**) starting from the geometry of the respective X-ray structures and on the intermediates **A** and **B** proposed in Scheme 2.3.

Geometry optimizations were carried out using the Gaussian09 program package:[28] B86[29] functional with a def2-SVP basis set[23] for C, H, B, O, and N. The optimized structures were in reasonable agreement with the observed molecular structures. All stationary points were characterized by frequency analyses. For all calculated molecules and intermediates there are no imaginary frequencies. The optimized structures were also subjected to natural bond orbital (NBO) analyses using the NBO 6.0 program.[30] It should be emphasized that the computation was carried out for a single, isolated (gas phase) species. There may well be significant differences among gas phase, solution, and solid-state data.
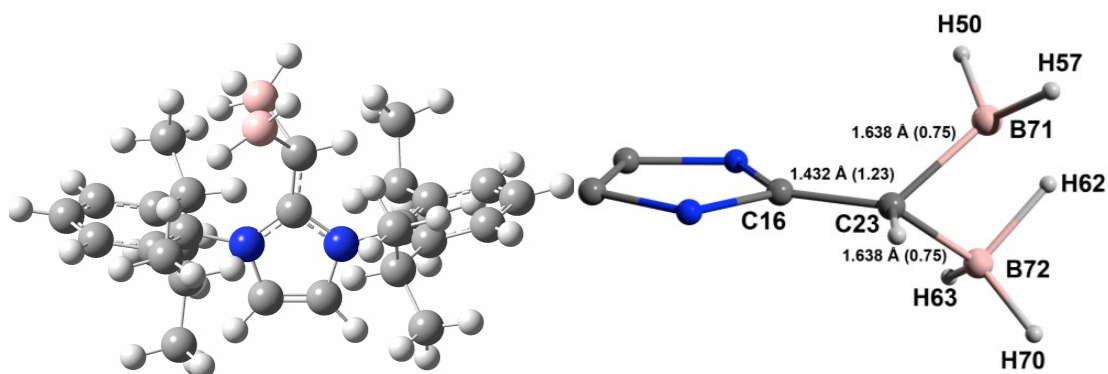
Figure 2.3. POV-ray depiction of the DFT-optimized structure of **3b** (left) with a second view (right) in which the Dipp-groups have been omitted for clarity. Selected computed bond lengths and Wiberg bond indices (in parentheses) are shown in the bottom view. xyz-coordinates for the optimized structure of [IPr–CH(BH$_2$)$_2$(μ-H)] have been checked to be a minimum on the energy hyper-surface by a frequency analysis.
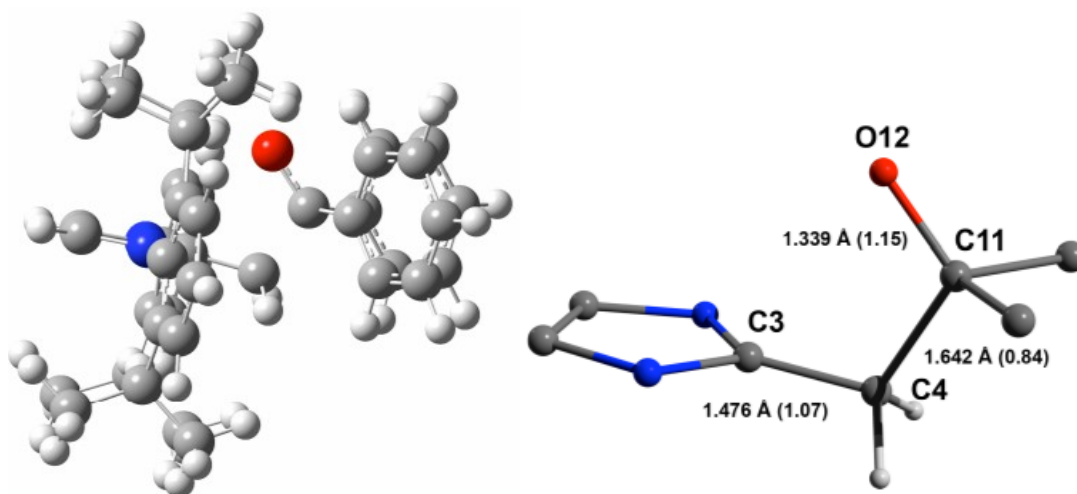
Figure 2.4. Ball-and-stick representation of the optimized structure of proposed intermediate **A** (left). Ball-and-stick depiction of the optimized structure of intermediate **A** (right) with Dipp-groups and hydrogen atoms on IPr and Ph_2CO omitted for clarity. Selected computed bond lengths and Wiberg bond indices (in parentheses) are shown in the bottom view. xyz-coordinates for the optimized structure of intermediate **A** and have been checked to be a minimum on the energy hypersurface by a frequency analysis.
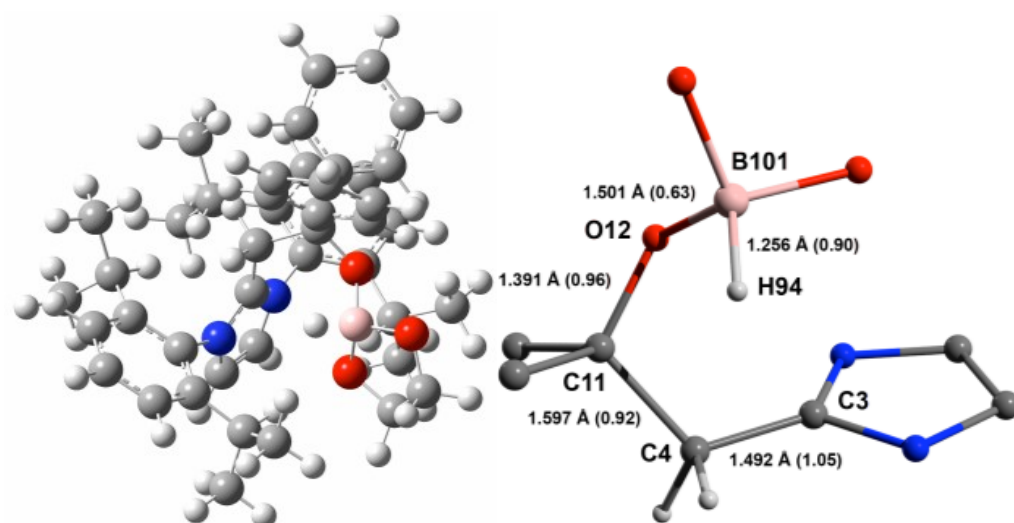
Figure 2.5. Ball-and-stick representation of the optimized structure of proposed intermediate **B** (left). Ball-and-stick depiction of the optimized structure of intermediate **B** (right) with Dipp-groups and hydrogen atoms on IPr and Ph$_2$CO omitted for clarity. Selected computed bond lengths and Wiberg bond indices (in parentheses) are shown in the bottom view. xyz-coordinates for the optimized structure of intermediate **B** and have been checked to be a minimum on the energy hyper-surface by a frequency analysis.
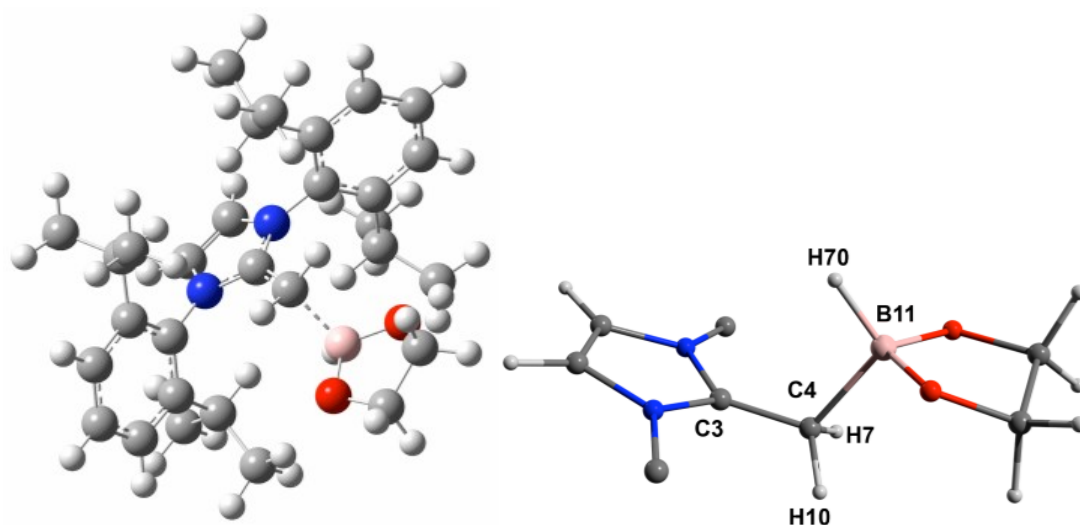
Figure 2.6. Ball-and-stick representation of the optimized structure of proposed intermediate **A2** (left). Ball-and-stick depiction of the optimized structure of intermediate **A2** (right) with Dipp-groups and hydrogen atoms on IPr omitted for clarity. Selected computed bond lengths and Wiberg bond indices (in parentheses) are shown in the bottom view. xyz-coordinates for the optimized structure of intermediate **A2** and have been checked to be a minimum on the energy hyper-surface by a frequency analysis.

2.4.4. Synthetic procedures

Synthesis of [^{Me}IPr–CH(BH$_2$)$_2$(μ-H)] (3a) from ^{Me}IPrCH(GeCl$_3$). To a mixture of ^{Me}IPrCH(GeCl$_3$) (0.148 g, 0.243 mmol) and Li[BH$_4$] (0.017 g, 0.75 mmol) was added 10 mL of Et$_2$O at room temperature, which was accompanied by vigorous bubbling. Stirring was continued for 4 h. The resulting yellow precipitate was allowed to settle and the supernatant filtered through a plug of Celite. The volatiles were evaporated from the filtrate to give [^{Me}IPr–CH(BH$_2$)$_2$(μ-H)] **(3a)** as an off-white solid (0.093 g, 85 %). X-ray diffraction quality crystals of **3a** were obtained by placing a saturated toluene solution layered with hexanes at −30 °C for 24 h.

Alternate Synthesis of [^{Me}IPr–CH(BH$_2$)$_2$(μ-H)] (3a) from ^{Me}IPrCH(SiMe$_3$). To ^{Me}IPrCH(SiMe$_3$) (0.084 g, 0.17 mmol) in 5 mL of toluene was added dropwise THF•BH$_3$ (1.0 M solution in THF, 0.340 mL, 0.34 mmol) at ambient temperature. After 12 h of stirring at room temperature, the resulting mixture was evaporated to dryness, and the remaining residue was washed with hexanes (2 × 3 mL) and the remaining solid dried *in vacuo* to yield [^{Me}IPr–CH(BH$_2$)$_2$(μ-H)] (3b) in the form of a white solid (0.065 g, 84 %). ^{1}H NMR (498 MHz, C$_6$D$_6$): δ = 7.21 (t, 2H, $^3J_{HH}$ = 7.3 Hz, Ar*H*), 7.07 (d, 4H, $^3J_{HH}$ = 7.3 Hz, Ar*H*), 2.77 (sept, 4H, $^3J_{HH}$ = 6.6 Hz, C*H*(CH$_3$)$_2$), 1.61 (br, 4H, B*H*$_2$), 1.44 (d, 12H, $^3J_{HH}$ = 7.3 Hz, CH(C*H*$_3$)$_2$), 1.38 (s, 6H, NC–C*H*$_3$), 1.01 (d, 12H, $^3J_{HH}$ = 6.6 Hz, CH(C*H*$_3$)$_2$), –0.88 ppm (br, 1H, (BH$_2$)$_2$-μ-*H*); ^{13}C\{^{1}H\} NMR (125 MHz, C$_6$D$_6$): δ = 9.3 (H$_3$*C*-CN), 11.9 (br, *C*CH(B$_2$H$_5$)), 24.2 (CH(*C*H$_3$)$_2$), 24.4 (CH(*C*H$_3$)$_2$), 29.0 (*C*H(CH$_3$)$_2$), 122.7 (N*C*-CH$_3$), 124.7 (Ar*C*), 130.6 (Ar*C*), 131.6 (Ar*C*), 146.7 (Ar*C*), 165.2 ppm (N*C*N); ^{11}B\{^{1}H\} (159.8 MHz, C$_6$D$_6$): δ = –29.0 ppm; element anal.: calcd. for C$_{30}$H$_{46}$N$_2$B$_2$: C, 78.96; H, 10.16; N, 6.14; found: C, 77.93; H, 10.30; N, 6.11 %; mp: 176 °C (dec.).

Synthesis of [IPr–CH(BH$_2$)$_2$(μ-H)] (3b). To a mixture of solid IPrCH(GeCl$_3$) (0.298 g, 0.508 mmol) and Li[BH$_4$] (0.032 g, 1.5 mmol) was added 10 mL of Et$_2$O at room temperature, leading to the immediate bubbling of the reaction mixture. Stirring was continued for 12 h. The resulting precipitate was allowed to settle and the supernatant was filtered through a plug of Celite. The volatiles were removed under vacuum from the filtrate to give [IPr–CH(BH$_2$)$_2$(μ-H)] (3b) as an off-white solid (0.201 g, 92 %). X-

ray diffraction quality crystals of **3b** were obtained from a saturated toluene solution layered with hexanes placed at $-30\ °C$ for 24 h. ^{1}H NMR (498 MHz, C_6D_6): $\delta = 7.18$ (t, 2H, $^3J_{HH} = 7.3$ Hz, Ar*H*), 7.04 (d, 4H, $^3J_{HH} = 7.3$ Hz, Ar*H*), 6.05 (s, 2H, N-C*H*), 2.87 (sept, 4H, $^3J_{HH} = 6.6$ Hz, C*H*(CH$_3$)$_2$), 1.67 (br, 1H, C*H*(B$_2$H$_5$)), 1.40 (d, 12H, $^3J_{HH} = 7.3$ Hz, CH(C*H*$_3$)$_2$), 1.10 (br, 4H, B*H*$_2$), 1.03 (d, 12H, $^3J_{HH} = 6.6$ Hz, CH(C*H*$_3$)$_2$), -0.89 ppm (br, 1H, (BH$_2$)$_2$-μ-*H*); ^{13}C{^{1}H} NMR (125 MHz, C_6D_6): $\delta = 12.5$ (br, *C*H(B$_2$H$_5$)), 21.4 (*C*CH(B$_2$H$_5$)), 24.0 (CH(*C*H$_3$)$_2$), 25.1 (CH(*C*H$_3$)$_2$), 29.2 (*C*H(CH$_3$)$_2$), 119.8 (N*C*H), 124.3 (Ar*C*), 130.8 (Ar*C*), 133.1 (Ar*C*), 146.5 (Ar*C*), 165.9 ppm (N*C*N); ^{11}B{^{1}H} NMR (159.8 MHz, C_6D_6): $\delta = -28.9$; element. anal.: calcd. for $C_{28}H_{42}N_2B_2$: C, 78.53; H, 9.89; N, 6.54; found: C, 77.34; H, 9.83; N, 6.66 %; mp: 136 °C (dec.). Despite repeated attempts, analyses for carbon content were repeatedly low.

Synthesis of [IPr–CH(BH$_2$){BH(OTf)}(μ-H)] (4). To [IPr–CH(BH$_2$)$_2$(μ-H)] (103 mg, 0.240 mmol) in 10 mL of fluorobenzene was added MeOTf (123 mg, 0.750 mmol) and stirring was continued for 16 h. The resulting cloudy mixture was filtered through a pad of Celite and the solvent was evaporated from the filtrate *in vacuo*. The remaining off-white solid was washed with hexanes (3 × 2 mL) and [IPr–CH(BH$_2$){BH(OTf)}(μ-H)] (**4**) was recovered as a white solid (0.115 g, 83 %). X-ray diffraction quality crystals of **4** were obtained from a saturated CH_2Cl_2 solution layered with hexanes, placed at $-30\ °C$ for 24 h. ^{1}H NMR (699.76 MHz, CDCl$_3$): $\delta = 7.12$ (t, 2H, $^3J_{HH} = 7.7$ Hz, Ar*H*), 7.00 (d, 2H, $^3J_{HH} = 7.7$ Hz, Ar*H*), 6.97 (d, 2H, $^3J_{HH} =$

7.7 Hz, ArH), 6.04 (d, 2H, $^3J_{HH}$ = 1.5 Hz, HCN), 2.63 (sept, 4H, $^3J_{HH}$ = 6.8 Hz, CH(CH$_3$)$_2$), 1.60 (d, 2H, -CHB$_2$H$_4$(OTf)), 1.39 (d, 6H, $^3J_{HH}$ = 7.0 Hz, CH(CH_3)$_2$), 1.32 (d, $^3J_{HH}$ = 7.0 Hz, 6H, CH(CH_3)$_2$), 0.96 (d, $^3J_{HH}$ = 6.8 Hz, 6H, CH(CH_3)$_2$), 0.95 ppm (d, $^3J_{HH}$ = 6.8 Hz, 6H, CH(CH_3)$_2$). The hydrides attached to the ^{11}B centers could not be detected reliably in variable temperature experiments due to severe broadening and possible overlap with Dipp ^{i}Pr-group signals; ^{13}C{^{1}H} NMR (125.7 MHz, CDCl$_3$): δ = 12.8 (br, CH(B$_2$H$_5$)), 22.5 (CH(CH$_3$)$_2$), 22.6 (CH(CH$_3$)$_2$), 25.1 (CH(CH$_3$)$_2$), 25.2 (CH(CH$_3$)$_2$), 29.3 (CH(CH$_3$)$_2$), 29.4 (CH(CH$_3$)$_2$), 120.9 (HCN), 124.53 (ArC), 124.55 (ArC), 131.6 (ArC), 131.7 (ArC), 145.9 (ArC), 146.3 (ArC), 161.5 ppm (NCN); ^{11}B{^{1}H} (159.8 MHz, C$_6$D$_6$): δ = -11.1 (-BH(OTf)) -26.7 ppm (-BH$_2$-). ^{19}F{^{1}H} NMR (376.3 MHz, C$_6$D$_6$): δ = -76.5 ppm; element. anal.: calcd. for C$_{29}$H$_{41}$B$_2$F$_3$N$_2$O$_3$S: C, 60.44; H, 7.17; N, 4.86; found C, 59.56; H, 7.16; N, 4.63 %; mp: 161 °C.

Reaction of IPrCH$_2$ with HBpin. IPrCH$_2$ (0.100 g, 0.248 mmol) was dissolved in 2 mL of THF and stirred for 5 minutes. To this solution, HBpin (0.032 g, 0.25 mmol) was added dropwise. ^{1}H NMR analysis after 30 hours, showed a 42 % conversion of IPrCH$_2$ to a product tentatively formulated as IPrCH$_2$B(H)pin and 7 % conversion to a new unknown product was observed. Attempts to isolate pure IPrCH$_2$B(H)pin by fractional crystallization have been unsuccessful so far. NMR data for IPrCH$_2$B(H)pin: ^{1}H NMR (500 MHz, C$_6$D$_6$): δ = 7.18-7.21 (m, 2H, ArH), 7.13-7.14 (m, 1H, ArH), 7.13-7.12 (m, 2H, ArH), 7.11-6.97 (m, 1H, ArH) 5.66 (s, 2H, HCN), 4.01 (sept, 2H, $^3J_{HH}$ = 7.0 Hz, CH(CH$_3$)$_2$), 3.86 (sept, 2H, $^3J_{HH}$ = 7.0 Hz, CH(CH$_3$)$_2$),

1.54 (s, 2H, CH_2B), 1.30 (d, 6H, $^3J_{HH}$ = 7.2 Hz, CH(CH_3)$_2$), 1.28 (d, $^3J_{HH}$ = 7.2 Hz, 6H, CH(CH_3)$_2$, 1.23 (d, 6H, $^3J_{HH}$ = 7.2 Hz, CH(CH_3), 1.16 (d, 6H, $^3J_{HH}$ = 7.2 Hz, CH(CH_3)$_2$ 1.01 ppm (s, 12H, BOC(CH_3)$_2$), the borate B-H resonance could not be found; ^{11}B NMR (128.2 MHz, C$_6$D$_6$): δ = 21.9 ppm.

2.4.5. General Procedure for the Hydroboration of Various Aldehydes and Ketones.

A solution containing the ketone/aldehyde (0.50 mmol) dissolved in 1.6 mL of THF was combined with a 0.40 mL THF solution of the NHO catalyst (1-5 mol%, 0.005-0.025 mmol; 0.010 g of IPrCH$_2$; 0.011 g of ^{Me}IPrCH$_2$ in a 20 mL scintillation vial and stirred for 5 minutes at room temperature. Afterwards, HBpin (0.070 g, 0.55 mmol) was added and the reaction progress was monitored by ^{1}H NMR spectroscopy, with sampling of 0.20 mL aliquots after various times. The results of these reactions can be seen in Table 2.1.

^{1}H NMR data for R-CH(OBpin)-R´ hydroboration products. ^{1}H NMR data matches previously reported literature values.

Ph$_2$C(OBpin):[31] ^{1}H NMR (498 MHz, C$_6$D$_6$): δ = 7.44 (m, 2H, ArH), 7.07 (m, 2H, ArH), 6.99 (m, 1H, ArH), 6.42 (s, 1H, Ph$_2$CH(OBpin)), 0.97 ppm (s, 12H, Bpin).

(4-Cl-C₆H₄)₂CH(OBpin):[32] ^{1}H NMR (498 MHz, C₆D₆): δ = 7.04 (br, 8H, Ar*H*), 6.11 (s, 1H, (4-Cl-C₆H₄)₂C*H*(OBpin)), 0.96 ppm (s, 12H, Bpin).

PhCH(OBpin)Me:[31] ^{1}H NMR (498 MHz, C₆D₆): δ = 7.34-7.38 (m, 2H, $^3J_{HH}$ = 7.3 Hz, Ar*H*), 7.02-7.16 (m, 3H, Ar*H*), 5.41 (q, 1H, $^3J_{HH}$ = 6.4 Hz, PhC*H*(OBpin)Me), 1.45 (d, 3H, $^3J_{HH}$ = 6.4 Hz, -C(OBpin)H(C*H₃*)), 1.02 (s, 6H, Bpin), 0.99 ppm (s, 6H, Bpin).

4-MeC(O)-C₆H₄-CH₂(OBpin):[32] ^{1}H NMR (500 MHz, C₆D₆): δ = 7.73 (d, 2H, $^3J_{HH}$ = 8.2 Hz, Ar*H*), 7.20 (d, 2H, $^3J_{HH}$ = 8.2 Hz, Ar*H*), 4.87 (s, 2H, 4-MeC(O)-C₆H₄-C*H₂*(OBPin)), 2.07 (s, 3H, 4-*H₃*CCO-), 1.03 ppm (s, 12H, Bpin).

MesCH₂(OBPin):[32] ^{1}H NMR (500 MHz, C₆D₆): δ = 6.72 (s, 2H, Ar*H*), 4.87 (s, 2H, MesC*H₂*(OBpin)), 2.37 (s, 6H, 2,6-Me in Mes), 2.10 (s, 3H, 4-Me in Mes), 1.03 ppm (s, 12H, Bpin).

Cy₂CH(OBpin):[32] ^{1}H NMR (700 MHz, C₆D₆): δ = 4.23 (quintet, 1H, $^3J_{HH}$ = 7.02 Hz, Cy₂C*H*(OBpin)), 1.12-1.91 (m, 22H, Cy-*H*), 1.07 ppm (s, 12H, Bpin).

CyCH₂(OBpin):[32] ^{1}H NMR (400 MHz, C₆D₆): δ = 3.73 (d, 2H, $^3J_{HH}$ = 4.5 Hz, CyC*H₂*(OBpin)), 1.38-1.71 (m, 11H, Cy-*H*), 1.07 ppm (s, 12H, Bpin).

Catalytic hydroboration of MesCHO using ^{Me}IPrCH₂ as a catalyst. MesCHO (0.50 mmol, 0.074 g) was dissolved in THF (1.6 mL) in a 20 mL scintillation vial and a solution containing ^{Me}IPrCH₂ (5 mol%, 0.025 mmol, 0.0090 g) in 0.40 mL of THF was added and the mixture stirred for 5 min at room temperature. Afterwards HBpin (0.070 g, 0.55 mmol) was added and the reaction progress was monitored by ^{1}H NMR

spectroscopy which indicated that full conversion to the borated product MesCH$_2$O(Bpin) was achieved after 5 minutes.

Catalytic hydroboration of MesCHO testing IPr as a catalyst. MesCHO (0.50 mmol, 0.074 g) was dissolved in THF (1.6 mL) in a 20 mL scintillation vial and a solution containing IPr (5 mol. %, 0.025 mmol, 0.0090 g) in 0.40 mL of THF was added and the mixture stirred for 5 min at room temperature. Afterwards HBpin (0.070 g, 0.55 mmol) was added and the extent of reaction was monitored by ^{1}H NMR spectroscopy with a 79 % conversion into MesCH$_2$O(Bpin) detected after 24 h.

Catalytic hydroboration of (4-Cl-C$_6$H$_4$)$_2$CO testing IPr as a catalyst. (4-ClC$_6$H$_4$)$_2$CO (0.126 g, 0.502 mmol) was dissolved in 1.6 mL of THF in a 20 mL scintillation vial and a solution containing IPr (5 mol%, 0.025 mmol, 0.0090 g) in 0.40 mL of THF was added, and the mixture stirred for 5 min at room temperature. Afterwards HBpin (0.070 g, 0.55 mmol) was added and the reaction progress was monitored by ^{1}H NMR spectroscopy, revealing the formation of a small amount (9 % conversion) of (4-ClC$_6$H$_4$)$_2$CHO(Bpin) after 24 h.

Catalytic hydrosilylation of MesCHO using IPrCH$_2$ as a catalyst. MesCHO (0.50 mmol, 0.074 g) was dissolved in THF (1.6 mL) in a 20 mL scintillation vial and a solution containing IPrCH$_2$ (5 mol%, 0.025 mmol, 0.0090 g) in 0.40 mL of THF was added and the mixture stirred for 5 min at room temperature. Afterwards Ph(Me)SiH$_2$

(0.066 g, 0.54 mmol) was added and the reaction progress was monitored by ^{1}H NMR spectroscopy, indicating a 28 % conversion into the previously unknown silylated product MesCH$_2$OSiH(Me)Ph after 2 h at 60 °C.[32] ^{1}H NMR (498 MHz, C$_6$D$_6$): δ = 7.53-7.60 (m, 2H, PhH), 7.12-7.23 (m, 3H, PhH), 6.72 (s, 2H, ArH in Mes), 5.08 (q, 1H, $^3J_{HH}$ = 2.9 Hz, SiH), 4.70 (s, 2H, CH_2), 2.26 (s, 6H, 2,6-Me in Mes), 2.11 (s, 3H, 4-Me in Mes), 0.32 ppm (d, 3H, $^3J_{HH}$ = 2.8 Hz, SiMe).

2.5. X-ray Crystallographic Data

Table 2.2. Crystallographic data for **3a** and **4**.

Compound	1	2
formula	C$_{28}$H$_{42}$B$_2$N$_2$	C$_{29}$H$_{41}$N$_2$B$_2$F$_3$O$_3$S
formula weight	532.12	576.32
crystal system	monoclinic	orthorhombic
Space Group	$P2_1/c$	$Pnma$
a (Å)	10.5280(2)	18.1783(3)
b (Å)	21.2551(4)	17.8683(3)
c (Å)	15.0977(3)	9.80200(10)
α (deg)	--	--
β (deg)	96.2795(13)	--
γ (deg)	--	--
V (Å^3)	3358.2(11)	3183.84(8)
Z	4	4
ρ_{calcd} (g cm^{-3})	1.035	1.202
Abs coeff (mm^{-1})	0.473	1.311
T (K)	173	173
$2\theta_{max}$ (°)	67.7	67.8
Total Data	22040	21558
Unique data (R$_{int}$)	6165 (0.049)	3336 (0.042)
Obs data [I>2(σ(I)]	4508	2950
Params	391	219
R$_1$ [I>2(σ(I)][a]	0.060	0.076
wR$_2$ [all data][a]	0.178	0.229
Max/min $\Delta\rho$ (e$^-$Å^{-3})	0.49/–0.41	0.47/–0.242

[a] $R_1 = \Sigma||F_o| - |F_c||/\Sigma|F_o|$; $wR_2 = [\Sigma w(F_o^2 - F_c^2)^2/\Sigma w(F_o^4)]^{1/2}$

2.6 References

1. a) Brown, H. C.; Rao, B. C. S. *J. Am. Chem. Soc.* **1956**, *78*, 5694-5695. b) Köster, R. *Liebigs Ann. Chem.* **1958**, *618*, 31-43.

2. a) Magano, J.; Dunetz, J. R. *Org. Process Res. Dev.* **2012**, *16*, 1156-1184. b) Clarke, M. L.; Roff, G. J. *The Handbook of Homogeneous Hydrogenation*, Wiley-VCH Verlag GmbH, 2008, pp. 413-454.

3. a) Suzuki, A. *J. Organomet. Chem.* **1999**, *576*, 147-168. b) Lennox, A. J. J.; Lloyd-Jones, G. C. *Chem. Soc. Rev.* **2014**, *43*, 412-443.

4. Hadlington, T. J.; Hermann, M.; Frenking, G.; Jones, C. *J. Am. Chem. Soc.* **2014**, *136*, 3028-3031.

5. Schneider, J.; Sindlinger, C. P.; Freitag, S. M.; Schubert, H.; Wesemann, L. *Angew. Chem. Int. Ed.* **2017**, *56*, 333-337.

6. a) Arrowsmith, M.; Hadlington, T. J.; Hill, M. S.; Kociok-Köhn, G. *Chem. Commun.* **2012**, *48*, 4567-4569. b) Fohlmeister, L.; Stasch, A. *Chem. Eur. J.* **2016**, *22*, 10235-10246.

7. a) Gudat, D. *Acc. Chem. Res.* **2010**, *43*, 1307-1316. b) Chong, C. C.; Kinjo, R. *ACS Catal.* **2015**, *5*, 3238-3259.

8. a) Mukherjee, D.; Osseili, H.; Spaniol, T. P.; Okuda, J. *J. Am. Chem. Soc.* **2016**, *138*, 10790-107930. b) Jakhar, V. K.; Barman, M. K.; Nembenna, S. *Org. Lett.* **2016**, *18*, 4710-4713. c) Bismuto, A.; Thomas, S. P.; Cowley, M. J. *Angew. Chem. Int. Ed.* **2016**, *55*, 15356-15359. d) Blake, A. J.; Cunningham, A.; Ford, A.; Teat, S. J.; Woodward, S. *Chem. Eur. J.* **2000**, *6*, 3586-3594.

9. a) Lummis, P. A.; Momeni, M. R.; Lui, M. W.; McDonald, R.; Ferguson, M. J.; Miskolzie, M.; Brown, A.; Rivard, E. *Angew. Chem. Int. Ed.* **2014**, *53*, 9347-9351. For reviews on zinc hydrides and main group element hydrides, see: b) Wiegand, A.-K.; Rit, A.; Okuda, J. *Coord. Chem. Rev.* **2016**, *314*, 71-82. c) Roy, M. M. D.; Omaña, A. A.; Wilson, A. S. S.; Hill, M. S.; Aldridge, S.; Rivard, E. *Chem. Rev.* **2021**, *121*, 12784-12965.

10. Roy, M. M. D.; Ferguson, M. J.; McDonald, R.; Rivard, E. *Chem. Eur. J.* **2016**, *22*, 18236-18246.

11. a) Hering-Junghans, C.; Andreiuk, P.; Ferguson, M. J.; McDonald, R; Rivard, E. *Angew. Chem. Int. Ed.* **2017**, *56*, 6272-6275. b) Roy, M. M. D.; Baird, S. R.; Dornsiepen, E.; Paul, L. A.; Miao, L.; Ferguson, M. J.; Zhou, Y.; Siewert, I.; Rivard, E. *Chem. Eur. J.* **2021**, *27*, 8572-8579.

12. Stephan, D. W. *Science* **2016**, *354*, aaf7229.

13. Légaré, M.-A.; Courtemanche, M.-A.; Rochette, É.; Fontaine, F.-G. *Science* **2015**, *349*, 513-516.

14. Lui, M. W.; Paisley, N. R.; McDonald, R.; Ferguson, M. J.; Rivard, E. *Chem. Eur. J.* **2016**, *22*, 2134-2145.

15. a) Kuhn, N.; Bohnen, H.; Kreutzberg, J.; Bläser, D.; Boese, R. *J. Chem. Soc., Chem. Commun.* **1993**, 1136-1137. b) Knappke, C. E. I.; Arduengo III, A. J.; Jiao, H.; Neudörfl, J.-M.; von Wangelin, A. J. *Synthesis* **2011**, 3784-3795. c) Al-Rafia, S. M. I.; Malcolm, A. C.; Liew, S. K.; Ferguson, M. J.; McDonald, R.; Rivard, E. *Chem. Commun.* **2011**, *47*, 6987-6989. d) Powers, K.; Hering-Junghans, C.; McDonald, R.; Ferguson, M. J.; Rivard, E. *Polyhedron* **2016**, *108*, 8-14.

16. For recent review articles see: a) Roy, M. M. D.; Rivard, E. *Acc. Chem. Res.* **2017**, *50*, 2017-2025. b) Crocker, R. D.; Nguyen, T. V. *Chem. Eur. J.* **2016**, *22*, 2208-2213. c) Saptal, V. B.; Bhanage, B. M. *ChemSusChem* **2016**, *9*, 1980-1985. d) Ghadwal, R. S. *Dalton Trans.* **2016**, *45*, 16081-16095. See also: e) Wang, Q.; Zhao, W.; He, J.; Zhang, Y.; Chen, E. Y.-X. *Macromolecules* **2017**, *50*, 123-136. f) Wang, Y.-B.; Wang, Y.-M.; Zhang, W.-Z.; Lu, X.-B. *J. Am. Chem. Soc.* **2013**, *135*, 11996-12003. g) Blümel, M.; Noy, J.-M.; Enders, D.; Stenzel, M. H.; Nguyen, T. V. *Org. Lett.* **2016**, *18*, 2208-2211. h) Naumann, S.; Thomas, A. W.; Dove, A. P. *Angew. Chem. Int. Ed.* **2015**, *54*, 9550-9554.

17. For a related silylated NHO, see: Ghadwal, R. S.; Reichmann, S. O.; Englehardt, F.; Andrada, D. M.; Frenking, G. *Chem. Commun.* **2013**, *49*, 9440-9442.

18. Despite the low quality of the X-ray data, atom connectivity in **3a** was confirmed. Closer inspection of the difference map revealed a minor germanium containing

component, IPrCH–GeH, which was allowed to refine freely with an occupancy of 4.5 %; the bulk sample of **3b** for which yield and analytical data was obtained did not have the Ge impurity.

19. Ghadwal, R. S.; Schürmann, C. J.; Andrada, D. M.; Frenking, G. *Dalton Trans.* **2015**, *44*, 14359-14367.

20. Petz, W.; Öxler, F.; Neumüller, B.; Tonner, R.; Frenking, G. *Eur. J. Inorg. Chem.* **2009**, 4507-4517.

21. Lafage, M.; Pujol, A.; Saffon-Merceron, N.; Mézailles, N. *ACS Catal.* **2016**, *6*, 3030-3035.

22. For recent work involving hybrid *N*-heterocyclic olefin-phosphine (NHOP) ligands as four-electron donors, see: a) Paisley, N. R.; Lui, M. W.; McDonald, R.; Rivard, E. *Dalton Trans.* **2016**, *45*, 9860-9870. b) Lui, M. W.; Shynkaruk, O.; Oakley, M. S.; Sinelnikov, R.; McDonald, R.; Ferguson, M. J.; Klobukowski, M.; Rivard, E. *Dalton Trans.* **2017**, *46*, 5946-5954.

23. Weigend, F.; Ahlrichs, R. *Phys. Chem. Chem. Phys.* **2005**, 7, 3297-3305.

24. Courtemanche, M.-A.; Légaré, M.-A.; Maron, L.; Fontaine, F.-G. *J. Am. Chem. Soc.* **2013**, *135*, 9326-9329.

25. Chong, C. C.; Hirao, H.; Kinjo, R. *Angew. Chem. Int. Ed.* **2014**, *54*, 190-194.

26. Sheldrick, G. M. *Acta. Crystallogr. Sect. A* **2015**, *A71*, 3-8.

27. Sheldrick, G. M. *Acta. Crystallogr. Sect. C* **2015**, *C71*, 3-8.

28. Frisch, M. J.; Trucks, G. W.; Schlegel, H. B.; Scuseria, G. E.; Robb, M. A.; Cheeseman, J. R.; Scalmani, G.; Barone, V.; Petersson, G. A.; Nakatsuji, H.; Li, X.; Caricato, M.; Marenich, A. V.; Bloino, J.; Janesko, B. G.; Gomperts, R.; Mennucci, B.; Hratchian, H. P.; Ortiz, J. V.; Izmaylov, A. F.; Sonnenberg, J. L.; Williams-Young, D.; Ding, F.; Lipparini, F.; Egidi, F.; Goings, J.; Peng, B.; Petrone, A.; Henderson, T.; Ranasinghe, D.; Zakrzewski, V. G.; Gao, J.; Rega, N.; Zheng, G.; Liang, W.; Hada, M.; Ehara, M.; Toyota, K.; Fukuda, R.; Hasegawa, J.; Ishida, M.; Nakajima, T.; Honda, Y.; Kitao, O.; Nakai, H.; Vreven, T.; Throssell, K.; Montgomery, J. A., Jr.; Peralta, J. E.; Ogliaro, F.; Bearpark, M. J.; Heyd, J. J.; Brothers, E. N.; Kudin, K. N.; Staroverov, V. N.; Keith, T. A.; Kobayashi, R.; Normand, J.; Raghavachari, K.; Rendell, A. P.; Burant, J. C.; Iyengar, S. S.; Tomasi, J.; Cossi, M.; Millam, J. M.; Klene, M.; Adamo, C.; Cammi, R.; Ochterski, J. W.; Martin, R. L.; Morokuma, K.; Farkas, O.; Foresman, J. B.; Fox, D. J. Gaussian 16, Revision A.03; Gaussian, Inc.: Wallingford, CT, **2016**.

29. Becke, A. D. *Phys. Rev. A* **1988**, *38*, 3098-3100.

30. a) Glendening, E. D.; Weinhold, F. *J. Comput. Chem.* **1998**, *19*, 593-609. b) Glendening, E. D.; Weinhold, F. *J. Comput. Chem.* **1998**, *19*, 610-627.

31. a) Hadlington, T. J.; Hermann, M.; Frenking, G.; Jones, C. *J. Am. Chem. Soc.* **2014**, *136*, 3028-3031. b) Arrowsmith, M.; Hadlington, T. J.; Hill, M. S.; Kociok-Köhn, G. *Chem. Commun.* **2012**, *48*, 4567-4569/

32. Chong, C. C.; Hirao, H.; Kinjo, R. *Angew. Chem. Int. Ed.* **2015**, *54*, 190-195.

Chapter 3: *N*-Heterocyclic Olefin-Ligated Palladium(II) Complexes as Pre-Catalysts for Buchwald–Hartwig Aminations

3.1 Introduction

Since the discovery of bottleable *N*-heterocyclic carbenes (NHCs) by Arduengo and coworkers (Chart 3.1, **I**),[1] these carbon-based donors have been used with great success as ligands in metal-mediated catalysis.[2] These studies were followed by the development of abnormal *N*-heterocyclic carbenes (aNHCs, **II**) that strongly coordinate metals through carbanionic backbone (C4 or C5) positions.[3] Furthermore, replacement of one ring-positioned N atom in an NHC for an sp³-hybridized carbon atom yields cyclic(alkyl)amino carbenes (CAACs, **III**), which are better π-acids and π-donors when compared with NHCs (Chart 3.1).[4]
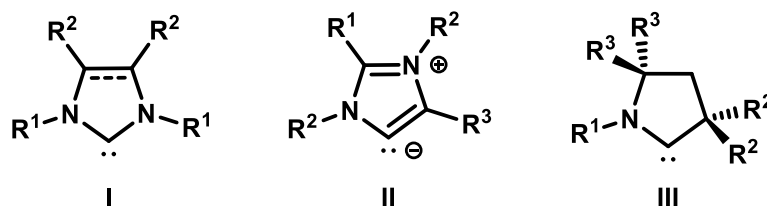
Chart 3.1. Generic Structures of NHCs (**I**), aNHCs (**II**), and CAACs (**III**).

Owing to their strong σ-donating properties and their easily tuneable steric and electronic properties, NHCs have joined phosphines as ligands of choice in palladium-catalyzed cross-coupling reactions.[5,6] The most commonly explored Pd(II)-containing pre-catalysts for cross-coupling are outlined in Chart 3.2, and include the 1:1 $PdCl_2$-ligand complex (**A**),[7] palladium-allyl species (**B**),[8] and generally active pyridine-

enhanced precatalyst preparation stabilization and initiation (PEPPSI) complexes bearing an NHC and 3-chloropyridine (3-Cl-pyr) in a mutually *trans* orientation (**C**).[9]
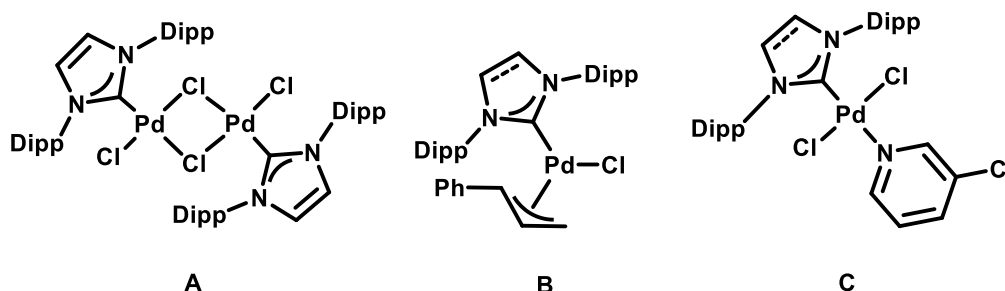
Chart 3.2. Widely investigated Pd(II) pre-catalysts bearing NHC co-ligands; Dipp = 2,6-^{i}Pr$_2$C$_6$H$_3$.

N-Heterocyclic olefins (NHOs) represent an emerging class of carbon-based donors that each contain a polarized, ylidic, alkylidene unit (=CH$_2$ or =CR$_2$) terminally bound to an *N*-heterocyclic carbene fragment (see Scheme 3.1 for contributing resonance forms).[10,11] The first isolable example of an NHO was described by Kaska and coworkers, followed by the example of (MeCNMe)$_2$C=CH$_2$, described by Kuhn and coworkers in 1993,[10,11] with nucleophilic/donor ability at the terminal carbon atom demonstrated.[10-13] Moreover, *N*-heterocyclic olefins are considered to be softer σ-donors than NHCs[13] and might yield stable coordination complexes with the soft Pd(0) centers found during cross-coupling catalysis. While the seminal work by Kuhn and co-workers introduced various NHO•M(CO)$_5$ complexes to the community (M = Cr, Mo and W),[10b] the number of metal complexes comprising NHOs as ligands is still limited, with examples of only W, Au, Ir and Rh complexes known.[12a,13-15] NHOs have also been used to stabilize reactive main group

element bonding environments,[12b,16] and an exciting new direction is the use of NHOs as organocatalysts.[11,17,18]
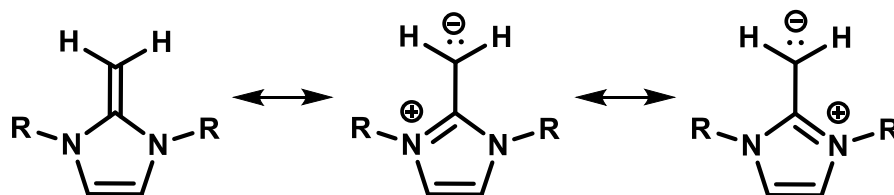
Scheme 3.1. Dominant canonical forms of *N*-heterocyclic olefins (NHOs).

In this Chapter, the synthesis of new *N*-heterocyclic olefin ligands, including those bearing extended backbone π-conjugation and functionalization at the terminal alkylidene group is described. In addition, it is shown that some NHO-Pd(II) complex combinations are viable pre-catalysts for the selective Buchwald-Hartwig C–N cross-coupling of hindered substrates, with evidence for heterogeneous catalysis modulated by Pd nanoparticles.

3.2. Results and Discussion

3.2.1 Synthesis of *N*-Heterocyclic Olefins (NHOs) and their Respective Pd(II) Complexes

In a previous report from the Rivard Group,[13] high yielding one-pot protocols were introduced to form the bulky NHOs ^{Me}IPrCH$_2$ and IPrCH$_2$ [^{Me}IPr = (MeCNDipp)$_2$C; IPr = (HCNDipp)$_2$C; Dipp = 2,6-^{i}Pr$_2$C$_6$H$_3$]. Depending on the approach used, either MeI (reaction i, Scheme 3.2) or the alkylchlorosilane ClCH$_2$SiMe$_3$ (reaction ii, Scheme 3.2) can be used as methylene sources.
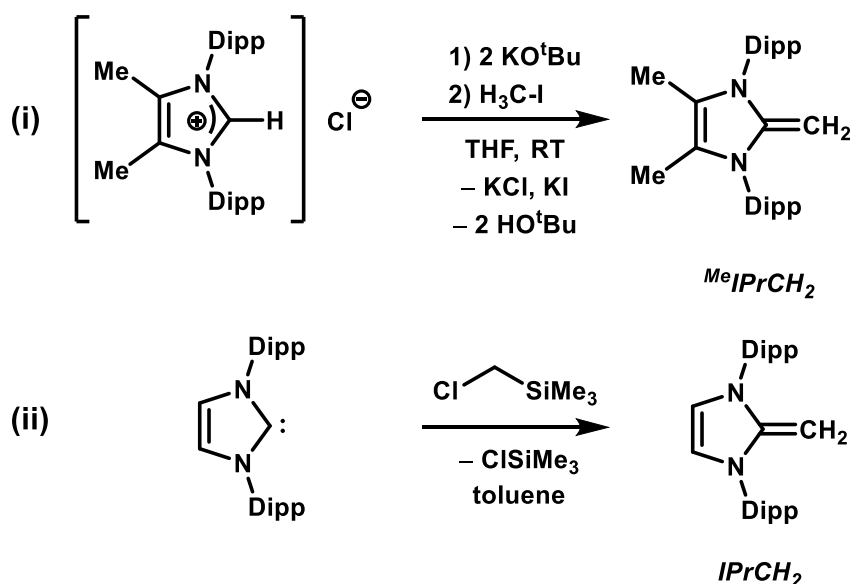
Scheme 3.2. Established synthetic routes towards ^{Me}IPrCH$_2$ (i, top) and IPrCH$_2$ (ii, bottom).

To expand the range of NHOs available and to introduce possibly new (stabilizing) binding modes with late transition metals, a variety of modified NHOs were prepared (Schemes 3.3 and 3.4). The first new ligand candidate synthesized in this work was the butadiene-NHO ^{Me}IPr=CH–CH=CH$_2$ (**1**). The structurally related species IPr=CH–CH=CH$_2$ was prepared by Jacobi von Wangelin and coworkers with nucleophilic character at the exocyclic α- and γ-C atoms postulated.[19,20] In a modified procedure, the known imidazolium salt [^{Me}IPrH]Cl was combined with allyl bromide in the presence of 2 equivalents of KO^{t}Bu to give ^{Me}IPr=CH–CH=CH$_2$ (**1**) in an 84 % yield as a yellow crystalline solid (Scheme 3.3 (iii) and Figure 3.1). Placement of Me groups at the backbone of **1** was designed to suppress possible C–H activation at the 4- or 5-positions in the presence of Pd(II) complex and base; related NHO ligand activation has been noted recently by Schumann and Hering-Junghans.[21] X-ray quality

crystals of **1** were obtained by slow evaporation of a saturated hexanes solution over the course of 24 hours.[22]
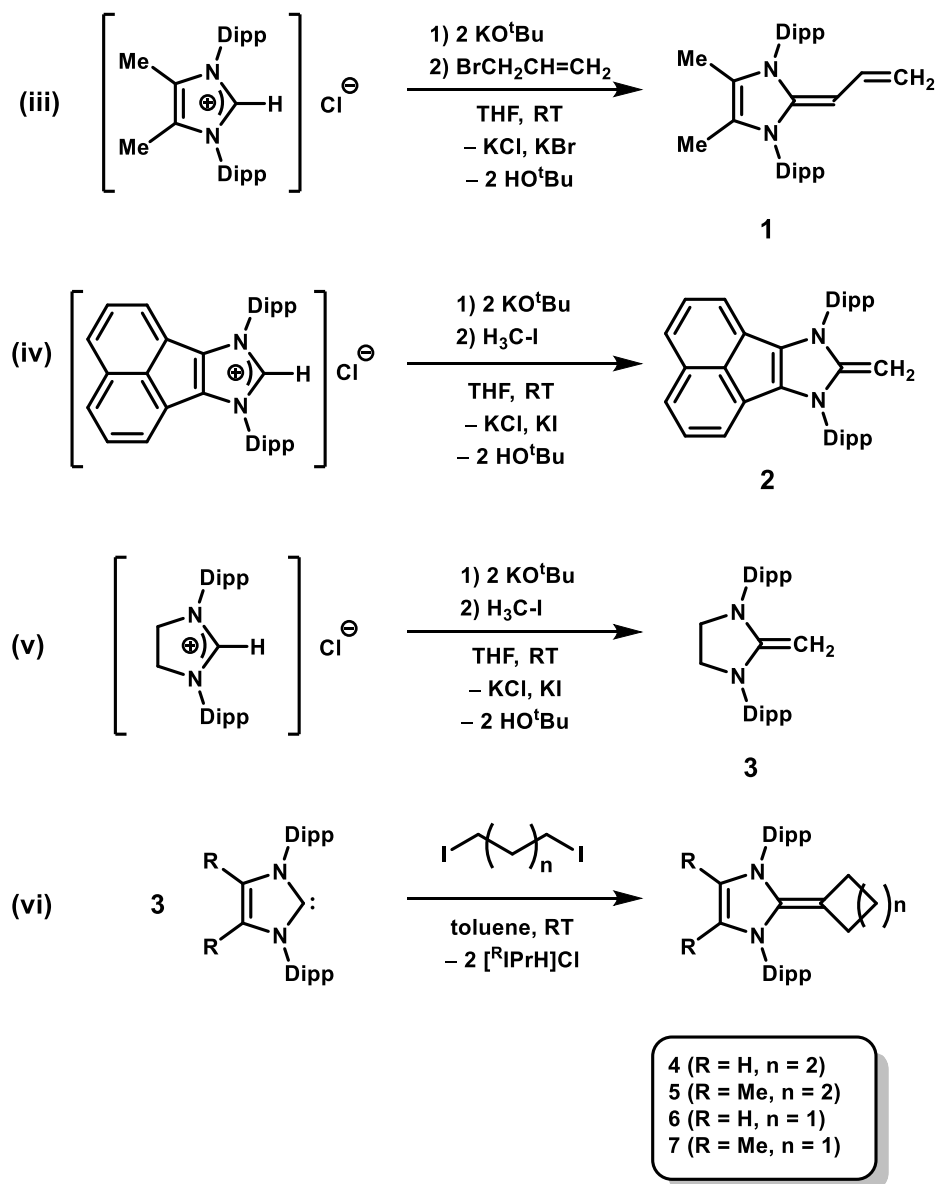
Scheme 3.3. Structurally modified NHOs (**1-7**) discussed in this Chapter.

An *N*-heterocyclic olefin bearing a π-extended acenaphthene backbone[23] IPr(BIAN)CH$_2$ (**2**) was also prepared using an analogous route to that used to obtain **1** (Scheme 3.3, reaction iv). IPr(BIAN)CH$_2$ (**2**) was isolated as a deep blue, air- and moisture-sensitive solid (87 % yield), and X-ray quality crystals were obtained from a benzene/hexanes mixture at 23 °C (Figure 3.1). In a similar fashion, the saturated analogue of IPrCH$_2$, SIPrCH$_2$ (**3**) (SIPr = [(H$_2$CNDipp)$_2$C]), previously reported by Ghadwal and coworkers,[24] was obtained as a colorless crystalline solid (Scheme 3.2) in 70 % yield using the modified one-pot procedure outlined in Scheme 3.3 (reaction v).
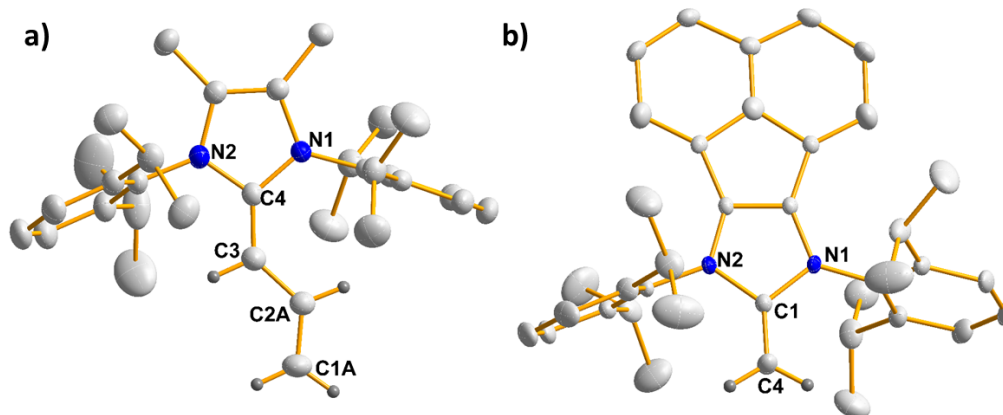
Figure 3.1. a) Molecular structure of ^{Me}IPr=CH-CH=CH$_2$ (**1**) with thermal ellipsoids shown at a 30 % probability level. Hydrogen atoms on the backbone and on the Dipp groups are omitted for clarity. Selected bond lengths [Å] and angles [°] with values belonging to a second molecule in the asymmetric unit in square brackets: C1A–C2A 1.328(3) [1.338(2)], C2A–C3 1.411(3) [1.282(1)], C3–C4 1.369(3) [1.369(3)]; N1–C4–N2 104.17(15) [104.17(15)], C1A–C2A–C3 127.1(3) [125.6(11)]. b) Molecular structure of IPr(BIAN)CH$_2$ (**2**) with thermal ellipsoids shown at a 30 % probability level. Hydrogen atoms on the backbone and on the Dipp groups are omitted for clarity. Selected bond lengths [Å] and angles [°]: C1–C4 1.336(3), N1–C1 1.405(2), N2–C1 1.403(2); N2–C1–N1 105.34(17).

The majority of the NHOs described in this study have been crystallographically characterized and are presented in Figures 3.1-3.3. ^{Me}IPr=CH–CH=CH$_2$ (**1**) shows bond alternation within the exocyclic =CH–CH=CH$_2$ group, as evidenced by shorter C4–C3 [1.369(3) Å] and C2A–C1A [1.328(3) Å] distances (Figure 3.1a) compared to the central C3–C2A bond [1.411(3) Å]. The exocyclic =CH–CH=CH$_2$ unit in **1** is in the same plane as the proximal 5-membered imidazole ring. The structure of the deep blue IPr(BIAN)CH$_2$ (**2**) was also determined by X-ray crystallography (Figure 3.1b) and the exocyclic C1–C4 linkage [1.336(3) Å] is of a typical length for an *N*-heterocyclic olefin;[11,12b] likewise standard metrical parameters for the backbone saturated SIPrCH$_2$ (**3**) are found (Figure 3.2).
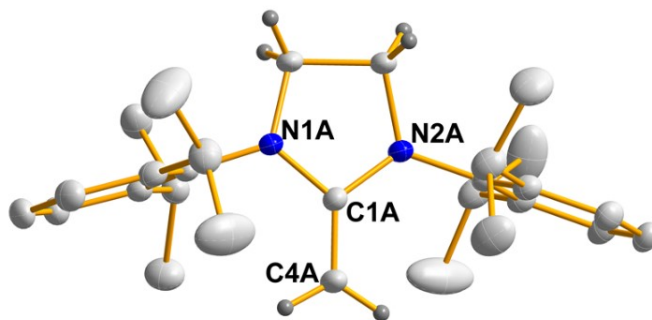
Figure 3.2. Molecular structure of SIPrCH$_2$ (**3**) with ellipsoids drawn at a 30 % probability level. Hydrogen atoms (except on C2A, C3A, and C4A) are omitted for clarity. Selected bond lengths [Å] and angles [°] [four independent molecules in the asymmetric unit]: N1A–C1A 1.3921(16) [1.3847(17), 1.3826(17), 1.3871(16)], N2A–C1A 1.3935(17) [1.3824(17), 1.3892(17), 1.3846(16)], C1A–C4A 1.3346(19) [1.3388(18), 1.3356(19), 1.3365(19)]; N1A–C1A–N2A 106.29(10) [106.66(11), 106.09(11), 106.11(11)].

A series of NHOs bearing ring-fused cycloalkane substituents (compounds **4-7**, Scheme 3.3, reaction vi) were generated in a one-pot procedure by treatment of the requisite 1,5-diiodoalkane with three equivalents of carbene (IPr or ^{Me}IPr) in toluene.

The resulting NHOs were soluble in organic solvents, facilitating their separation from the insoluble imidazolium salt by-product ([IPrH]I or [^{Me}IPrH]I) via filtration. The X-ray crystal structures of the ring-fused compounds IPr=C(CH$_2$)$_4$ (**4**) and IPr=C(CH$_2$)$_3$ (**6**) (Figure 3.3) revealed identical ylidic C=C distances of 1.343(2) Å and 1.3432(21) Å, respectively. The hydrocarbon five-membered ring (=C(CH$_2$)$_4$) in **4** is non-planar, while the related four-membered ring in IPr=C(CH$_2$)$_3$ (**6**) is planar. A recent computational study revealed a high proton affinity of ring-fused NHOs, with their basicity reaching the high-end of "superbasicity" (*e.g.,* absolute proton affinities > 245.3 kcal/mol).[25]
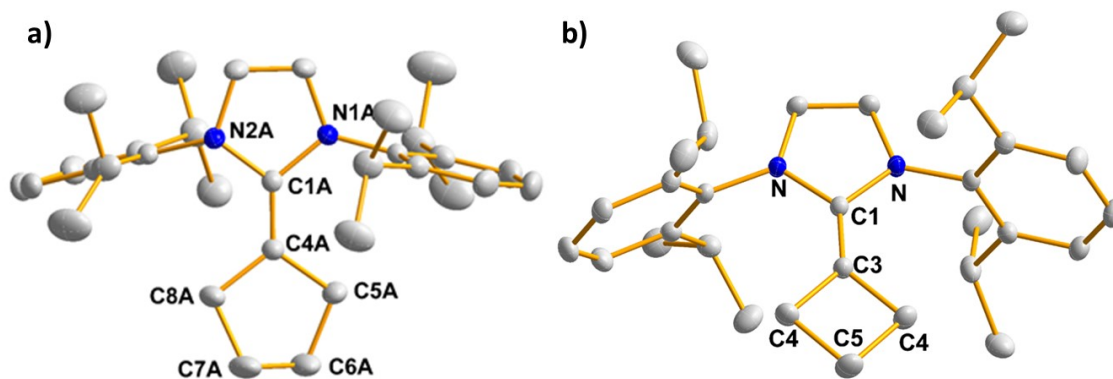
Figure 3.3. a) Molecular structure of IPr=C(CH$_2$)$_4$ (**4**) with thermal ellipsoids shown at a 30 % probability level. Hydrogen atoms are omitted for clarity. Selected bond lengths [Å] and angles [°] with values belonging to a second molecule in the asymmetric unit in square brackets: N1A–C1A 1.414(2) [1.4096(19)], N2A–C1A 1.420(2) [1.4068(19)], C1A–C4A 1.343(2) [1.353(2)], C4A–C5A 1.522(2) [1.521(2)], C6A–C7A 1.446(4) [1.522(2)]; N1A–C1A–N2A 103.98(13) [103.48(13)], C4A–C5A–C6A 103.65(17) [103.79(13)]. b) Molecular structure of IPr=C(CH$_2$)$_3$ (**6**) with ellipsoids drawn at a 30 % probability level. Hydrogen atoms are omitted for clarity. Selected bond lengths [Å] and angles [°]: N–C1 1.4029(12), 1.343(2), C3–C4 1.5182(15), C4–C5 1.5485(17); N–C1–N 103.82(12), C3–C4–C5 88.29(9), C4–C5–C4′ 90.55(13).

To evaluate possible differences in donor capability amongst the NHOs **1-4** and **6**, computations at the B3LYP/6-31G+(d,p) level of density functional theory (DFT) were carried out. As expected, these NHOs possess exocyclic double bonds with substantially polarized terminal C=C π-components, leading to accumulation of negative charge on the exocyclic carbon atom. For IPr(BIAN)CH$_2$ (**2**) and SIPrCH$_2$ (**3**) the charge on the terminal CH_2 carbon atom was computed to be -0.69e and -0.67e, respectively (as determined by a natural population analysis, NPA). In contrast, the corresponding degree of C=C bond polarization in the bicyclic NHOs **4** and **6** is less pronounced, as reflected by lower NPA charges of -0.23e and -0.24e, respectively, and less polarized π-components of the corresponding C=C double bonds according to Natural Bond Orbital (NBO) analysis. In ^{Me}IPr=CH-CH=CH$_2$ (**1**) the largest negative charge (-0.53e) is found on the terminal exocyclic carbon atom, suggesting preferential metal ligation via an end-on mode (*vide infra*; see also Chapter 4).

To determine whether the bicyclic NHOs **4-7** mentioned above were able to act as formal two-electron donors, ^{Me}IPr=C(CH$_2$)$_4$ (**5**) was combined with MeOTf. As expected, this reaction afforded the alkylated product [^{Me}IPrC(Me)(CH$_2$)$_4$]OTf (**8**) (Scheme 3.4 and Figure 3.4).
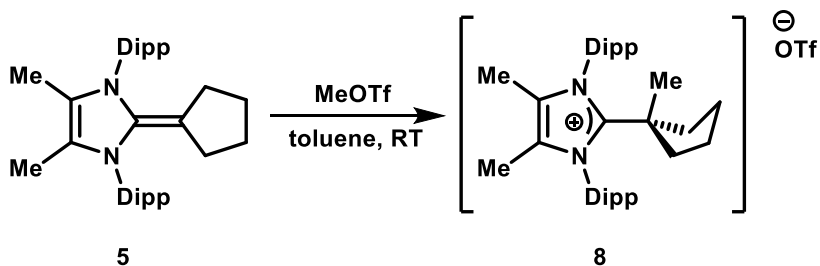
Scheme 3.4. Methylation of $^{Me}IPr=C(CH_2)_4$ (**5**) with MeOTf.
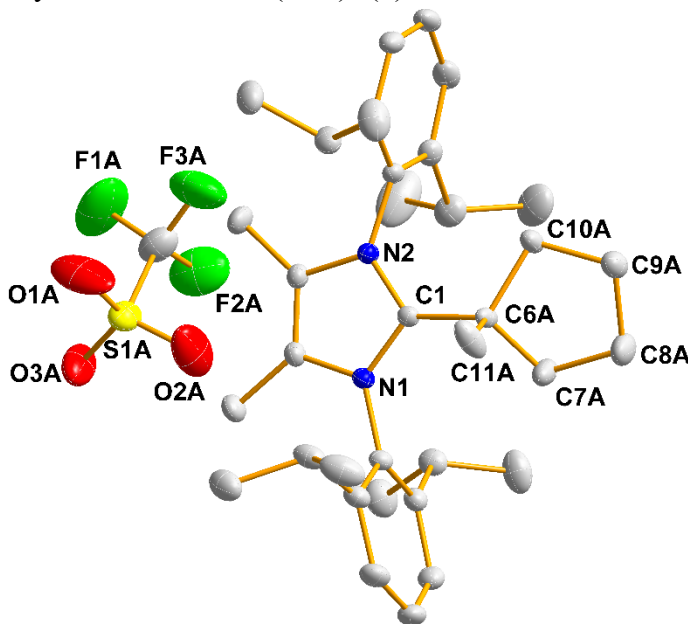
Figure 3.4. Molecular structure of [$^{Me}IPrC(Me)(CH_2)_4$]OTf (**8**) with thermal ellipsoids shown at a 30 % probability level. Hydrogen atoms have been omitted for clarity. Selected bond lengths [Å] and angles [°]: C1-N1 1.3542(17), C1-N2 1.3526(18), C1-C6A 1.546(9), C6A-C11A 1.508(8), C8A-C9A 1.531(8); N2-C1-N1 105.85(12), C1-C6A-C11A 107.7(5), C6A-C10A-C9A 103.9(5).

The ^1H NMR spectrum of $^{Me}IPr=CH-CH=CH_2$ (**1**) shows four distinct resonances for the =CH-CH=CH$_2$-group with the CH proton at the terminal vinylic position being downfield-shifted compared to NHOs **2** and **3**. *N*-Heterocyclic olefins **1-7** show ^1H NMR resonances (in C$_6$D$_6$) consistent with the formulated structures with upfield-positioned terminal methylene =C*H*$_2$ resonances ranging from 2.42 to 2.72 ppm, with the most deshielded environment arising within the π-electron-rich

NHO IPr(BIAN)CH$_2$ (**2**). The resulting ^{13}C{^{1}H} NMR shifts for the NHC-appended methylene carbon atoms (=CR$_2$) range from 48.3 ppm in IPr(BIAN)CH$_2$ (**2**) to 75.3 ppm for the bicyclic NHO ^{Me}IPr=C(CH$_2$)$_4$ (**5**), showing that NHOs **1-7** have varying ylidic character about the methylene carbon atoms.

With an expanded library of *N*-heterocyclic olefin ligands in hand, their coordinating ability towards Pd(II) centers was explored, with the ultimate goal of accessing suitable pre-catalysts for C–N bond formation (*e.g.,* Buchwald-Hartwig amination). The first Pd-NHO was prepared by combining a slight molar excess of ^{Me}IPrCH$_2$ with *trans*-[Cl$_2$Pd(NCPh)$_2$] in toluene, leading to the deposition of a red crystalline precipitate. This product was identified by X-ray crystallography (Figure 3.5) as the centrosymmetric μ-Cl-bridged dimer [(^{Me}IPrCH$_2$)PdCl(μ-Cl)]$_2$ (**9**) (Scheme 3.5). The most drastic structural change within the NHO ligand upon coordination is elongation of the once terminal C=C bond from a length of 1.349(2) Å[13] to a single bond C1-C4 distance of 1.453(3) Å in **9**, consistent with transfer of exocyclic C=C π-electron density from ^{Me}IPrCH$_2$ to Pd. The resulting coordinative Pd1−C4 distance of 2.026(2) Å in **9** is *ca*. 0.07 Å longer than in the Pd–C bonds of the corresponding NHC-capped PdCl$_2$ complex [(IPr)Pd(μ-Cl)]$_2$ [1.955(3) Å], which retains a similar overall geometry as in **9**.[8,26]
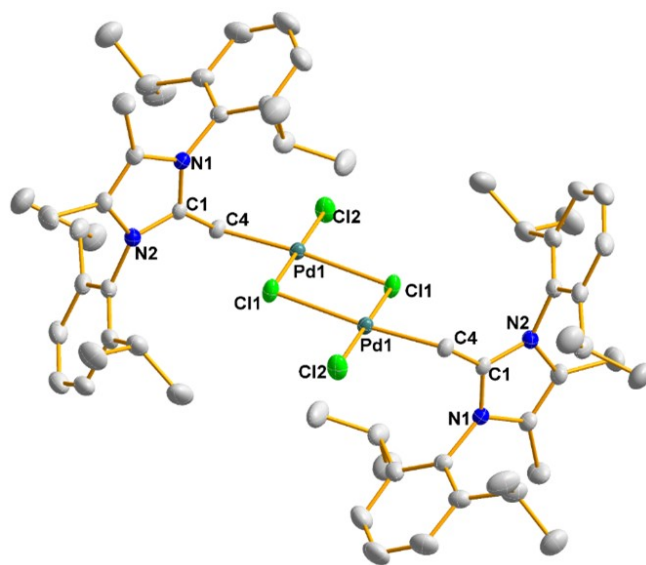
Figure 3.5. Molecular structure of [(^{Me}IPrCH$_2$)PdCl(μ-Cl)]$_2$ (**9**) with ellipsoids drawn at a 30 % probability level. Hydrogen atoms are omitted for clarity. Selected bond lengths [Å] and angles [°]: Pd1-C4 2.026(2), Pd1-Cl2 2.3002(6), Pd1-Cl1 2.3169(6), N1-C1 1.352(3), N1-C2 1.403(3), C1-C4 1.453(3); N1-C1-N2 106.66(18), C1-C4-Pd1 118.69(14).

Prior work by Organ and co-workers revealed that their (NHC)PdCl$_2$(3-Cl-pyr) "PEPPSI" complexes were active in C–N bond forming catalysis, and they selectively achieved either mono- or diarylation of primary amines (ArNH$_2$) depending on the choice of NHC and base.[27] Given the lower steric bulk of NHOs in relation to NHCs and possibly enhanced soft-soft NHO-Pd(0) interactions during catalysis, the potential pre-catalyst [(^{Me}IPrCH$_2$)PdCl$_2$(3-Cl-pyr)] (**10**) was prepared by addition of 3-chloropyridine to a solution of **9** in CH$_2$Cl$_2$ (Scheme 3.5).
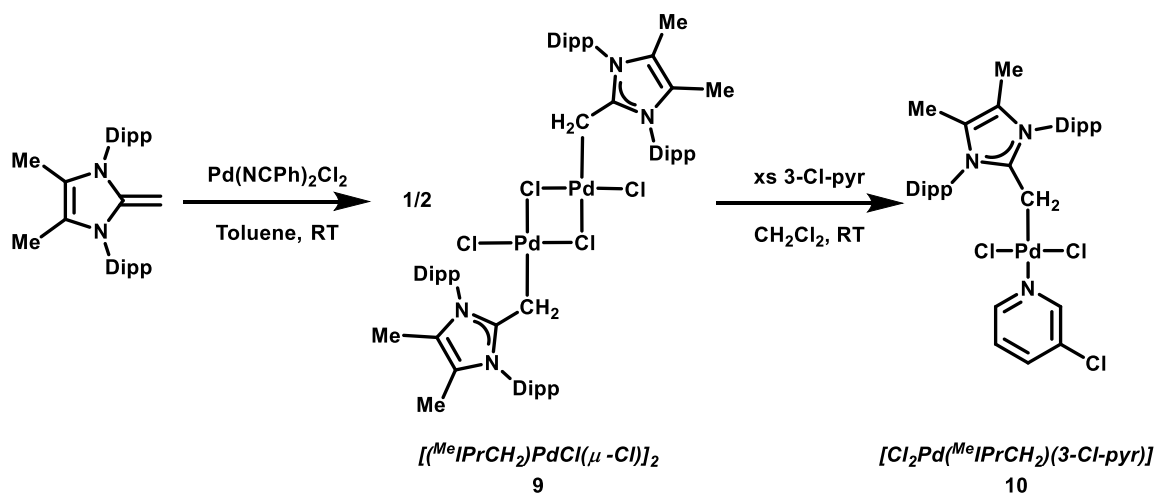
Scheme 3.5. Synthesis of [(^{Me}IPrCH$_2$)PdCl(μ-Cl)]$_2$ (**9**) and [(^{Me}IPrCH$_2$)PdCl$_2$(3-Cl-pyr)] (**10**).

After work-up of the reaction mixture, including product recrystallization from CH$_2$Cl$_2$/hexanes (−30 °C), yellow X-ray quality crystals of [(^{Me}IPrCH$_2$)PdCl$_2$(3-Cl-pyr)] (**10**) were obtained in 67 % yield (Figure 3.6). The ligating Pd−C$_{NHO}$ interaction in [(^{Me}IPrCH$_2$)PdCl$_2$(3-Cl-pyr)] (**10**) [2.043(6) Å] is the same length (within experimental error) as in the pyridine-free precursor **9**, while the *trans*-disposed Pd–N$_{3\text{-Cl-pyr}}$ bond has a length [2.137(6) Å] that is the same as the related Pd–N distance of 2.137(2) Å in the *N*-heterocyclic carbene complex [(IPr)PdCl$_2$(3-Cl-pyr)].[9a]
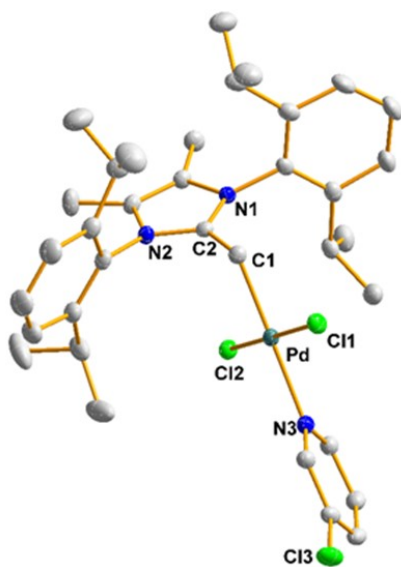
Figure 3.6. Molecular structure of [(^{Me}IPrCH$_2$)PdCl$_2$(3-Cl-pyr)] (**10**) with thermal ellipsoids shown at a 30 % probability level. Hydrogen atoms have been omitted for clarity. Selected bond lengths [Å] and angles [°]: N1-C2 1.354(5), N2-C2 1.351(5), C1-C2 1.448(7), Pd1-N3 2.137(6), Pd1-C1 2.043(6); N2-C2-N1 107.0(3), C2-C1-Pd1 116.7(3).

IPr(BIAN)CH$_2$ (**2**) adopts parallel coordination chemistry as outlined for ^{Me}IPrCH$_2$, which enabled the stepwise formation of the red complex [{IPr(BIAN)CH$_2$}PdCl(μ-Cl)]$_2$ (**11**) (Figure 3.7) and its yellow 3-chloropyridine adduct [{IPr(BIAN)CH$_2$}PdCl$_2$(3-Cl-pyr)] (**12**) (Scheme 3.6 and Figure 3.8). The synthesis of the dimeric NHO-PdCl$_2$ adduct **11** proceeded in a low isolated yield of 31 %, and despite repeated attempts, this compound routinely contained *ca.* 10 % unknown impurities; thus the 3-chloropyridine adduct **12** was prepared from *in situ* generated **11**.
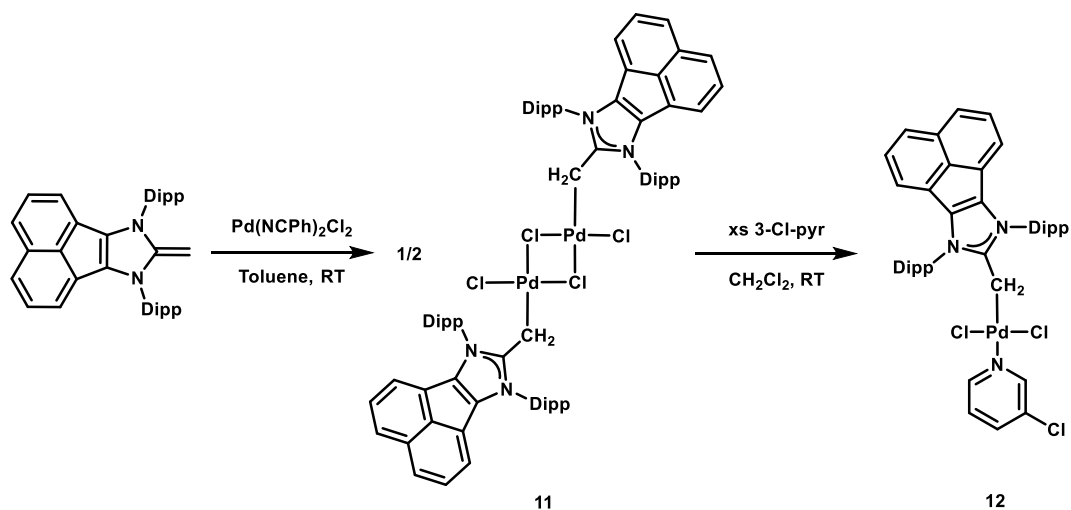
Scheme 3.6. Synthesis of [{IPr(BIAN)}PdCl(μ-Cl)]₂ (**11**) and [{IPr(BIAN)}PdCl₂(3-Cl-pyr)] (**12**).

Despite the change in the structure of the coordinating NHO, the metrical parameters involving the Pd center in the IPr(BIAN)CH₂ complexes **12** were similar to its ^{Me}IPrCH₂ analogue (Figure 3.6). Our attempts to yield isolable Pd(II) complexes between the ring-fused NHOs **4-7** and Pd(II) precursors gave no reaction in each case; this observation is likely due to the small steric pocket that would result upon coordinating **4-7** to Pd (*vide supra*).
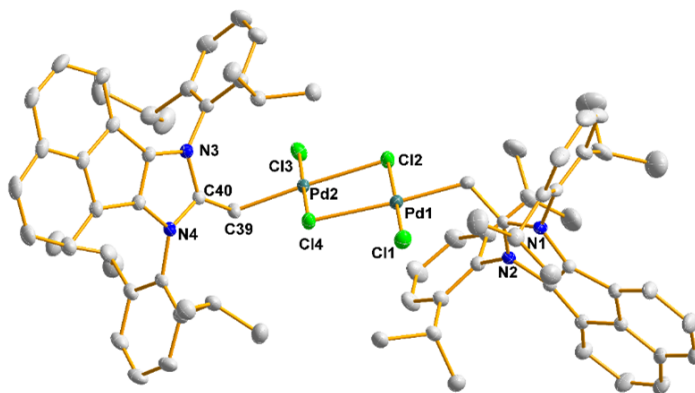
Figure 3.7. Molecular structure of [{IPr(BIAN)}PdCl(μ-Cl)]₂ (**11**) with ellipsoids drawn at a 30 % probability level. Hydrogen atoms are omitted for clarity. Selected bond lengths [Å] and angles [°]: N1-C2 1.364(3), N2-C2 1.364(3), Cl1-Pd1 2.2916(6), Cl2-Pd1 2.3462(6), Cl2-Pd2 2.4473(6), Cl3-Pd2 2.3000(6), Cl4-Pd2 2.3245(6), Cl4-Pd1 2.4738(6), Pd1-C1 2.028(2), Pd2-C39 2.033(2), C1-C2 1.465(3), N3-C40 1.364(3), N4-C40 1.361(3), C39-C40 1.458(3); N2-C2-N1 107.32(19), N4-C40-N3 107.69(19), C2-C1-Pd1 116.99(16), C40-C39-Pd2 116.45(16).
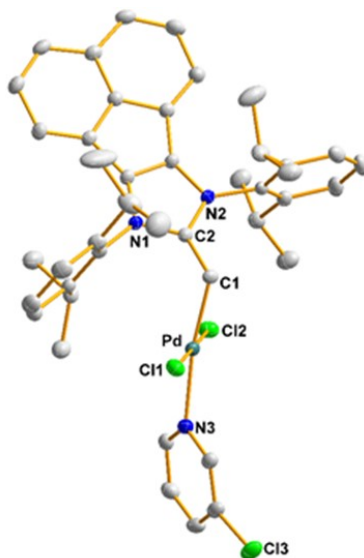
Figure 3.8. Molecular structure of [{IPr(BIAN)}PdCl₂(3-Cl-pyr)] (**12**) with thermal ellipsoids shown at a 30 % probability level. Hydrogen atoms have been omitted for clarity. Selected bond lengths [Å] and angles [°]: N1-C2 1.368(3), N2-C2 1.373(3), C1-C2 1.447(3), Pd1-C1 2.045(2), Pd1-N3 2.147(2); N1-C2-N2 107.41(19), C1-Pd1-N3 171.65(9), C2-C1-Pd1 120.09(17).

$^{\text{Me}}$IPr=CH-CH=CH$_2$ (**1**) was also complexed with Pd(II) centers in order to verify if η^1-coordination occurs via the α- or γ-position of the NHO, or whether an allyl-type η^3-coordination mode prevails. It was also hoped that during catalysis, the presence of an added olefinic unit could lead to Pd(0) complex stabilization via metal to C=C π^* back-bonding. When complex **1** was combined in toluene with *trans*-[Cl$_2$Pd(NCPh)$_2$], the formation of a red precipitate (presumably [($^{\text{Me}}$IPrCHCHCH$_2$)PdCl(μ-Cl)]$_2$, *vide infra*) was observed. This compound was difficult to purify in a consistent fashion (*cf.* compound **11** above), thus crude samples of this complex were subsequently combined with an excess of 3-chloropyridine to yield [($^{\text{Me}}$IPrCHCHCH$_2$)PdCl$_2$(3-Cl-pyr)] (**13**) as an analytically pure red solid in a 44 % yield (Scheme 3.7). As shown in Figure 3.9, coordination of the NHO **1** to Pd is achieved through the less sterically hindered γ-position with a Pd–C distance of 2.0393(18) Å.
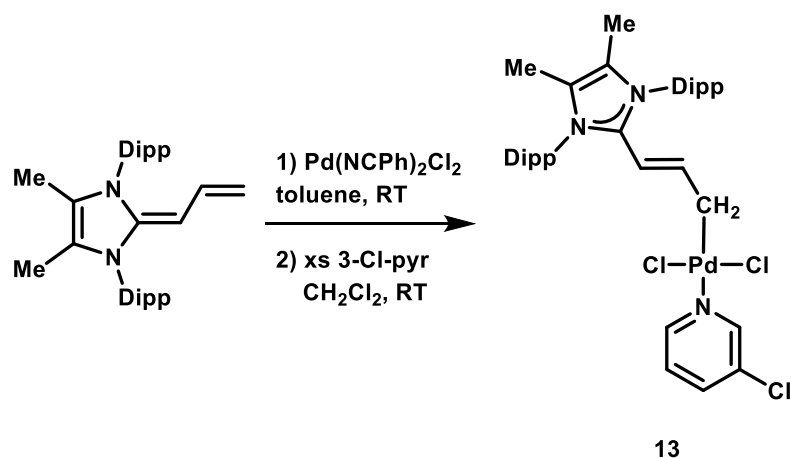
Scheme 3.7. Synthesis of [($^{\text{Me}}$IPrCHCHCH$_2$)PdCl$_2$(3-Cl-pyr)] (**13**).
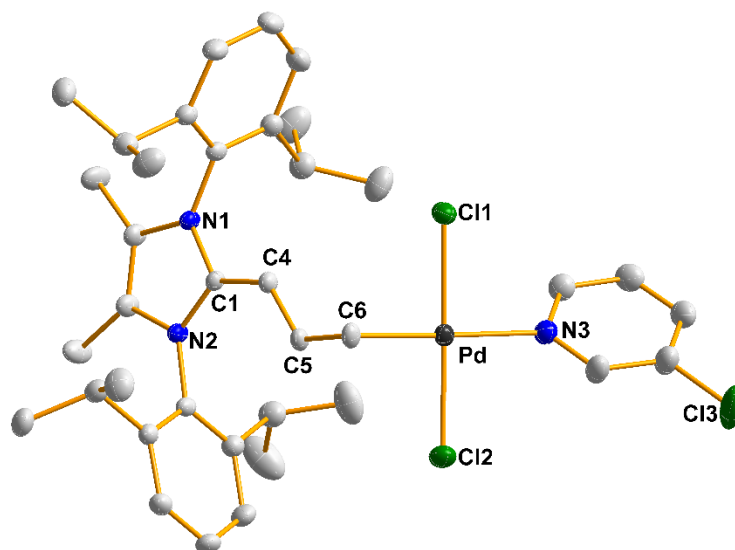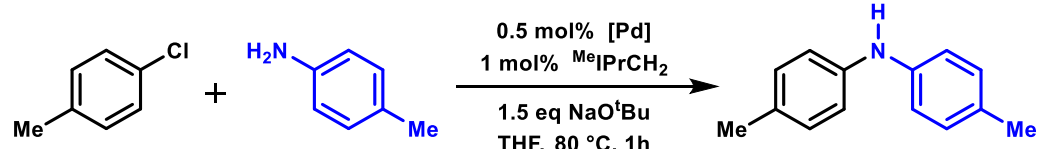
Figure 3.9. Molecular structure of [(^{Me}IPrCHCHCH$_2$)PdCl$_2$(3-Cl-pyr)] (**13**) with thermal ellipsoids shown at a 30 % probability level. Hydrogen atoms are omitted for clarity. Selected bond lengths [Å] and angles [°]: N1-C1 1.353(2), N2-C1 1.348(2), C1-C4 1.433(2), C4-C5 1.353(2), C5-C6 1.453(2), C6-Pd 2.0393(18), Pd-N3 2.1487(1); N2-C1-N1 106.28(13), C5-C6-Pd 103.23(12).

3.2.2. Catalytic Buchwald-Hartwig Aminations

Motivated by the ability of (NHC)PdCl$_2$(3-Cl-pyr) complexes to act as effective pre-catalysts for cross-coupling,[9,27] initial efforts were focused on screening the (NHO)PdCl$_2$(3-Cl-pyr) analogues **12** and **13** for C–N bond catalysis. Upon examining cross-coupling with the test substrates *p*-toluidine (4-methylaniline) and 4-chlorotoluene, no catalytic activity in the presence of pre-catalysts **12** and **13** was observed when 0.5 mol% of pre-catalyst was reacted for 1 hour at 80 °C, with sodium *tert*-butoxide acting as a base. The choice of solvent did not change this outcome whether the reaction was performed in THF, toluene, or 1,4-dioxane. With the goal of preparing more active homogeneous Pd(0) complexes *in situ*, catalyst mixtures derived from mixing the Pd sources [Pd(cinnamyl)Cl]$_2$, Pd$_2$(dba)$_3$ (dba =

dibenzylideneacetone), $Pd(OAc)_2$ or $PdCl_2$ with two equivalents of the common NHO

donor, $^{Me}IPrCH_2$ in THF (80 °C, NaO^{t}Bu) were evaluated for catalytic activity. As

outlined in Table 3.1, this general procedure led to the efficient catalytic coupling of

p-toluidine and 4-chlorotoluene. Based on an average of three runs per Pd source, it

was found that the highest conversion, along with the best reproducibility, occurred

with the [Pd(cinnamyl)Cl]$_2$/$^{Me}IPrCH_2$ pre-catalyst mixture (93 ± 5 % conversion after

1 hour at 80 °C). Attempts to facilitate the reduction of Pd(II) complexes to Pd(0) via

addition of NEt$_3$ were made,[28] however, only marginal improvement in the case of

$PdCl_2$ as a metal source was found (Table 3.1, entries 5 and 6).

Table 3.1. Optimization of palladium source for the cross-coupling of p-toluidine and 4-chlorotoluene.

Entry	Palladium Source	Yield [%][b]
1	[Pd(cinnamyl)$_2$Cl]$_2$	93(5)
2	Pd$_2$(dba)$_3$	85(15)
3	Pd(OAc)$_2$	41(7)
4	Pd(OAc)$_2$^{a}	39(6)
5	PdCl$_2$	31(15)
6	PdCl$_2$^{a}	44(4)
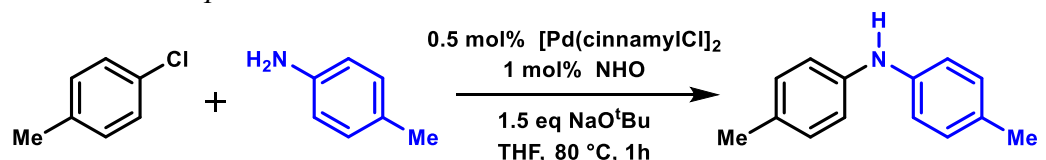
a) 0.5 mol% NEt$_3$ were used b) Yield determined by ^{1}H NMR using 1,3,5-trimethoxybenzene as an internal standard. (+/-) in parentheses for triplicate runs

The influence of different NHO ligands on the catalytic activity when

partnered with [Pd(cinnamyl)Cl]$_2$ as a common Pd source was explored (Table 3.2).

In these trials, the influence of the saturation of the imidazole backbone (*cf.* entry 4), on appending π-extended units (entries 2 and 5), and upon substitution at the terminal methylidene group (=CH$_2$ vs. a ring-fused =C(CH$_2$)$_4$ unit; entries 1 and 3) were examined. It was found that NHOs with an unsaturated backbone showed comparably excellent catalytic activity (> 93 % conversion after 1 hour, 80 °C, NaO^{t}Bu), with the exception of IPr(BIAN)CH$_2$ (**2**), which only facilitated the coupling of *p*-toluidine with 4-chlorotoluene up to a conversion of 9 ± 2 % (Table 3.2, entry 5). As a result, ^{Me}IPrCH$_2$ was selected as the ligand of choice for all future cross-coupling trials as it is a commonly used NHO that can be synthesized easily on a > 20 g scale. The ability of ^{Me}IPr, the NHC analogue to ^{Me}IPrCH$_2$, to perform the cross-coupling of *p*-toluidine and 4-chlorotoluene was compared with the NHO. The ^{Me}IPr/[Pd(cinnamyl)Cl]$_2$ pre-catalyst system promoted the reaction quickly, with complete conversion after 20 minutes under the same conditions.

The role of solvent on this cross-coupling was also explored, and it was found that THF (Table 3.3) consistently gave better yields for the *p*-toluidine/4-chlorotoluene coupling than reactions conducted in 1,4-dioxane or toluene. It should also be mentioned that the use of pre-dried THF from a commercial solvent-purification system further dried over sodium/benzophenone and distilled gave the best yields, whereas if one does not take care to exclude water/oxygen from the THF, then a lowering of conversion occurred (<47 % yield for conditions in entry 4, Table 3.3).
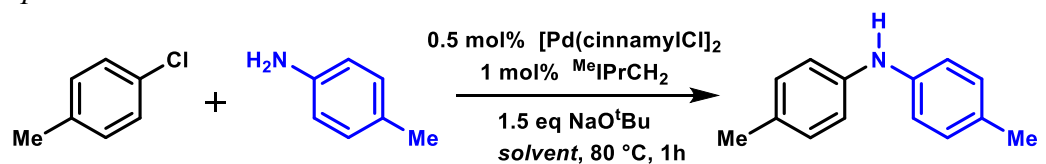
Table 3.2. Optimization of the NHO ligand used for the cross-coupling of 4-chlorotoluene and *p*-toluidine.

Entry	Ligand[a]	Yield [%][b]
1	^{Me}IPrCH$_2$	93(5)
2	^{Me}IPr=CH-CH=CH$_2$	96(4)
3	^{Me}IPrC(CH$_2$)$_4$	97(3)
4	SIPrCH$_2$	7(7)
5	IPr(BIAN)$_2$	99(1)
6	^{Me}IPr[a]	44(4)[c]

a) 1 mol% was used; b) Yield determined by ^{1}H NMR using 1,3,5-trimethoxybenzene as an internal standard. (+/-) in parentheses for triplicate runs; c) Conversion completed after 20 minutes.

Table 3.3. Optimization of the solvent used for the cross-coupling of 4-chlorotoluene and *p*-toluidine.

Entry	Solvent	Yield [%][a]
1	1.4-dioxane	63(2)
2	THF	93(5)
3	toluene	17(5)
4	THF[b]	47(7)

a) Yield determined by ^{1}H NMR using 1,3,5-trimethoxybenzene as an internal standard. (+/-) in parentheses for triplicate runs. b) THF was not distilled from sodium and benzophenone.

The abovementioned catalyst-screening trials led to the selection of [Pd(cinnamyl)Cl]$_2$/^{Me}IPrCH$_2$ as the preferred pre-catalyst for Buchwald–Hartwig aminations, and subsequent studies involved expanding the scope of this reaction. The motivating postulates behind exploring NHOs as ligands for this chemistry were: a) the soft nature of *N*-heterocyclic olefin (NHO) donors might help stabilize Pd^0 intermediates during catalysis, and b) that the lower steric bulk of NHOs compared with *N*-heterocyclic carbenes could facilitate Pd–X/amine exchange (X = halide).[28]

To start, the coupling of sterically encumbered arylhalides with bulky arylamines (Scheme 3.8) was examined. In all cases the selective formation of secondary diarylamines occurred. For example, mesitylamine (MesNH$_2$) was coupled with 4-bromotoluene (see Scheme 3.8 for conditions) to give the mono-coupled product Mes(*p*-tolyl)NH in a 81 % isolated yield. Coupling of 2,6-diisopropylaniline (DippNH$_2$) with 4-bromotoluene under the same conditions did not give full conversion; even after heating the mixture for two days at 80 °C only 12 % of the product Dipp(*p*-tolyl)NH was observed after purification by flash chromatography. Interestingly, the coupling of the sterically more demanding bromomesitylene (MesBr) with DippNH$_2$ proceeded smoothly, and full conversion was noted after 1 h (as determined by ^{1}H NMR spectroscopy); after workup, Mes(Dipp)NH was isolated in a 93 % yield. Having established the coupling of sterically demanding substrates, effort was focused on 9-bromoanthracene (BrAnth) to show that π-extended functional groups could be coupled. Accordingly, *p*-toluidine was coupled with

9-bromoanthracene to exclusively afford the mono-coupled product N-(4-methylphenyl)anthracen-9-amine, Anth(p-tolyl)NH, in a 97 % yield. 4-Bromoanisole and 4-bromo-1-fluorobenzene were each coupled to 4-toluidine to investigate the effect of electron-donating and electron-withdrawing groups (respectively) during cross-coupling (Scheme 3.8). The yields of these reactions were 98 % and 99 %, respectively, showing that the presence of either electron-donating or electron-withdrawing groups does not hinder the effectiveness of the catalyst system. The scope of this system was then expanded to include the coupling of a primary alkylamine (p-methylbenzylamine), a secondary alkylamine (morpholine), and the secondary aniline PhNHMe with 4-chlorotoluene; in all cases, successful monocoupling was found to give the expected products in >80 % yield of isolated material (Scheme 3.8). Of added note, the coupling of 4-chlorotoluene with p-toluidine could be scaled up, to give 1.84 g of di(p-tolyl)amine (94 % yield). It is worth noting that attempts to lower the temperature of these reactions below 80 °C resulted in no conversion, save for the coupling of 9-bromoanthracene and p-toluidine (see Figure 3.12).
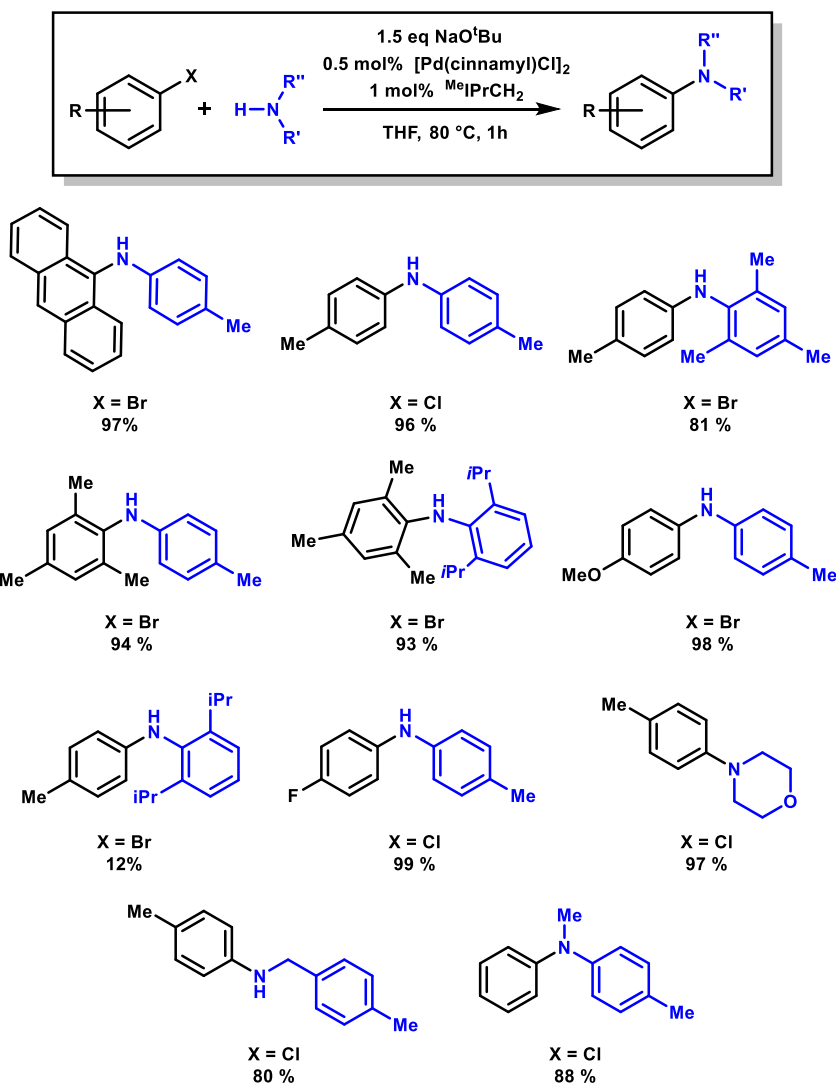
Scheme 3.8. The substrate scope investigated in this Chapter. DippNH₂ was distilled under vacuum prior to use. Each reaction was conducted in duplicate with average isolated yields reported (see Table 3.4).

Table 3.4. A summary of coupling trials depicted in Scheme 3.8.

Substrate 1	Substrate 2	Isolated yield [%] trial 1	Isolated yield [%] trial 2	Isolated yield [%] average	Max. deviation [%]	Product description
9-Br-Anth	*p*-toluidine	99	95	97	2	Orange solid
4-Cl-Tol	*p*-toluidine	96	95	96	1	White solid
4-Br-Tol	MesNH$_2$	79	82	81	2	Off-white solid
2-Br-Mes	*p*-toluidine	91	97	94	3	Yellow oil
2-Br-Mes	DippNH$_2$	95	91	93	2	White solid
4-Br-anisole	*p*-toluidine	99	97	98	1	White solid
4-Br-Tol	DippNH$_2$	12	12	12	0	White solid
4-Br-1F-benzene	*p*-toluidine	98	99	99	1	Off-white solid
4-Cl-Tol	morpholine	98	96	97	1	Off-white solid
4-Cl-Tol	4-Me-benzylamine	62	97	80	18	Off-white solid
4-Cl-Tol	N-Me-Aniline	94	83	89	6	Yellow oil

3.2.3 Poisoning, Kinetic, and Imaging of Pd^0 Nanoparticles

It was not clear whether the active species in these catalytic reactions was a well-defined Pd-NHO complex or if it was the presence of catalytically active Pd nanoparticles that catalyzed the cross-coupling reactions.[29] In an attempt to elucidate the active species of the catalytic system, elemental mercury was added 30 minutes into the reaction of 4-chlorotoluene and *p*-toluidine performed under the conditions featured in Scheme 3.8. If the active species of the system is colloidal in nature, the active palladium nanoparticles can form an amalgam when introduced to elemental mercury thereby halting catalytic activity by poisoning the catalyst.[29,30] Upon mercury

addition to the cross-coupling reaction of *p*-toluidine and 4-bromotoluene, catalytic activity halted which indicates the active species are in fact Pd nanoparticles. (Figure 3.10).
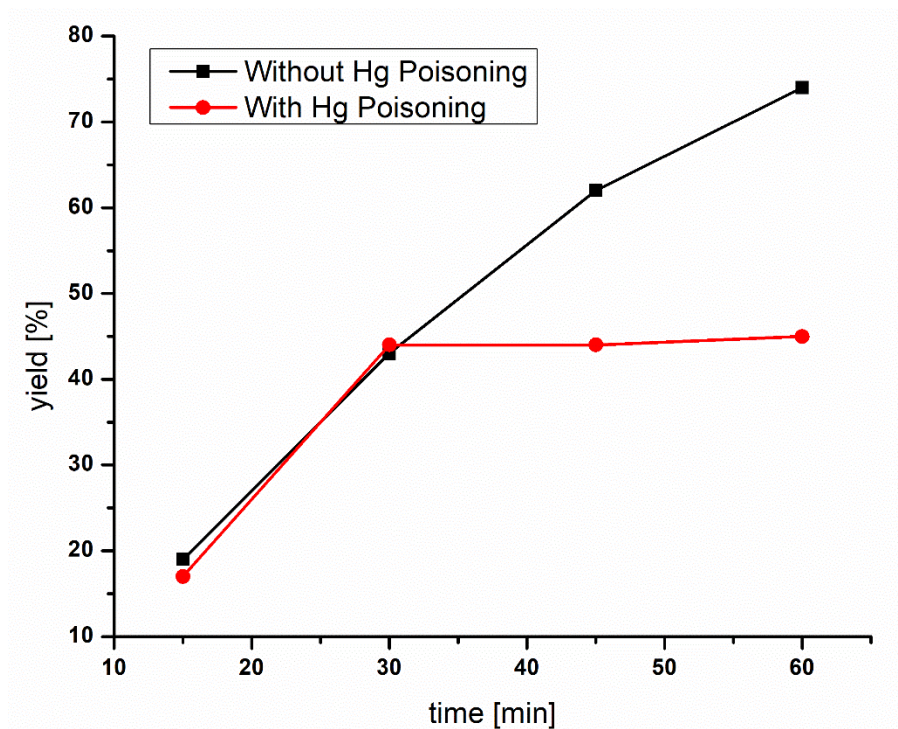
Figure 3.10. A plot of percent yield over time in the reaction of *p*-toluidine and 4-chlorotoluene at 80 °C in THF with 1.5 eq of NaO^{t}Bu as a base, [Pd(cinnamyl)Cl]$_2$ (0.5 mol%) as a palladium source, and ^{Me}IPrCH$_2$ (1 mol%) as a ligand. Elemental mercury was added at time = 30 min leading to a halt in catalysis.

Although the observed cessation of catalysis upon addition of Hg can indicate that a mercury-palladium amalgam formed, thereby rendering catalytically active Pd nanoparticles inert, reactions involving a homogeneous Pd^0 species and mercury are also possible.[29,31] As such, an additional catalyst poisoning experiment using substoichiometric amounts of PMe$_3$ was conducted. By using substoichiometric amounts of poisoning phosphine in relation to the Pd present, further support can be

offered for the presence of catalytic palladium colloids because the bulk of palladium present in these nanoparticles is buried in the core of the particles, so small amounts (*ca.* 15 % relative to the amount of palladium) of poisoning ligand will halt catalysis.[30] As with the mercury poisoning experiment, PMe$_3$ was added 30 minutes into the reaction time and a similar halt in catalysis was noted (Figure 3.11), thus adding further support for the initial presence of catalytically active Pd nanoparticles.
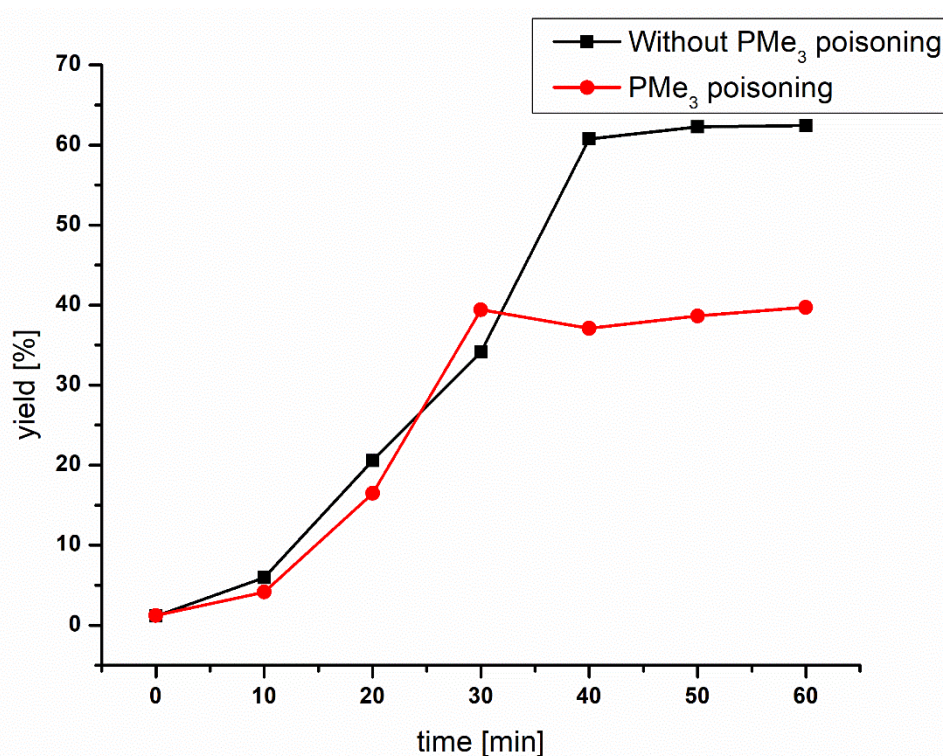
Figure 3.11. Plot of percent yield over time of the reaction of *p*-toluidine and 4-chlorotoluene at 80 °C in THF with 1.5 eq of NaO^{t}Bu as a base, [Pd(cinnamyl)Cl]$_2$ (0.5 mol%) as a palladium source, and ^{Me}IPrCH$_2$ (1 mol%) as a ligand. PMe$_3$ was added at time = 30 min leading to a halt catalysis.

To gain a greater understanding of the system, the cross-coupling reaction of *p*-toluidine with 9-bromoanthracene in THF-d$_8$ at room temperature with 1.5

133

equivalents of NaO^{t}Bu as a base, [Pd(cinnamyl)Cl]$_2$ (0.5 mol%) as a palladium source, and ^{Me}IPrCH$_2$ (1 mol%) as a ligand was monitored *in situ* via ^{1}H NMR spectroscopy over the course of 8 h with scans every 5 minutes. In performing this experiment, it became possible to observe the disappearance of 9-bromoanthracene and *p*-toluidine over time (Figure 3.12).

The kinetic data collected from the above *in situ* experiment was fitted to the Finke–Watzky model and can be seen in Figure 3.12.[32] This model is based on a two-step process for nanoparticle formation: 1) a slow, continuous nucleation step, and 2) an autocatalytic surface-growth step. This model was chosen to fit the kinetic data because it relates directly to physical properties of the reaction, yielding rate constants k$_1$ and k$_2$ for each distinct step in nanoparticle growth. The Finke–Watzky model works on the assumption that the step that consumes the reagent being monitored (in this case 9-bromoanthracene, *vide supra*) is fast compared with the rate of nanoparticle formation, and as such can be used to monitor the disappearance of [Pd(cinnamyl)Cl]$_2$ and thus formation of catalytically active nanoparticles. Given that the model fits reasonably well with the experimental data presented in Figure 3.12, it can be stated that the Buchwald–Hartwig amination occurring is faster than the formation of catalytically active nanoparticles. As shown in Figure 3.12, there is reasonable agreement between the two-step Finke–Watzky model and the experimentally derived concentration of [Pd(cinnamyl)Cl]$_2$ precursor, with an R^2 value of 0.988. This suggests, in accordance with other evidence provided, that nanoparticles are being formed which, in turn, perform catalytic Buchwald–Hartwig

amination. It is worth noting, however, that the induction period is not entirely flat, so there is some catalytic activity before the rate of catalysis increases. Curve fitting to the Finke-Watzky model was done using Origin8 to obtain values of k_1 and k_2 to fit the experimental concentration of 9-bromoanthracene to the following equation, where the values of k_1 and k_2 obtained by curve-fitting are 1.62×10^{-2} h^{-1} and 9.89×10^2 M^{-1} h^{-1}.

$$[A_t] = \frac{\frac{k_1}{k_2} + [A_0]}{1 + \frac{k_1}{k_2[A_0]} * \exp(k_1 + k_2[A_0]) t}$$
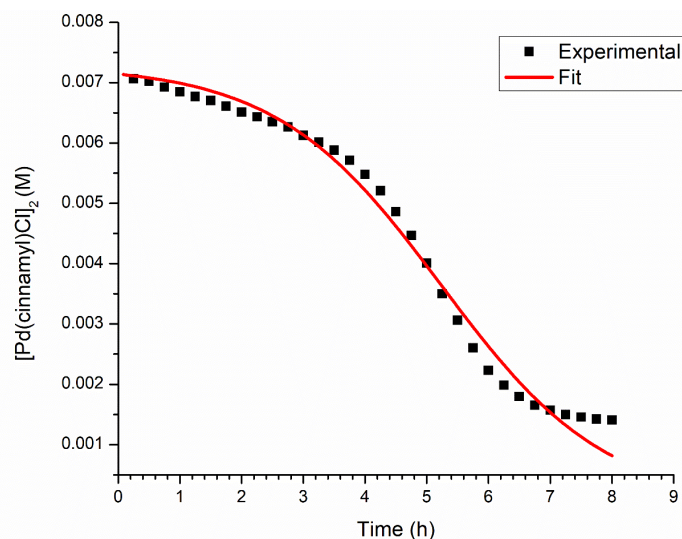
Figure 3.12. A plot of the concentration of [Pd(cinnamyl)Cl]$_2$ versus time (h) during the cross-coupling of 9-bromoanthracene and *p*-toluidine as observed by *in situ* ^{1}H NMR spectroscopy with 1,3,5-trimethoxybenzene as an internal standard. The reaction was performed in THF-d$_8$ at room temperature with 1.5 eq NaO^{t}Bu as a base, [Pd(cinnamyl)Cl]$_2$ (0.5 mol%) as a palladium source, and ^{Me}IPrCH$_2$ (1 mol%) as a ligand. Using the Finke–Watzky model, disappearance of pre-catalyst [Pd(cinnamyl)Cl]$_2$ and thus formation of Pd nanoparticles can be tracked by correlating the formation of nanoparticles to the disappearance of 9-bromoanthracene. Only every third data point is shown in the plot, for clarity.

With evidence supporting heterogeneous catalysis in hand, the fate of the NHO ligand after palladium nanoparticle formation was examined further. One possibility would be Heck-type coupling between 4-chlorotoluene and the ^{Me}IPrCH$_2$ ligand.[33] Accordingly, one equivalent each of ^{Me}IPrCH$_2$ and 4-chlorotoluene were combined in the presence of 0.5 mol% [Pd(cinnamyl)Cl]$_2$ and 1.5 equivalents of NaO^{t}Bu (at 80 °C in THF); however, only unreacted starting materials were detected by ^{1}H NMR spectroscopy. Stoichiometric amounts of p-toluidine, 4-chlorotoluene, and ^{Me}IPrCH$_2$ were combined with a half equivalent of [Pd(cinnamyl)Cl]$_2$ and 1.5 equivalents of NaO^{t}Bu (at 80 °C in THF) and the only NHO-containing species observed was free ^{Me}IPrCH$_2$. This leads me to believe that the majority NHO is left unchanged after Pd-mediated cross-coupling.

To obtain images of the catalytically active nanoparticles, it was necessary to isolate the palladium nanoparticles and capture images of them using various Transmission Electron Microscopy (TEM) techniques, such as high angle annular dark field (HAADF) imaging and scanning transmission electron microscopy (STEM). After performing the cross-coupling of p-toluidine and 4-chlorotoluene as per the conditions in Scheme 3.8, the resulting suspended Pd nanoparticles were isolated by centrifugation and washed 3 times with water to remove the sodium chloride. The resulting particles were re-suspended in anhydrous ethanol,[34] then drop-cast on a holey carbon TEM grid. The solvent was then removed under vacuum followed by heating to 300 °C overnight to remove excess organic material.
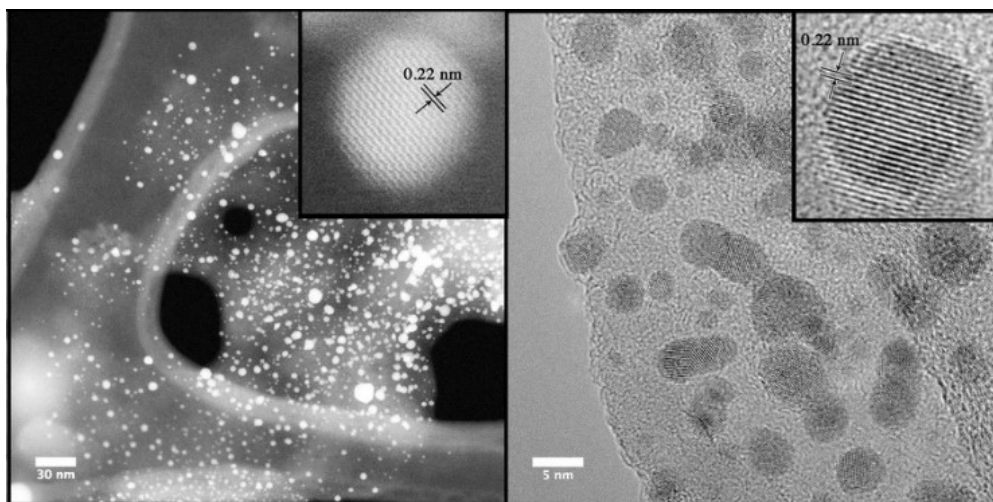
Figure 3.13. A pair of high resolution transmission electron microscopy (HRTEM) images of Pd nanoparticles isolated after the completion of aryl amination of *p*-toluidine and 4-chlorotoluene under the conditions shown in Scheme 3.8. The nanoparticles were heated at 300 °C overnight to remove excess organic material. Left: An HAADF image showing Pd nanoparticles as well as their lattice fringes. Right: A STEM image depicting Pd nanoparticles and their lattice fringes.

The resulting spherical nanoparticles have high contrast compared with the grid, and thus were readily observable by TEM. Lattice fringes with a spacing of 0.22 nm were obtained in both high-resolution and high-angle angular dark-field (HAADF) scanning mode (Figure 3.13) and indexed to Pd [111] faces.[35] A control sample was prepared by drop-casting the anhydrous ethanol Pd nanoparticle suspension onto a TEM grid and removing solvent under vacuum overnight, to ensure that heating the grid did not dramatically affect the particles (Figure 3.14).
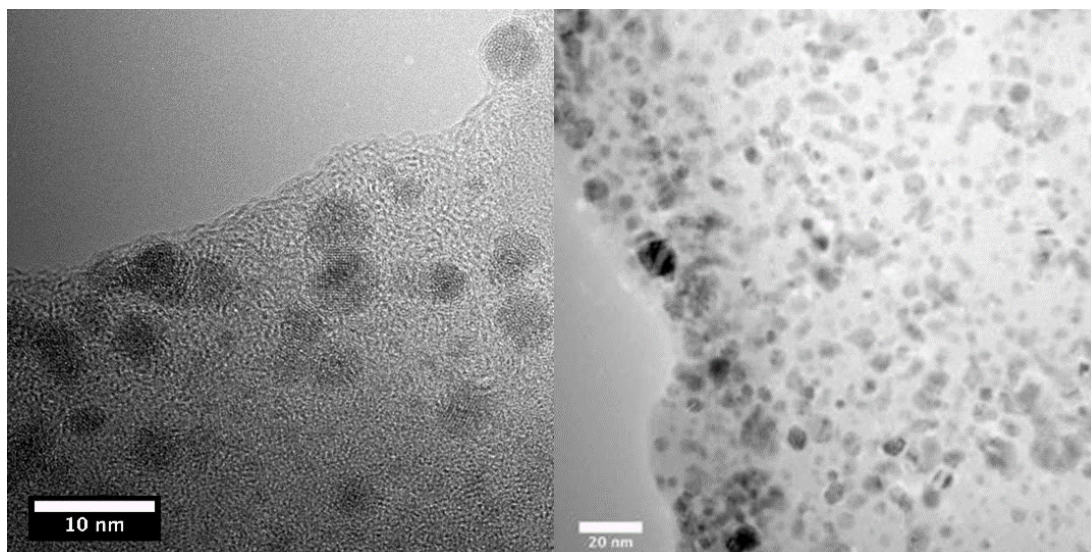
Figure 3.14. A pair of STEM images of Pd nanoparticles isolated after the completion of the aryl amination of *p*-toluidine and 4-chlorotoluene under the conditions shown in Scheme 3.8. The nanoparticles were not heated prior to imaging.

300 particles were measured averaging 4.80 ± 0.84 nm in size (Figures 3.14 and 3.15) and are similar in size to the control sample prepared by vacuum drying (4.72 ± 0.91 nm) (Figure 3.16). The composition of nanoparticles was further confirmed with an energy dispersive X-ray (EDX) detector. A good overlap of the nanoparticles in the dark-field image with palladium signal mapping was observed (Figure 3.16).
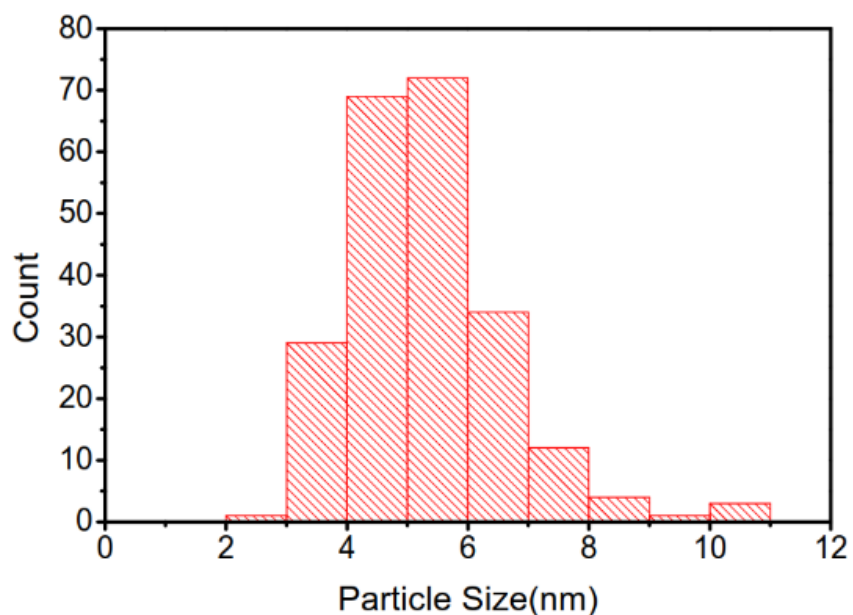
Figure 3.15. A histogram showing the size distribution of the nanoparticles generated during the Buchwald-Hartwig amination of *p*-toluidine and 4-chlorotoluene according to the conditions in Scheme 3.8. More than 300 particles were measured.
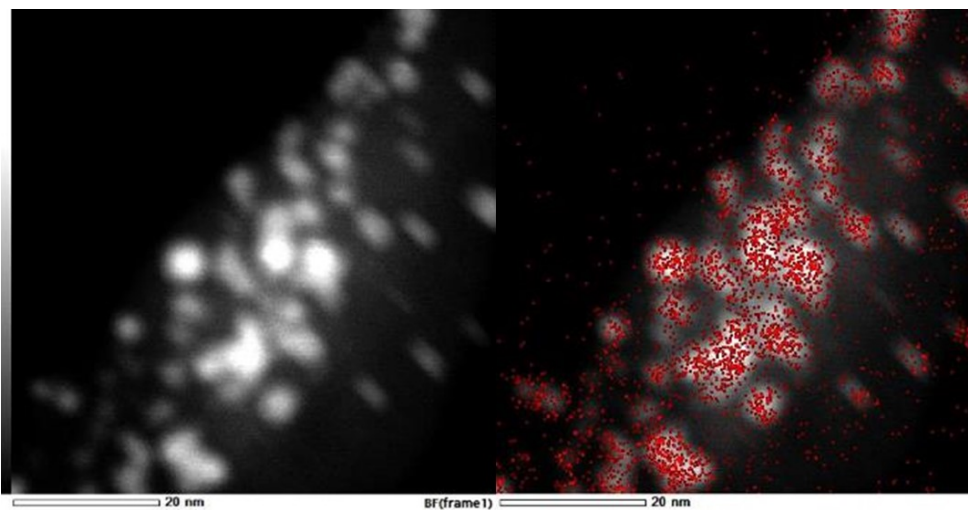
Figure 3.16. Left: A HAADF STEM image of the Pd nanoparticles generated during the Buchwald-Hartwig amination of *p*-toluidine and 4-chlorotoluene according to the conditions in Scheme 3.8. Right: The same HAADF STEM image as above with a Pd EDX map overlayed, showing that the observed nanoparticles contain palladium.

3.3. Conclusion

A series of structurally distinct *N*-heterocyclic olefins (NHOs) have been prepared, including analogues with extended π-frameworks. In line with prior work involving NHOs, metal coordination through the terminal C atoms (η^1) was found in each case. A variety of [(NHO)PdCl$_2$(3-Cl-pyr)] complexes were prepared, however, these species proved to be ineffective in Buchwald–Hartwig cross-coupling between arylchlorides and primary arylamines. A suitable catalyst system containing Pd nanoparticles was obtained by combining the readily accessible NHO ^{Me}IPrCH$_2$ with the Pd source [Pd(cinnamyl)Cl]$_2$ in the presence of NaO^{t}Bu in THF at 80 °C. This system was active for the coupling of a wide range of arylhalides with arylamines (including high conversion with bulky substrates), whereas also avoiding over-arylation to tertiary triarylamines. Catalyst poisoning experiments revealed that addition of Hg or substoichiometric amounts of PMe$_3$ halts catalysis, thus pointing to the observed catalysis being heterogeneous in nature, a feature that is likely more common in cross-coupling reactions than previously noted.

3.4 Experimental Section

3.4.1 Materials and Instrumentation

All reactions were performed using standard Schlenk line techniques under an atmosphere of nitrogen or in an inert-atmosphere glovebox (MBraun Labmaster 100). Solvents were dried using a Grubbs-type solvent-purification system manufactured by Innovative Technology, Inc. and stored under an atmosphere of nitrogen and over 4 Å

molecular sieves prior to use. THF used as a solvent for cross-coupling experiments, was dried over sodium/benzophenone and distilled under nitrogen prior to use. [MeIPrH]Cl,[37] [SIPrH]Cl,[38] [IPr(BIAN)H]Cl,[39] IPr,[40] MeIPr,[40] and MeIPrCH$_2$[13] were prepared according to literature procedures. [Pd(cinnamyl)(μ-Cl)]$_2$ was purchased from MilliporeSigma and used as received. Allyl bromide was purchased from Alfa Aesar and degassed through freeze–pump–thaw cycles before use. NaO^{t}Bu and KO^{t}Bu were purchased from MilliporeSigma and used as received. 3-Chloropyridine was purchased form Oakwood Chemicals and distilled before storing in a glovebox before use. 1,5-Diiodopentane, 1,4-diiodobutane, and methyl iodide were purchased from MilliporeSigma and freeze–pump–thaw degassed before use. Methyl trifluoromethylsulfonate (MeOTf) was purchased from Oakwood Chemicals and used as received. Bis(benzonitrile)palladium(II) dichloride was purchased from Strem Chemicals and used as received. ^{1}H, ^{13}C{^{1}H}, and ^{19}F{^{1}H} NMR spectra were recorded on 500 MHz and 700 MHz Varian Inova spectrometers and referenced externally to SiMe$_4$ (^{1}H, ^{13}C{^{1}H}) and FCCl$_3$ (^{19}F{^{1}H}). Elemental analyses were performed by the Analytical and Instrumentation Laboratory at the University of Alberta. Melting points were measured in sealed glass capillaries under nitrogen using a MelTemp melting-point apparatus and are uncorrected.

3.4.2 Transmission Electron Microscopy

TEM images were obtained from a JEOL JEM-ARM200CF Transmission Electron Microscope. Samples were prepared from the Buchwald–Hartwig amination

of *p*-toluidine and 4-chlorotoluene as earlier described in Scheme 3.8. Samples were centrifuged (3000 rpm, 5 min) to separate the Pd nanoparticles from the supernatant. The isolated Pd nanoparticles were then washed with 3×2 mL of water, and then suspended in 3 mL of anhydrous ethanol. This suspension was then drop cast onto a holey carbon grid, placed under vacuum for 3–4 h, followed by heating to 300 °C overnight to remove organic material. To ensure that heating the samples at 300 °C overnight was not inducing nanoparticle formation, samples were prepared in the same manner as above except that the samples were put under high vacuum overnight to remove volatile organic material instead of heating at 300 °C.

3.4.3 X-ray Crystallography

Crystals of appropriate quality for X-ray diffraction studies were removed from either a Schlenk flask under a stream of nitrogen, or from a vial (glove box) and immediately covered with a thin layer of hydrocarbon oil (Paratone-N). A suitable crystal was then selected, attached to a glass fiber, and quickly placed in a low-temperature stream of nitrogen. All data were collected using a Bruker APEX II CCD detector/D8 diffractometer using $Mo_{K\alpha}$ or $Cu_{K\alpha}$ radiation, with the crystal cooled to -100 °C or -80 °C, respectively. The data were corrected for absorption through Gaussian integration from indexing of the crystal faces. Structures were solved using the direct methods programs SHELXT-2014,[41] and refinements were completed using the program SHELXL-2014.[42] Hydrogen atoms were assigned positions based on the

sp^2- or sp^3-hybridization geometries of their attached carbon atoms, and were given thermal parameters 20 % greater than those of their parent atoms.

3.4.4 Computational Methods

Computational work for this Chapter was performed by Dr. Christian Hering-Junghans. Density functional theory (DFT) calculations (full geometry optimization) were carried out on **1**–**3**, **4**, and **6** starting from the geometry of their respective X-ray structures. Geometry optimizations were carried out using the Gaussian09 program package:[3] B3LYP[44] functional with a 6-31+G(d,p) basis set[45] for C, H, and N. The optimized structures were in reasonable agreement with the observed molecular structures. All stationary points were characterized by frequency analyses. For all calculated molecules and intermediates there are no imaginary frequencies. The optimized structures were also subjected to natural bond orbital (NBO) analyses using the NBO 6.0 program.[46] It should be emphasized that the computation was carried out for a single, isolated (gas phase) species. There may well be significant differences among gas phase, solution, and solid state data.
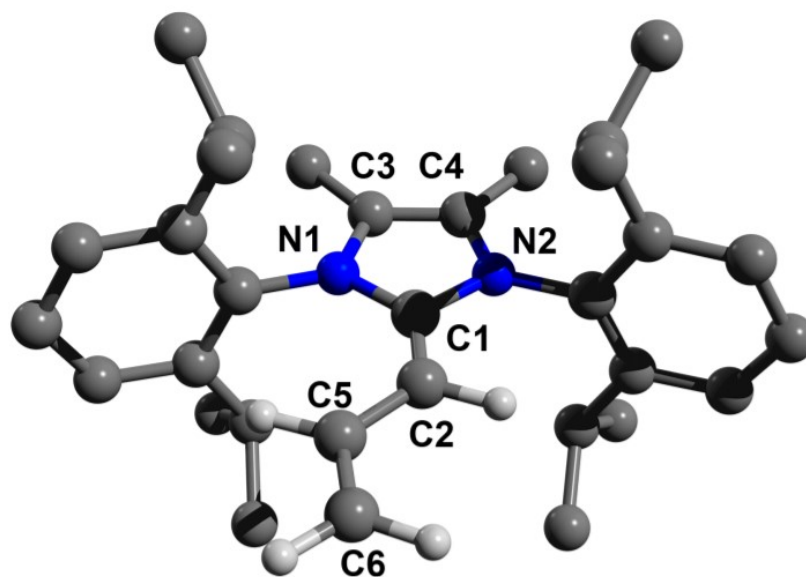
Figure 3.17. Optimized structure of ^{Me}IPr=CH-CH=CH$_2$ (**1**). Natural population analysis (NPA charges): C1 0.43, C2 -0.46, C5 -0.25, C6 -0.53, N1 -0.46, N2 -0.46. Wiberg bond indices (WBI): C1-C2 1.50, C2-C5 1.20, C5-C6 1.80.
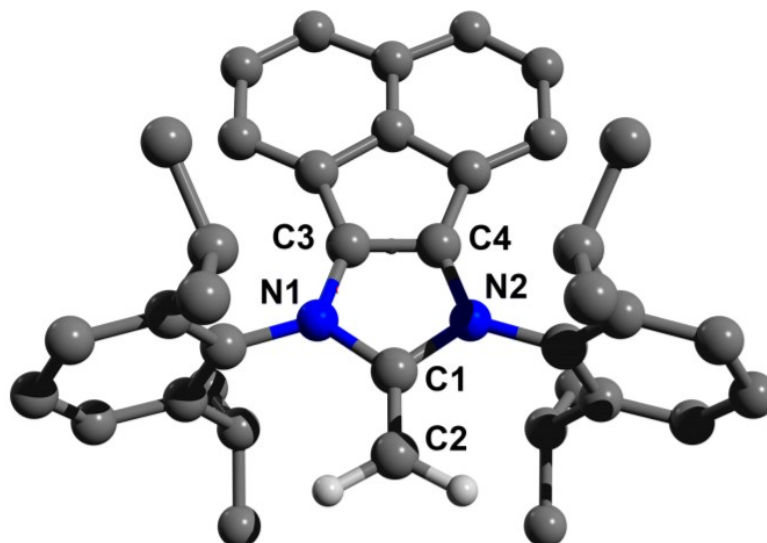
Figure 3.18. Optimized structure of IPr(BIAN)CH$_2$ (**2**). Natural population analysis (NPA charges): C1 0.40, C2 -0.70, N1 -0.45, N2 -0.45. Wiberg bond indices (WBI): C1-C2 1.67
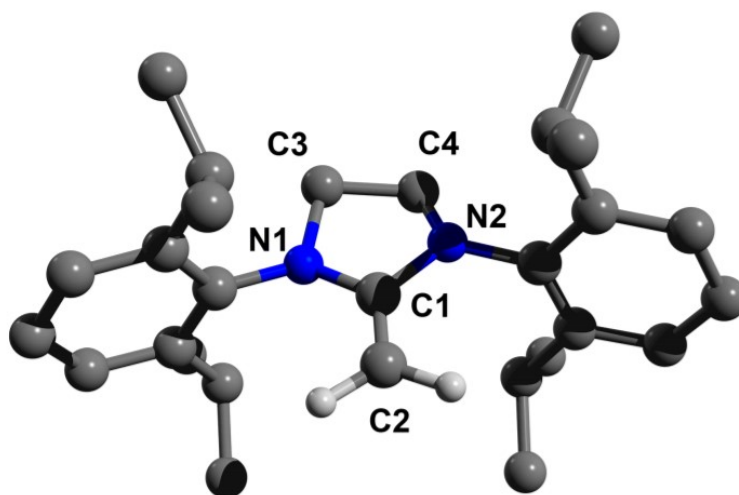
Figure 3.19. Optimized structure of SIPrCH$_2$ (**3**). Natural population analysis (NPA charges): C1 0.41, C2 -0.68, N1 -0.54, N2 -0.54. Wiberg bond indices (WBI): C1-C2 1.70.
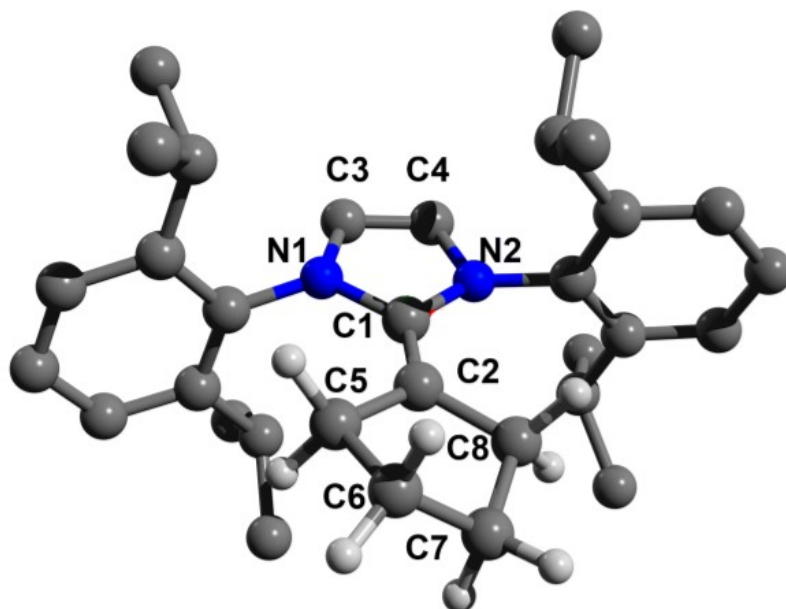
Figure 3.20. Optimized structure of IPr=C(CH$_2$)$_4$ (**4**). Natural population analysis (NPA charges): C1 0.38, C2 -0.23, N1 -0.48, N2 -0.48. Wiberg bond indices (WBI): C1-C2 1.63.
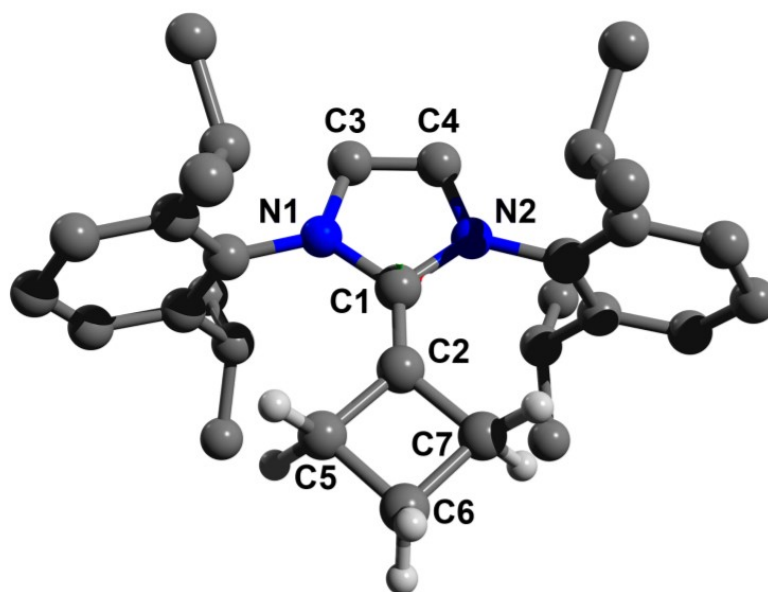
Figure 3.21. Optimized structure of IPr=C(CH$_2$)$_3$ (**6**). Natural population analysis (NPA charges): C1 0.38, C2 -0.24, N1 -0.47, N2 -0.47. Wiberg bond indices (WBI): C1-C2 1.61.

3.4.5 *In situ* Reaction Monitoring and Kinetic Data

Solutions of [Pd(cinnamyl)Cl]$_2$ (0.0027 g, 0.050 mmol) and ^{Me}IPrCH$_2$ (0.0043 g, 0.010 mmol) were made in 1.00 mL of THF. 200 µL portions of these stock solutions were transferred into separate vials and solvent was removed *in vacuo*. 9-Bromoanthracene (0.0256 g, 0.100 mmol), *p*-toluidine (0.0128 g, 0.119 mmol), 1,3,5-trimethoxybenzene (0.0168 g, 0.100 mmol), sodium *tert*-butoxide (0.0188 g, 0.150 mmol) and the [Pd(cinnamyl)Cl]$_2$ and ^{Me}IPrCH$_2$ were combined in 700 µL THF-d$_8$, placed into an J-Young NMR tube, and the sealed tube placed into a 400 MHz NMR spectrometer. 16 scans were taken of the mixture every 5 minutes for 320 minutes. Curve fitting to match experimental data to the Finke-Watzky model was performed using Origin 8.

3.4.6 Synthetic Procedures

Synthesis of ^{Me}IPr=CH−CH=CH₂ (1). To a mixture of [^{Me}IPrH]Cl (0.445 g, 0.984 mmol) and KO^tBu (0.232 g, 2.07 mmol) in THF (10 mL) was added dropwise a solution of allyl bromide (0.127 g, 1.05 mmol) in THF (2 mL). The resulting suspension was stirred at room temperature for 12 h. The precipitate was allowed to settle and the deep-yellow supernatant was filtered through a plug of Celite. The volatiles were evaporated under vacuum from the filtrate and the yellow residue was extracted with toluene (10 mL). Filtration of the toluene extract followed by evaporation of the toluene gave ^{Me}IPr=CH−CH=CH₂ (**1**, 0.285 g, 84 %) as a bright-yellow solid. X-ray quality crystals of **1** were obtained by slowly evaporating a saturated hexanes solution over a period of 24 h at room temperature. ^{1}H NMR (500 MHz, C₆D₆): δ = 7.27–7.20 (m, 2H, ArH), 7.11–7.15 (m, 4H, ArH), 5.60–5.70 (m, 1H, C−CH=CH₂), 4.29 (dd, 1H, $^3J_{HH}$ = 16.1 Hz, $^2J_{HH}$ = 2.8 Hz, *cis*-CH=CH_2), 4.03 (d, 1 H, $^3J_{HH}$ = 11.5 Hz, C=CH-CH), 3.97 (dd, 1H, $^3J_{HH}$ = 10.7 Hz, $^2J_{HH}$ = 2.8 Hz, *trans*-CH=CH_2), 3.26 (sept, 2H, $^3J_{HH}$ = 6.8 Hz, CH(CH₃)₂), 3.16 (sept, 2H, $^3J_{HH}$ = 6.9 Hz, CH(CH₃)₂), 1.47–1.52 (m, 6H, H_3C-CN), 1.43 (d, 6H, $^3J_{HH}$ = 6.8 Hz, CH(CH_3)₂), 1.38 (d, 6H, $^3J_{HH}$ = 6.8 Hz, CH(CH_3)₂), 1.18 (d, 6H, $^3J_{HH}$ = 6.9 Hz, CH(CH_3)₂), 1.17 ppm (d, 6H, $^3J_{HH}$ = 6.9 Hz, CH(CH_3)₂); ^{13}C{^{1}H} NMR (125 MHz, C₆D₆): δ = 9.1 (H₃C−CN), 9.5 (H₃C−CN), 23.8 (CH(CH₃)₂), 24.1 (CH(CH₃)₂), 24.8 (CH(CH₃)₂), 28.9 (CH(CH₃)₂), 29.0 (CH(CH₃)₂), 72.2 (CH=CH₂), 95.3 (=CH−CH), 116.6 (NC−CH₃), 117.2 (NC−CH₃), 124.4 (ArC), 124.6 (ArC), 129.7 (ArC), 129.8 (ArC), 132.4 (ArC), 132.6 (CH=CH₂), 134.4 (ArC), 146.0 (ArC), 148.7 (ArC), 149.2

(ArC), 206.5 ppm (NCN); element. anal.: calcd for $C_{28}H_{42}N_2B_2$: C, 84.16; H, 9.71; N, 6.13, found: C, 83.49; H, 9.74; N, 5.91 %; mp: 146–149 °C.

Synthesis of IPr(BIAN)CH₂ (2). [IPr(BIAN)H]Cl (0.105 g, 0.192 mmol) and KO^{t}Bu (0.044 g, 0.39 mmol) were combined in a 1:1 mixture of toluene/THF (10 mL) at room temperature and the mixture was stirred for 30 min. To the resulting yellow suspension was added MeI (0.031 g, 0.21 mmol) and the color immediately changed to deep blue. Stirring was continued for 12 h and the precipitate was allowed to settle. The supernatant was filtered through a plug of Celite. The volatiles were removed from the filtrate *in vacuo* and IPr(BIAN)CH₂ (**2**, 0.088 g, 87 %) was obtained as a blue solid. X-ray quality crystals of **2** were obtained from a saturated benzene solution layered with hexanes at room temperature after 24 h. ^{1}H NMR (498 MHz, C_6D_6): δ = 7.33 (t, 2H, $^3J_{HH}$ = 7.7 Hz, ArH), 7.27 (d, 4H, $^3J_{HH}$ = 7.7 Hz, ArH), 7.14-7.15 (m, 2H, Napht-H), 6.85-6.88 (m, 2H, Napht-H), 6.67 (d, 2H, $^3J_{HH}$ = 7.0 Hz, Napht-H), 3.59 (sept, 4H, $^3J_{HH}$ = 7.0 Hz, CH(CH₃)₂), 2.73 (s, 2H, C=CH_2), 1.39 (d, 12H, $^3J_{HH}$ = 7.0 Hz, CH(CH_3)₂), 1.16 ppm (d, 12H, $^3J_{HH}$ = 7.0 Hz, CH(CH_3)₂); ^{13}C{^{1}H} NMR (125 MHz, C_6D_6): δ = 24.0 (CH(CH₃)₂), 24.4 (CH(CH₃)₂), 29.2 (CH(CH₃)₂), 48.3 (CH₂), 118.5 (ArC), 124.8 (ArC), 126.1 (ArC), 127.5 (ArC), 128.9 (ArC), 129.4 (ArC), 129.7 (ArC), 132.0 (ArC), 133.5 (ArC), 149.1 (ArC), 157.6 ppm (NCN); UV/Vis (THF): λ_{max} (ϵ) = 286 (6.40 × 10^5 L mol^{-1} cm^{-1}), 406 (1.86 × 10^4 L mol^{-1} cm^{-1}), 686 nm (1.03 × 10^4 L mol^{-1} cm^{-1}); element. anal.: calcd for $C_{33}H_{46}N_2$: C, 86.64; H, 8.04; N, 5.32; found: C, 86.02; H, 8.00; N, 5.17 %; mp: >260 °C.

Synthesis of SIPrCH₂ (3). A 20 mL scintillation vial was charged with [SIPrH]Cl (0.4271 g, 1.000 mmol), KO^{t}Bu (0.2468 g, 2.200 mmol) and THF (5 mL) were added. The mixture was stirred for 10 minutes, then MeI (0.1419 g, 1.100 mmol) in THF (2 mL) was added dropwise and the reaction mixture was stirred overnight. The resulting precipitate was allowed to settle and the supernatant was filtered through a pad of Celite. The volatiles were removed from the filtrate *in vacuo* to give **3** as a white solid (0.2671 g, 70 %). X-ray quality crystals were obtained from a saturated toluene solution at −25 °C for 24 h. ^{1}H NMR (500 MHz, C₆D₆): δ = 7.23 (t, 2H, $^3J_{HH}$ = 7.2 Hz, Ar*H*), 7.14 (d, 4H, $^3J_{HH}$ = 7.5 Hz, Ar*H*), 3.40 (s, 4H, NC*H₂*), 3.37 (sept, 4H, $^3J_{HH}$ = 6.8 Hz, C*H*(CH₃)₂), 2.42 (s, 2H, C=C*H₂*), 1.36 (d, 12H, $^3J_{HH}$ = 6.7 Hz, CH(C*H₃*)₂), 1.27 ppm (d, 12H, $^3J_{HH}$ = 6.7 Hz, CH(C*H₃*)₂); ^{13}C{^{1}H} NMR (126 MHz, C₆D₆): δ = 156.1 (N*C*N), 149.5 (Ar*C*), 137.2 (Ar*C*), 128.5 (Ar*C*), 124.5 (Ar*C*), 51.8 (N*C*H₂), 50.4 (C=*C*H₂), 28.7 (*C*H(CH₃)₂), 24.7 (CH(*C*H₃)₂), 24.5 ppm (CH(*C*H₃)₂; element. anal.: calcd for C₂₈H₄₀N₂: C, 83.11; H, 9.96; N, 6.92; found: C, 82.92; H, 10.07; N, 6.77 %; mp: 132–134 °C.

Synthesis of IPr=C(CH₂)₄ (4). To a solution of IPr (0.335 g, 0.861 mmol) in toluene (10 mL) was added dropwise 1,5-diiodopentane (0.098 g, 0.30 mmol) in toluene (2 mL). The resulting suspension was stirred at room temperature for 8 h. The colorless precipitate ([IPrH]I) was allowed to settle and the yellow supernatant was filtered through a pad of Celite. The volatiles were removed from the filtrate under vacuum and the yellow residue was extracted with hexanes (10 mL). Evaporation of the

hexanes afforded **4** (0.110 g, 84 %) as a bright yellow solid. X-ray quality crystals of **4** were obtained by slow evaporation (under N_2) of a saturated hexanes solution over a period of 24 h at room temperature. ^{1}H NMR (498 MHz, C_6D_6): δ = 7.20 (t, 2H, $^3J_{HH}$ = 7.7 Hz, Ar*H*), 7.07 (d, 4H, $^3J_{HH}$ = 7.7 Hz, Ar*H*), 5.77 (s, 2H, NCH), 3.59 (sept, 2H, $^3J_{HH}$ = 6.9 Hz, C*H*(CH$_3$)$_2$), 1.73–1.880 (m, 4H, C*H$_2$*), 1.32–1.37 (m, 4H, C*H$_2$*), 1.32 (d, 12H, $^3J_{HH}$ = 7.0 Hz, CH(C*H$_3$*)$_2$), 1.25 ppm (d, 12H, $^3J_{HH}$ = 7.0 Hz, CH(C*H$_3$*)$_2$); ^{13}C{^{1}H} NMR (125 MHz, C_6D_6): δ = 22.8 (CH(CH$_3$)$_2$), 25.0 (CH(CH$_3$)$_2$), 28.2 ((CH$_2$)$_4$), 28.7 (CH(CH$_3$)$_2$), 29.9 ((CH$_2$)$_4$), 75.3 (C=C), 116.8 (N*C*-H), 123.5 (Ar*C*), 128.7 (Ar*C*), 137.8 (Ar*C*), 138.4 (Ar*C*), 148.3 ppm (N*C*N); element. anal.: calcd for $C_{32}H_{44}N_2$: C, 84.16; H, 9.71; N, 6.13; found: C, 83.47; H, 9.56; N, 6.64 %; mp: 105 °C (dec.).

Synthesis of ^{Me}IPr=C(CH$_2$)$_4$ (5). To a solution of ^{Me}IPr (0.417 g, 1.00 mmol) in 10 mL of toluene was added dropwise 1,5-diiodopentane (0.118 g, 0.364 mmol) in toluene (2 mL). The resulting suspension was stirred at room temperature for 8 h. The colorless precipitate was allowed to settle and the yellow supernatant was filtered through a pad of Celite. The volatiles were evaporated from the filtrate under vacuum and the yellow residue was extracted with hexanes (10 mL). Evaporation of hexanes afforded **5** (0.135 g, 77 %) as a bright-yellow solid. X-ray quality crystals of **5** were obtained by storing a saturated hexanes solution in the freezer at −30 °C over a period of 24 h. ^{1}H NMR (498 MHz, C_6D_6): δ = 7.22 (t, 2H, $^3J_{HH}$ = 7.6 Hz, Ar*H*), 7.08 (d, 4H, $^3J_{HH}$ = 7.6 Hz, Ar*H*), 3.48 (sept, 2H, $^3J_{HH}$ = 6.9 Hz, C*H*(CH$_3$)$_2$), 1.69–1.75 (m, 4H,

CH_2), 1.37 (d, 12H, $^3J_{HH}$ = 7.0 Hz, CH(CH_3)$_2$), 1.30–1.36 (m, 4H, CH_2), 1.20 ppm (d, 12H, $^3J_{HH}$ = 7.0 Hz, CH(CH_3)$_2$); ^{13}C{^{1}H} NMR (125 MHz, C$_6$D$_6$): δ = 9.9 (NC$-$$CH_3$), 23.6 (CH($CH_3$)$_2$), 24.3 (CH($CH_3$)$_2$), 28.1 (($CH_2$)$_4$), 28.5 ($C$H(CH$_3$)$_2$), 30.0 (($CH_2$)$_4$), 73.5 (C=$C$(CH$_2$)$_2$), 116.8 (N$C$$-$Me), 123.4 (Ar$C$), 128.7 (Ar$C$), 136.5 (Ar$C$), 139.6 (Ar$C$), 149.4 ppm (N$C$N); element. anal.: calcd for C$_{34}$H$_{48}$N$_2$: C, 84.24; H, 9.98; N, 5.78; found: C, 83.41; H, 9.91; N, 5.76 %; mp: 117 °C (dec.).

Synthesis of IPr=C(CH$_2$)$_3$ (6). To a solution of IPr (1.017 g, 2.621 mmol) in toluene (10 mL) was added dropwise 1,4-diiodobutane (0.280 g, 0.903 mmol) in toluene (2 mL). The resulting suspension was stirred at room temperature for 12 h. The colorless precipitate ([IPrH]I) was allowed to settle and the yellow supernatant was filtered through a pad of Celite. The volatiles were removed from the filtrate under vacuum and the yellow residue was extracted with hexanes (10 mL). Evaporation of hexanes resulted afforded **6** as a solid (0.300 g, 74 %) as a bright-yellow solid. X-ray quality crystals of **6** were obtained by storing a saturated hexanes solution in the freezer at −30 °C over a period of 24 h. ^{1}H NMR (498 MHz, C$_6$D$_6$): δ = 7.20 (t, 2H, $^3J_{HH}$ = 7.7 Hz, ArH), 7.07 (d, 4H, $^3J_{HH}$ = 7.7 Hz, ArH), 5.73 (s, 2H, $H$$-$CN), 3.53 (sept, 4H, $^3J_{HH}$ = 6.9 Hz, CH(CH$_3$)$_2$), 2.16 (t, 4H, $^3J_{HH}$ = 7.5 Hz, CH_2), 1.79 (quint, 2H, $^3J_{HH}$ = 7.5 Hz, CH_2), 1.41 (d, 12H, $^3J_{HH}$ = 6.9 Hz, CH(CH_3)$_2$), 1.25 ppm (d, 12H, $^3J_{HH}$ = 6.9 Hz, CH(CH_3)$_2$); ^{13}C{^{1}H} NMR (125 MHz, C$_6$D$_6$): δ = 20.0 (CH$_2$), 23.0 (CH(CH$_3$)$_2$), 24.7 (CH(CH$_3$)$_2$), 28.2 (CH$_2$), 28.8 (CH(CH$_3$)$_2$), 69.7 (C=C(CH$_2$)$_2$), 115.6 (N$C$$-$H), 123.3 (Ar$C$), 128.8 (Ar$C$), 136.2 (Ar$C$), 137.2 (Ar$C$), 149.2 ppm (N$C$N); element. anal.:

calcd for $C_{31}H_{42}N_2$: C, 84.11; H, 9.56; N, 6.33; found: C, 83.29; H, 9.62; N, 6.14 %; despite subsequent recrystallizations, an impurity of about 6 % free IPr was present, mp: 84 °C (dec.).

Synthesis of ^{Me}IPr=C(CH$_2$)$_3$ (7). To a solution of ^{Me}IPr (0.133 g, 0.294 mmol) in toluene (10 mL) was added dropwise 1,4-diiodobutane (0.038 g, 0.123 mmol) in toluene (2 mL). The resulting suspension was stirred at room temperature for 12 h. The colorless precipitate ([^{Me}IPrH]I) was allowed to settle and the yellow supernatant was filtered through a pad of Celite. The volatiles were removed from the filtrate under vacuum and the yellow residue was extracted with hexanes (5 mL) and filtered. Evaporation of the hexanes gave **7** (0.050 g, 82 %) as a bright yellow solid. ^{1}H NMR (498 MHz, C_6D_6): δ = 7.22 (t, 2H, $^3J_{HH}$ = 7.7 Hz, ArH), 7.08 (d, 4H, $^3J_{HH}$ = 7.7 Hz, ArH), 3.44 (sept, 4H, $^3J_{HH}$ = 7.0 Hz, CH(CH$_3$)$_2$), 2.11 (t, 4H, $^3J_{HH}$ = 7.5 Hz, CH_2), 1.76 (quint, 2H, $^3J_{HH}$ = 7.5 Hz, CH_2), 1.53 (s, 6H, H_3C−CN), 1.45 (d, 12H, $^3J_{HH}$ = 7.0 Hz, CH(CH_3)$_2$), 1.21 ppm (d, 12H, $^3J_{HH}$ = 7.0 Hz, CH(CH_3)$_2$); ^{13}C{^{1}H} NMR (125 MHz, C_6D_6): δ = 9.4 (H_3C−CN), 19.7 (CH$_2$), 23.8 (CH(CH_3)$_2$), 24.2 (CH(CH_3)$_2$), 28.6 (2C, CH$_2$), 28.7 (CH(CH$_3$)$_2$), 68.1 (C=C(CH$_2$)$_2$), 115.9 (NC−Me), 123.3 (ArC), 128.8 (ArC), 134.6 (ArC), 138.2 (ArC), 149.8 ppm (NCN); element. anal.: calcd for $C_{33}H_{46}N_2$: C, 84.20; H, 9.85; N, 5.95; found: C, 83.48; H, 9.87; N, 5.69 %; mp: 108 °C (dec.).

Synthesis of [^{Me}IPrC(Me)(CH$_2$)$_4$]OTf (8). To a solution of ^{Me}IPr=C(CH$_2$)$_4$ (0.050 g, 0.10 mmol) in hexanes (5 mL) was added dropwise a solution of MeOTf (0.020 g, 0.12 mmol) in hexanes (1 mL) at room temperature. The resulting suspension was stirred at room temperature for 12 h. The colorless precipitate was isolated by filtration and washed with hexanes (2 mL). Afterwards the precipitate was dissolved in CH$_2$Cl$_2$ (1 mL) and the resulting solution layered with hexanes, which resulted in the formation of colorless X-ray quality crystals of **8** after 24 h at −30 °C (0.030 g, 47 %). ^{1}H NMR (399 MHz, CDCl$_3$): δ = 7.65 (t, 2H, $^3J_{HH}$ = 7.8 Hz, Ar*H*), 7.40 (d, 4H, $^3J_{HH}$ = 7.8 Hz, Ar*H*), 2.34 (sept, 4H, $^3J_{HH}$ = 6.7 Hz, C*H*(CH$_3$)$_2$), 2.08 (s, 6H, *H*$_3$C−CN), 1.30–1.56 (m, 8H, C*H*$_2$), 1.20–1.35 (m, 4H CH(C*H*$_3$)$_2$), 1.33 (d, 12H, $^3J_{HH}$ = 6.7 Hz, CH(C*H*$_3$)$_2$), 1.22 (d, 12H, $^3J_{HH}$ = 6.7 Hz, 12 H, CH(C*H*$_3$)$_2$), 1.11 ppm (s, 3H, -C*H*$_3$); ^{13}C{^{1}H} NMR (176 MHz, CDCl$_3$): δ = 10.5 (*H*$_3$C−CN), 21.1 (C-CH$_2$-*C*H$_2$), 23.5 (CH(*C*H$_3$)$_2$), 24.5 (CH(*C*H$_3$)$_2$), 25.3 (CH(*C*H$_3$)$_2$), 29.2 (*C*H(CH$_3$)$_2$), 37.4 (C-*C*H$_2$-CH$_2$), 46.3 (NC−*C*), 125.7 (Ar*C*), 129.9 (Ar*C*), 130.5 (Ar*C*), 132.5 (Ar*C*), 145.5 (Ar*C*), 151.4 ppm (N*C*N); ^{19}F{^{1}H} NMR (376 MHz, CDCl$_3$): δ= −78.0 ppm (s); element. anal.: calcd for C$_{36}$H$_{51}$F$_3$N$_2$O$_3$S: C, 66.64; H, 7.92; N, 4.32; S, 4.94; found: C, 66.52; H, 7.92; N, 4.24; S, 4.63 %; mp: >300 °C.

Synthesis of [(^{Me}IPrCH$_2$)PdCl(μ-Cl)]$_2$ (9). A solution of ^{Me}IPrCH$_2$ (0.053 g, 0.12 mmol) in toluene (2 mL) was added dropwise to a solution of *trans*-[Cl$_2$Pd(NCPh)$_2$] (0.035 g, 0.091 mmol) in toluene (1 mL) at room temperature. A red crystalline solid precipitated from the reaction mixture after stirring for 2 h. This precipitate was

isolated by filtration and washed with fresh toluene (2 mL). The collected solid was re-dissolved in a minimum amount of CH_2Cl_2 and the resulting solution was layered with hexanes. X-ray quality red crystals of **9** (0.061 g, 72 %) were then obtained after storing this layered solution at $-30\,°C$ for 24 h. ^{1}H NMR (498 MHz, CDCl$_3$): $\delta = 7.54$ (t, 4H, $^3J_{HH} = 7.6$ Hz, ArH), 7.37 (d, 8H, $^3J_{HH} = 7.8$ Hz, ArH), 2.69 (sept, 8H, $^3J_{HH} = 6.9$ Hz, CH(CH$_3$)$_2$), 2.42 (s, 4H, CCH_2Pd), 1.86 (s, 12H, NC-CH_3), 1.52 (d, 24H, $^3J_{HH} = 6.7$ Hz, CH(CH_3)$_2$), 1.08 ppm (d, 24H, $^3J_{HH} = 6.7$ Hz, CH(CH_3)$_2$); ^{13}C{^{1}H} NMR (125 MHz, CDCl$_3$): $\delta = 10.2$ (NC(CH$_3$)), 10.7 (CCH$_2$Pd), 25.2 (CH(CH$_3$)$_2$), 25.7 (CH(CH$_3$)$_2$), 29.0 (CH(CH$_3$)$_2$), 125.6 (NC(CH$_3$)), 129.1 (ArC), 131.2 (ArC), 132.4 (ArC), 145.8 (ArC), 146.7 ppm (NCN); element. anal.: calcd for C$_{74}$H$_{100}$N$_4$Pd$_2$Cl$_4$ (**9**·2 C$_7$H$_8$): C, 63.47; H, 7.20; N, 4.00; found: C, 62.86; H, 7.18; N, 3.96 %; mp: 163 °C (dec.).

Synthesis of [(^{Me}IPrCH$_2$)PdCl$_2$(3-Cl-pyr)] (10). To a solution of [(^{Me}IPrCH$_2$)PdCl(μ-Cl)]$_2$ (0.020 g, 0.014 mmol) in CH_2Cl_2 (2 mL) was added 3-chloropyridine (0.010 g, 0.08 mmol) at room temperature. Stirring was continued for 2 h and afterwards the volatiles were removed under vacuum. The residue was dissolved in CH_2Cl_2 (0.2 mL) and filtered through a plug of Celite. The filtrate was concentrated to incipient crystallization and layered with hexanes. After placing the sample at $-30\,°C$ for 24 h, pale-yellow crystals of **10** formed (0.015 g, 67 %) that were suitable for X-ray crystallographic analysis. ^{1}H NMR (498 MHz, CDCl$_3$): $\delta = 8.62$ (d, 1H, $^3J_{HH} = 2.2$ Hz, 3-Cl-pyr), 8.54 (d, 1H, $^3J_{HH} = 5.4$ Hz, 3-Cl-pyr), 7.57 (t, 2H, $^3J_{HH} =$

7.8 Hz, Ar*H*), 7.53–7.56 (m, 1H, 3-Cl-pyr), 7.39 (d, 4H, $^3J_{HH}$ = 7.8 Hz, Ar*H*), 7.09 (dd, 1H, $^3J_{HH}$ = 8.0 Hz, $^3J_{HH}$ = 5.7 Hz, 3-Cl-pyr), 2.60 (sept, 4H, $^3J_{HH}$ = 6.7 Hz, C*H*(CH$_3$)$_2$), 2.60 (s, 2H, CC*H*$_2$−Pd), 1.96 (s, 6H, NC−C*H*$_3$), 1.44 (d, 24H, $^3J_{HH}$ = 6.7 Hz, CH(C*H*$_3$)$_2$), 1.13 ppm (d, 12H, $^3J_{HH}$ = 6.7 Hz, CH(C*H*$_3$)$_2$); ^{13}C{^{1}H} NMR (126 MHz, CDCl$_3$): δ = 10.4 (NC(*C*H$_3$)), 25.0 (CH(*C*H$_3$)$_2$), 25.3 (CH(*C*H$_3$)$_2$), 28.8 (*C*H(CH$_3$)$_2$), 124.2 (Ar*C*), 125.5 (Ar*C*), 126.1 (Ar*C*), 129.9 (Ar*C*), 131.2 (Ar*C*), 136.6 (Ar*C*), 146.8 (Ar*C*), 149.4 (Ar*C*), 150.5 (Ar*C*), 163.8 ppm (N*C*N); element. anal.: calcd for C$_{34}$H$_{45}$Cl$_3$N$_3$Pd: C, 58.26; H, 6.43; N, 5.80; found: C, 58.51; H, 6.20; N, 5.82 %; mp: 178 °C (dec).

Synthesis of [{IPr(BIAN)CH$_2$}PdCl(μ-Cl)]$_2$ (11). A solution of IPr(BIAN)CH$_2$ (0.063 g, 0.12 mmol) in toluene (2 mL) was added dropwise to a solution of *trans*-[Cl$_2$Pd(NCPh)$_2$] (0.046 g, 0.12 mmol) in toluene (1 mL) at room temperature. A red crystalline solid precipitated from the solution after stirring for 2 h. The precipitate was isolated by filtration and washed with fresh toluene (2 mL). The collected solid was re-dissolved in a minimum amount of CH$_2$Cl$_2$, and the resulting solution was layered with hexanes. X-ray quality red crystals of **11** (0.030 g, 31 %) were obtained from this layered solution after cooling at −30 °C for 24 h. Despite obtaining crystalline material, the bulk sample routinely contained approximately 10 % impurity. ^{1}H NMR (498 MHz, CDCl$_3$): δ = 7.84 (d, 4H, $^3J_{HH}$ = 6.9 Hz, Napht-*H*), 7.82 (t, 4H, $^3J_{HH}$ = 7.9 Hz, Ar*H*), 7.59 (d, 8H, $^3J_{HH}$ = 7.9 Hz, Ar*H*), 7.46 (dd, 4H, $^3J_{HH}$ = 6.9 Hz, $^3J_{HH}$ = 8.1 Hz, Napht-*H*), 7.02 (d, 4H, $^3J_{HH}$ = 6.9 Hz, Napht-*H*),

2.95 (sept, 8H, $^3J_{HH}$ = 6.9 Hz, CH(CH$_3$)$_2$), 2.57 (s, 4H, CCH_2−Pd), 1.49 (d, 24H, $^3J_{HH}$ = 6.7 Hz, CH(CH_3)$_2$), 0.98 ppm (d, 24H, $^3J_{HH}$ = 6.7 Hz, CH(CH_3)$_2$).

[{IPr(BIAN)CH$_2$}PdCl$_2$(3-Cl-pyr)] **(12).** To a solution of crude [{IPr(BIAN)CH$_2$}PdCl(μ-Cl)]$_2$ (0.034 g, 0.021 mmol) in CH$_2$Cl$_2$ (2 mL) was added 3-chloropyridine (0.015 g, 0.13 mmol) at room temperature. Stirring was continued for 2 h and the solvent was then removed under vacuum. The residue was dissolved in CH$_2$Cl$_2$ (0.2 mL) and filtered through a plug of Celite. The filtrate was concentrated to incipient crystallization and layered with hexanes. After placing the sample at −30 °C for 24 h, **12** (0.012 g, 32 %) was obtained in the form of yellow crystals suitable for X-ray crystallographic analysis. ^{1}H NMR (498 MHz, CDCl$_3$): δ = 8.80 (d, 1H, $^3J_{HH}$ = 2.4 Hz, 3-Cl-pyr), 8.70 (dd, 1H, $^3J_{HH}$ = 5.5, $^3J_{HH}$ = 1.4 Hz, 3-Cl-pyr), 7.81 (d, 2H, $^3J_{HH}$ = 8.2 Hz, Napht-H), 7.69 (t, 2H, $^3J_{HH}$ = 7.9 Hz, ArH), 7.53–7.56 (m, 1H, 3-Cl-pyr), 7.50 (d, 4H, $^3J_{HH}$ = 7.9 Hz, ArH), 7.40 (dd, 2H, $^3J_{HH}$ = 8.2 Hz, $^3J_{HH}$ = 7.0 Hz, Napht-H), 7.11 (dd, 1H, $^3J_{HH}$ = 8.1 Hz, $^3J_{HH}$ = 5.5 Hz, 3-Cl-pyr), 7.02 (d, 2H, $^3J_{HH}$ = 7.0 Hz, Napht-H), 3.15 (sept, 8H, $^3J_{HH}$ = 6.9 Hz, CH(CH$_3$)$_2$), 2.86 (s, 4H, CCH_2-Pd), 1.44 (d, 12H, $^3J_{HH}$ = 6.7 Hz, CH(CH_3)$_2$), 1.01 ppm (d, 12H, $^3J_{HH}$ = 6.7 Hz, CH(CH_3)$_2$); ^{13}C{^{1}H} NMR (126 MHz, CDCl$_3$): δ = 23.9 (CH(CH_3)$_2$), 25.8 (CH(CH_3)$_2$), 29.4 (CH(CH$_3$)$_2$), 122.6 (Napht-C), 124.3 (pyr-C), 127.7 (Napht-C), 129.2 (ArC), 129.8 (ArC), 129.9 (ArC), 130.9 (Napht-C), 132.0 (ArC), 131.7 (ArC), 132.0 (ArC), 136.6 (pyr-C), 146.6 (pyr-C), 149.6 (pyr-C), 150.7 (pyr-C), 168.3 ppm (NCN); element. anal.: calcd for: C, 63.71; H, 5.67; N, 5.14; found: C, 61.72; H, 5.65;

N, 5.01. Despite repeated attempts, combustion analysis gave consistently low carbon values.

[(^MeIPrCHCHCH₂)PdCl₂(3-Cl-pyr)] (13). A solution of ^MeIPr=CH−CH=CH₂ (0.110 g, 0.241 mmol) in toluene (1 mL) was added dropwise a solution of *trans*-[Cl₂Pd(NCPh)₂] (0.070 g, 0.18 mmol) in toluene (5 mL) at room temperature. After 2 h a red precipitate formed, which was isolated by filtration and washed with toluene (2 mL). This solid was then dissolved in CH_2Cl_2 (1 mL) and 3-chloropyridine (0.027 g, 0.24 mmol) was then added. The resulting mixture was filtered through Celite and the volatiles were removed in vacuo from the filtrate. The crude product was then recrystallized from an acetonitrile/hexanes mixture that was cooled to −30 °C for 24 h, affording red X-ray quality crystals of **13** (0.0712 g, 46 %). ^{1}H NMR (498 MHz, CDCl₃): δ = 8.86 (br, 1H, 3-Cl-pyr), 8.76 (br, 1H, 3-Cl-pyr), 7.63 (t, 2H, $^3J_{HH}$ = 8.0 Hz, Ar*H*), 7.57 (d, 1H, $^3J_{HH}$ = 8.0 Hz, 3-Cl-pyr), 7.42 (d, 4H, $^3J_{HH}$ = 8.0 Hz, Ar*H*), 7.13 (br, 1H, 3-Cl-pyr), 5.99–6.08 (m, 1H, CH=C*H*), 5.92 (d, 1H, $^3J_{HH}$ = 15.5 Hz, C*H*=CH), 3.01 (d, 2H, $^3J_{HH}$ = 9.3 Hz, CHC*H₂*Pd), 2.45 (sept, 4H, $^3J_{HH}$ = 6.9 Hz, C*H*(CH₃)₂), 1.98 (s, 6 H, NCC*H₃*), 1.36 (d, 12H, $^3J_{HH}$ = 7.0 Hz, CH(C*H₃*)₂), 1.25 ppm (d, 12H, $^3J_{HH}$ = 7.0 Hz, CH(C*H₃*)₂); ^{13}C{^{1}H} NMR (125.7 MHz, CDCl₃): δ = 9.4 (NC*C*H₃), 19.7 (CH=CH−*C*H₂), 23.8 (CH(*C*H₃)₂), 24.3 (CH(*C*H₃)₂), 29.2 (*C*H(CH₃)₂, 97.7 (*C*H=CH−CH₂), 125.3 (3-Cl-pyr), 125.7 (Ar*C*), 128.6 (3-Cl-pyr), 132.2 (Ar*C*), 145.2 (3-Cl-pyr), 146.3 (3-Cl-pyr), 156.8 ppm (CH=*C*H−CH₂); element. anal.: calcd

for $C_{51}H_{39}Cl_3N_3Pd$: C, 59.14; H, 6.57; N, 5.61; found: C, 59.14; H, 6.57; N, 5.79; mp: 154–156 °C (dec).

3.4.6. Buchwald–Hartwig Cross-Coupling Procedure

Preparation of the reaction mixtures were conducted in a glovebox under an argon atmosphere. A 0.100 M stock solution of $^{Me}IPrCH_2$ and a 0.0125 M stock solution of [Pd(cinnamyl)Cl]$_2$ were prepared. To a mixture of 1.00 mmol of arylhalide, 1.20 mmol of arylamine and 144 mg (1.50 mmol) of NaO^{t}Bu in THF (2 mL) in a vial was added 100 μL (0.0100 mmol) of the $^{Me}IPrCH_2$ stock solution and 400 μL (0.00500 mmol) of the [Pd(cinnamyl)Cl]$_2$ stock solution. Molecular sieves (4 Å) were added and the vial was capped using a cap with a PTFE septa. The reaction mixture was stirred for 1 h at 80 °C. The reaction mixture was sampled through a syringe for NMR analysis. To isolate the product, after cooling to room temperature the vial was opened to air, filtered, then evaporated using a rotary evaporator. The products were isolated by column chromatography (silica, n-hexane/ethyl acetate 10:1) or flash chromatography (silica, n-hexane eluent).

3.4.7. Preparation of Cross-Coupling Products According to the Procedure in Section 3.4.6.

2,6-Diisopropyl-N-(p-tolyl)aniline (14a).[47] Compound **14a** was prepared from 171 mg (1.00 mmol) of 4-bromotoluene [4-Br-Tol] and 213 mg (1.20 mmol) of 2,6-diisopropylaniline (DippNH$_2$). Flash chromatography (silica, n-hexane) afforded 32

mg (0.12 mmol, 12 %) of 2,6-diisopropyl-N-(p-tolyl)aniline as a white solid. ^{1}H NMR (300 MHz, CDCl$_3$): δ = 7.23-7.34 (m, 3H, ArH), 6.99 (d, 2H, $^3J_{HH}$ = 8.2 Hz, ArH), 6.44 (d, 2H, $^3J_{HH}$ = 7.8 Hz, ArH), 5.06 (br, 1H, NH), 3.24 (septet, 2H, $^3J_{HH}$ = 6.9 Hz, CH(CH$_3$)$_2$), 2.27 (s, 3H, CH_3 tolyl), 1.18 (d, 12H, $^3J_{HH}$ = 6.9 Hz, CH(CH_3)$_2$).

N-(p-Tolyl)-2,4,6-trimethylaniline (14b).[48] *Preparation A*: Compound **14b** was prepared from 171 mg (1.00 mmol) of 4-bromotoluene and 162 mg (1.20 mmol) of mesitylamine (MesNH$_2$). Flash chromatography (silica, n-hexane) afforded 183 mg (0.81 mmol, 81 %) of N-(p-tolyl)-2,4,6-trimethylaniline as an off-white solid. *Preparation B*: Compound **14b** was also prepared from 199 mg (1.00 mmol) of 2-bromomesitylene [2-Br-Mes] and 129 mg (1.20 mmol) of p-toluidine. Flash chromatography afforded 212 mg (0.94 mmol, 94 %) of N-(p-tolyl)-2,4,6-trimethylaniline as a yellow oil. ^{1}H NMR (300 MHz, CDCl$_3$): δ = 6.96 (d, 2H, $^3J_{HH}$ = 8.2 Hz, ArH tolyl), 6.93 (s, 2H, ArH Mes), 6.43 (d, 2H, $^3J_{HH}$ = 8.1 Hz, ArH tolyl), 2.30 (s, 3H, CH_3), 2.24 (s, 3H, CH_3), 2.17 (s, 6H, CH_3).

N-(2,6-Diisopropylphenyl)-2,4,6-trimethylaniline (14c).[48] Compound **14c** was prepared from 1.99 mg (1.00 mmol) of 2-bromomesitylene and 213 mg (1.20 mmol) of 2,6-diisopropylaniline. Flash chromatography afforded 275 mg (0.93 mmol, 93 %) of N-(2,6-diisopropylphenyl)-2,4,6-trimethylaniline (Dipp)MesNH as a colorless oil. ^{1}H NMR (300 MHz, CD$_2$Cl$_2$): δ = 7.10 (m, 3H, ArH), 6.75 (s, 2H, ArH Mes), 4.75 (s,

1H, NH), 3.13 (septet, 2H, $^3J_{HH}$ = 6.9 Hz, CH(CH$_3$)$_2$), 2.21 (s, 3H, CH_3 Mes), 1.95 (s, 6H, CH_3 Mes), 1.11 (d, $^3J_{HH}$ = 6.9 Hz, 12H, CH(CH_3)$_2$).

Di(*p*-tolyl)amine (14d).[49] *Small Scale*: Compound **14d** was prepared using 127 mg (1.00 mmol) of 4-chlorotoluene [4-Cl-Tol] and 129 mg (1.20 mmol) of *p*-toluidine. Flash chromatography (silica, *n*-hexane) afforded 189 mg (0.96 mmol, 96 %) of di(*p*-tolyl)amine as a white solid. *Large Scale*: Starting from 1.27 g (10.0 mmol) of 4-chlorotoluene and 1.29 g (12.0 mmol) of *p*-toluidine in an overall volume of 20 mL of THF, with otherwise identical conditions as above. This resulted in an isolated yield of 1.85 g (9.4 mmol, 94 %) of (*p*-tolyl)$_2$NH as a colorless solid. ^{1}H NMR (300 MHz, CDCl$_3$): δ = 7.07 (d, 4H, $^3J_{HH}$ = 8.1 Hz, ArH), 6.96 (d, 4H, $^3J_{HH}$ = 8.3 Hz, ArH), 5.72 (br, 1H, NH), 2.29 (s, 6H, CH_3).

***N*-(*p*-Tolyl)anthracene-9-amine (14e).**[49] Compound **14e** was prepared from 257 mg (1.00 mmol) of 9-bromoanthracene [9-Br-anth] and 129 mg (1.20 mmol) of *p*-toluidine. Column chromatography (silica, *n*-hexane/ethyl acetate 10:1) afforded 275 mg (0.97 mmol, 97 %) of *N*-(4-tolyl)anthracene-9-amine as an orange solid. ^{1}H NMR (300 MHz, CDCl$_3$): δ = 8.40 (s, 1H, ArH), 8.20 (d, 2H, $^3J_{HH}$ = 9.0 Hz, ArH), 8.05 (d, 2H, $^3J_{HH}$ = 8.6 Hz, ArH tolyl), 7.47 (dp, 4H, $^3J_{HH}$ = 8.5 Hz, $^3J_{HH}$ = 1.8 Hz, ArH), 6.98 (d, 2H, $^3J_{HH}$ = 8.6 Hz, ArH tolyl), 6.53 (d, 2H, $^3J_{HH}$ = 8.1 Hz, ArH), 5.93 (br, 1H, NH), 2.26 (s, 3H, CH_3).

4-Fluoro-4′-methyldiphenylamine (14f).[47] Compound **14f** was prepared from 175 mg (1.00 mmol) of 4-bromo-1-fluorobenzene [4-Br-1-F-benzene] and 129 mg (1.20 mmol) of *p*-toluidine. Column chromatography (silica, *n*-hexane/ethyl acetate 10:1) afforded 199 mg (0.99 mmol, 99 %) of 4-fluoro-4′-methyldiphenylamine as a white solid. ^{1}H NMR (300 MHz, CDCl$_3$): δ = 7.08 (d, 2H, $^3J_{HH}$ = 8.0 Hz, Ar*H*), 6.90-7.00 (m, 6H, Ar*H*), 5.46 (br, 1H, N*H*), 2.30 (s, 3H, C*H*$_3$).

4-Methoxy-*N*-(*p*-tolyl)aniline (14g).[47] Compound **14g** was prepared from 187 mg (1.00 mmol) of *p*-bromoanisole [4-Br-anisole] and 129 mg (1.20 mmol) of *p*-toluidine. Column chromatography (silica, *n*-hexane/ ethyl acetate 10:1) afforded 209 mg (0.98 mmol, 98 %) of 4-methoxy-*N*-*p*-tolylaniline as a white solid. ^{1}H NMR (300 MHz, CDCl$_3$): δ = 7.03-7.06 (m, 4H, Ar*H*), 6.84-6.88 (m, 4H, Ar*H*), 5.40 (br, 1H, N*H*), 3.81 (s, 3H, OC*H*$_3$), 2.30 (s, 3H, C*H*$_3$).

N-(*p*-Tolyl)morpholine (14h).[50] Compound **14h** was prepared starting from 127 mg (1.00 mmol) of 4-chlorotoluene and 105 mg (1.20 mmol) of morpholine. Column chromatography (silica, *n*-hexane/ ethyl acetate 10:1) afforded 172 mg (0.97 mmol, 97 %) of *N*-(*p*-tolyl)morpholine as an off-white solid. ^{1}H NMR (300 MHz, CDCl$_3$): δ = 7.09 (d, 2H, $^3J_{HH}$ = 7.11 Hz, Ar*H*), 6.84 (d, 2H, $^3J_{HH}$ = 7.1 Hz, Ar*H*), 3.86 (s, 4H, C*H*$_2$), 3.11 (s, 4H, C*H*$_2$), 2.28 (s, 3H, C*H*$_3$).

***N*-(*p*-Methylbenzyl)-*p*-methylylaniline (14i).**[60] Compound **14i** was prepared starting from 127 mg (1.00 mmol) of 4-chlorotoluene and 145 mg (1.20 mmol) of *p*-methylbenzylamine. Column chromatography (silica, *n*-hexane/ ethyl acetate 10:1) afforded 169 mg (0.80 mmol, 80 %) of *N*-(*p*-methylbenzyl)-*p*-methylaniline as off-white solid. ^{1}H NMR (300 MHz, CDCl$_3$): δ = 7.28 (d, 2H, $^3J_{HH}$ = 7.2 Hz, Ar*H*), 7.16 (d, 2H, $^3J_{HH}$ = 7.8 Hz, Ar*H*), 7.00 (d, 2H, $^3J_{HH}$ = 8.3 Hz, Ar*H*), 6.54 (d, 2H, $^3J_{HH}$ = 8.4 Hz, Ar*H*), 4.28 (s, 2H, C*H*$_2$), 3.95 (br, 1H, N*H*), 2.36 (s, 3H, C*H*$_3$), 2.25 (s, 3H, C*H*$_3$).

***N*,4-Dimethyl-*N*-phenylaniline (14j).**[51] Compound **14j** was prepared starting from 127 mg (1.00 mmol) of 4-chlorotoluene and 129 mg (1.20 mmol) of methylphenylamine. Column chromatography (silica, *n*-hexane/ethyl acetate 10:1) afforded 173 mg (0.88 mmol, 88 %) of *N*,4-dimethyl-*N*-phenylaniline as a yellow oil. ^{1}H NMR (300 MHz, CDCl$_3$): δ = 7.20-7.31 (m, 2H, Ar*H* Ph), 7.14 (d, 2H, $^3J_{HH}$ = 8.5 Hz, Ar*H* p-Tol), 7.02 (d, 2H, $^3J_{HH}$ = 8.4 Hz, Ar*H* p-Tol), 6.85-6.99 (m, 3H, Ar*H* Ph), 3.31 (s, 3H, C*H*$_3$), 2.35 (s, 3H, C*H*$_3$).

3.5. Crystallography Data

Table 3.5. Crystallographic data for **1**, **2**, and **3**.

Compound	1	2	3
formula	$C_{32}H_{44}N_2$	$C_{38}H_{42}N_2$	$C_{28}H_{40}N_2$
formula weight	456.72	526.77	404.64
crystal system	monoclinic	monoclinic	triclinic
Space Group	$P2_1/c$	$P2_1/n$	$P\bar{1}$
a (Å)	18.976(3)	12.8745(3)	13.9578(3)
b (Å)	9.2917(16)	19.6382(4)	16.6138(3)
c (Å)	16.597(3)	13.0964(3)	23.1281(5)
α (deg)	--	--	79.1412(9)
β (deg)	92.188(2)	109.661(1)	80.9639(8)
γ (deg)	--	--	78.9657(10)
V (Å^3)	2924.24(90)	3118.15(12)	5128.92(18)
Z	4	4	8
ρ_{calcd} (g cm^{-3})	1.037	1.122	1.048
Abs coeff (mm^{-1})	0.06	0.49	0.45
T (K)	193	173	173
$2\theta_{max}$ (°)	51.0	140.4	148.4
Total Data	23183	17449	36843
Unique data (R_{int})	5431 (0.054)	5917 (0.059)	11405 (0.077)
Obs data [I>2(σ(I)]	3154	4379	8244
Params	366	361	1081
R_1 [I>2(σ(I)][a]	0.049	0.082	0.053
wR_2 [all data][a]	0.135	0.249	0.149
Max/min $\Delta\rho$ (e$^-$Å^{-3})	0.16/–0.13	0.49/–0.34	0.35/–0.36

[a] $R_1 = \Sigma||F_o| - |F_c||/\Sigma|F_o|$; $wR_2 = [\Sigma w(F_o^2 - F_c^2)^2/\Sigma w(F_o^4)]^{1/2}$

Table 3.6. Crystallographic data for **4**, **6**, and **8**.

Compound	**4**	**6**	**8**
formula	$C_{32}H_{44}N_2$	$C_{31}H_{42}N_2$	$C_{36}H_{51}F_3N_2O_3S$
formula weight	456.69	442.66	648.84
crystal system	orthorhombic	monoclinic	monoclinic
Space Group	*Pbca*	*C2/c*	*P2$_1$/c*
a (Å)	18.8447(3)	16.2856(3)	12.8230(2)
b (Å)	17.8189(3)	9.4045(2)	14.6646(2)
c (Å)	34.4726(6)	17.6620(3)	19.6088(3)
α (deg)	--	--	--
β (deg)	--	91.4804(6)	105.5340(10)
γ (deg)	--	--	--
V (Å^3)	11575.66(3)	2704.17(9)	3552.63(9)
Z	16	4	4
ρ_{calcd} (g cm^{-3})	1.048	1.087	1.213
Abs coeff (mm^{-1})	0.45	0.47	1.24
T (K)	173	173	173
$2\theta_{max}$ (°)	144.4	148.0	144.0
Total Data	72189	8665	24355
Unique data (R_{int})	11405 (0.077)	2653(0.015)	6978 (0.03)
Obs data [I>2(σ(I)]	8244	2463	6002
Params	613	152	541
R_1 [I>2(σ(I)]^a	0.0549	0.041	0.051
wR_2 [all data]^a	0.1659	0.117	0.141
Max/min $\Delta\rho$ (e$^-$Å^{-3})	0.56/–0.32	0.23/–0.21	0.47/–0.37

^{a} $R_1 = \Sigma||F_o| - |F_c||/\Sigma|F_o|$; $wR_2 = [\Sigma w(F_o^2 - F_c^2)^2/\Sigma w(F_o^4)]^{1/2}$

Table 3.7. Crystallographic data for **9**, **10**, and **11**.

Compound	**9**	**10**	**11**
formula	$C_{60}H_{84}Cl_4N_2Pd_2$	$C_{35}H_{46}Cl_3N_3Pd$	$C_{76}H_{84}Cl_4N_4Pd_2$
formula weight	1212.35	808.44	1592.33
crystal system	monoclinic	triclinic	monoclinic
Space Group	$P2_1/n$	$P\bar{1}$	$C2/c$
a (Å)	12.1465(5)	10.70(4)	43.1349(7)
b (Å)	19.6523(8)	13.72(4)	15.9471(2)
c (Å)	15.1820(6)	14.50(6)	24.9880(4)
α (deg)	--	75.62(11)	--
β (deg)	94.124(1)	74.4(2)	113.714(1)
γ (deg)	--	71.15(9)	--
V (Å^3)	3614.7(3)	1909(13)	15737.3(4)
Z	2	2	8
ρ_{calcd} (g cm^{-3})	1.286	1.405	1.344
Abs coeff (mm^{-1})	0.69	0.86	5.30
T (K)	193	193	173
$2\theta_{max}$ (°)	55.0	54	144.8
Total Data	57138	16491	54413
Unique data (R_{int})	8305 (0.046)	8335 (0.022)	15403 (0.025)
Obs data [$I>2(\sigma(I)$]	7023	6931	13905
Params	441	390	901
R_1 [$I>2(\sigma(I)$]^a	0.034	0.030	0.031
wR_2 [all data]^a	0.093	0.076	0.087
Max/min $\Delta\rho$ (e$^-$Å^{-3})	1.13/–0.34	0.47/–0.27	0.65/–0.87

^{a} $R_1 = \Sigma||F_o| - |F_c||/\Sigma|F_o|$; $wR_2 = [\Sigma w(F_o^2 - F_c^2)^2/\Sigma w(F_o^4)]^{1/2}$

Table 3.8. Crystallographic data for **12** and **13**.

Compound	**12**	**13**
formula	$C_{43}H_{46}Cl_3N_3Pd$	$C_{36}H_{46}Cl_3N_3Pd$
formula weight	944.96	855.25
crystal system	triclinic	triclinic
Space Group	$P\bar{1}$	$P\bar{1}$
a (Å)	12.2664(9)	10.4610(5)
b (Å)	12.7814(10)	14.4418(8)
c (Å)	15.4035(12)	17.0423(9)
α (deg)	84.26(1)	77.0821(18)
β (deg)	87.172(1)	86.8222(16)
γ (deg)	65.803(1)	69.2001(19)
V (Å^3)	2191.7(3)	2345.15(19)
Z	2	2
ρ_{calcd} (g cm^{-3})	1.432	1.211
Abs coeff (mm^{-1})	0.82	4.988
T (K)	193	173
$2\theta_{max}$ (°)	52.96	147.96
Total Data	34741	16804
Unique data (R_{int})	10020 (0.035)	9113 (0.0215)
Obs data [I>2(σ(I)]	8072	8832
Params	514	399
R_1 [I>2(σ(I)][a]	0.038	0.0289
wR_2 [all data][a]	0.106	0.0787
Max/min $\Delta\rho$ (e$^-$Å^{-3})	0.78/–0.44	0.911/–0.823

[a] $R_1 = \Sigma||F_o| - |F_c||/\Sigma|F_o|$; $wR_2 = [\Sigma w(F_o{}^2 - F_c{}^2)^2/\Sigma w(F_o{}^4)]^{1/2}$

3.6 References

1. Arduengo, A. J.; Harlow, R. L.; Kline, M. *J. Am. Chem. Soc.* **1991**, *113*, 361-363.

2. Nolan, S. P.; Cazin, C. S. J. *Science of Synthesis: N-Heterocyclic Carbenes in Catalytic Organic Synthesis, Vol. 1* (Eds.: S. P. Nolan, C. S. J. Cazin), Thieme, Stuttgart, 2017, pp. 161-182.

3. a) Grendemann, S.; Kovacevic, A.; Albrecht, M.; Faller, J. W.; Crabtree, R. H. *J. Am. Chem. Soc.* **2002**, *124*, 10473-10481. b) Lebel, H.; Janes, M. K.; Charette, A. B.; Nolan, S. P. *J. Am. Chem. Soc.* **2004**, *126*, 5046-5047. c) Schuster, O.; Yang, L.; Raubenheimer, H. G.; Albrecht, M. *Chem. Rev.* **2009**, *109*, 3445-3478.

4. Melaimi, M.; Jazzar, R.; Soleilhavoup, M.; Bertrand, G. *Angew. Chem. Int. Ed.* **2017**, *56*, 10046-10068.

5. a) Dröge, T.; Glorius, F. *Angew. Chem. Int. Ed.* **2010**, *49*, 6940-6952. b) Hopkinson, M. N.; Richter, C.; Schedler, M.; Glorius, F. *Nature* **2014**, *510*, 485-496.

6. Fortman, G. C.; Nolan, S. P. *Chem. Soc. Rev.* **2011**, *40*, 5151-5169.

7. Viciu, M. S.; Kissling, R. M.; Stevens, E. D.; Nolan, S. P. *Org. Lett.* **2002**, *4*, 2229-2231.

8. a) Viciu, M. S.; Germaneau, R. F.; Navarro-Fernandez, O.; Stevens, E. D.; Nolan, S. P. *Organometallics* **2002**, *21*, 5470-5472. b) Marion, N.; Navarro-Fernandez, O.; Mei, J.; Stevens, E. D.; Scott, N. M.; Nolan, S. P. *J. Am. Chem. Soc.* **2006**, *128*, 4101-4111.

9. a) O'Brien, C. J.; Kantchev, E. A. B.; Valente, C.; Hadei, N.; Chass, G. A.; Lough, A. J.; Hopkinson, A. C.; Organ, M. G. *Chem. Eur. J.* **2006**, *12*, 4743-4748. b) Organ, M. G.; Abdel-Hadi, M.; Avola, S.; Dubovyk, I.; Hadei, N.; Kantchev, E. A. B.; O'Brien, C. J.; Sayah, M.; Valente, C. *Chem. Eur. J.* **2008**, *14*, 2443-2452. c) Tu, T.; Fang, W.; Jiang, J. *Chem. Commun.* **2011**, *47*, 12358-12360.

10. a) Kuhn, N.; Bohnen, H.; Kreutzberg, J.; Bläser, D.; Boese, R. *J. Chem. Soc. Chem. Commun.* **1993**, 1136-1137. b) Kuhn, N.; Bohnen, H.; Bläser, D.; Boese, R.; *Chem. Ber.* **1994**, *127*, 1405-1407. c) Ponti, P. P.; Baldwin, J. C.; Kaska, W. C. *Inorg. Chem.* **1979**, *18*, 873-875. d) For a related study on triazolylidene-based NHOs, see: Enders, D.; Breuer, K.; Raabe, G.; Runsink, J.; Teles, J. H.; Melder, J.-P.; Ebel, K.; Brode, S. *Angew. Chem. Int. Ed. Engl.* **1995**, *34*, 1021-1023.

11. Roy, M. M. D.; Rivard, E. *Acc. Chem. Res.* **2017**, *50*, 2017-2025.

12. a) Fürstner, A.; Alcarazo, M.; Goddard, R.; Lehmann, C. W. *Angew. Chem. Int. Ed.* **2008**, *47*, 3210-3214. b) Al-Rafia, S. M. I.; Malcolm, A. C.; Liew, S. K.; Ferguson, M. J.; McDonald, R.; Rivard, E. *Chem. Commun.* **2011**, *47*, 6987-6989. c) Knappke, C. E. I.; Arduengo III, A. J.; Jiao, H.; Neudörfl, J. M.; von Wangelin, A. J. *Synthesis* **2011**, 3784-3795.

13. Powers, K.; Hering-Junghans, C.; McDonald, R.; Ferguson, M. J.; Rivard, E. *Polyhedron* **2016**, *108*, 8-14.

14. Kronig, S.; Jones, P. G.; Tamm, M. *Eur. J. Inorg. Chem.* **2013**, 2301-2314.

15. a) Iglesias, M.; Iturmendi, A.; Sanz Miguel, P. J.; Polo, V.; Pérez-Torrente, J. J; Oro, L. A. *Chem. Commun.* **2015**, *51*, 12431-12434. b) Iturmendi, A.; García, N.; Jaseer, E. A.; Munárriz, J.; Sanz Miguel, P. J.; Polo, V.; Iglesias, M.; Oro, L. A. *Dalton Trans.* **2016**, *45*, 12835-12845.

16. Al-Rafia, S. M. I.; Ferguson, M. J.; Rivard, E. *Inorg. Chem.* **2011**, *50*, 10543-10545. b) Al-Rafia, S. M. I.; Momeni, M. R.; Ferguson, M. J; McDonald, R.; Brown, A.; Rivard, E. *Organometallics* **2013**, *32*, 6658-6665. c) Wang, Y.; Abraham, M. Y.; Gilliard, Jr., R. J.; Sexton, D. R.; Wei, P.; Robinson, G. H. *Organometallics* **2013**, *32*, 6639-6642. d) Berger, C. J.; He, G.; Merten, C.; McDonald, R.; Ferguson, M. J.; Rivard, E. *Inorg. Chem.* **2014**, *53*, 1475-1486. e) Ghadwal, R. S.; Schermann, C. J.; Engelhardt, F.; Steinmetzger, C. *Eur. J. Inorg. Chem.* **2014**, 4921-4926. f) Lee, W.-H.; Lin, Y.-F.; Lee, G.-H.; Peng, S.-M.; Chiu, C.-W. *Dalton Trans.* **2016**, *45*, 5937-5940. g) Hering-Junghans, C.; Andreiuk, P.; Ferguson, M. J.; McDonald, R.; Rivard, E. *Angew. Chem. Int. Ed.* **2017**, *56*, 6272-6275. h) Causero, A.; Elsen, H.; Pahl, J.; Harder, S. *Angew. Chem. Int. Ed.* **2017**, *56*, 6906-6910. i) Roy, M. M. D.; Ferguson, M. J.; McDonald, R.; Zhou, Y.; Rivard, E. *Chem. Sci.* **2019**, *10*, 6476-6481.

17. For recent examples, see: a) Wang, Q.; Zhao, W.; Zhang, S.; He, J.; Zhang, S.; Chen, E. Y.-X. *ACS Catal.* **2018**, *8*, 3571-3578. b) Walther, P.; Naumann, S. *Macromolecules* **2017**, *50*, 8406-8416. c) Hering-Junghans, C.; Watson, I. C.; Ferguson, M. J.; McDonald, R.; Rivard, E. *Dalton Trans.* **2017**, *46*, 7150-7153. d) Kaya, U.; Tran, U. P. N.; Enders, D.; Ho, J.; Nguyen, T. V. *Org. Lett.* **2017**, *19*, 1398-1401.

18. Crocker, R. D.; Nguyen, T. V. *Chem. Eur. J.* **2016**, *22*, 2208-2213.

19. Knappke, C. E. I.; Neudörfl, J. M.; von Wangelin, A. J. *Org. Biomol. Chem.* **2010**, *8*, 1695-1705.

20. For related fulvalene-type NHOs, see: Kunz, D.; Johnsen, E. Ø.; Monsler, B.; Rominger, F. *Chem. Eur. J.* **2008**, *14*, 10909-10914.

21. Schumann, A.; Hering-Junghans, C. *Eur. J. Inorg. Chem.* **2018**, 2584-2588.

22. CCDC 1903754, 1903755, 1903756, 1903757, 1903758, 1903759, 1903760, 1903761, 1903762, 1903763, 1903764 contain the supplementary crystallographic data for this Chapter. These data are provided free of charge by The Cambridge Crystallographic Data Centre.

23. Gasperini, M.; Ragaini, F.; Cenini, S. *Organometallics* **2002**, *21*, 2950-2957.

24. Ghadwal, R. S.; Reichmann, S. O.; Engelhardt, F.; Andrada, D. M.; Frenking, G. *Chem. Commun.* **2013**, *49*, 9440-9442.

25. a) Schuldt, R.; Kästner, J.; Naumann, S. *J. Org. Chem.* **2019**, *84*, 2209-2218. b) Raczyńska, E. D.; Decouzon, M.; Gal, J.-F.; Maria, P.-C.; Woźniak, K.; Kurg R.; Carins, S. N. *Trends Org. Chem.* **1998**, *7*, 996-103.

26. Lesieur, M.; Slawin, A. M. Z.; Cazin, C. S. *Org. Biomol. Chem.* **2014**, *12*, 5586-5589.

27. a) Hoi, K. H.; Coggan, J. A.; Organ, M. G. *Chem. Eur. J.* **2013**, *19*, 843-845. b) Pompeo, M.; Farmer, J. L.; Froese, R. D. J.; Organ, M. G. *Angew. Chem. Int. Ed.*

2014, *53*, 3223-3226. c) Sharif, S.; Rucker, R. P; Chandrasoma, N.; Mitchell, D.; Rodriquez, M. J.; Froese, R. D. J.; Organ, M. G. *Angew. Chem. Int. Ed.* **2015**, *54*, 9507-9511.

28. Surry, D. S.; Buchwald, S. L. *Chem. Sci.* **2011**, *2*, 27-50.

29. Crabtree, R. H. *Chem. Rev.* **2012**, *112*, 1536-1554.

30. Higman, C. S.; Lanterna, A. E.; Marin, M. L.; Scaiano, J. C.; Fogg, D. E. *ChemCatChem* **2016**, *8*, 2446-2449.

31. Gorunova, O. N.; Novitskiy, I. M.; Grishin, Y. K.; Gloriozov, I. P.; Roznyatovsky, V. A.; Khrustalev, V. N.; Kochetkov, K. A.; Dunina, V. V. *Organometallics* **2018**, *37*, 2842-2858.

32. Watzky, M. A.; Finke, R. G. *J. Am. Chem. Soc.* **1997**, *119*, 10382-10400.

33. McGuinness, D. S.; Saendig, N.; Yates, B. F.; Cavell, K. J. *J. Am. Chem. Soc.* **2001**, *123*, 4029-4040.

34. Sable, V.; Maindan, K.; Kapdi, A. R.; Shejwalker, P. S.; Hara, K. *ACS Omega* **2017**, *2*, 204-217.

35. Navaladian, S.; Viswanathan, B.; Varadarajan, T. K.; Viswanath, R. P. *Nanoscale Res. Lett.* **2009**, *4*, 181-186.

36. Arduengo III, A. J.; Krafczyk, R.; Schmutzler, R.; Craig, H. A.; Goerlich, J. R.; Marshall, W. J.; Unverzagt, M. *Tetrahedron* **1999**, *55*, 14523-14534.

37. Gaillard, S.; Bantreil, X.; Slawin, A. M. Z.; Nolan, S. P. *Dalton Trans.* **2009**, 6967-6971.

38. Vasudevan, K. V.; Butorac, R. R.; Abernathy, C. D.; Cowley, A. H. *Dalton Trans.* **2010**, *39*, 7401-7408.

39. Bantreil, X.; Nolan, S. P. *Nat. Protoc.* **2011**, *6*, 69-77.

40. Ryan, S. J; Schimler, S. D.; Bland, D. C.; Sanford, M. S. *Org. Lett.* **2015**, *17*, 1866-1869.

41. Sheldrick, G. M. *Acta. Crystallogr. Sect. A* **2015**, *71*, 3-8.

42. Sheldrick, G. M *Acta. Crystallogr. Sect. C* **2015**, *71*, 3-8.

43. Frisch, M. J.; Trucks, G. W.; Schlegel, H. B.; Scuseria, G. E.; Robb, M. A.; Cheeseman, J. R.; Scalmani, G.; Barone, V.; Mennucci, B.; Petersson, G. A.; Nakatsuji, H.; Caricato, M.; Li, X.; Hratchian, H. P,; Izmaylov, A. F.; Bloino, J.; Zheng, G.; Sonnenberg, J. L.; Hada, M.; Ehara, M.; Toyota, K.; Fukuda, R.; Hasegawa, J.; Ishida, M.; Nakajima, T.; Honda, Y.; Kitao, O.; Nakai, H.; Vreven, T.; Montgomery, Jr., J. A.; Peralta, J. E.; Ogliaro, F.; Bearpark, M.; Heyd, J. J.; Brothers, E.; Kudin, K. N.; Staroverov, V. N.; Kobayashi, R.; Normand, J.; Raghavachari, K.; Rendell, A.; Burant, J. C.; Iyengar, S. S.; Tomasi, J.; Cossi, M.; Rega, N.; Millam, J. M.; Klene, M.; Knox, J. E.; Cross, J. B.; Bakken, V.; Adamo, C.; Jaramillo, J.; Gomperts, R.; Stratmann, R. E.; Yazyev, O.; Austin, A. J.; Cammi, R.; Pomelli, C.; Ochterski, J. W.;. Martin, R. L.; Morokuma, K.; Zakrzewski, V. G.; Voth, G. A.; Salvador, P.; Dannenberg, J. J.; Dapprich, S.; Daniels, A. D.; Farkas, Ö.; Foresman, J.

B.; Ortiz, J. V.; Cioslowski, J.; Fox, D. J. Gaussian 09, Revision E.01, Gaussian, Inc., Wallingford CT, **2009**.

44. Becke, A. D. *J. Chem. Phys.* **1993**, *98*, 5648-5652.

45. a) Petersson, G. A.; Bennett, A.; Tensfeldt, T. G.; Al-Laham, M. A.; Shirley, W. A.; Mantzaris, J. *J. Chem. Phys.* **1988**, *89*, 2193-2218. b) Petersson, G. A.; Al-Laham, M. A. *J. Chem. Phys*. **1991**, *94*, 6081-6090.

46. a) Glendening, E. D.; Badenhoop, J. K.; Reed, A. E.; Carpenter, J. E.; Bohmann, J. A.; Morales, C. M.; Landis, C. R.; Weinhold, F. *NBO* 6.0, Theoretical Chemistry Institute, University of Wisconsin, Madison, 2013. b) Carpenter, J. E.; Weinhold, F. J. *Mol. Struct.* **1988**, *169*, 41–62. c) Weinhold, F.; Carpenter, J. E. *The Structure of Small Molecules and Ions*, Plenum, New York, 1988. d) Weinhold, F.; Landis, C. R. *Valency and Bonding. A Natural Bond Orbital Donor-Acceptor Perspective*, Cambridge University Press, Cambridge, 2005.

47. Tian, X.; Lin, J.; Zuo, S.; Lv, J.; Huang, Q.; Zhu, J.; Huang, S.; Wang, Q. *J. Organomet. Chem.* **2018**, *861*, 125-130.

48. Kim, M.; Shin, T.; Lee, A.; Kim, H. *Organometallics* **2018**, *19*, 3253-3258.

49. Sugahara, T.; Murakami, K.; Yorimitsu, H.; Osuka, A. *Angew. Chem. Int. Ed.* **2014**, *53*, 9329-9333.

50. Sai, M. *Adv. Synth. Catal.* **2021,** *363*, 5422-5428.

51. Cui, X.; Dai, X.; Deng, Y.; Shi, F. *Chem. Eur. J.* **2013**, *19,* 3665-3675.

Chapter 4: Trialkylaluminum *N*-Heterocyclic Olefin (NHO) Adducts as Catalysts for the Polymerization of Michael-Type Monomers

4.1 Introduction

N-Heterocyclic olefins (NHOs), first reported by Kaska with following reports by Kuhn in the mid-1990s,[1] are an emerging class of ylidic carbon-based donors that has attracted recent attention due to the ability of NHOs to stabilize various reactive main group species.[2] Related to *N*-heterocyclic carbenes (NHCs), NHOs feature an exocyclic alkylidene unit (=CR$_2$) attached to a heterocyclic imidazole ring, and are good σ-donating ligands but lack the ability to act as π-acceptors.[3]

NHOs have also been explored as organocatalysts/initiators within the realms or synthetic organic and polymer chemistry.[4] For example, Naumann and coworkers showed that NHOs can be used as initiators in the polymerization of dimethylacrylamide (DMAA).[4c] Furthermore, Chen and coworkers demonstrated that NHO•Al(C$_6$F$_5$)$_3$ Lewis pairs are capable of polymerizing lactones and challenging Michael-type monomers, such as crotonates;[5] in addition, the Lu Group showed that methyl methacrylate (MMA) can be polymerized with NHO•Al(C$_6$F$_5$)$_3$ complexes as initiators.[6] In related work, Chen and coworkers used NHC•AlR$_3$ adducts to polymerize methyl methacrylate.[7]

In this Chapter, the preparation of NHO•AlR$_3$ adducts, such as ^{Me}IPrCH$_2$•AlMe$_3$ (Chart 1) (^{Me}IPrCH$_2$ = (MeCNDipp)$_2$C=CH$_2$; Dipp = 2,6-^{i}Pr$_2$C$_6$H$_3$) are reported. These complexes are structurally related to the NHC or *N*-heterocyclic imine (NHI) adducts made previously by the groups of Robinson and Masuda, respectively (Chart 4.1).[8] One of the newly prepared NHO•AlR$_3$ complexes in this study was found to be a competent catalyst for the polymerization of Michael-type monomers at room temperature.
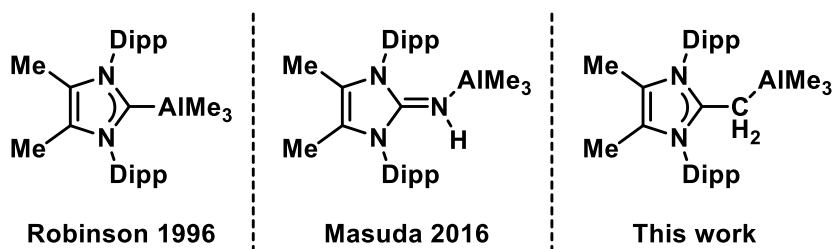
Chart 4.1. Examples of trimethylaluminum adducts with *N*-heterocyclic donors.

4.2 Results and Discussion

The first NHO•AlR$_3$ adduct presented in this Chapter, ^{Me}IPrCH$_2$•AlMe$_3$ (**1**), was obtained in a 68 % yield as a colorless solid by combining ^{Me}IPrCH$_2$ with one equivalent of AlMe$_3$ in toluene at room temperature (Scheme 4.1). As these results were encouraging, a similar reaction was performed between ^{Me}IPrCH$_2$ and AlEt$_3$, leading to the formation of the monoadduct ^{Me}IPrCH$_2$•AlEt$_3$ (**2**). Upon binding of ^{Me}IPrCH$_2$ to either AlMe$_3$ or AlEt$_3$, an upfield shift in the ^{1}H NMR signals (in C$_6$D$_6$) is observed relative to the free NHO. Specifically, the exocyclic C*H$_2$* resonance shifts

from 2.33 ppm in free ^{Me}IPrCH$_2$ to values of 2.01 ppm and 1.89 ppm in adducts **1** and

2, respectively. The ^{1}H NMR resonances belonging to the AlR$_3$ moieties in **1** and **2** are

also upfield-shifted in comparison to those found in the uncomplexed alanes AlMe$_3$

and AlEt$_3$; for example, the methyl resonance for the AlMe$_3$ group in **1** is found at

–0.52 ppm in C$_6$D$_6$, while the corresponding resonance for (dimeric) AlMe$_3$ in C$_6$D$_6$ is

–0.37 ppm.
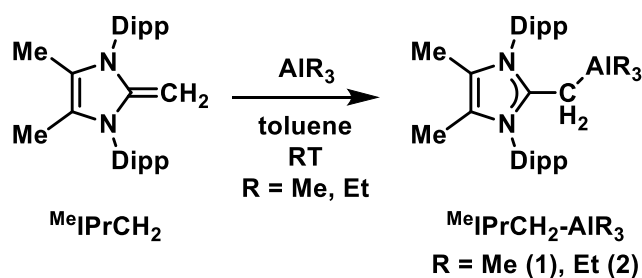
Scheme 4.1. Preparation of ^{Me}IPrCH$_2$•AlMe$_3$ (**1**) and ^{Me}IPrCH$_2$•AlEt$_3$ (**2**).

Figure 4.1 shows the structure of ^{Me}IPrCH$_2$•AlMe$_3$ (**1**), as determined by X-ray

crystallography, as well as the structure of ^{Me}IPrCH$_2$•AlEt$_3$ (**2**). The coordinative

C$_{NHO}$-Al bond in **1** is 2.1198(13) Å, and is similar in length as the C$_{NHC}$-Al distance

found in Robinson's NHC•AlMe$_3$ adduct [2.124(6) Å] in Chart 4.1,[8a] while longer

than the coordinative N$_{NHI}$-Al interaction in Masuda's IPr=NH•AlMe$_3$ complex

[1.9648(19) Å] (Chart 4.1).[8b] The latter observation follows a general trend of shorter

ligand-element bonds with *N*-heterocyclic imine (NHI) adducts in comparison to

NHO-element bonds.[9] While the carbene adduct IPr•AlEt$_3$ (IPr = [(HCNDipp)$_2$C:])

has been previously synthesized by Dagorne and coworkers in 2017,[10] an X-ray

crystal structure has not been reported, obviating the chance to directly compare its structure with that of ^{Me}IPrCH$_2$•AlEt$_3$ (**2**).
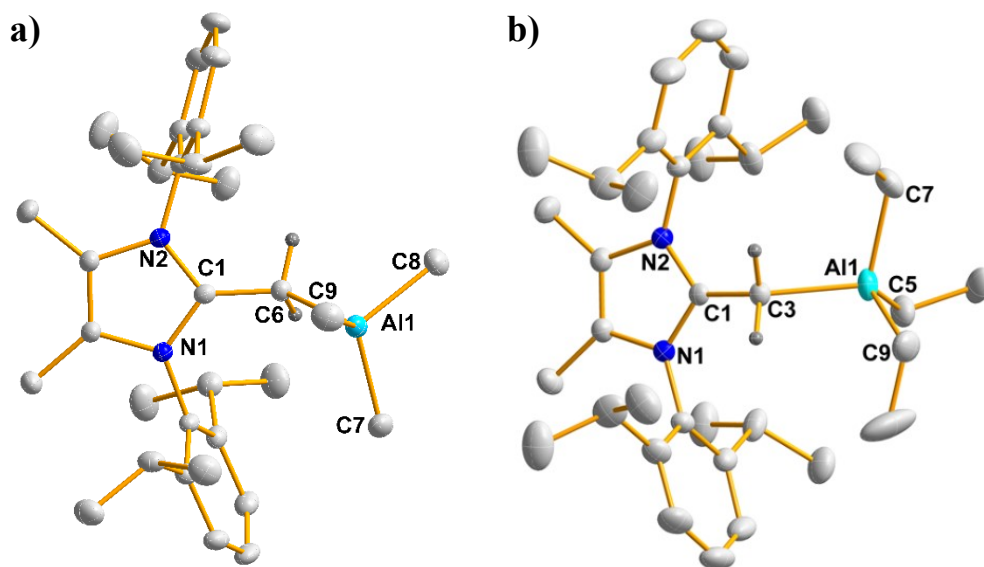
Figure 4.1. a) Molecular structure of ^{Me}IPrCH$_2$•AlMe$_3$ (**1**) with thermal ellipsoids shown at a 30 % probability level. All hydrogen atoms except those on C6 have been omitted for clarity. Selected bond lengths [Å] and angles [°]: C1–C6 1.4439(17), C6–Al1 2.1198(13), Al1–C8 1.9925(16); C1–C6–Al1 130.01(9), C7–Al1–C8 109.59(7). b) Molecular structure of ^{Me}IPrCH$_2$•AlEt$_3$ (**2**) with thermal ellipsoids shown at a 30 % probability level. All hydrogen atoms except those on C3 have been omitted for clarity. Selected bond length [Å] and angles [°]: C1–C3 1.439(2), C3–Al1 2.0954(17), Al1–C5 1.999(4); C3–Al1–C5 117.43(17).

^{Me}IPr=CH–CH=CH$_2$, an allyl-appended NHO with two potential sites to accommodate a Lewis acid, has been reported previously by the Rivard Group (Scheme 4.2a).[11] In this previously published study, only evidence of coordination via the terminal exocyclic carbon atom to palladium was found (see Chapter 3), presumably due to the steric crowding imparted by the flanking Dipp groups in ^{Me}IPr=CH–CH=CH$_2$.[11] In this current study, it was postulated that an alternate

coordination mode might be possible when complexes were formed with less hindered Lewis acids, such as AlMe$_3$. Upon combining ^{Me}IPr=CH-CH=CH$_2$ with AlMe$_3$ in a 1:1 ratio, the corresponding adduct ^{Me}IPrCHCHCH$_2$•AlMe$_3$ (**3**) was obtained (Scheme 4.2b). X-ray crystallography (Figure 4.2) revealed a similar terminal NHO-AlMe$_3$ binding mode was present as in previously reported Pd complexes.[11] As with ^{Me}IPrCH$_2$•AlMe$_3$ (**1**), a diagnostic upfield shift in the methyl resonance for the AlMe$_3$ group in **3** was found (to a value of –0.42 ppm in C$_6$D$_6$). The formally dative Al-C$_{NHO}$ distance of 2.1135(13) Å in **3** (Al-C4; Figure 4.2) is similar to the corresponding Al-C$_{NHO}$ interaction in ^{Me}IPrCH$_2$•AlMe$_3$ (**1**) [2.1198(13) Å]. The terminal olefin coordination mode in **3** is adopted for two plausible reasons: 1) the steric bulk close to the heterocycle makes binding to the proximal exocyclic carbon (C2 in Figure 4.2) difficult, and 2) Natural population analysis (NPA)[11] of ^{Me}IPr=CH-CH=CH$_2$ showed a more negative charge at the terminal carbon compared to the one adjacent to the ^{Me}IPr unit (-0.53e$^-$ vs. -0.46e$^-$), making the terminal site slightly more Lewis basic.
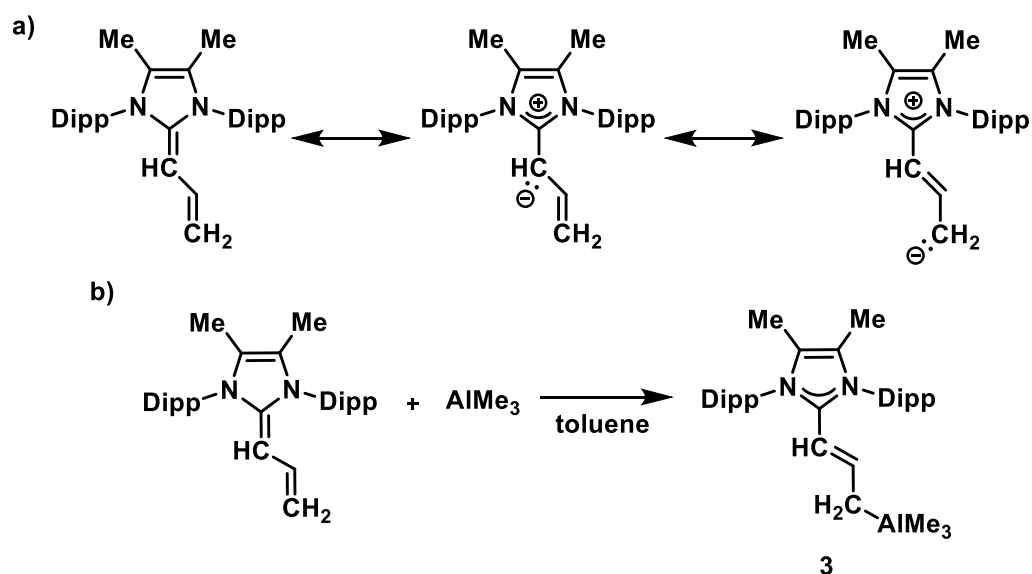
Scheme 4.2. a) Important resonance forms associated with $^{Me}IPr=CH–CH=CH_2$, illustrating two potential sites of coordination. b) Preparation of $^{Me}IPrCHCHCH_2 \cdot AlMe_3$ (**3**).
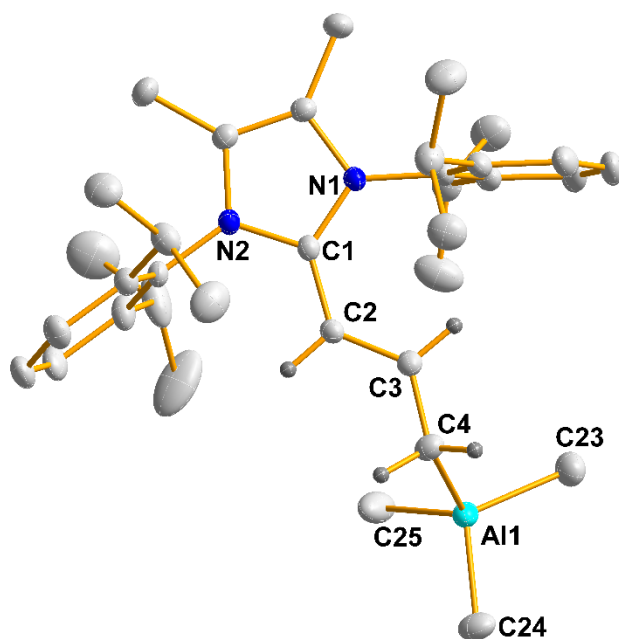
Figure 4.2. Molecular structure of $^{Me}IPrCHCHCH_2 \cdot AlMe_3$ (**3**) with thermal ellipsoids shown at a 30 % probability level. Co-crystallized toluene solvate and all hydrogen atoms besides those on C2, C3 and C4 have been omitted for clarity. Selected bond lengths [Å] and angles [°]: C1–C2 1.4205(16), C2–C3 1.3665(17), C3–C4 1.4203(17), Al1–C4 2.1135(13); C1–C2–C3 128.34(11), C3–C4–Al1 116.12(9).

The new NHO•AlR$_3$ adducts **1-3** are only sparingly soluble in C$_6$D$_6$, which made the acquisition of ^{13}C{^{1}H} NMR spectra a challenge. When **1-3** were dissolved in THF-d$_8$ (to possibly obtain more intense ^{13}C{^{1}H} NMR resonances), the dissociation of these adducts into free NHO and AlR$_3$ was observed (Figure 4.3). Variable temperature ^{1}H NMR analysis of ^{Me}IPrCH$_2$•AlMe$_3$, ^{Me}IPrCH$_2$•AlEt$_3$, and ^{Me}IPrCH$_2$CHCH$_2$•AlMe$_3$ was performed in toluene-d$_8$ over the temperature range of –60 to + 80 °C to determine whether or not these Lewis adducts could be separated thermally. However, none of these Lewis pair adducts (**1-3**) showed any evidence of separating into their respective free Lewis acid and base under the conditions explored.
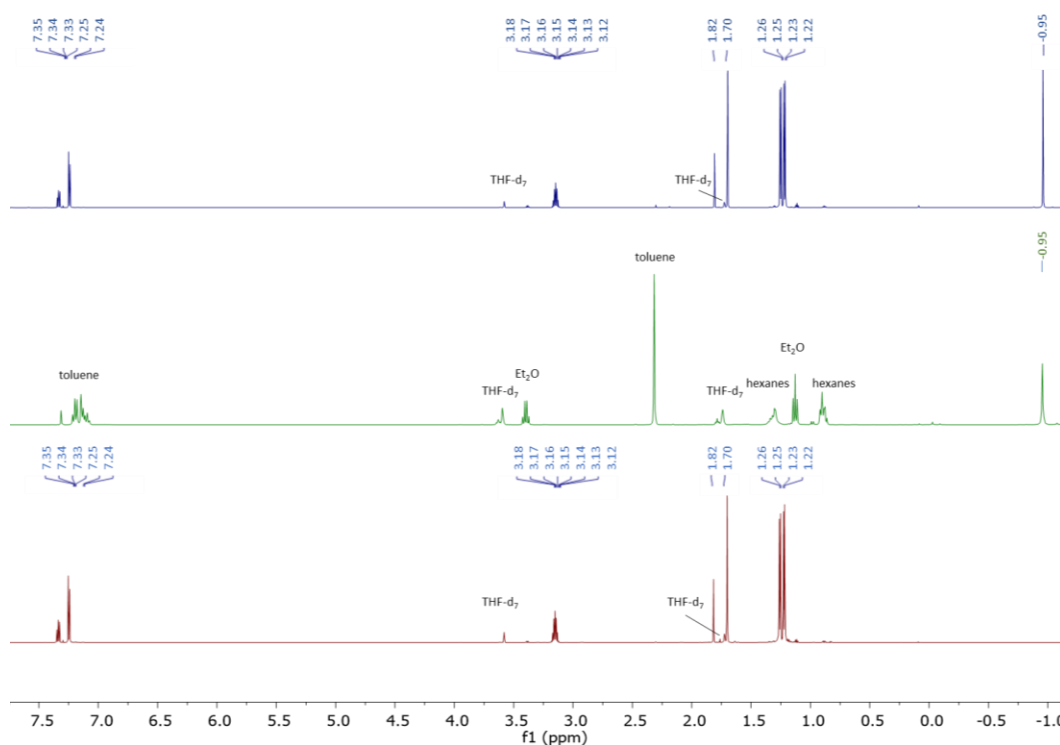
Figure 4.3. A series of stacked ^{1}H NMR spectra showing ^{Me}IPrCH$_2$•AlMe$_3$ recorded in THF-d$_8$ (top), AlMe$_3$ (2.0 M in toluene) recorded in THF-d$_8$ (middle), and ^{Me}IPrCH$_2$ recorded in THF-d$_8$.

Prior work involving the use of frustrated Lewis pairs (FLPs) as initiators prompted the investigation of ^{Me}IPrCH$_2$•AlMe$_3$ (**1**) as a viable polymerization catalyst for Michael-type monomers (Scheme 4.3).[4c,6,7,12] Polymerization trials were conducted by first combining dimethylacrylamide (DMAA) with 0.5 mol.% of **1** in THF. Upon adding 0.5 mol% of **1** to a stirring solution of DMAA in THF, a rapid increase in temperature was noted, as is typical for this type of polymerization. After stirring for 1 h, the reaction mixture was quenched by the addition of ethanol, and the resulting polymer was isolated and purified via precipitation from a concentrated solution of the polymer in CH$_2$Cl$_2$ into cold (–30 °C) pentanes. According to gel permeation chromatography (GPC) on the isolated polymer sample in THF/H$_2$O (with 9 g/L [^{n}Bu$_4$N]Br added to increase the ionic strength), a number average molecular weight (M$_n$) of 150 kDa and a polydispersity index (PDI) of 1.18 was found (Table 4.1). For comparison, the use of **1** as a catalyst afforded higher molecular weight polymer versus Naumann's NHO-only polymerization, with (MeCNMe)$_2$C=CMe$_2$ as an initiator (67 % conversion, 2 h, 0.5 mol% NHO).[4c] Of note, the expected molecular weight of the resulting polymer if **1** instigated the living polymerization of DMAA would be *ca.* 20 kDa (*i.e.* a degree of polymerization, DP, of 200); however, the higher molecular weight obtained (150 kDa), while keeping a low PDI, is consistent with a low effective initiator efficiency (*I**).[13] Another notable system is the polymerization of DMAA by the NHC-alane adduct [(DippNC(H)C(H)N^{i}Pr)C]•Al(C$_6$F$_5$)$_3$, which transpired in only 4 min., significantly faster than **1**, with a low PDI (*ca.* 1.05) and an M$_n$ of 170 kDa.[7] This is consistent with

the observation that the polymerization of Michael-type monomers occurs quickly in the presence of strong Lewis acids.[14]

Table 4.1. Polymerization of various Michael-type monomers using 0.5 mol% of ^{Me}IPrCH$_2$•AlMe$_3$ as an initiator in THF (1 h).

Monomer	Isolated yield (%)	M_n ($\times 10^3$ kDa)	PDI (M_w/M_n)
DMMA	> 99	150	1.18
2VP	98	840	1.35
MA	5	10	2.08
DEVP	No polymerization	N/A	N/A

Knowing that DMAA is polymerized by **1**, the polymerization of several other monomers was attempted (Scheme 4.3 and Table 4.1). Methylacrylate (MA), 2-vinylpyridine (2VP), and diethylvinylphosphonate (DEVP) were each combined with **1** under the same conditions used for DMAA (*vide supra*). While the polymerizations MA and 2VP were successful (Table 4.1), diethylvinylphosphonate (DEVP) failed to yield any polymers. DEVP is known to be more sterically demanding than DMAA and 2VP, and this could explain the failure of ^{Me}IPrCH$_2$·AlMe$_3$ to promote this polymerization.[15]
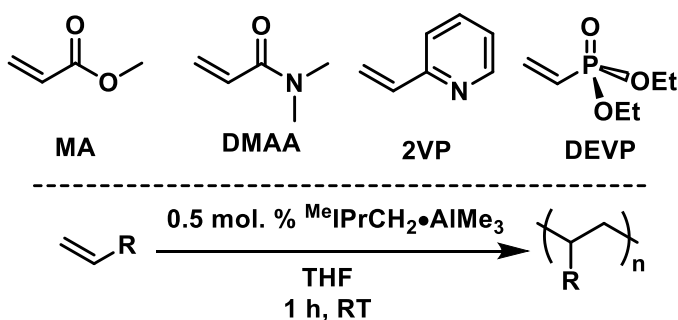
Scheme 4.3. (top) The Michael-type monomers investigated in this study; (bottom) polymerization conditions.

The polymerization of 2-vinylpyridine (2VP) with catalytic **1** afforded very high molecular weight polymer, with M_n values exceeding 800 kDa (Table 1). 2VP has also been polymerized with NHC/Al$(C_6F_5)_3$ systems (with excess Lewis acid) to yield polymer with molecular weights (M_n) in the 10-80 kDa range.[16]

Chen has demonstrated that a ImMe$_4$CMe$_2$•AlMe$_3$ Lewis pair (ImMe$_4$ = (MeCNMe)$_2$C) can promote the slow polymerization of methyl methacrylate (MMA) (38 % yield over 12 h), however, no reactions were tried with the less hindered monomer methylacrylate (MA).[14] Combining 0.5 mol% of **1** with MA in THF only gave a small amount of isolated poly(methylacrylate) *(ca.* 5 % yield) with a low M_n value of 10 kDa (PDI = 2.08; Table 4.1). According to findings in the literature, Lewis pair polymerization has not been used to polymerize MA previously. Notably, poly(methyacrylate) with a narrow PDI (1.03) and high *I** (*ca.* 80 %) was obtained from MA via group transfer polymerization with 1-triisopropylsiloxy-1-methoxy-2-methyl-1-propene (MTS^{iPr}) as an initiator and C$_6$F$_5$CHTf$_2$ as a catalyst (Tf = SO$_2$CF$_3$).[17] Industrially, the polymerization of acrylic

monomers is typically achieved using radical initiators,[18] however, these methods often yield high PDI values,[18c] making Frustrated Lewis pair catalysis attractive when smaller PDI values are desired.

Polymerization trials with MA and 2VP monomer using ^{Me}IPrCHCHCH$_2$•AlMe$_3$ (**3**) as a catalyst were undertaken. However, these trials gave disappointingly low yields of polymer (3 and 15 % for poly(methylacrylate) and poly(2-vinylpyridine), respectively; thus, this catalyst was not explored further. The ability of ^{Me}IPrCH$_2$•AlEt$_3$ (**2**) to act as a catalyst was not investigated due to the constant presence of a minor amount of unidentified NHO-containing impurity (according to ^{1}H NMR analysis), which could not be removed via washing or recrystallization protocols.

To verify that the FLP pair of **1** in THF was performing the polymerizations opposed to either the Lewis acid or base alone, the interaction of 2-vinylpyridine (2VP) with both ^{Me}IPrCH$_2$ and AlMe$_3$ individually was examined. When ^{Me}IPrCH$_2$ was combined with 2VP under the same conditions outlined in Table 4.1, no polymerization was detected *in situ* by ^{1}H NMR spectroscopy (in THF-d$_8$). Likewise, treatment of 2VP with AlMe$_3$ gave no evidence of polymerization by *in situ* ^{1}H NMR analysis of the mixture in THF-d$_8$. Interestingly, when the mixture of AlMe$_3$ and 2VP was quenched with methanol, a vigorous exothermic reaction was observed, as expected upon the reaction of AlMe$_3$ with alcohol; however, surprisingly, a small amount of poly(2-vinylpyridine) was observed (6 % isolated yield). Knowing that unstabilized 2VP can autopolymerize at –20 °C over the course of a week,[18b] it is

thought that the heat generated by quenching the mixture with MeOH is responsible for some polymerization of 2VP.

4.3 Conclusion

The syntheses of the new NHO-trialkylaluminum complexes (**1-3**) have been described and it has been found that ^{Me}IPrCH$_2$•AlMe$_3$ (**1**) shows FLP-type behavior in THF, leading to the polymerization of several Michael-type monomers under very mild conditions. Future work will involve targeting the synthesis of more electron deficient and lower coordinate NHO-aluminum species bearing anionic NHOs[19] as supporting ligands, as increased Lewis acidity of an alane leads to greater effectiveness in Lewis pair polymerization.[14]

4.4 Experimental Section

4.4.1 Materials and Instrumentation

All reactions were performed using standard Schlenk line techniques under an atmosphere of nitrogen or in an inert atmosphere glovebox (Innovative Technology Inc.). Solvents were dried using a Grubbs-type solvent purification system manufactured by Innovative Technology Inc., and stored under an atmosphere of nitrogen over 4 Å molecular sieves prior to use. ^{Me}IPrCH$_2$[3] and ^{Me}IPr=CH–CH=CH$_2$[11] were prepared according to literature procedures. Trimethylaluminum (2.0 M solution in toluene) and triethylaluminum (1.0 M solution in hexanes) were purchased from MilliporeSigma and used as received. Dimethylacrylamide (DMMA) and 2-

vinylpyridine (2VP) were purchased from MilliporeSigma, distilled over calcium hydride and freeze-thaw degassed before use. Methylacrylate (MA) was purchased from MilliporeSigma, washed with a saturated NaOH solution, distilled over calcium hydride, and freeze-thaw degassed before use. THF-d_8 was purchased from MilliporeSigma and distilled from sodium benzophenone, then stored over Na/K before use. ^{1}H and ^{13}C$\{^1$H$\}$ NMR spectra were recorded on 400 MHz, 500 MHz, and 700 MHz Varian Inova spectrometers and referenced externally to SiMe$_4$ (^{1}H, ^{13}C$\{^1$H$\}$). Elemental analyses were performed by the Analytical and Instrumentation Laboratory at the University of Alberta. Melting points were measured in sealed glass capillaries under nitrogen using a MelTemp melting point apparatus and are uncorrected. GPC measurements for poly(2-vinylpyridine) and poly(methylacrylate) were performed at 40 °C using THF as the eluent at a flow rate of 0.5 mL per minute. A Viscotek VE 2001 autosampler, one Viscotek T6000M column, GPC 270 Max dual detector, and Viscotek VE 3580 refractive index detector were used for sample analysis and data collection. Multidetector calibration was done using refractive index (RI) detection in conjunction with low angle light scattering (LALS) and right angle light scattering (RALS), using 99 kDa polystyrene to create the calibration method and 235 kDa polystyrene to verify the calibration. GPC measurements for poly(dimethylacrylamide) were performed using two PL Polargel columns in THF:H$_2$O [1:1; v:v] (with 272 mg/L 3,5-di-tert-butyl-4-hydroxytoluene and 9 g/L of tetrabutylammonium bromide (TBAB) as the eluent. The determination of the absolute molecular weights was performed with multi-angle light scattering on a

Wyatt Dawn Heleos II instrument equipped with an Wyatt Optilab rEX 536 RI detector for concentration determination. The dn/dc value for the absolute molecular weight measurements was determined to be 0.1282 mL/g.

4.4.2 X-Ray Crystallography

Crystals of appropriate quality for X-ray diffraction studies were removed from either a Schlenk flask under a stream of nitrogen, or from a vial (glove box) and immediately covered with a thin layer of hydrocarbon oil (Paratone-N). A suitable crystal was then selected, attached to a glass fiber, and quickly placed in a low-temperature stream of nitrogen. All data were collected using a Bruker APEX II CCD detector/D8 diffractometer using Mo Kα or Cu Kα radiation, with the crystal cooled to −100 °C or −80 °C, respectively. The data were corrected for absorption through Gaussian integration from indexing of the crystal faces. Structures were solved using the direct methods programs SHELXT-2014,[20] and refinements were completed using the program SHELXL-2014.[21] Hydrogen atoms were assigned positions based on the sp^2- or sp^3-hybridization geometries of their attached carbon atoms, and were given thermal parameters 20 % greater than those of their parent atoms.

4.4.3 Synthetic Procedures

Synthesis of ^{Me}IPrCH$_2$•AlMe$_3$ (1). A solution of AlMe$_3$ (0.210 mL, 2.0 M solution in toluene, 0.42 mmol) was layered atop of a solution of ^{Me}IPrCH$_2$ (0.181 g, 0.420 mmol) in 1.5 mL of toluene. After allowing the mixture to remain undisturbed for 4 h,

colorless X-ray quality crystals formed. The supernatant was decanted away and the remaining crystals of ^{Me}IPrCH$_2$•AlMe$_3$ (**1**) were washed with 3 × 2 mL of cold (-30 °C) toluene, and dried *in vacuo* (0.143 g, 68 %). ^{1}H NMR (500 MHz, C$_6$D$_6$): δ = 7.21 (t, 2H, $^3J_{HH}$ = 7.6 Hz, Ar*H*), 7.17 (d, 4H, $^3J_{HH}$ = 7.6 Hz, Ar*H*), 2.80 (m, 4H, C*H*(CH$_3$)$_2$), 2.01 (s, 2H, CC*H$_2$*AlMe$_3$), 1.38 (s, 6H, CN-C*H$_3$*), 1.38 (d, 12H, $^3J_{HH}$ = 6.8 Hz, CH(C*H$_3$*)$_2$), 0.98 (d, 12H, $^3J_{HH}$ = 6.8 Hz, CH(C*H$_3$*)$_2$), –0.52 ppm (s, 9H, –Al(C*H$_3$*)$_3$); ^{13}C{^{1}H} NMR (125 MHz, C$_6$D$_6$): δ = –4.4 (-Al(*C*H$_3$)$_3$), 9.6 (H$_3$*C*CN), 24.5 (CH(*C*H$_3$)$_2$), 24.6 (CH(*C*H$_3$)$_2$), 28.8 (*C*H(CH$_3$)$_2$), 125.3 (Ar*C*), 128.0 (Ar*C*), 128.2 (Ar*C*), 128.4 (Ar*C*), 131.0 (Ar*C*), 145.5 (N*C*N), 146.9 ppm (*C*CH$_2$-AlEt$_3$). One of the Ar*C* resonances could not be observed; element. anal.: calcd. for C$_{33}$H$_{55}$AlN$_2$: C, 78.84; H, 10.23; N, 5.57; found: C, 78.69; H, 10.23; N, 5.46 %; mp: 229 °C (dec.).

Synthesis of ^{Me}IPrCH$_2$•AlEt$_3$ (2). A solution of AlEt$_3$ (1.0 M solution in hexanes, 1.476 mL, 1.5 mmol) was layered atop of a solution of ^{Me}IPrCH$_2$ (0.6357 g, 1.476 mmol) in 1.5 mL of toluene. After allowing the mixture to remain undisturbed for 4 h, colorless crystals of ^{Me}IPrCH$_2$•AlEt$_3$ (**2**) deposited. The supernatant was then decanted away and the remaining crystals washed with 3 × 2 mL of cold (–30 °C) hexanes and dried *in vacuo* (0.6115 g, 75 %). ^{1}H NMR (700 MHz, C$_6$D$_6$): δ = 7.22 (t, 2H, $^3J_{HH}$ = 7.8 Hz, Ar*H*), 7.12 (d, 4H, $^3J_{HH}$ = 7.8 Hz, Ar*H*), 2.70 (sept, 4H, $^3J_{HH}$ = 6.8 Hz, C*H*(CH$_3$)$_2$), 1.89 (s, 2H, CC*H$_2$*-AlEt$_3$), 1.37 (d, 12H, $^3J_{HH}$ = 6.8 Hz, CH(C*H$_3$*)$_2$), 1.34 (t, 9H, $^3J_{HH}$ = 8.1 Hz, AlCH$_2$C*H$_3$*), 1.33 (s, 6H, *H$_3$*CCN), 0.95 (d, 12H, $^3J_{HH}$ = 6.9 Hz, CH(C*H$_3$*)$_2$), 0.01 ppm (q, 6H, $^3J_{HH}$ = 8.1 Hz, AlC*H$_2$*CH$_3$); ^{13}C{^{1}H} NMR (175 MHz,

C$_6$D$_6$): δ = 3.0 (–Al(CH_2CH$_3$)$_3$), 9.5 (H$_3$CCN), 11.4 (Al(CH$_2$CH$_3$)$_3$), 24.3 (CH(CH_3)$_2$), 24.4 (CH(CH_3)$_2$), 28.8 (CH(CH$_3$)$_2$), 125.3 (ArC), 125.7 (ArC), 128.3 (ArC), 128.4 (ArC), 131.0 (ArC), 131.8 (ArC), 145.8 (NCN), 146.6 ppm (CCH$_2$-AlEt$_3$); element. anal.: calcd. for C$_{36}$H$_{57}$AlN$_2$: C, 79.36; H, 10.55; N, 5.14; found: C, 78.82; H, 10.47; N, 4.99 %; mp: 132 °C (dec.).

Synthesis of ^{Me}IPrCHCHCH$_2$•AlMe$_3$ (3). A solution of AlMe$_3$ (2.0 M solution in toluene, 0.193 mL, 0.39 mmol) was layered atop of a solution of ^{Me}IPr=CH-CH=CH$_2$ (0.1760 g, 0.3854 mmol) in 1.5 mL of toluene. The mixture was then left undisturbed for 16 h, resulting in the formation of colorless crystals of ^{Me}IPrCHCHCH$_2$•AlMe$_3$ (3). The supernatant was decanted away and the remaining crystals were washed with 3 mL of cold (–30 °C) toluene and dried *in vacuo* (0.1271 g, 62 %). ^{1}H NMR (700 MHz, C$_6$D$_6$): δ = 7.22 (t, 2H, $^3J_{HH}$ = 7.7 Hz, Ar*H*), 7.08 (d, 4H, $^3J_{HH}$ = 7.8 Hz, Ar*H*), 6.57 (dt, 1H, $^3J_{HH}$ = 14.3 Hz, $^3J_{HH}$ = 10.7 Hz, CHC*H*CH$_2$-AlMe$_3$), 4.67 (d, 1H, $^3J_{HH}$ = 14.3 Hz, C*H*CHCH$_2$–AlMe$_3$), 2.79 (d, 2H, $^3J_{HH}$ = 10.7 Hz, CHCHC*H$_2$*–AlMe$_3$), 2.60 (sept, 4H, $^3J_{HH}$ = 6.9 Hz, C*H*(CH$_3$)$_2$), 1.30 (s, 6H, *H$_3$*C-CN), 1.29 (d, 12H, $^3J_{HH}$ = 7.4 Hz, CH(C*H$_3$*)$_2$), 1.01 (d, 12H, $^3J_{HH}$ = 6.9 Hz, CH(C*H$_3$*)$_2$), -0.42 ppm (s, 9H, –Al(C*H$_3$*)$_3$); ^{13}C{^{1}H} NMR (175 MHz, C$_6$D$_6$): δ = –6.1 (–Al(C*H$_3$*)$_3$), 8.7 (H$_3$CCN), 23.6 (CH(C*H$_3$*)$_2$), 24.2 (CH(C*H$_3$*)$_2$), 29.1 (*C*H(CH$_3$)$_2$), 58.6 (CH-*C*HCH$_2$–AlMe$_3$), 85.3 (CHCH*C*H$_2$–AlMe$_3$), 121.4 (ArC), 125.3 (ArC), 127.9 (ArC), 128.4 (ArC), 130.4 (ArC), 131.4 (ArC), 146.7 (H$_3$C*C*N), 147.5 (N*C*N), 162.2 ppm (*C*HCHCH$_2$–AlMe$_3$);

element. anal.: calcd. for $C_{35}H_{53}AlN_2$: C, 79.50; H, 10.10; N, 5.30; found: C, 79.39; H, 9.91; N, 5.12 %; mp: 218 °C (dec.).

General Procedure for the polymerization of Michael-type monomers. ^{Me}IPrCH$_2$•AlMe$_3$ (0.025 g, 0.050 mmol) was added to a solution of monomer (10 mmol) in 5 mL of THF. After 1 h of stirring the reaction mixture was quenched with *ca*. 0.5 mL of ethanol, and the volatiles were removed *in vacuo*. The resulting solid was dissolved in *ca.* 5 mL of dichloromethane and precipitated into 100 mL of pentanes at –0 °C. The resulting polymer was dried under high vacuum while heated at 50 °C.

4.5 Crystallographic Data

Table 4.2. Crystallographic data for **1**, **2**, and **3**.

Compound	1	2	3
formula	$C_{33}H_{51}AlN_2$	$C_{36}H_{57}AlN_2$	$C_{42}H_{61}AlN_2$
formula weight	502.73	544.81	620.90
crystal system	monoclinic	orthorhombic	triclinic
Space Group	$P2_1/n$	$Pnma$	$P\bar{1}$
a (Å)	10.5356(10)	17.7601(2)	10.7726(2)
b (Å)	19.8481(18)	18.5390(3)	11.7427(2)
c (Å)	15.5870(14)	10.7479(2)	18.0916(3)
α (deg)	--	--	95.9354(8)
β (deg)	103.9165(12)	--	101.5030(8)
γ (deg)	--	--	114.7611(8)
V (Å^3)	3163.7(5)	3538.79(10)	1990.98(6)
Z	4	4	2
ρ_{calcd} (g cm^{-3})	1.055	1.023	1.036
Abs coeff (mm)	0.086	0.660	0.641
T (K)	193	173	193
$2\theta_{max}$ (°)	52.96	148.31	144.92
Total Data	73202	139725	13979
Unique data (R_{int})	73202 (0.0310)	3717 (0.0516)	7617 (0.0142)
Obs data [I>2(σ(I)]	5549	3472	6844
Params	330	246	412
R_1 [I>2(σ(I)][a]	0.0429	0.0440	0.0428
wR_2 [all data][a]	0.1250	0.1261	0.1243
Max/min $\Delta\rho$ (e$^-$Å^{-3})	0.261/–0.193	0.230/–0.191	0.367/–0.296

[a] $R_1 = \Sigma||F_o| - |F_c||/\Sigma|F_o|$; $wR_2 = [\Sigma w(F_o^2 - F_c^2)^2/\Sigma w(F_o^4)]^{1/2}$

4.6 References

1. a) Ponti, P. P.; Baldwin, J. C.; Kaska, W. C. *Inorg. Chem.* **1979**, *18*, 873-875. b) Kuhn, N.; Bohnen, H.; Kreutzberg, J.; Bläser, D.; Boese, R. *J. Chem. Soc., Chem. Commun.* **1993**, 1136-1137. c) Kuhn, N.; Bohnen, H.: Bläser, D.; Boese, R. *Chem. Ber.* **1994**, *127*, 1405-1407.

2. a) Roy, M. M. D.; Rivard, E. *Acc. Chem. Res.* **2017**, *50*, 2017-2025. b) Al-Rafia, S. M. I.; Malcolm, A. C.; Liew, S. K.; Ferguson, M. J.; McDonald, R.; Rivard, E. *Chem. Commun.* **2011**, *47*, 6987-6989. c) Wang, Y. W.; Abraham, M. Y.; Gilliard Jr., R. J.; Sexton, D. R.; Wei, P.; Robinson, G. H. *Organometallics* **2013**, *32*, 6639-6642. d) Al-Rafia, S. M. I.; Momeni, M. R.; Ferguson, M. J.; McDonald, R.; Brown, A.; Rivard, E. *Organometallics* **2013**, *32*, 6658-6665. e) Ghadwal, R. S.; Schürmann, C. J.; Andrada, D. M.; Frenking, G. *Dalton Trans*. **2015**, *44*, 14359-14367. f) Ghadwal, R. S. *Dalton Trans.* **2016**, *45*, 16081-16095. g) Lee, W.-H.; Lin, Y.-F.; Lee, G.-H.; Peng, S.-M.; Chiu, C.-W. *Dalton Trans.* **2016**, *45*, 5937-5940. h) Eymann, L. Y. M.; Varava, R.; Shved, A. M.; Curchod, B. F. E.; Liu, Y.; Planes, O. M.; Sienkiewicz, A.; Scopelliti, R.; Tirani, F. F.; Severin, K. *J. Am. Chem. Soc.* **2019**, *141*, 17112-17116.

3. Powers, K.; Hering-Junghans, C.; McDonald, R.; Ferguson, M. J.; Rivard, E. *Polyhedron* **2016**, *108*, 8-14.

4. For selected reviews and articles, see: a) Naumann, S. *Chem. Commun.* **2019**, *55*, 11658-11670. b) Crocker, R. D.; Nguyen, T. V. *Chem. Eur. J.* **2016**, *22*, 2208-2213. c) Naumann, S.; Mudsinger, K.; Cavallo, L.; Falivene, L. *Polym. Chem.* **2017**, *8*, 5803-

5812. d) Hering-Junghans, C.; Watson, I. C.; Ferguson, M. J.; McDonald, R.; Rivard, E. *Dalton Trans.* **2017**, *46*, 7150-7153. e) Walther, P.; Krauβ, A.; Naumann, S. *Angew. Chem. Int. Ed.* **2019**, *58*, 10737-10741.

5. McGraw, M.; Chen, E. Y.-X. *ACS Catal.* **2018**, *8*, 9877-9887.

6. Jia, Y.-B.; Wang, Y.-B.; Ren, W.-M.; Xu, T.; Wang, J.; Lu, X.-B. *Macromolecules* **2014**, *47*,1966-1972.

7. Zhang, Y.; Miyake, G. M.; Chen, E. Y.-X. *Angew. Chem. Int. Ed.* **2010**, *49*, 10158-10162.

8. a) Li, X.-W.; Su, J.; Robinson, G. *Chem. Commun.* **1996**, 2683-2684. b) Todd, A. D. K.; McClennan, W. L.; Masuda, J. D. *RSC Adv.* **2016**, *6*, 69270-69276.

9. a) Hering-Junghans, C.; Andreiuk, P.; Ferguson, M. J.; McDonald, R.; Rivard, E. *Angew. Chem. Int. Ed.* **2017**, *56*, 6272-6275. b) Lui, M.; Merten, C.; Ferguson, M. J.; McDonald, R.; Xu, Y.; Rivard, E. *Inorg. Chem.* **2015**, *54*, 2040-2049. For a review on NHI complexes, see: c) Ochiai, T.; Franz, D.; Inoue, S. *Chem. Soc. Rev.* **2016**, *45*, 6327-6344.

10. Schnee, G.; Bolley, A.; Hild, F.; Specklin, D.; Dagorne, S. *Catal. Today* **2017**, *289*, 204-210.

11. Watson, I. C.; Schumann, A.; Yu, H.; Davy, E. C.; McDonald, R.; Ferguson, M. J.; Hering-Junghans, C.; Rivard, E. *Chem. Eur. J.* **2019**, *25*, 9678-9690.

12. Weger, M.; Grötsch, R. K.; Knaus, M. G.; Giuman, M. M.; Mayer, D. C.; Altmann, P. J.; Mossou, E., Dittrich, B.; Pöthig, A.; Rieger, B. *Angew. Chem. Int. Ed.* **2019**, 58, 9797-9801.

13. a) Zhao, Z.; Wang, Q.; He, J.; Zhang, Y. *Polym. Chem.* **2019**, *10*, 4328-4335. b) Xu, T.; Chen, E. Y.-X. *J. Am. Chem. Soc.* **2014**, *136*, 1774-1777.

14. Wang, Q.; Zhao, W.; Zhang, S.; He, J.; Zhang, Y.; Chen, E. Y.-X. *ACS Catal.* **2018**, *8*, 3571-3578.

15. For the polymerization of DEVP, see: Weger, M.; Pahl, P.; Schmidt, F.; Soller, B. S.; Altmann, P. J.; Pöthig, A.; Gemmecker, G.; Eisenreich, W.; Rieger, B. *Macromolecules* **2019**, *24*, 7073-7080 and references therein.

16. He, J.; Zhang, Y.; Chen, E. Y.-X. *Synlett* **2014**, *25*, 1534-1538.

17. Takada, K.; Fuchise, K.; Chen, Y.; Satoh, T.; Kakuchi, T. *J. Polym. Sci., Part A: Polym. Chem.* **2012**, *50*, 3560-3566.

18. a) Radical Polymerization in Industry, *Encyclopedia of Radicals in Chemistry, Biology and Materials* [Online]; John Wiley & Sons, Posted March 15, 2012. https://onlinelibrary.wiley.com/doi/full/10.1002/9781119953678.rad080 (accessed December 12, 2019). b) Kennemur, J. G. *Macromolecules* **2019**, 52, 1354-1370. c) Rudin, A.; Choi, P. *The Element of Polymer Science & Engineering, 3rd* ed.; Academic Press: Waltham, MA, USA, 2013; pg. 380.

19. For work on complexes supported by anionic NHO ligands, see: a) Al-Rafia, S. M. I.; Ferguson, M. J.; Rivard, E. *Inorg. Chem.* **2011**, *50*, 10543-10545. b) Ghadwal, R. S.; Reichmann, S. O.; Engelhardt, F.; Andrada, D. M.; Frenking, G. *Chem. Commun.* **2013**, *49*, 9440-9442. c) Paisley, N. R., Lui, M. W.; McDonald, R.; Ferguson, M. J.; Rivard, E. *Dalton Trans.* **2016**, *45*, 9860-9870. d) Chong, C. C.; Rao, B.; Ganguly, R.; Li, Y.; Kinjo, R. *Inorg. Chem.* **2017**, *56*, 8608-8614. e) Roy, M. M. D.; Ferguson, M. J.; McDonald, R.; Zhou, Y.; Rivard, E. *Chem. Sci.* **2019**, *10*, 6476-6481. f) Sharma, M. K.; Blomeyer, S.; Neumann, B.; Stammler, H.-G.; van Gastel, M.; Hinz, A.; Ghadwal, R. S. *Angew. Chem. Int. Ed.* **2019**, *58*, 17599-17603. g) Hupf, E.; Kaiser, F.; Lummis, P. A.; Roy, M. M. D.; McDonald, R.; Ferguson, M. J.; Kühn, F.; Rivard, E. *Inorg. Chem.* **2020**, *59*, 1592-1601. h) Sharma, M. K.; Neumann, B.; Stammler, H.-G.; Andrada, D. M.; Ghadwal, R. S. *Chem. Commun.* **2019**, *55*, 14669-14672. i) Roy, M. M. D.; Baird, S. R.; Dornsiepen, E.; Paul, L. A.; Miao, L.; Ferguson, M. J.; Zhou, Y.; Siewert, I.; Rivard, E. *Chem. Eur. J.* **2021**, *27*, 8572-8579.

20. Sheldrick, G. M. *Acta. Crystallogr. Sect. A* **2015**, *71*, 3-8.

21. Sheldrick, G. M. *Acta. Crystallogr. Sect. C* **2015**, *71*, 3-8.

Chapter 5: Zinc-Mediated Transmetallation as a Route to Anionic *N*-Heterocyclic Olefin Complexes in the p-Block

5.1. Introduction

Transmetallation is a central reaction type in organometallic chemistry, with Frankland's historic 1861 study of the reaction of ZnEt$_2$ with main group halides representing the birth of this field.[1] In the domain of catalysis, transmetallation processes involving carbon-based substrates are key to the widely used Suzuki-Miyaura,[2] Negishi,[3] and Stille cross-coupling protocols.[4] Of particular interest to the current study is the use of organozinc(II) reagents as easy-to-handle sources of organic nucleophiles, as exemplified by Piers' use of the thermally stable Zn(C$_6$F$_5$)$_2$ to install –C$_6$F$_5$ groups onto boron centers (*in lieu* of the potentially explosive and more reducing Li[C$_6$F$_5$]).[5] Examples of transmetallation involving sterically hindered ZnR$_2$ sources, such as zincocenes (*e.g.*, Cp$_2$Zn and its structural analogues),[6] and the reaction of Zn–R and Zn–OR moieties with hydride sources to form catalytically active zinc hydride complexes are also noteworthy.[7] The Rivard Group's interest in transmetallation stems from the use of zirconium-based reagents (and Zr-element exchange) to yield conjugated and often luminescent materials based on heavy p-block elements.[8]

N-Heterocyclic olefins (NHOs) are a class of carbon-based donor wherein the terminal/exocyclic olefin unit in these R$_2$C=CH$_2$ frameworks (where R$_2$C is a

nitrogen-containing heterocycle) is sufficiently polarized/ylidic to enable coordination chemistry and organocatalysis to transpire.[9] The formally deprotonated analogues of NHOs, termed here as anionic *N*-heterocyclic olefins (aNHOs; Scheme 5.1), are highly electron-releasing ligands that can act as $2\sigma,2\pi$-electron donors. Anionic NHOs have been used in the Rivard Group to stabilize the acyclic silylene **A** (Scheme 5.1)[10,11] and by Kinjo and coworkers to access a stable cyclophosphenium cation (**B** in Scheme 5.1).[12] There are three common routes by which an aNHO ligand can be installed onto a main group center: 1) by *in situ* deprotonation of an NHO using an exogenous base in the presence of the main group center (*e.g.*, see preparation of **B** in Scheme 5.1),[11,12] 2) reaction of an element halide with a terminally-silylated NHO (*cf.* formation of the germyl-complex **C** in Scheme 5.1),[11] or, 3) reaction of a pre-formed lithiated aNHO complex with element halides (*e.g.,* preparation of silylene **A** in Scheme 5.1).[10] Routes 1 and 2 occasionally do not work due to a low nucleophilicity of the NHO source, while route 3 is challenging as the known (isolable) lithiated aNHO (Scheme 5.1) is unstable in THF and decomposes over time in solution and even slowly in the solid state at –35 °C.[10] Herein, the synthesis of a thermally stable Zn(II) source of anionic *N*-heterocyclic olefin (^{Me}IPrCH)$_2$Zn (**1**) is described and its use as a transmetallating agent with both halide- and hydride-containing main group substrates (Scheme 5.1).
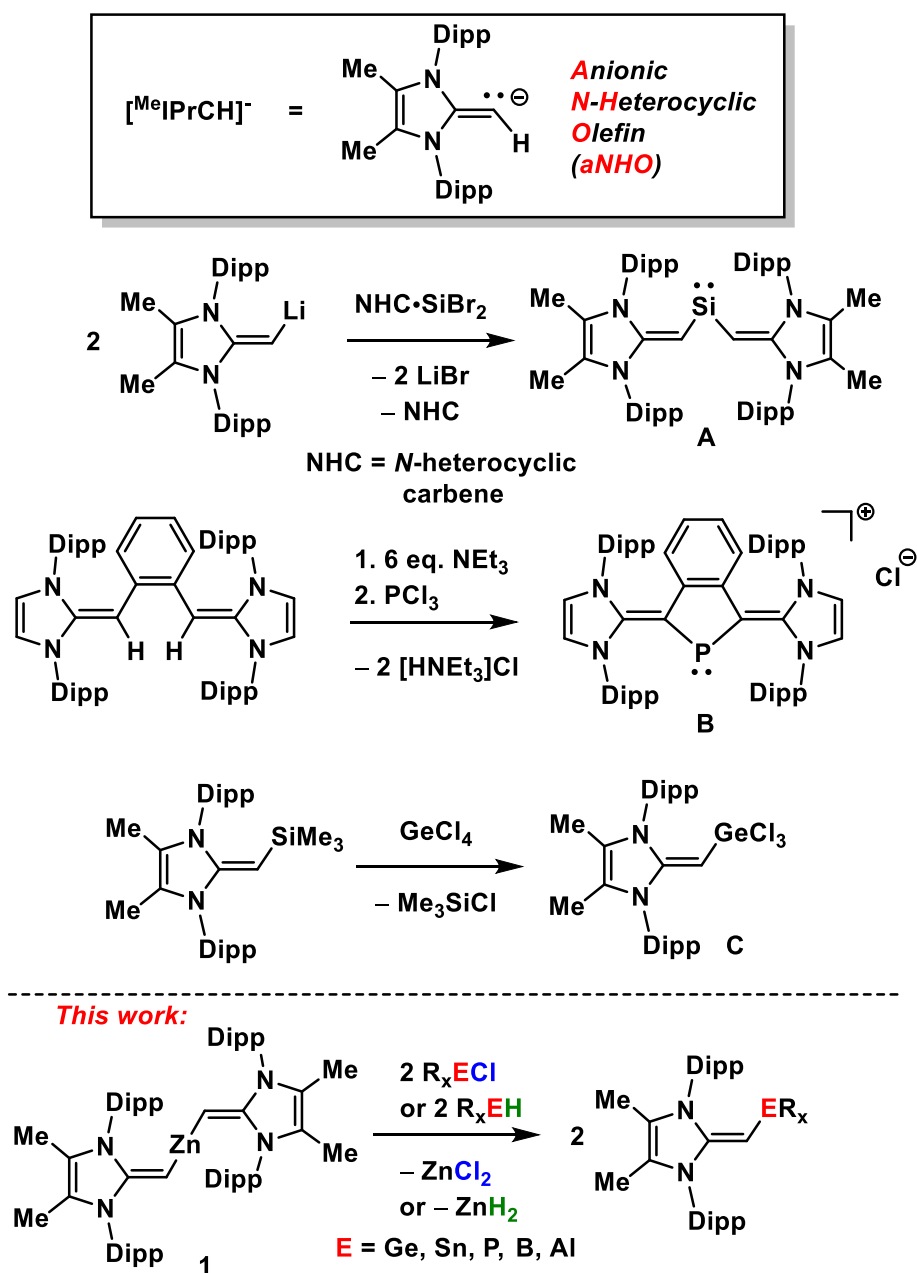
Scheme 5.1. Selected routes used to install anionic *N*-heterocyclic olefin (aNHO) ligands onto main group centers and the zinc-metathesis route introduced in this Chapter.

5.2. Results and Discussion

Recently, the preparation of $(^{Me}IPrCH)Li$ $(^{Me}IPrCH = [(MeCNDipp)_2CH]^-$; Dipp = 2,6-^{i}Pr$_2C_6H_3$) was reported, a reagent that can be used to install $[^{Me}IPrCH]^-$ groups onto inorganic Group 14 elements via salt metathesis.[10] A highlight of this work was the isolation of the first two-coordinate acyclic diorganosilylene $(^{Me}IPrCH)_2Si$: (**A** in Scheme 1).[10] While $(^{Me}IPrCH)Li$ is a useful reagent, it is unstable in THF and has a limited shelf life, even when kept at –35 °C in the solid state (decomposition becomes noticeable after one week). As such, the preparation of $(^{Me}IPrCH)_2Zn$ (**1**) became a synthetic target in hopes that this diorganozinc(II) reagent could be an easy-to-handle source of the bulky anionic N-heterocyclic olefin (aNHO) ligand $[^{Me}IPrCH]^-$ via transmetallation. As expected, $(^{Me}IPrCH)_2Zn$ (**1**) can be prepared in a high yield of 88 % as yellow crystals, by adding two equivalents of $(^{Me}IPrCH)Li$ to ZnCl$_2$ in a mixture of Et$_2$O/THF (Scheme 5.2); the reaction time was short enough (1 h) to prevent substantial decomposition of $(^{Me}IPrCH)Li$ in the THF/Et$_2$O mixture. Compound **1** is soluble in typical non-protic organic solvents (THF, Et$_2$O, toluene, and benzene) and is thermally stable up to 196 °C in the solid state (under N$_2$), while **1** can be heated to 120 °C in toluene-d$_8$ for 24 h without decomposition. Moreover, $(^{Me}IPrCH)_2Zn$ (**1**) can be made in an efficient one-pot procedure starting from the precursor to the lithiated aNHO, $^{Me}IPr=CH(I)$ (Scheme 5.2).[10] By adding ^{n}BuLi to $^{Me}IPr=CH(I)$ followed by the addition of half an equivalent of ZnCl$_2$ in THF, $(^{Me}IPrCH)_2Zn$ (**1**) can be obtained in a very high overall yield of 98

%. This approach has the advantage of avoiding the isolation of (^{Me}IPrCH)Li, which has limited shelf life (*vide supra*).
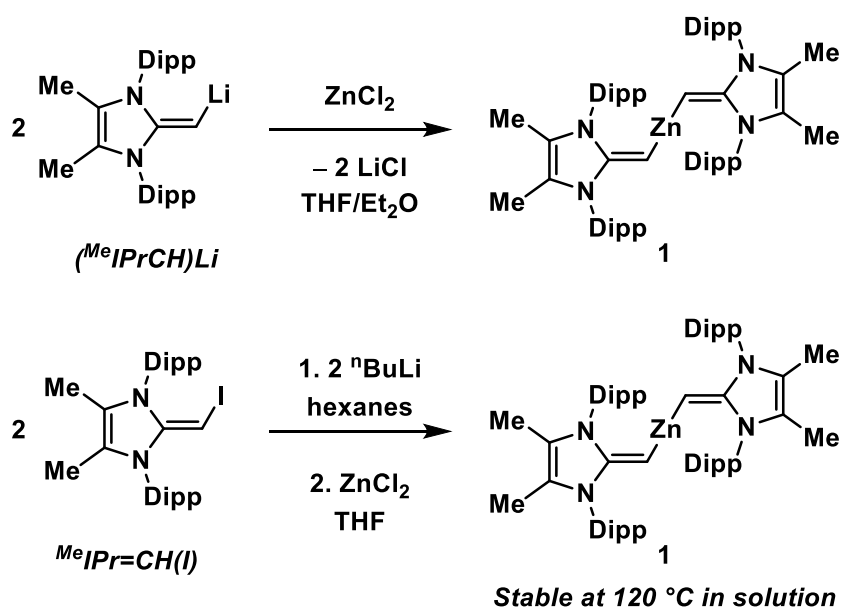
Scheme 5.2. Syntheses of (^{Me}IPrCH)$_2$Zn (**1**) starting from either (^{Me}IPrCH)Li (top) or ^{Me}IPr=CH(I) (bottom).

Yellow crystals of compound **1** were grown from a concentrated toluene solution at –35 °C and the resulting refined structure from single-crystal X-ray diffraction is presented as Figure 5.1. The exocyclic C1–C4 bond length of the aNHO ligands in **1** are each 1.351(3) Å (symmetry imposed by an inversion center at Zn), which is the same within experimental error as the corresponding exocyclic C=C distance in ^{Me}IPr=CH(SiMe$_3$) [1.361(4) Å];[11d] moreover, the C1–C4/C1–C4′ units in compound **1** maintain much of the olefinic character that is observed in the free ligand ^{Me}IPr=CH$_2$ [C=C bond length of 1.3489(18) Å].[13] The Zn–C bond distances in **1** are 1.8879(18) Å and match those found in Roesky's Zn(CAAC)$_2$[14] complex [1.8850(17)

200

Å] (CAAC = cyclic(alkyl)amino carbene), but are shorter than the C_{sp3}–Zn linkages in dimethylzinc [1.927(6) Å].[15] Compound **1** adopts a linear geometry at Zn, much like in other diorganozinc(II) species.[14,15]
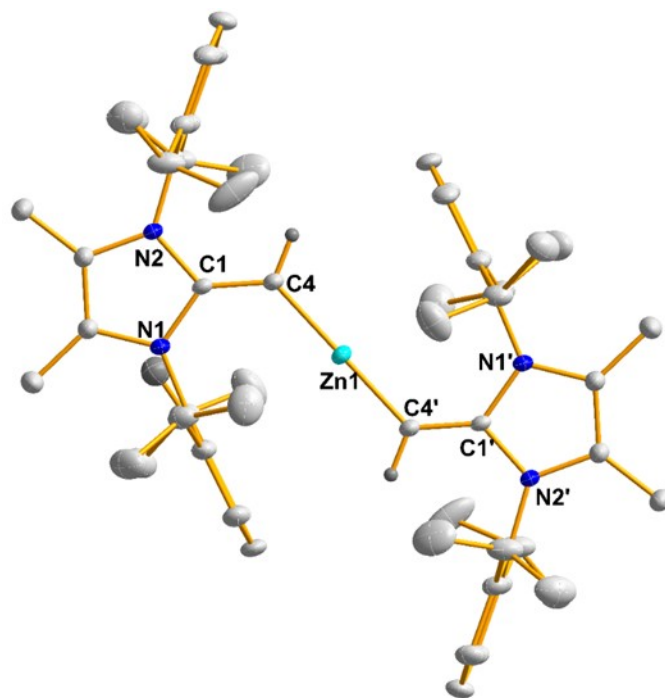
Figure 5.1. Molecular structure of (^{Me}IPrCH)$_2$Zn (**1**) with thermal ellipsoids shown at a 30 % probability level. All hydrogen atoms except for those on C4 and C4´ have been omitted for clarity. Selected bond lengths [Å] and angles [°]: C4–Zn1 1.8879(18), C1–C4 1.351(3); C4–Zn1–C4´180.00(15), Zn1–C4–C1 129.02(14). Primed atoms are related to unprimed ones by an inversion center at Zn.

To test the ability of (^{Me}IPrCH)$_2$Zn (**1**) to undergo transmetallation chemistry, this Zn reagent was combined with one equivalent of Cl$_2$Ge•dioxane in toluene in an attempt to form the known divinylgermylene (^{Me}IPrCH)$_2$Ge.[11d] While a small amount of this divinylgermylene (*ca.* 10 %) was observed by ^{1}H NMR analysis, the major product formed was a new species. After work-up of the soluble fraction of the

reaction mixture, X-ray quality crystals of the purified purple solid (66 % yield) were grown from fluorobenzene, revealing that a germylene-zinc chloride adduct (^{Me}IPrCH)$_2$Ge•ZnCl$_2$ (**2**) had been formed (Scheme 5.3 and Figure 5.2); this product was indeed derived from aNHO-transmetallation from Zn to Ge, however, the Ge(II) center was further coordinated by the ZnCl$_2$ by-product. Fluorobenzene was chosen as the solvent of crystallization for **2** due to the enhanced solubility of the adduct in this medium in comparison to other (more common) aromatic solvents. The insoluble fraction of the same reaction mixture was extracted with THF and a very small amount of yellow solid was crystallized. This product was identified as [(^{Me}IPrCHGe)$_2$(μ–Cl)][ZnCl$_3$(THF)] (**3**) by single-crystal X-ray crystallography (Figure 5.3). Compound **3** could be prepared in bulk form (45 % yield) by repeating the reaction between (^{Me}IPrCH)$_2$Zn (**1**) and Cl$_2$Ge•dioxane in a 1:2 mole ratio, as summarized in Scheme 5.3. Compound **3** can also be prepared by adding Cl$_2$Ge•dioxane to the metallogermylene adduct (^{Me}IPrCH)$_2$Ge•ZnCl$_2$ (**2**) (Scheme 5.3).
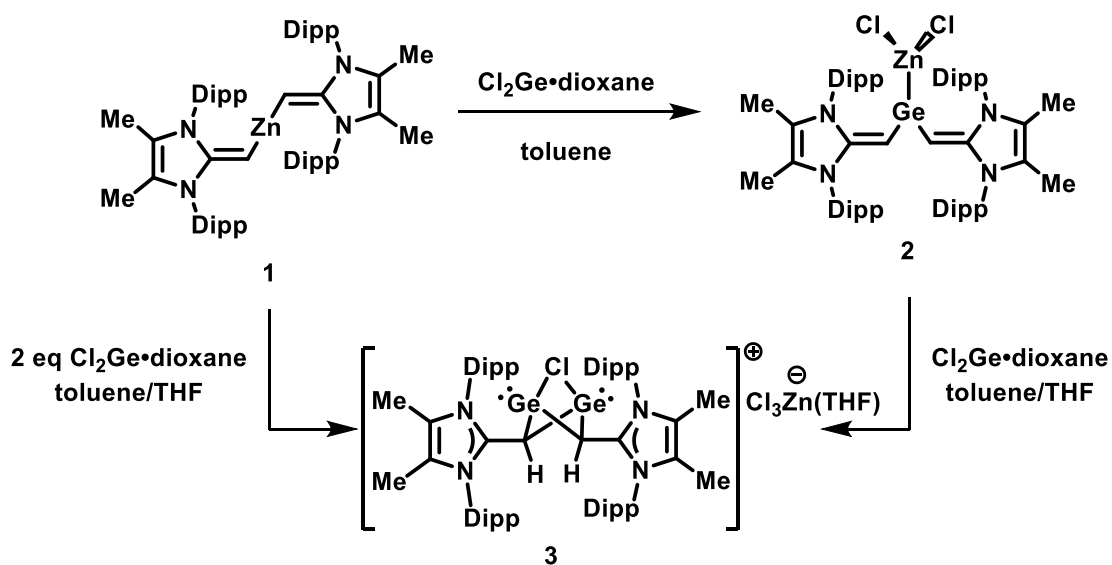
Scheme 5.3. Reaction of (^{Me}IPrCH)$_2$Zn (**1**) with one and two equivalents of Cl$_2$Ge•dioxane, leading to the new Ge(II) products (^{Me}IPrCH)$_2$Ge•ZnCl$_2$ (**2**) and [(^{Me}IPrCHGe)$_2$(μ-Cl)][ZnCl$_3$(THF)] (**3**), respectively.

(^{Me}IPrCH)$_2$Ge•ZnCl$_2$ (**2**) is a rare example of a molecular species with a localized germanium-zinc single bond[16] and is, to my knowledge, the only Ge–Zn bonded species involving a three-coordinate Ge center. The Ge–Zn distance in **2** is 2.4315(10) Å and is slightly elongated with respect to the Ge–Zn distance [2.3839(11) Å] found in Power's four-coordinate Ge complex [(Ar^{Me6})$_2$Ge(Et)-ZnEt], derived from the reaction of the germylene Ar^{Me6}$_2$Ge with ZnEt$_2$ (Ar^{Me6} = 2,6-Mes$_2$C$_6$H$_3$; Mes = 2,4,6-Me$_3$C$_6$H$_2$).[17] The Ge and Zn centers in (^{Me}IPrCH)$_2$Ge•ZnCl$_2$ (**2**) adopt trigonal planar geometries [bond angle sum near 360°], with the Cl–Zn–Cl unit canted with respect to the C–Zn–C array by a torsion angle of 72.16(15)° (C4A–Ge1A–Zn1A–Cl2A, Figure 5.2); thus, the ZnCl$_2$ unit twists away from co-planarity due to the steric impact of the flanking Dipp groups of the ^{Me}IPrCH ligands (Figure 5.2).
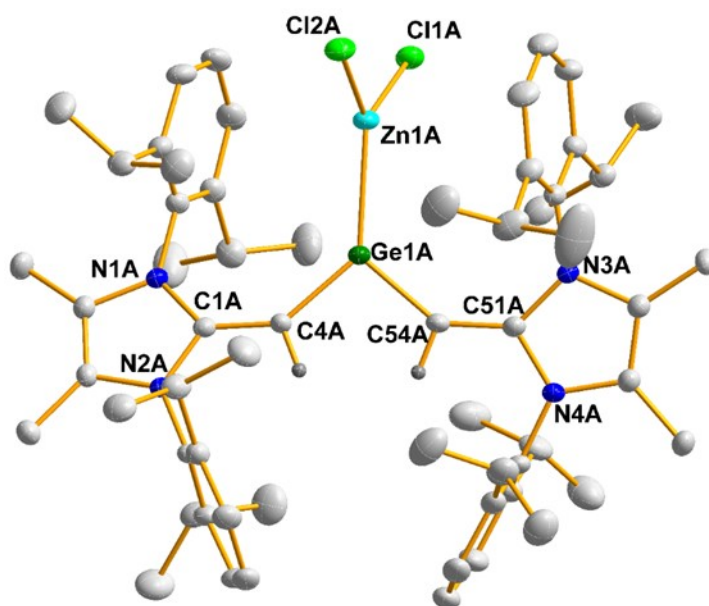
Figure 5.2. Molecular structure of (^{Me}IPrCH)$_2$Ge•ZnCl$_2$ (**2**) with thermal ellipsoids shown at a 30 % probability level. Hydrogen atoms except for those on C4A and C54A as well as fluorobenzene solvate molecules have been omitted for clarity. Selected bond lengths [Å] and angles [°] with values belonging to a second molecule in the unit cell in square brackets: C1A–C4A 1.387(4) [1.383(5)], Ge1A–C4A 1.870(3) [1.871(3)], Zn1A–Ge1A 2.4315(10) [2.4415(11)], Zn1A–Cl2A 2.2302(10) [2.2151(12)]; C1A–C4A–Ge1A 140.2(2) [140.8(3)], C4A–Ge1A–Zn1A 133.92(10) [131.91(10)], Ge1A–Zn1A–Cl1A 124.35(3) [122.82(4)], Ge1A–Zn1A–Cl2A 120.94(3) [124.52(4)], C4A–Ge1A–C54A 97.92(14) [97.18(14)]; torsion angle C4A–Ge1A–Zn1A–Cl2A 72.16(15) [72.17(16)].

The structure of the cationic, propellane-shaped, unit [(^{Me}IPrCHGe)$_2$(μ–Cl)]$^+$ in **3** is shown in Figure 5.3, and is nearly isostructural to the same cationic species found in the previously reported salt [(^{Me}IPrCHGe)$_2$(μ–Cl)][BAr$^F_4$] (Ar^F = 3,5-(F$_3$C)$_2$C$_6$H$_3$).[18] While the intramolecular Ge---Ge separation in **3** [2.7614(5) Å] falls just outside a typical value for a Ge–Ge single bond, comprehensive DFT computations on the isostructural species [(^{Me}IPrCHGe)$_2$(μ–Cl)]BAr$^F_4$ (**D**) (which has a similar crystallographically determined Ge---Ge separation as in **3**; 2.7547(6) Å)

204

showed a lack of Ge–Ge bonding.[18] The Ge–C distances in the propellane Ge_2C_2Cl

core in **3** fall in the range of 2.061(3) to 2.079(2) Å, and are consistent with single

bond character. While the mechanism by which $[(^{Me}IPrCHGe)_2(\mu–Cl)][Cl_3Zn(THF)]$

(**3**) forms is not entirely certain, one possible route involves the initial formation of the

known germanium(II) chloride dimer $[(\mu–^{Me}IPrCH)GeCl]_2$ (**E**) (from an aNHO-ligand

scrambling reaction between $(^{Me}IPrCH)_2Ge$ (**F**) and $Cl_2Ge\bullet dioxane$),[18] followed by

halide abstraction with $ZnCl_2$ to yield the zincate anion $[Cl_3Zn(THF)]^-$ and

$[(^{Me}IPrCHGe)_2(\mu–Cl)]^+$ cation in **3** (Scheme 5.4).
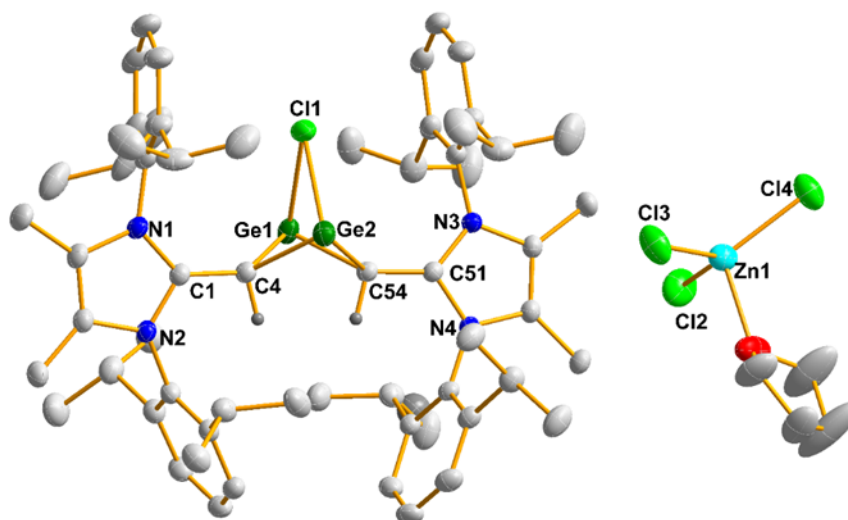
Figure 5.3. Molecular structure of $[(^{Me}IPrCHGe)_2(\mu–Cl)][ZnCl_3(THF)]$ (**3**) with thermal ellipsoids shown at a 30 % probability level. Hydrogen atoms except those on C4 and C54 have been omitted for clarity. Selected bond lengths [Å] and angles [°]: C1-C4 1.434(4), C51-C54 1.434(3), Ge1-C4 2.068(3), Ge2-C4 2.061(3), Ge1-C54 2.067(3), Ge2-C54 2.079(2), Ge1-Cl1 2.5159(10), Ge2-Cl1 2.5095(10), Ge1---Ge2 2.7614(5); Ge1-Cl1-Ge2 66.66(2).
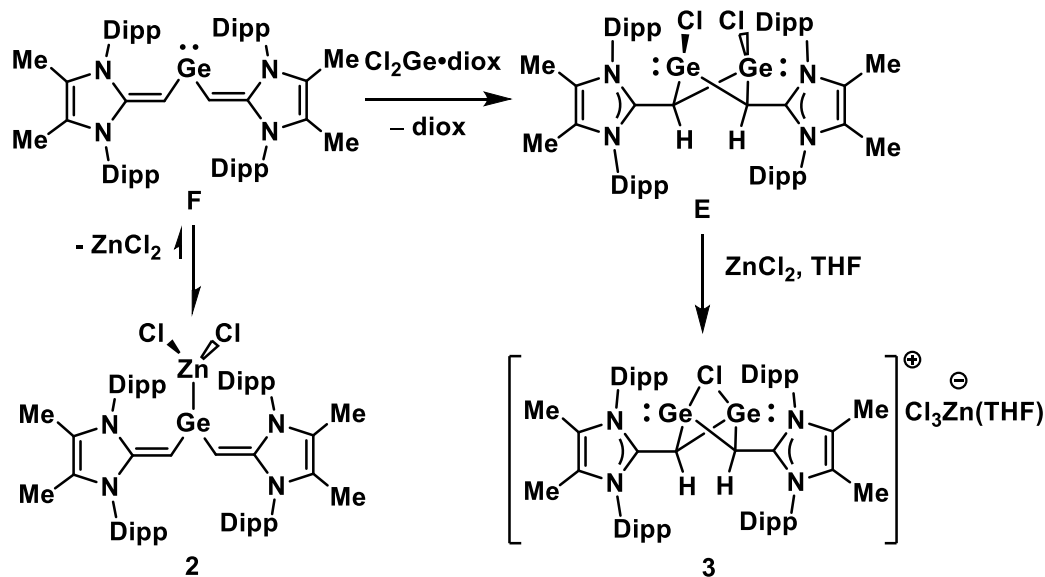
Scheme 5.4. Possible route by which (^{Me}IPrCH)$_2$Ge•ZnCl$_2$ (**2**) is converted into [(^{Me}IPrCHGe)$_2$(μ–Cl)][Cl$_3$Zn(THF)] (**3**); the formation of the intermediate [(μ–^{Me}IPrCH)GeCl]$_2$ (**E**) follows known chemistry reported in the Rivard Group.[18]

A striking feature of (^{Me}IPrCH)$_2$Ge•ZnCl$_2$ (**2**) is its deep purple color, both in solution (λ_{max} = 558 nm [ε = 8490 L mol^{-1} cm^{-1}] and 368 nm [ε = 3310 L mol^{-1} cm^{-1}] in toluene) and in the solid state. As such, a time-dependent density functional theory (TD-DFT) study was carried out on **2** at the B3LYP/def2-TZVP level of theory, wherein the most intense and red-shifted electronic transition arises from a HOMO to LUMO transition at 490 nm, while a HOMO-1 to LUMO transition of substantial oscillator strength occurs at 349 nm (Figure 5.4). Specifically, the long wavelength HOMO to LUMO transition in **2** consists of a charge-transfer process with the HOMO bearing considerable C=C π contribution from the ^{Me}IPrCH ligands, while the LUMO is dominated by a Ge p-orbital; there is negligible orbital participation from the ZnCl$_2$ unit on the electronic transitions that occur in the visible spectral region in **2**.
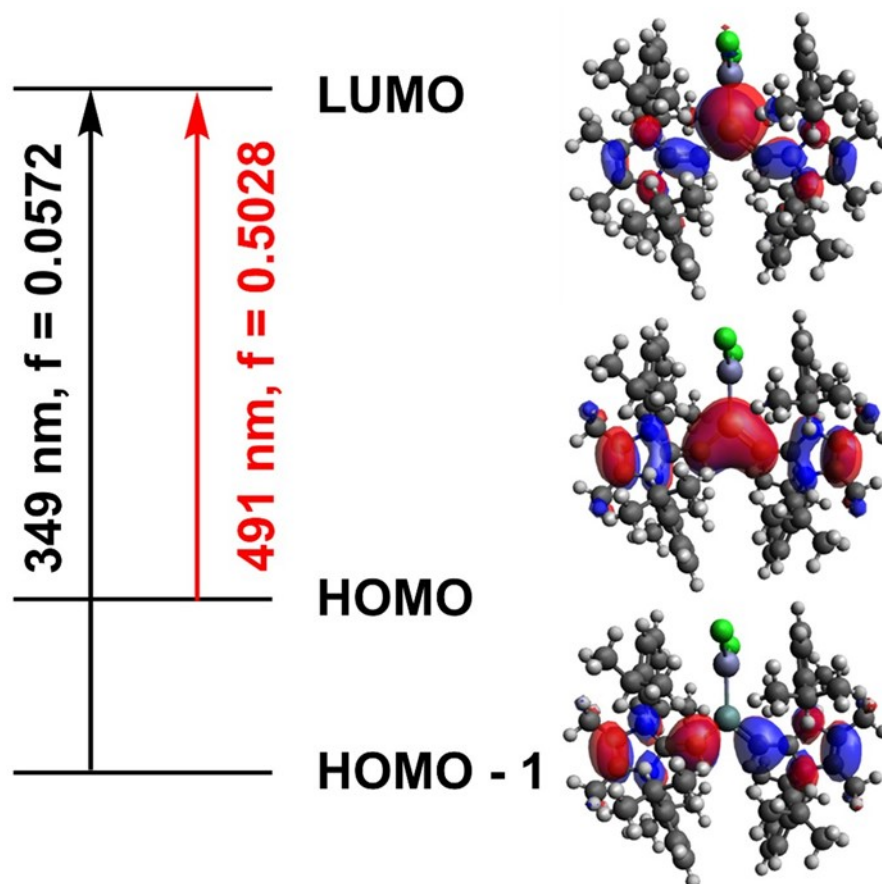
Figure 5.4. TD-DFT [B3LYP/def2-TZVP] computed electronic transitions for (^{Me}IPrCH)$_2$Ge•ZnCl$_2$ (**2**), including excitation wavelengths and oscillator strengths (*f*) and the associated molecular orbitals involved.

Exploration was continued on the transmetallation reactivity of (^{Me}IPrCH)$_2$Zn (**1**) to include its interaction with the Sn(II) dihalide, Cl$_2$Sn•dioxane. As outlined in Equation 5.1, the new product obtained was not the metallostannylene (^{Me}IPrCH)$_2$Sn•ZnCl$_2$, but instead the halide-bridged Sn(II) product [(^{Me}IPrCHSn)$_2$(μ–Cl)]$_2$[Zn$_2$Cl$_6$] (**4**), bearing a similar propellane E$_2$C$_2$Cl core (E = Group 14 element) as in **3** (*vide supra*). The highest isolated yield of the yellow solid **4** (45 %) transpired when (^{Me}IPrCH)$_2$Zn (**1**) was combined with two equivalent of Cl$_2$Sn•dioxane in

toluene (Equation 5.1). Crystals of **4** that were of suitable quality for single-crystal X-ray diffraction were grown, and the resulting structure is presented in Figure 5.5. As expected, the average exocyclic aNHO C1–C4/C1A–C4A bond length in **4** (two independent molecules in unit cell) is 1.430(11) Å [1.425(10) Å for C51–C54/C51A–C54A], which is longer than the corresponding exocyclic C=C bonds in the starting material (^{Me}IPrCH)$_2$Zn (**1**) [1.351(3) Å, *vide supra*], since each aNHO ligand in **4** acts as a 4-electron donor via the formation of two Sn–C bonds. As expected, the average Sn–Cl distance involving the bridging Cl atom in **4** [2.662(6) Å] is substantially longer than the bridging Ge–Cl interactions in the Ge congener **3** [2.5127(10) Å]. While the average intramolecular Sn---Sn separation in **4** [3.0824(11) Å] hint at some form of intramolecular bonding, however, DFT computations show a lack of direct Sn–Sn bonding in **4** (Figure 5.5).

1   **4**

(5.1)
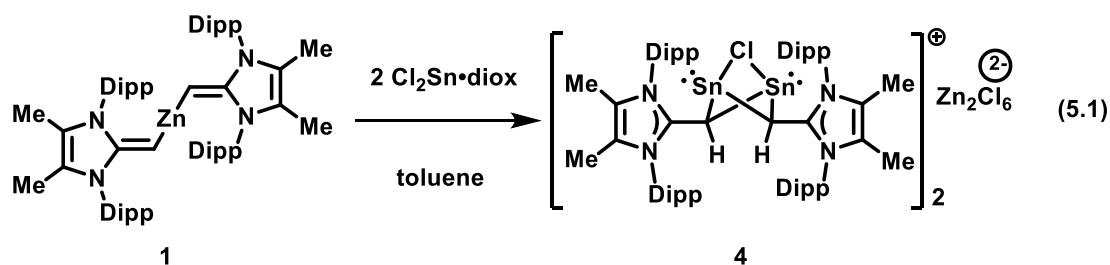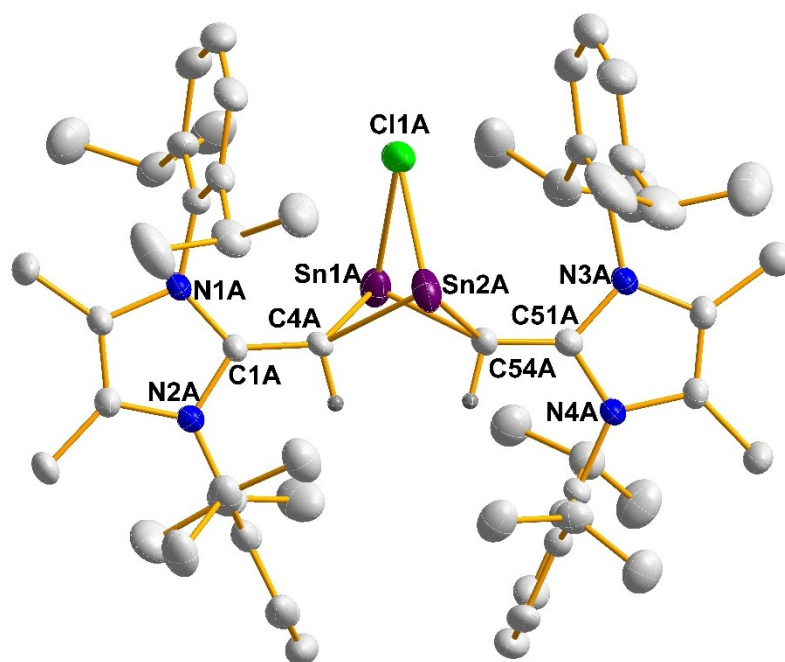
Figure 5.5. Molecular structure of $[(^{Me}IPrCHSn)_2(\mu–Cl)]_2[Zn_2Cl_6]$ (**4**) with thermal ellipsoids shown at a 30 % probability level. Hydrogen atoms, except those on C4A and C54A, and the $[Zn_2Cl_6]^{2-}$ anion have been omitted for clarity. Selected bond lengths [Å] and angles [°] with values belonging to a second molecule in the unit cell in square brackets: C1A–C4A 1.422(7) [1.438(8)], C4A–Sn1A 2.255(6) [2.271(6)], C4A–Sn2A 2.249(5) [2.252(6)], Sn1A–Cl1A 2.650(3) [2.660(3)], Sn2A–Cl1 2.656(3) [2.681(3)], C51A–C54A 1.423(7) [1.427(7)], C54A–Sn1A 2.263(6) [2.256(6)], C54A–Sn2A 2.258(6) [2.224(6)], Sn1A---Sn2A 3.0846(7) [3.0801(8)]; Sn1A–Cl1A–Sn2A 71.10(5) [70.44(15)], C1A–C4A–Sn1A 124.4(4) [127.7(5)], C1A–C4A–Sn2A 132.2(4) [131.4(5)], Sn1A–C54A–C51A 131.4(4) [132.4(4)], Sn2A–C54A–C51A 126.8(4) [127.3(4)].

Compounds **3** and **4** each contain a C_2E_2Cl propellane core as part of the cationic units. For comparison, all-inorganic Group 14 element-based propellanes are known in the literature with examples by the Sita,[19] Breher,[20] and Power[21] Groups summarized in Chart 5.1 (compounds **G-I**). The abovementioned Ge---Ge separation in **3** is 2.7614(5) Å, and is the same within experimental error as the transannular Ge---Ge distance in Breher's $[(Mes_2Si)_3Ge_2]$ cluster (**G**) [2.767(1) Å], but significantly

shorter than the corresponding value in Power's expanded propellane [(Ar^{Me6}SnCl)$_3$Ge$_2$] (**H**) [3.363(1) Å]. Lastly, Sita and coworkers prepared an all-Sn propellane [(Dep$_2$Sn)$_3$Sn$_2$] (**I**) (Dep = 2,6-Et$_2$C$_6$H$_3$) with a Sn---Sn separation involving the ligand-free Sn atoms [3.367(1) Å] that is elongated by *ca.* 0.29 Å in relation to the Sn---Sn separation in **4**.
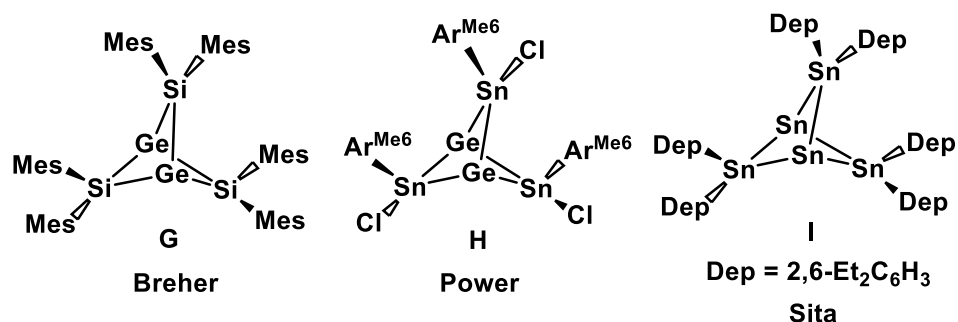
Chart 5.1. Salient examples of all-inorganic Group 14 propellanes.

(^{Me}IPrCH)$_2$Zn (**1**) was also combined with the Si(II)- and Pb(II)-based halides ^{Me}IPr•SiBr$_2$[10] and PbBr$_2$, however, no reaction was found in toluene at room temperature after 24 h. It is likely that the low solubility of PbBr$_2$ suppressed transmetallation with **1**, while in the case of ^{Me}IPr•SiBr$_2$, it is likely the lower reactivity of Si–X (X = halide) bonds in transmetallation[8a] that prevents any reaction; heating a mixture of **1** and ^{Me}IPr•SiBr$_2$ to 100 °C in toluene for 16 h gave no reaction. Combining **1** and PbBr$_2$ in THF resulted in decomposition into the free NHO ^{Me}IPrCH$_2$ over the course of 16 h.

Next, an aNHO framework was installed onto a phosphorus center by reacting (^{Me}IPrCH)$_2$Zn (**1**) with two equivalents of ClPPh$_2$ in toluene (Equation 5.2). This

procedure afforded the expected phosphine (^{Me}IPrCH)PPh$_2$ (**5**) along with insoluble ZnCl$_2$ as a by-product (Equation 5.2). Compound **5** is analogous to the phosphine-ligand (IPrCH)PPh$_2$ (IPrCH = [(HCNDipp)$_2$CH]$^-$) reported previously by the Rivard Group;[22] notably, (IPrCH)PPh$_2$ was shown to bind two equivalents of gold(I) chloride, through coordination to both carbon (IPrCH-) and phosphorus (-PPh$_2$) centers.[23]
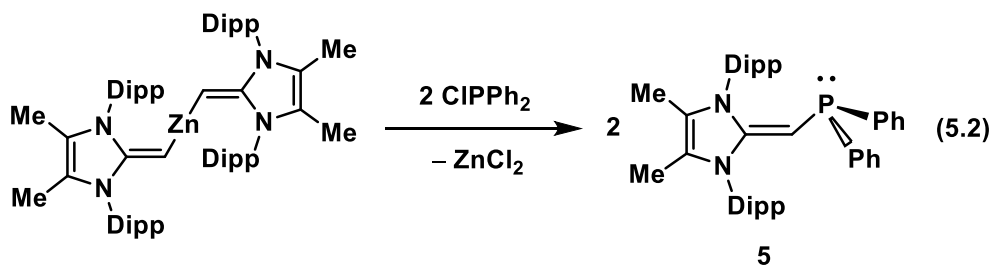
Looking to expand the range of substrates that undergo transmetallation with (^{Me}IPrCH)$_2$Zn (**1**), motivation was found in prior studies by Okuda and coworkers (and others)[7,24] who studied the formation of zinc hydrides by reacting organozinc precursors with molecular hydride sources. There also is a desire to prepare new boryl species of the general form ^{Me}IPrCH–BR$_2$, with the hope for interesting luminescent properties stemming from an inherent "push-pull" electronic architecture.[25] To access a borated aNHO complex, (^{Me}IPrCH)$_2$Zn (**1**) was combined with two equivalents of catecholborane (HBcat) in toluene. Upon mixing these reagents, the immediate formation of ZnH$_2$ as a white precipitate (as confirmed by IR spectroscopy) and the desired product (^{Me}IPrCH)Bcat (**6**) was obtained from the soluble fraction as a white crystalline solid (77 % yield; Scheme 5.5, Figure 5.6). Attempts to form the analogous pinacolborane derivative (^{Me}IPrCH)Bpin by combining **1** with HBpin in toluene (with

heating up to 100 °C) led to no reaction, possibly due to a decreased electrophilicity at the boron center in HBpin (*vs.* HBcat), thus making transmetallation less favorable.

Heartened by the observed reactivity of (^{Me}IPrCH)$_2$Zn (**1**) with HBcat, the transmetallation of **1** was explored with primary arylboranes. Mixing **1** with two equivalents of mesitylborane (MesBH$_2$) in toluene resulted in the gradual formation of (^{Me}IPrCH)B(Mes)H (**7**) over the span of 18 h at room temperature; similarly, combination of **1** with TripBH$_2$ (Trip = 2,4,6-^{i}Pr$_3$C$_6$H$_2$) afforded (^{Me}IPrCH)B(Trip)H (**8**) (Scheme 5.5). The aNHO-boryl species **7** and **8** were obtained as colorless crystals in 90 % and 85 % yields, respectively, and their structures are presented as part of Figures 5.7 and 5.8.
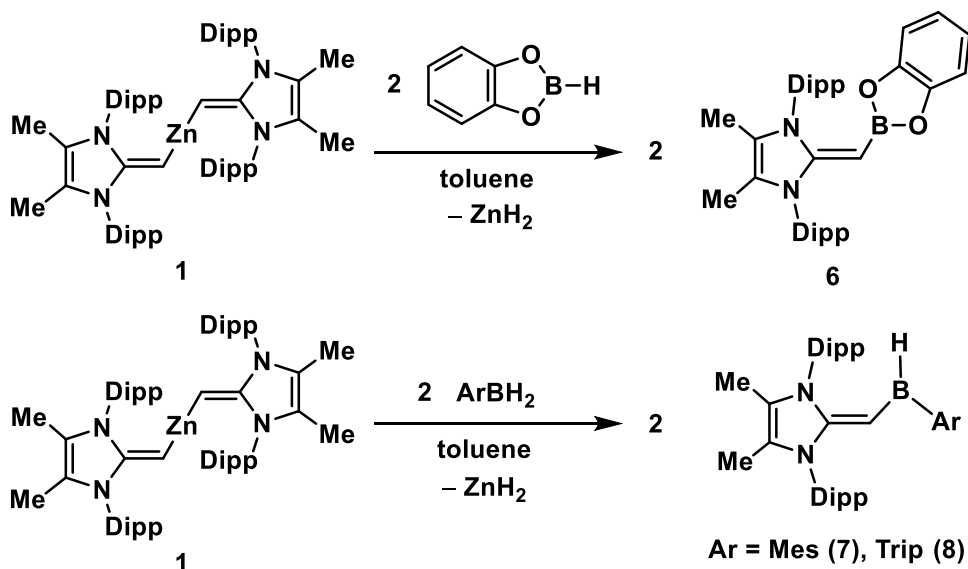
Scheme 5.5. Synthesis of (^{Me}IPrCH)Bcat (**6**), (^{Me}IPrCH)B(Mes)H (**7**), and (^{Me}IPrCH)B(Trip)H (**8**).
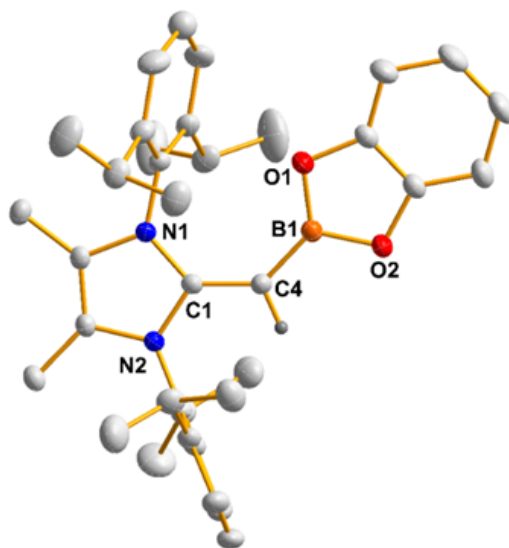
Figure 5.6. Molecular structure of (^{Me}IPrCH)Bcat (**6**) with thermal ellipsoids shown at a 30 % probability level. Hydrogen atoms except for that shown on C4 have been omitted for clarity. Selected bond lengths [Å] and angles [°]: C1–C4 1.3867(17), C4–B1 1.4813(18); C1–C4–B1 134.28(12).
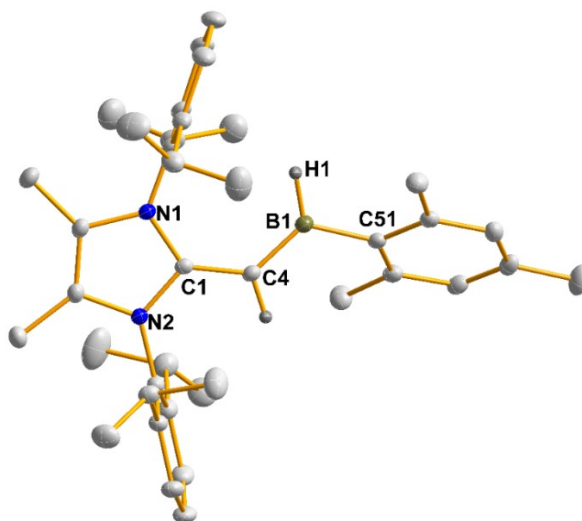
Figure 5.7. Molecular structure of (^{Me}IPrCH)B(Mes)H (**7**) with thermal ellipsoids shown at 30 % probability level. Hydrogen atoms other than those on C4 and B1 have been omitted for clarity. Selected bond lengths [Å] and angles [°]: C1–C4 1.4022(15), C4–B1 1.4783(16), B1–H1 1.104(15); C1–C4–B1 130.68(10), C4–B1–H1 122.0(8).
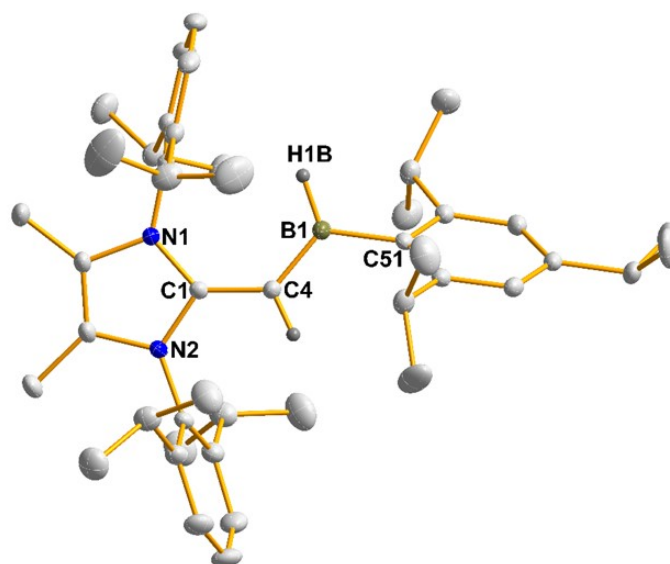
Figure 5.8. Molecular structure of (^{Me}IPrCH)B(Trip)H (**8**) with thermal ellipsoids shown at a 30 % probability level. Hydrogen atoms other than those on C4 and B1 have been omitted for clarity. Selected bond lengths [Å] and angles [°]: C1–C4 1.4033(14), C4–B1 1.4741(15), B1–H1B 1.098(13); C4–B1–H1B 122.18(9).

The C_{aNHO}–B bond length (C4-B1) in (^{Me}IPrCH)Bcat (**6**) (Figure 5.6) is 1.4813(18) Å and the same within experimental error as the corresponding C_{aNHO}–B bonds in (^{Me}IPrCH)B(Mes)H (**7**) [1.4783(16) Å] and (^{Me}IPrCH)B(Trip)H (**8**) [1.4741(15) Å] (Figures 5.7 and 5.8). Notably, each of these C–B bonds are shorter than those found in BPh$_3$ [*avg.* 1.689(6) Å],[26] suggesting the presence of some C–B π-character within the ^{Me}IPrCH-BR$_2$ products **6-8**. Indeed, DFT computations show C–B π interactions in the HOMO of **6** and **8**, with corresponding C–B Wiberg bond indices of 1.14 and 1.23, respectively (see Figures 5.9, 5.15, and 5.16). The hydrides at the boron centers in **7** and **8** could be located in the electron difference map and refined to final B–H bond lengths of 1.104(15) and 1.098(13) Å, respectively; for comparison, a

similar (*avg.*) B–H bond length of 1.15(3) Å has been determined for $H_3B \cdot NH_3$.[27] It is salient to point out that compounds **6-8** are structurally related to a series of *N*-heterocyclic imine-boryl complexes IPr=N-BR$_2$ reported by the Rivard Group.[28]
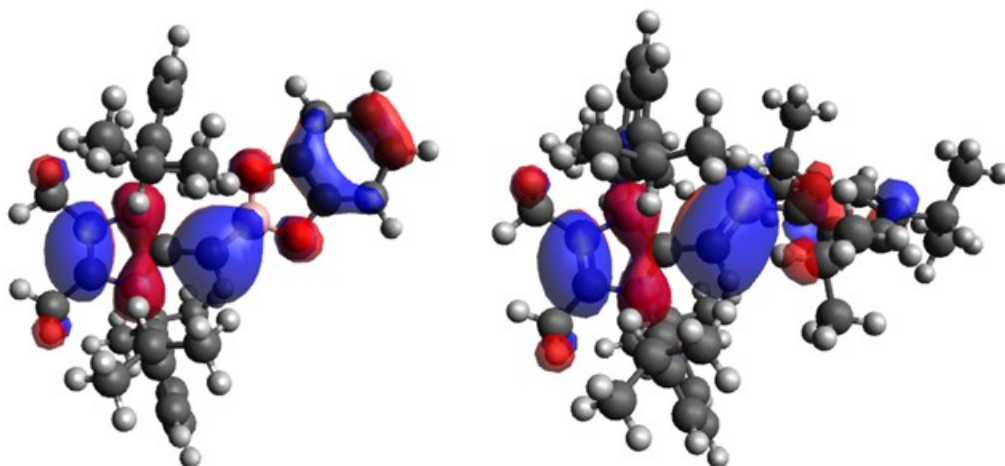
Figure 5.9. Computed HOMOs of (^{Me}IPrCH)Bcat (**6**) (left) and (^{Me}IPrCH)B(Trip)H (**8**) (right).

Compound **1** was also combined with PhSiH$_3$ and heated at 120 °C in toluene, however, no reaction transpired. Likewise, an attempt to form the abovementioned phosphine (^{Me}IPrCH)PPh$_2$ (**5**) by heating a 1:2 mixture of (^{Me}IPrCH)$_2$Zn (**1**) and HPPh$_2$ at 80 °C in toluene, also failed to give an observable reaction. While combining $H_3B \cdot NMe_3$ with **1** did not afford any new products (according to NMR analysis), mixing **1** with two equivalents of the more reactive borane adduct $H_3B \cdot SMe_2$ in toluene gave the known[29] boryl-borane complex [^{Me}IPrCH(BH$_2$)$_2$(μ–H)] (**9**) as a white solid in a 61 % yield (Equation 5.3); previously, [^{Me}IPrCH(BH$_2$)$_2$(μ–H)]

(**9**) was prepared by reacting the silylated aNHO ^{Me}IPr=CH(SiMe$_3$) with excess

H$_3$B•THF in toluene (as seen in Chapter 2).[30]

(5.3)
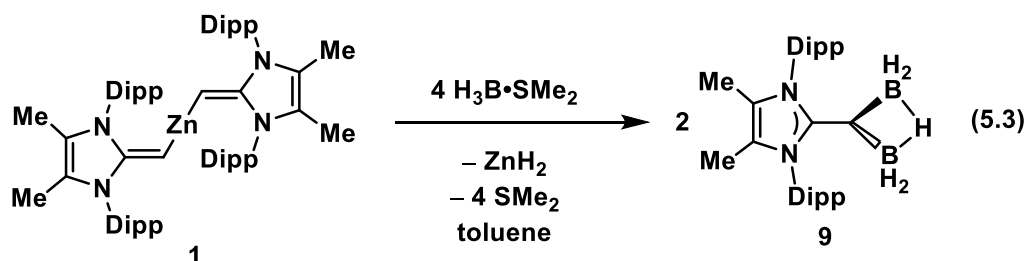
According to DFT computations, (^{Me}IPrCH)B(Trip)H (**8**) contains a B–H bond

with considerable hydridic character, as evidenced by a computed charge of –0.079

via natural population analysis (NPA) (Figure 5.16). With the goal of abstracting a

hydride to form a two-coordinate borenium ion [^{Me}IPrCH-B-Mes]$^+$,

(^{Me}IPrCH)B(Mes)H (**7**) was combined with trityl triflate [Ph$_3$C]OTf in toluene,

leading to the rapid formation of a precipitate. ^{1}H NMR analysis of the supernatant

revealed that Gomberg's dimer (Ph$_2$C=C$_6$H$_4$-CPh$_3$, Scheme 5.6) formed. The

remaining precipitate was dissolved in THF, and the solution layered with hexanes to

give colorless crystals of a new product after storage at –35 °C for one week. Single-

crystal X-ray analysis revealed that the expected borenium cation did not form.

Instead, an unusual triflate salt was present [(^{Me}IPrCHMes)B(THF)(OTf)H][OTf] (**10**)

(Scheme 5.6, Figure 5.10), wherein a formal [HB]$^{2+}$ dication is coordinated by a

neutral *N*-heterocyclic olefin ^{Me}IPrC(H)Mes (formed by a 1,2-Mes migration), and

further bound by THF and OTf$^-$ units. The exocyclic C1-C4 bond length in **10** is

1.515(3) Å, and is substantially elongated in comparison to the exocyclic C=C distance of 1.4022(15) Å in the starting material (^{Me}IPrCH)B(Mes)H (**7**) (Figure 5.7), in line with a loss of exocyclic C–C π-bonding in **10**. The boron center in **10** adopts a tetrahedral environment with a B–H bond length of 1.13(3) Å. This B–H bond length is similar to those found in boronium cations reported by the groups of Vedejs [Me$_2$NCH(Me)(C$_6$H$_4$)B(H)•pyr]$^+$ [1.130(19)] and Braunschweig [{(Me$_3$Si)-$_2$N}B(H)•TMEDA]$^+$ [1.16(4) Å] (pyr = pyridine; TMEDA = Me$_2$NCH$_2$CH$_2$NMe$_2$).[30] While the structure of **10** is complicated, there is a possible pathway to this species from (^{Me}IPrCH)B(Mes)H (**7**) that involves initial oxidation of a C=C π-bond within the ^{Me}IPrCH$^-$ ligand to yield a carbon-based radical and Ph$_3$C• (and its subsequent dimerization to give Gomberg's dimer). The resulting radical cation [(^{Me}IPrCH)B(Mes)H]$^{•+}$ could then undergo a 1,2-Mes shift to yield a boryl-type radical, which is then oxidized by another equivalent of [Ph$_3$C]$^+$ (Scheme 5.6). Despite repeated attempts, it was not possible obtain pure samples of **10** on a bulk scale.
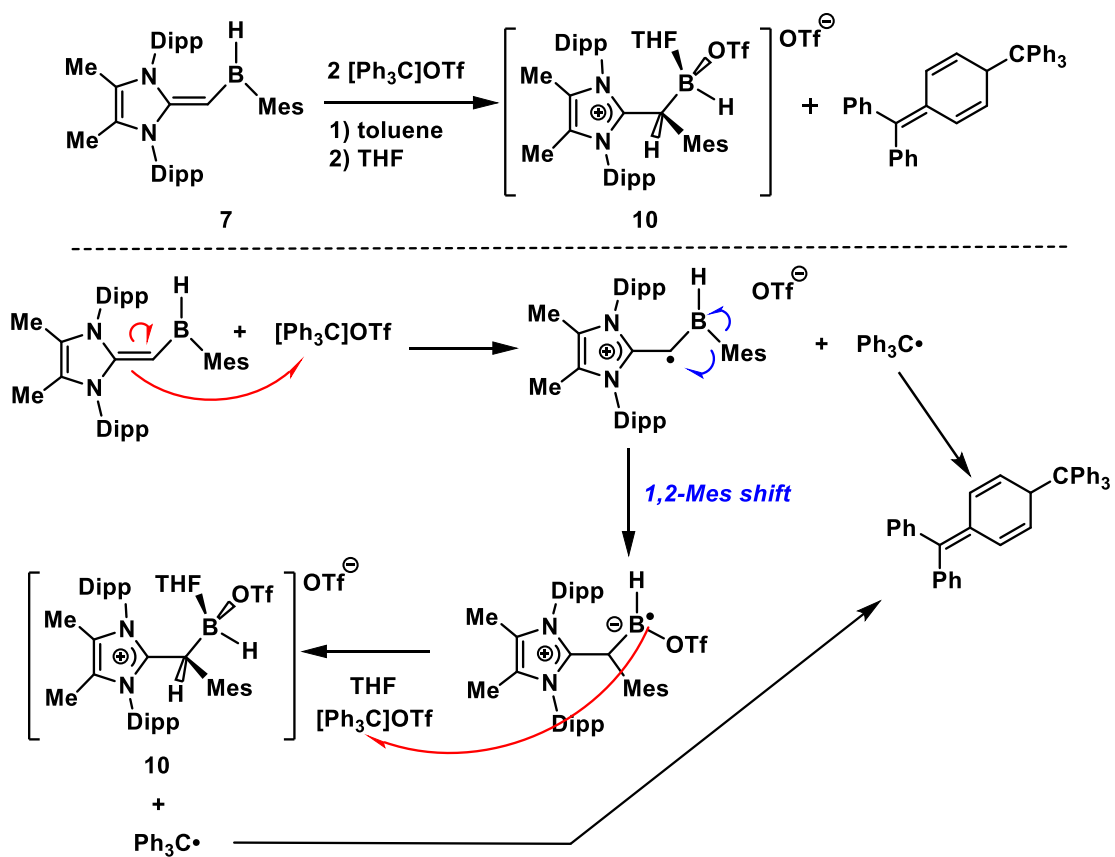
Scheme 5.6. Synthesis of [(^MeIPrCHMes)B(THF)(OTf)H][OTf] (**10**) and a possible mechanism for its formation.
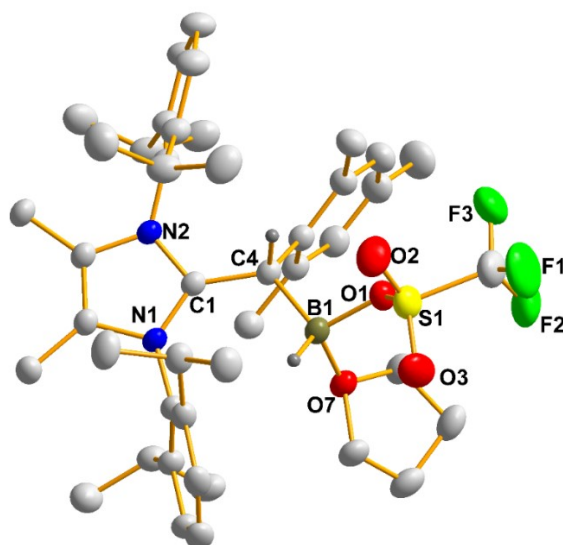
Figure 5.10. Molecular structure of the $[(^{Me}IPrCHMes)B(THF)(OTf)H]^+$ cation in **10** with thermal ellipsoids shown at a 30 % probability level. Hydrogen atoms other than those on C4 and B1 and the triflate anion have been omitted for clarity. Selected bond lengths [Å] and angles [°]: C1-C4 1.515(3), C4-B1 1.623(3), B1-H1 1.13(3); C4-B1-O1 106.9(2), C4-B1-H1 114.6(13).

With confirmation that zinc dihydride elimination can drive transmetallation from $(^{Me}IPrCH)_2Zn$ (**1**), one last example of this reaction type was explored. Specifically, treatment of **1** with diisobutylaluminum hydride (DIBAL-H, $[^iBu_2AlH]_2$) led to conversion into the new aluminyl-alane product $[^{Me}IPrCH(Al^iBu_2)_2(\mu-H)]$ (**11**) (Equation 5.4); this process likely proceeds via $^{Me}IPr=CH-Al^iBu_2$ as an intermediate, wherein the ylidic $^{Me}IPr=CH$ group is sufficiently nucleophilic to coordinate an extra molecule of HAl^iBu_2. The impact of dual coordination at the terminal carbon atom in the $^{Me}IPrCH$ ligand in **11** is manifest by the presence of an exocyclic (C1-C4) single

bond [1.434(2) Å], as determined by single-crystal X-ray diffraction (Figure 5.11). The adjacent C_{aNHO}–Al bonds in **11** are slightly shorter [2.0513(17) and 2.0328(15) Å] than the dative Al–C_{NHO} bond length in the recently reported *N*-heterocyclic olefin (NHO)-alane adduct $^{Me}IPrCH_2 \cdot AlMe_3$ [2.1198(13) Å, see Chapter 4].[31] The bridging hydride in **11** could be located and refined, leading to Al–H distances of 1.662(18) and 1.753(18) Å; these bond lengths are similar to the average bridging Al–H bond length found in α-AlH$_3$ (1.715 Å).[32] While not structurally authenticated, Gavrilenko and coworkers described the preparation of an anionic analogue of **11**, [{Me(CH$_2$)$_4$C(H)}(Al^{i}Bu)$_2$(μ–H)]$^-$ in 1981, wherein a similar bridging hydride unit sandwiched between -Al^{i}Bu$_2$ units was proposed.[33]

220
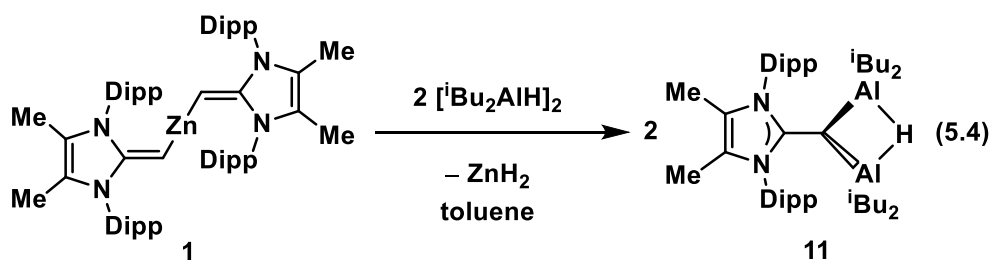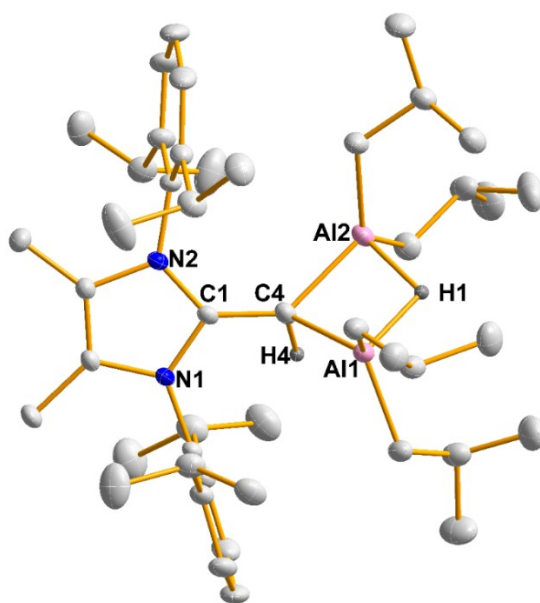
Figure 5.11. Molecular structure of [^{Me}IPrCH(Al^{i}Bu$_2$)$_2$(μ–H)] (**11**) with thermal ellipsoids shown at a 30 % probability level. Hydrogen atoms other than those on C4 and bridged between Al1 and Al2 have been omitted for clarity. A second minor conformation of the {(Al^{i}Bu$_2$)$_2$(μ-H)} subunit exists (7 %) within the same unit cell. Selected bond lengths [Å] and angles [°] with values for the minor conformation in square brackets: C1-C4 1.434(2), C4-Al1 2.0513(17) [1.95(2)], C4-Al2 2.0328(15) [1.94(2)], Al1-H1 1.662(18) [1.61(2)], Al2-H1 1.753(18) [1.869(19)]; C1-C4-Al1 127.02(11) [127.02(11)], C1-C4-Al2 135.86(12) [135.86(12)], Al1-C4-Al2 82.75(6) [87.4(12)].

5.3. Conclusion

In this study, the number of known anionic *N*-heterocyclic olefin (aNHO)-supported main group complexes has been expanded with the use of the new organozinc(II) species (^{Me}IPrCH)$_2$Zn (**1**) as a ligand source. This Zn reagent has the advantage of being stable up to 120 °C in solution, is soluble in organic solvents, and can participate in transmetallation chemistry with both main group halide and

hydrides. Future work will include exploring the use of this versatile chemistry to gain access to luminescent main group "push-pull" systems, the development of new frustrated Lewis pairs (FLPs) bearing synergistic Lewis basic ^{Me}IPrCH and acidic ($-ER_x$) units, the application of these FLPs in olefin polymerization and small molecule activation, and the preparation of new aNHO ligands.

5.4. Experimental Section

5.4.1. Materials and Instrumentation

All reactions were performed using standard Schlenk techniques under an atmosphere of nitrogen or argon or in a nitrogen/argon-filled glovebox (Innovative Technology, Inc./MBraun). Solvents were dried using a Grubbs-type solvent purification system[34] manufactured by Innovative Technology, Inc, degassed, and stored under an atmosphere of nitrogen or argon prior to use. Fluorobenzene was dried by heating to reflux over calcium hydride, followed by distillation, degassing (freeze–pump–thaw method), and storage over 4 Å molecular sieves prior to use. Cl$_2$Ge•dioxane, ZnCl$_2$, diisobutylaluminum hydride (1.0 M solution in hexanes), MesBr, ^{i}PrOBpin, HPPh$_2$, ClPPh$_2$, PhSiH$_3$, and HBcat were obtained from MilliporeSigma and used as received. Li[AlH$_4$] (1.0 M solution in Et$_2$O) and HCl (4.0 M solution in 1,4-dioxane) were purchased from Acros Organics. HBpin was purchased from Oakwood Chemicals. ^{Me}IPr=CH(I),[10] (^{Me}IPrCH)Li,[10] Cl$_2$Sn•dioxane,[35] and [Ph$_3$C]OTf[36] were prepared according to literature procedures. MesBH$_2$,[37]

MesB(OMe)$_2$,[37] TripBpin,[38] and TripBH$_2$[38] were prepared according to modified literature procedures (see Section 5.4.4 for more details). ^{1}H, ^{13}C{^{1}H}, ^{11}B{^{1}H}, ^{19}F{^{1}H}, and ^{31}P{^{1}H} NMR spectra were recorded on a Varian Inova-400, Varian Inova-500, Bruker AVHD500 cryo, Bruker AV400, or Varian Inova-700 spectrometer and referenced externally to SiMe$_4$ (^{1}H, ^{13}C{^{1}H}), F$_3$B•OEt$_2$ (^{11}B), ClCF$_3$ (^{19}F{^{1}H}), and 85 % H$_3$PO$_4$ (^{31}P{^{1}H}), respectively. Elemental analyses were performed at the Analytical and Instrumentation Laboratory at the University of Alberta. Melting points were measured in sealed glass capillaries under nitrogen using MelTemp apparatus. UV-Vis spectroscopy was performed on a Thermo Scientific Genesys 10S UV-Vis Spectrometer.

5.4.2. X-ray Crystallography

Appropriate X-ray quality crystals were coated with a small amount of hydrocarbon oil (Paratone-N) and removed from the glovebox in a vial. Crystals were quickly mounted onto a glass fiber and placed in a low temperature stream of nitrogen on the X-ray diffractometer. All data was collected using a Bruker APEX II CCD detector/D8 or PLATFORM diffractometer using Mo Kα (0.71073 Å) or Cu Kα (1.54178 Å) radiation, with the crystals cooled to –80 °C or –100 °C. The data was corrected for absorption through Gaussian integration from the indexing of crystal faces.[39] Crystal structures were solved using intrinsic phasing (SHELXT)[40] and refined using SHELXL-2014.[41] The assignment of hydrogen atom positions are based on the sp^2- or sp^3-hybridization geometries of their attached carbon atoms and given

thermal parameters 20 % greater than those of their parent atoms. Molecular structures are shown with ellipsoids at a 30 % probability level and have been imaged using SHELXP ORTEPs.

5.4.3. Computational Studies

Geometry optimizations of the gas-phase structures were performed using DFT with the B3LYP[42] functional and the def2-TZVP [43] basis set for compounds **1**, **2**, **4**, **6**, **8**, and **10** (only the cations of **4** and **10** hereafter referred to as **[4]**$^+$ and **[10]**$^+$). The initial structures were taken from the experimental obtained X-ray structures of the respective compounds. All calculations were performed with the Gaussian16 software.[44] The molecular orbitals (MOs) were extracted from the Gaussian16 checkpoint files, and the final molecular geometries were used to compute the NBOs using the NBO6 program.[45]

Atoms	$Q_{NPA}(e)$
Zn1	1.34
C2	-1.09
C4	0.354

Bonds	WBI
Zn1-C2	0.45
C2-C4	1.65
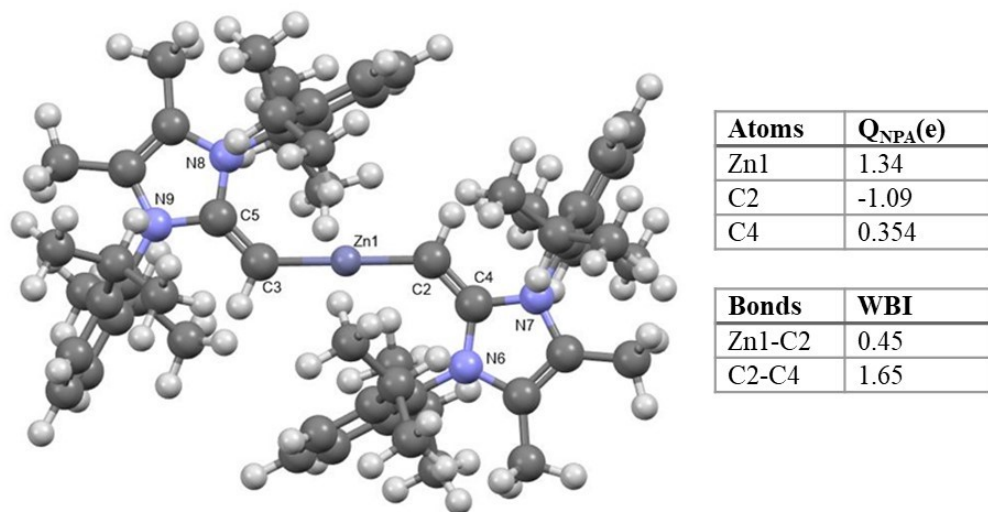
Figure 5.12. Optimized structure, natural charges (Q_{NPA}), and Wiberg bond indices (WBI) derived from natural bonding orbital (NBO) analysis of (^{Me}IPrCH)$_2$Zn (**1**).

Atoms	$Q_{NPA}(e)$
Ge21	0.62
Zn25	1.33
C15	-0.89
C10	0.41

Bonds	WBI
C15-Ge21	1.06
Ge21-Zn25	0.41
C10-C15	1.43
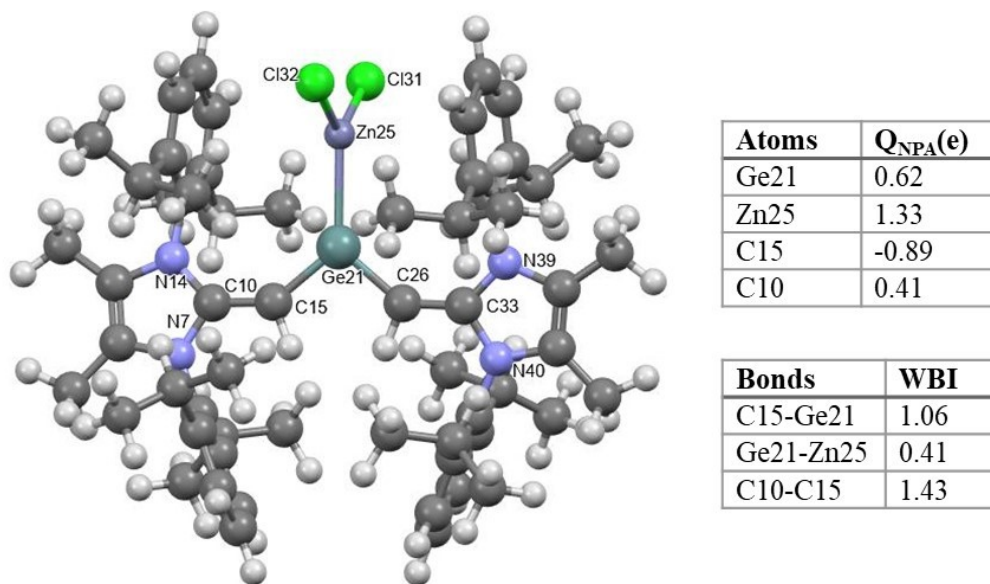
Figure 5.13. Optimized structure, natural charges (Q_{NPA}), and Wiberg bond indices (WBI) derived from natural bonding orbital (NBO) analysis of (^{Me}IPrCH)$_2$Ge•ZnCl$_2$ (**2**).

Atoms	$Q_{NPA}(e)$
Sn32	1.09
Sn33	1.09
Cl39	-0.56
C24	-1.17
C40	-1.17

Bonds	WBI
C24-Sn32	0.48
C24-Sn33	0.51
Sn32-Sn33	0.05
Sn32-Cl39	0.35
Sn33-Cl39	0.35
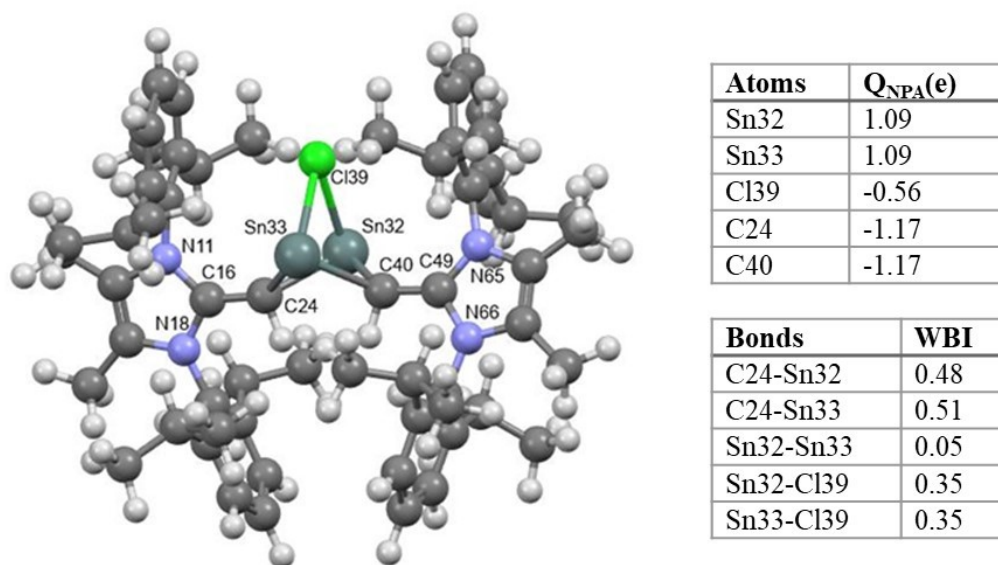
Figure 5.14. Optimized structure, natural charges (Q_{NPA}), and Wiberg bond indices (WBI) derived from natural bonding orbital (NBO) analysis of $[(^{Me}IPrCHSn)_2(\mu–Cl)]^+$ [**4$^+$**].

Atoms	$Q_{NPA}(e)$
C7	-0.80
B3	1.00
O1	-0.69
O6	-0.68

Bonds	WBI
C7-C11	1.45
C11-B3	1.14
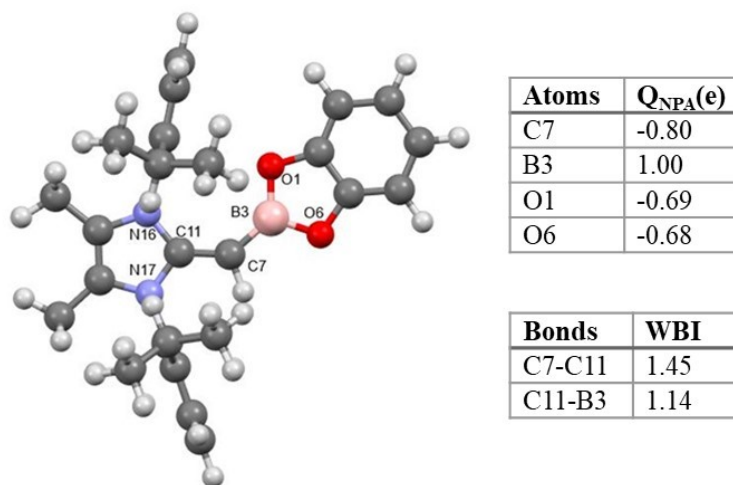
Figure 5.15. Optimized structure, natural charges (Q_{NPA}), and Wiberg bond indices (WBI) derived from natural bonding orbital (NBO) analysis of $(^{Me}IPrCH)Bcat$ (**6**).

Atoms	$Q_{NPA}(e)$
C6	-0.77
B13	0.44
H25	-0.08

Bonds	WBI
C2-C6	1.39
C6-B13	1.23
B13-H25	0.94
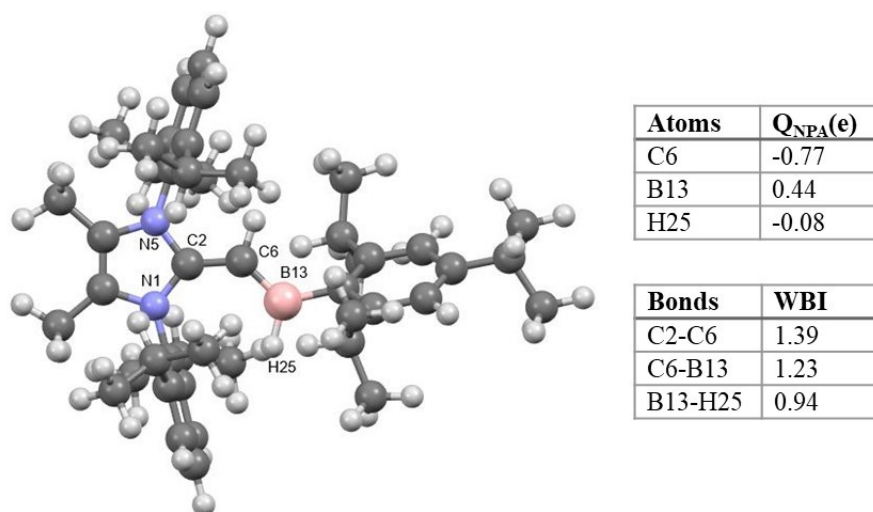
Figure 5.16. Optimized structure, natural charges (Q_{NPA}), and Wiberg bond indices (WBI) derived from natural bonding orbital (NBO) analysis of (^{Me}IPrCH)B(Trip)H (**8**).

Atoms	$Q_{NPA}(e)$
O2	-0.89
S1	2.31
B6	0.69
C10	-0.61
H56	-0.07

Bonds	WBI
C10-C11	1.02
O1-S2	0.83
O2-B6	0.65
B6-C10	0.82
B6-H56	0.95
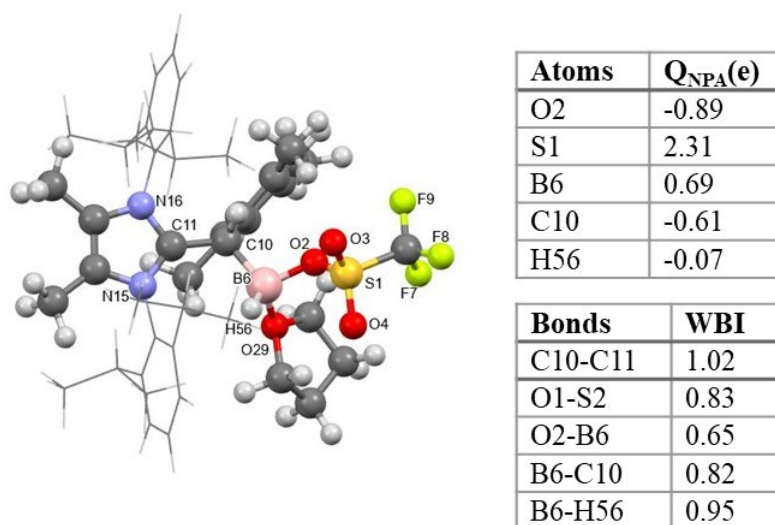
Figure 5.17. Optimized structure, natural charges (Q_{NPA}), and Wiberg bond indices (WBI) derived from natural bonding orbital (NBO) analysis of [(^{Me}IPrCHMes)B(THF)(OTf)H]$^+$ [**10**$^+$]; Dipp groups shown as wireframes for clarity.

5.4.4. Synthetic Procedures

Synthesis of (^{Me}IPrCH)$_2$Zn (1). (^{Me}IPrCH)Li (0.1015 g, 0.2325 mmol) in 8 mL of Et$_2$O was added dropwise to a solution of ZnCl$_2$ (0.0158 g, 0.116 mmol) in 6 mL of THF and the mixture was stirred for one hour. The mixture was filtered through a pad of Celite and the volatiles were removed from the filtrate *in vacuo*, yielding (^{Me}IPrCH)$_2$Zn (**1**) as a yellow solid (0.0947 g, 88 %). X-ray quality crystals (yellow) were grown from a concentrated toluene at –30 °C. ^{1}H NMR (700 MHz, C$_6$D$_6$): δ = 7.38 (t, 2H, $^3J_{HH}$ = 7.7 Hz, Ar*H*), 7.29 (d, 4H, $^3J_{HH}$ = 7.6 Hz, Ar*H*), 7.02 (d, 4H, $^3J_{HH}$ = 7.7 Hz, Ar*H*), 6.89 (t, 2H, $^3J_{HH}$ = 7.7 Hz, Ar*H*), 3.22 (sept, 4H, $^3J_{HH}$ = 6.9 Hz, C*H*(CH$_3$)$_2$), 3.15 (sept, 4H, $^3J_{HH}$ = 6.9 Hz, C*H*(CH$_3$)$_2$), 1.59 (s, 6H, CN-C*H$_3$*), 1.54 (s, 6H, CN-C*H$_3$*), 1.43 (d, 12H, $^3J_{HH}$ = 6.9 Hz, CH(C*H$_3$*)$_2$), 1.35 (d, 12H, $^3J_{HH}$ = 6.9 Hz, CH(C*H$_3$*)$_2$), 1.27 (s, 2H, C=C*H*), 1.26 (d, 12H, $^3J_{HH}$ = 6.9 Hz, CH(C*H$_3$*)$_2$), 1.12 ppm (d, 12H, $^3J_{HH}$ = 6.9 Hz, CH(C*H$_3$*)$_2$); ^{13}C{^{1}H} NMR (176 MHz, C$_6$D$_6$): δ = 9.9 (NC-*C*H$_3$), 10.0 (NC-*C*H$_3$), 24.0 (CH(*C*H$_3$)$_2$), 24.3 (CH(*C*H$_3$)$_2$), 24.9 (CH(*C*H$_3$)$_2$), 25.3 (CH(*C*H$_3$)$_2$), 28.6 (*C*H(CH$_3$)$_2$), 28.9 (*C*H(CH$_3$)$_2$), 57.6 (C=*C*H), 115.2 (Ar*C*), 116.0 (Ar*C*), 124.0 (Ar*C*), 125.7 (Ar*C*), 128.7 (Ar*C*), 129.4 (Ar*C*), 134.2 (Ar*C*), 134.5 (Ar*C*), 149.0 (N*C*-CH$_3$), 150.0 (N*C*-CH$_3$), 158.1 ppm (*C*=CH); element. anal.: calcd. for C$_{60}$H$_{82}$ZnN$_4$: C, 77.93; H, 8.94; N, 5.87; found: C, 77.35; H, 8.91; N, 5.93 %; mp: 196 °C (dec.); UV-vis (toluene): λ_{max} = 328 nm (1.15 × 10^4 L mol^{-1} cm^{-1}).

One-pot synthesis of (^{Me}IPrCH)$_2$Zn (1) from ^{Me}IPr=CH(I). ^{n}BuLi (65 μL, 0.16 mmol, 2.5 M solution in hexanes) was added to a solution of ^{Me}IPr=CH(I) (0.0899 g, 0.162 mmol) in 3 mL of hexanes. The resulting red mixture was stirred for 20 min, to

which a solution of ZnCl$_2$ (0.0110 g, 0.0808 mmol) in 2 mL of THF was then added. The resulting yellow mixture was stirred for 20 min then the volatiles were removed *in vacuo*, followed by extraction of the product with 10 mL of toluene. The volatiles were removed from the filtrate *in vacuo* resulting in (^{Me}IPrCH)$_2$Zn (**1**) as a bright yellow solid (0.0738 g, 98 %). NMR data matches that reported in the above preparation.

Synthesis of (^{Me}IPrCH)$_2$Ge•ZnCl$_2$ (2). Cl$_2$Ge•dioxane (0.0301 g, 0.130 mmol) was stirred in 12 mL of toluene for 20 min (until dissolved) and then added dropwise over 3 min to (^{Me}IPrCH)$_2$Zn (**1**) (0.1200 g, 0.1297 mmol) in 6 mL of toluene. The resulting solution was stirred for 45 min and then filtered through a pad of Celite. The volatiles were removed from the filtrate *in vacuo* and the resulting solid was washed with three 5 mL portions of pentane. This remaining solid was dissolved in 1 mL of fluorobenzene and layered with 4 mL of pentane and stored at –35 °C for one day to yield a purple solid. The supernatant was decanted and the solid was dried under vacuum yielding (^{Me}IPrCH)$_2$Ge•ZnCl$_2$ (**2**) as a dark purple solid (0.0901 g, 66 %). X-ray quality crystals (deep purple) were grown from a concentrated fluorobenzene solution at –35 °C. ^{1}H NMR (400 MHz, C$_6$D$_6$): δ = 7.76 (t, 2H, $^3J_{HH}$ = 7.9 Hz, ArH), 7.62 (d, 4H, $^3J_{HH}$ = 7.7 Hz, ArH), 7.27 (t, 2H, $^3J_{HH}$ = 7.6 Hz, ArH), 7.05 (d, 4H, $^3J_{HH}$ = 7.2 Hz, ArH), 4.18 (s, 2H, C=CH), 2.81 (br, 4H, CH(CH$_3$)$_2$), 2.67 (br, 4H, CH(CH$_3$)$_2$), 1.58 (d, 12H, $^3J_{HH}$ = 6.7 Hz, CH(CH_3)$_2$), 1.36 (s, 6H, CN-CH_3), 1.10 (d, 24H, $^3J_{HH}$ = 6.9 Hz, CH(CH_3)$_2$), 1.02 ppm (d, 12H, $^3J_{HH}$ = 6.2 Hz, CH(CH_3)$_2$); compound **2**

decomposes over time in solution, thus making the recording of meaningful $^{13}C\{^1H\}$ NMR data not possible; element. anal.: calcd. for $C_{60}H_{82}ZnGeCl_2N_4$: C, 67.46; H, 7.74; N, 5.24; found: C, 67.43; H, 7.83; N, 4.78 %; mp: 250 °C (dec.); UV-vis (toluene): λ_{max} = 558 nm (8490 L mol^{-1} cm^{-1}), 368 nm (3310 L mol^{-1} cm^{-1}).

Synthesis of [(^{Me}IPrCHGe)$_2$(µ-Cl)][ZnCl$_3$(THF)] (3). Cl$_2$Ge•dioxane (0.0551 g, 0.239 mmol) was stirred in 12 mL of toluene for 20 min (until dissolved) and then added dropwise over 3 min to a solution of (^{Me}IPrCH)$_2$Zn (**1**) (0.103 g, 0.119 mmol) in 6 mL of toluene, and the mixture was stirred for another 2 h. The volatiles were then removed from the reaction mixture and 2 mL of THF was added, followed by stirring for 1 h. The volatiles were removed from the resulting solution *in vacuo* and the resulting solid was triturated with 2 mL of pentane and dried under vacuum to yield [(^{Me}IPrCHGe)$_2$(µ–Cl)][ZnCl$_3$(THF)] (**3**) (0.0632 g, 45 %) as a pale-yellow solid. X-ray quality crystals (pale-yellow) were grown from a concentrated THF solution that was layered with hexanes and stored at –35 °C for 1 day. ^1H NMR (400 MHz, CD$_2$Cl$_2$): δ = 7.47 (t, 4H, $^3J_{HH}$ = 7.8 Hz, Ar*H*), 7.22 (d, 8H, $^3J_{HH}$ = 7.8 Hz, Ar*H*), 3.78-3.87 (m, 4H, Zn-OC*H*$_2$CH$_2$), 2.55 (sept, 8H, $^3J_{HH}$ = 6.8 Hz, C*H*(CH$_3$)$_2$), 1.88 (s, 12H, NC-C*H*$_3$), 1.13 (d, 24H, $^3J_{HH}$ = 6.8 Hz, CH(C*H*$_3$)$_2$), 1.04 (d, 24H, $^3J_{HH}$ = 6.8 Hz, CH(C*H*$_3$)$_2$), 0.84-0.89 (m, 4H, Zn-OCH$_2$C*H*$_2$), 0.10 ppm (s, 2H, C=C*H*); $^{13}C\{^1H\}$ NMR (100 MHz, CD$_2$Cl$_2$): δ = 10.1 (NC-*C*H$_3$), 24.2 (CH(*C*H$_3$)$_2$), 24.4 (CH(*C*H$_3$)$_2$), 29.1 (*C*H(CH$_3$)$_2$), 50.7 (C=*C*H), 125.1 (Ar*C*), 125.6 (Ar*C*), 126.0 (Ar*C*), 129.3 (Ar*C*), 130.3 (Ar*C*), 131.4 (Ar*C*), 146.2 (N*C*-CH$_3$), 156.9 ppm (N*C*N); element. anal.: calcd.

for $C_{64}H_{90}Cl_4N_4OZn$: C, 59.87; H, 7.07 N, 4.36; found: C, 56.13; H, 6.69; N, 3.73 %; despite repeated attempts, analyses were consistently low in carbon content. mp: 210-212 °C.

Alternative synthesis of [(^{Me}IPrCHGe)$_2$(μ–Cl)][ZnCl$_3$(THF)] (3). Cl$_2$Ge•dioxane (0.0091 g, 0.039 mmol) in 5 mL of toluene was added dropwise to a solution of (^{Me}IPrCH)$_2$Ge•ZnCl$_2$ (**2**) (0.0382 g, 0.0357 mmol) in 10 mL of toluene. Volatiles were removed *in vacuo* and the resulting solid was washed with 4 mL of hexanes. The remaining solid dissolved in 2 mL of THF then precipitated by the addition of 10 mL of hexanes. The mother liquor was decanted and the remaining solid dried *in vacuo* to yield [(^{Me}IPrCHGe)$_2$(μ–Cl)][ZnCl$_3$(THF)] (**3**) as a yellow solid (0.0301 g, 80 %). NMR data matches that reported in the above preparation.

Synthesis of [(^{Me}IPrCHSn)$_2$(μ–Cl)]$_2$[Zn$_2$Cl$_6$] (4). Cl$_2$Sn•dioxane complex (30.6 mg, 0.112 mmol) was stirred in 12 mL of toluene for 20 min (until dissolved) and then added dropwise over 3 min to a solution of (^{Me}IPrCH)$_2$Zn (**1**) (52.0 mg, 0.0562 mmol) in 6 mL of toluene. The resulting mixture was stirred for 30 min then the solid was collected on a piece of glass fiber filter paper via filtration. The solid was dissolved in 15 mL of fluorobenzene, concentrated to a final volume of *ca.* 0.5 mL, and stored at –35 °C for 4 h to give [(^{Me}IPrCHSn)$_2$(μ–Cl)]$_2$[Zn$_2$Cl$_6$] (**4**) (49.9 mg, 34 %) as pale-yellow crystals, which were isolated and dried. ^{1}H NMR (700 MHz, CH$_2$Cl$_2$-d$_2$): δ = 7.49 (t, 4H, $^3J_{HH}$ = 7.4 Hz, Ar*H*), 7.24 (d, 8H, $^3J_{HH}$ = 7.8 Hz, Ar*H*), 2.60 (sept, 8H, $^3J_{HH}$ = 6.8 Hz, C*H*(CH$_3$)$_2$), 1.87 (s, 12H, NC-C*H*$_3$), 1.14 (d, 24H, $^3J_{HH}$ = 7.4 Hz, CH(C*H*$_3$)$_2$), 1.00 (d, 24H, $^3J_{HH}$ = 7.4 Hz, CH(C*H*$_3$)$_2$), -0.17 ppm (s, 2H, C=C*H*);

$^{13}C\{^1H\}$ NMR (176 MHz, C_6D_6): δ = 10.3 (NC-CH_3), 24.5 (CH($CH_3)_2$), 24.6 (CH($CH_3)_2$), 29.1 ($CH(CH_3)_2$), 54.4 (CH-Sn), 115.6 (ArC) 124.1 (ArC), 125.8 (ArC), 126.2 (ArC), 130.5 (ArC), 131.4 (ArC), 146.5 (NC-CH$_3$), 158.5 ppm (NCN); element. anal.: calcd. for $C_{120}H_{164}Cl_8N_8Sn_4Zn_2$: C, 55.27; H, 6.34; N, 4.30; found: C, 53.16; H, 6.46; N, 3.92 %; despite repeated attempts, analyses were consistently low in carbon content; mp: 192 °C (dec.).

Synthesis of (^{Me}IPrCH)PPh$_2$ (5). A solution of ClPPh$_2$ (23.3 mg, 0.106 mmol) in 1 mL of toluene was added to a solution of (^{Me}IPrCH)$_2$Zn (**1**) (46.5 mg, 0.0502 mmol) in 5 mL of toluene and the mixture was stirred for 3 h. Then the resulting mixture was filtered through a pad of Celite and the volatiles removed from the filtrate *in vacuo* to give (^{Me}IPrCH)PPh$_2$ (**5**) as a white solid (39.6 mg, 64 %); this product contained *ca.* 3 % of Ph$_2$P-PPh$_2$ as a by-product, thus obtaining satisfactory elemental analyses was not possible. ^1H NMR (700 MHz, C_6D_6): δ = 7.36-7.40 (m, 2H, PhH), 7.30-7.36 (m, 4H, PhH), 7.20-7.26 (m, 2H, PhH), 7.18 (d, 2H, $^3J_{HH}$ = 6.1 Hz, ArH), 6.97-7.03 (m, 4H, ArH), 6.92-6.96 (m, 2H, PhH), 3.26 (d, 1H, $^2J_{HP}$ = 6.0 Hz, C=CH), 3.23 (sept, 2H, $^3J_{HH}$ = 6.8 Hz, CH(CH$_3)_2$), 3.18 (sept, 2H, $^3J_{HH}$ = 6.8 Hz, CH(CH$_3)_2$), 1.52 (d, 6H, $^3J_{HH}$ = 10.6 Hz, CH(C$H_3)_2$), 1.35 (d, 6H, $^3J_{HH}$ = 6.9 Hz, CH(C$H_3)_2$), 1.16 (d, 6H, $^3J_{HH}$ = 6.9 Hz, CH(C$H_3)_2$), 1.15 (s, 6H, NC-CH_3), 1.12 ppm (d, 6H, $^3J_{HH}$ = 6.9 Hz, CH(C$H_3)_2$); $^{13}C\{^1H\}$ NMR (175 MHz, C_6D_6): δ = 9.5 (NC-CH_3), 9.8 (NC-CH_3), 23.7 (CH($CH_3)_2$), 23.7 (CH($CH_3)_2$), 24.1 (CH($CH_3)_2$), 24.2 (CH($CH_3)_2$), 24.5 (CH($CH_3)_2$), 29.0 (CH(CH$_3)_2$), 51.7 (C=CH), 117.5 (NC-CH$_3$), 118.0 (NC-CH$_3$), 124.6 (d, J_{CP} =

25.8 Hz, PhC), 126.7 (ArC), 127.7 (d, J_{CP} = 6.0 Hz, ArC), 128.4 (ArC), 129.8 (d, J_{CP} = 40.5 Hz, PhC), 132.5 (ArC), 132.6 (ArC), 132.8 (ArC), 135.0 (d, J_{CP} = 3.9 Hz, PhC), 146.6 (d, J_{CP} = 12.5 Hz, PhC), 148.2 (NCN), 148.9 (ArC), 154.3 ppm (d, J_{CP} = 37.7 Hz, PhC); ^{31}P{^{1}H} NMR (162 MHz, C$_6$D$_6$): δ = -31.4 ppm (s); mp: 125-127 °C.

Synthesis of (^{Me}IPrCH)Bcat (6). HBcat (25.4 mg, 0.106 mmol) in 2 mL of toluene was added dropwise to a solution of (^{Me}IPrCH)$_2$Zn (**1**) (97.8 mg, 0.106 mmol) in 2 mL of toluene and stirred for 4 h. The resulting mixture was filtered through a pad of Celite, and the volatiles removed from the filtrate *in vacuo* yielding (^{Me}IPrCH)Bcat (**6**) as a white solid (89.4 mg, 77 %). Colorless X-ray quality crystals were grown from a saturated toluene solution over the course of 5 days at –35 °C. ^{1}H NMR (700 MHz, C$_6$D$_6$): δ = 7.44 (t, 1H, $^{3}J_{HH}$ = 7.7 Hz, ArH), 7.22-7.26 (m, 1H, ArH), 7.21 (d, 2H, $^{3}J_{HH}$ = 7.7 Hz, ArH), 7.11-7.13 (m, 2H, ArH), 6.71-6.74 (m, 4H, Bcat), 3.03-3.11 (m, 2H, CH(CH$_3$)$_2$), 3.04 (s, 1H, C=CH), 2.94-3.00 (m, 2H, CH(CH$_3$)$_2$), 1.52 (s, 3H, NC-CH_3), 1.49 (s, 3H, NC-CH_3), 1.32 (d, 6H, $^{3}J_{HH}$ = 7.7 Hz, CH(CH_3)$_2$), 1.24 (d, 6H, $^{3}J_{HH}$ = 6.7 Hz, CH(CH_3)$_2$), 1.18 (d, 6H, $^{3}J_{HH}$ = 7.0 Hz, CH(CH_3)$_2$), 1.13 ppm (d, 6H, $^{3}J_{HH}$ = 7.0 Hz, CH(CH_3)$_2$); ^{13}C{^{1}H} NMR (176 MHz, C$_6$D$_6$): δ = 9.4 (NC-CH$_3$), 9.5 (NC-CH$_3$), 23.7 (CH(CH$_3$)$_2$), 23.8 (CH(CH$_3$)$_2$), 24.4 (CH(CH$_3$)$_2$), 24.7 (CH(CH$_3$)$_2$), 29.0 (CH(CH$_3$)$_2$), 29.1 (CH(CH$_3$)$_2$), 45.4 (C=CH), 110.6 (ArC in Bcat), 120.7 (ArC in Bcat), 124.1 (ArC), 124.7 (ArC), 128.8 (ArC), 129.6 (ArC), 130.1 (ArC), 148.4 (ArC), 150.3 (ArC in Bcat), 156.2 ppm (NCN); ^{11}B NMR (128 MHz, C$_6$D$_6$): δ = 31.0

ppm (s); element. anal.: calcd. for $C_{36}H_{45}BN_2O_2$: C, 78.82; H, 8.27; N, 5.11; found: C, 78.41; H, 8.27; N, 4.97 %; mp: 230 °C (dec.).

Modified Synthesis of MesB(OMe)$_2$. Magnesium turnings (3.28 g, 0.135 mol) and a single crystal of I_2 were placed into a 250 mL Schlenk flask with 20 mL of THF, and then a solution of MesBr (15.52 g, 0.07795 mol) in 50 mL of THF was added dropwise over 20 minutes. The mixture was stirred for 6 h and then filtered using a glass fiber filter-tipped cannula. The resulting Grignard reagent was added dropwise to B(OMe)$_3$ (25.07 g, 0.2413 mol) in 30 mL of Et$_2$O at –78 °C, allowed to warm to room temperature and stirred for 16 h. Then 100 mL of hexanes was added, the mixture filtered with a glass fiber filter-tipped cannula, and the volatiles removed from the filtrate *in vacuo* to yield MesB(OMe)$_2$ as a colorless oil (6.2778 g, 61 %). ^{1}H NMR (500 MHz, C$_6$D$_6$): δ = 6.75 (s, 2H, Ar*H*), 3.45 (s, 6H, OC*H*$_3$), 2.25 (s, 6H, *o*-C*H*$_3$ in Mes), 2.16 ppm (s, 3H, *p*-C*H*$_3$ in Mes); ^{11}B{^{1}H} (128 MHz, C$_6$D$_6$): δ = 31.4 ppm (s).

Modified Synthesis of MesBH$_2$. Li[AlH$_4$] (16.7 mL, 1.0 M solution in Et$_2$O, 17 mmol) was added dropwise to a solution of MesB(OMe)$_2$ (3.044 g, 15.84 mmol) in 60 mL of Et$_2$O at –78 °C. The resulting mixture was allowed to warm to room temperature and stirred for 16 h. The resulting mixture was filtered with a glass fiber filter-tipped cannula and the filtrate cooled to –78 °C. Then HCl (4.0 mL, 4.0 M

solution in 1,4-dioxane, 16 mmol) was added dropwise to the filtrate and the mixture stirred for 16 h. The reaction mixture was then filtered with a glass fiber filter-tipped cannula, the volatiles removed from the filtrate *in vacuo*, and the resulting solid extracted into 10 mL of toluene. The volatiles were removed from the resulting toluene solution *in vacuo* to give MesBH$_2$ (0.6490 g, 31 %) as a white solid. ^{1}H NMR (500 MHz, C$_6$D$_6$): δ = 7.00 (s, 2H, ArH), 4.25 (s, br, 2H, BH_2), 2.60 (s, 6H, *o*-CH_3 in Mes), 2.30 ppm (s, 3H, *p*-CH_3 in Mes); ^{11}B{^{1}H} (128 MHz, C$_6$D$_6$): δ = 24.9 ppm (s).

Synthesis of (^{Me}IPrCH)B(Mes)H (7). MesBH$_2$ (37.9 mg, 0.276 mmol) in 3 mL of toluene was added dropwise to a solution of (^{Me}IPrCH)$_2$Zn (**1**) (127.4 mg, 0.1378 mol) in 5 mL of toluene. The reaction mixture was allowed to stir for 18 h, then the mixture was filtered through a pad of Celite and the volatiles removed from the filtrate *in vacuo*, yielding (^{Me}IPrCH)B(Mes)H (**7**) as a pure white solid (0.1396 g, 90 %). The resulting solid was dissolved in 0.5 mL toluene and stored at –35 °C, leading to the formation of colorless X-ray quality crystals after 3 days. ^{1}H NMR (400 MHz, C$_6$D$_6$): δ = 7.25 (t, 2H, $^3J_{HH}$ = 7.7 Hz, ArH), 7.13 (d, 4H, $^3J_{HH}$ = 7.7 Hz, ArH), 6.74 (s, 2H, ArH in Mes), 5.08 (s, 1H, BH), 4.29 (d, 1H, $^3J_{HH}$ = 10.7 Hz, C=CH), 2.99 (sept, 4H, $^3J_{HH}$ = 7.2 Hz, CH(CH$_3$)$_2$), 2.35 (s, 6H, *o*-CH_3 in Mes), 2.17 (s, 3H, *p*-CH_3 in Mes), 1.49 (s, 6H, NC-CH_3), 1.36 (d, 12H, $^3J_{HH}$ = 6.8 Hz, CH(CH_3)$_2$), 1.13 ppm (s, 12H, $^3J_{HH}$ = 6.8 Hz, CH(CH_3)$_2$); ^{13}C{^{1}H} NMR (176 MHz, C$_6$D$_6$): δ = 9.3 (NC-CH$_3$), 21.3 (*p*-CH$_3$ in Mes), 23.7 (CH(CH$_3$)$_2$), 23.8 (*o*-CH$_3$ in Mes), 24.3 (CH(CH$_3$)$_2$), 29.0 (CH(CH$_3$)$_2$), 84.0 (C=CH), 119.4 (ArC), 124.7 (ArC), 127.4 (ArC), 128.3 (ArC),

129.3 (ArC), 130.0 (ArC), 134.2 (ArC), 139.1 (ArC), 147.2 (NC-CH$_3$), 156.2 ppm (NCN); ^{11}B{^{1}H} NMR (128 MHz, C$_6$D$_6$): δ = 46.8 ppm (s); element. anal.: calcd. for C$_{39}$H$_{53}$BN$_2$: C, 83.55; H, 9.53; N, 5.00; found: C, 82.88; H, 9.48; N, 4.92 %; mp: 120 °C (dec.).

Alternate Synthesis of TripBpin. ^{n}BuLi (6.2 mL, 2.5 M solution in hexanes, 17 mmol) was added dropwise to a solution of TripBr (4.262 g, 15.05 mmol) in 50 mL of THF at –78 °C. The resulting mixture was stirred for 2 h at –78 °C, followed by the dropwise addition of ^{i}PrOBpin (3.079 g, 16.55 mmol) to the mixture at –78 °C and stirred overnight. The reaction mixture was quenched with 20 mL of brine followed by the addition of 20 mL of Et$_2$O. The organic fraction was separated and washed with 20 mL of water. Then the organic layer was collected, dried over MgSO$_4$, filtered then the volatiles removed on a rotovap. The resulting solid was dissolved in 5 mL of hexanes and stored for 16 h at –35 °C. TripBpin was then collected as a white microcrystalline solid and dried (4.324 g, 87 %). ^{1}H NMR (500 MHz, C$_6$D$_6$): δ = 7.12 (s, 2H, ArH), 3.28 (sept, 2H, $^3J_{HH}$ = 7.0 Hz, o-CH(CH$_3$)$_2$ in Trip), 2.83 (sept, 1H, $^3J_{HH}$ = 7.0 Hz, p-CH(CH$_3$)$_2$ in Trip), 1.37 (d, 12H, $^3J_{HH}$ = 7.0 Hz, o-CH(CH_3)$_2$ in Trip), 1.26 (d, 6H, $^3J_{HH}$ = 7.0 Hz, p-CH(CH_3)$_2$ in Trip), 1.19 ppm (s, 12H, OC-CH_3); ^{13}C{^{1}H} (124 MHz, C$_6$D$_6$): δ = 24.0 (p-CH(CH$_3$)$_2$ in Trip), 24.4 (OC(CH$_3$)$_2$), 24.7 (o-CH(CH$_3$)$_2$ in Trip), 34.2 (o-CH(CH$_3$)$_2$ in Trip), 34.7 (p-CH(CH$_3$)$_2$ in Trip), 83.2 OC(CH$_3$)$_2$), 119.6 (ArC), 149.7 (ArC), 152.3 ppm (ArC); ^{11}B{^{1}H} (159 MHz, C$_6$D$_6$): δ = 33.0 ppm (s).

Modified Synthesis of TripBH₂. Li[AlH₄] (4.2 mL, 1.0 M solution in Et₂O, 4.2 mmol) was added dropwise to a solution of TripBpin (1.2574 g, 3.8066 mmol) in 60 mL of Et₂O at –78 °C, and the mixture was stirred for 16 h. The mixture was then filtered with a glass fiber filter-tipped cannula, and the resulting filtrate was cooled to –78 °C. HCl (0.95 mL, 4.0 M solution in 1,4-dioxane, 3.8 mmol) was added dropwise to the filtrate. The mixture was allowed to warm to room temperature and stirred for 18 h. The mixture was filtered with a glass fiber filter-tipped cannula, the volatiles removed from the filtrate *in vacuo*, and the resulted solid was extracted with 15 mL of toluene. The volatiles were removed from the resulting solution *in vacuo* yielding TripBH₂ as a spectroscopically pure white solid (0.700 g, 85 %). ^{1}H NMR (500 MHz, C₆D₆): δ = 7.18 (s, 2H, Ar*H*), 5.33 (br, 2H, B*H₂*), 3.14 (sept, 2H, $^3J_{HH}$ = 6.9 Hz, *o*-C*H*(CH₃)₂ in Trip), 2.87 (sept, 1H, $^3J_{HH}$ = 6.9 Hz, *p*-C*H*(CH₃)₂ in Trip), 1.33 (d, 12H, $^3J_{HH}$ = 6.8 Hz, *o*-CH(C*H₃*)₂ in Trip), 1.29 ppm (d, 6H, $^3J_{HH}$ = 6.8 Hz, *p*-CH(C*H₃*)₂ in Trip); ^{11}B{^{1}H} (159 MHz, C₆D₆): δ = 31.2 ppm (s).

Synthesis of (ᴹᵉIPrCH)B(Trip)H (8). A solution of TripBH₂ (0.0518 g, 0.239 mmol) in 3 of mL toluene was added dropwise to a solution of (ᴹᵉIPrCH)₂Zn (**1**) (0.1005 g, 0.1087 mol) in 5 mL of toluene. The reaction mixture was allowed to stir for 18 h, after which the mixture was filtered through a pad of Celite and the volatiles removed from the filtrate *in vacuo*, yielding (ᴹᵉIPrCH)B(Trip)H (**8**) as a white solid (0.1194 g, 85 %). This sample was dissolved in 0.5 mL of toluene and storing the solution at –35 °C gave colorless X-ray quality crystals of **8** after 4 days. ^{1}H NMR (700 MHz, C₆D₆):

δ = 7.25 (t, 2H, $^3J_{HH}$ = 7.7 Hz, ArH), 7.13 (d, 4H, $^3J_{HH}$ = 7.8 Hz, ArH), 7.03 (s, 2H, ArH in Trip), 5.16 (br, 1H, BH), 4.22 (d, 1H, $^3J_{HH}$ = 10.9 Hz, C=CH), 3.28 (sept, 2H, $^3J_{HH}$ = 6.8 Hz, o-CH(CH$_3$)$_2$ in Trip), 2.98 (sept, 4H, $^3J_{HH}$ = 6.9 Hz, CH(CH$_3$)$_2$), 2.86 (sept, 1H, $^3J_{HH}$ = 6.9 Hz, p-CH(CH$_3$)$_2$ in Trip), 1.50 (s, 6H, NC-CH_3), 1.34 (d, 12H, $^3J_{HH}$ = 6.9 Hz, CH(CH_3)$_2$), 1.29 (d, 6H, $^3J_{HH}$ = 6.9 Hz, CH(CH_3)$_2$), 1.19 (d, 12H, $^3J_{HH}$ = 6.9 Hz, CH(CH$_3$)$_2$), 1.13 ppm (d, 12H, $^3J_{HH}$ = 6.9 Hz, $^3J_{HH}$ = 6.9 Hz, CH(CH_3)$_2$); ^{13}C{^{1}H} NMR (175 MHz, C$_6$D$_6$): δ = 9.4 (NC-CH$_3$), 23.6 (CH(CH$_3$)$_2$), 24.0 (CH(CH$_3$)$_2$), 24.7 (CH(CH$_3$)$_2$), 25.0 (CH(CH$_3$)$_2$), 29.0 (CH(CH$_3$)$_2$, 33.2 (CH(CH$_3$)$_2$), 35.0 (CH(CH$_3$)$_2$), 83.6 (C=CH), 146.1 (ArC), 147.1 (ArC), 149.9 (NC-CH$_3$), 155.8 ppm (NCN); ^{11}B{^{1}H} NMR (128 MHz, C$_6$D$_6$): δ = 47.1 ppm (s); element. anal.: calcd. for C$_{45}$H$_{65}$BN$_2$: C, 83.82; H, 10.16; N, 4.34; found: C, 83.15; H, 10.21; N, 4.34 %; mp: 179 °C (dec.).

Synthesis of [^{Me}IPrCH(BH$_2$)$_2$(μ–H)] (9). A solution of H$_3$B•SMe$_2$ (2.0 M solution in THF, 70 μL, 0.14 mmol) in 2 mL toluene was added dropwise to a solution of (^{Me}IPrCH)$_2$Zn (**1**) (0.0292 g, 0.0316 mmol). The reaction mixture was allowed to stir for 16 h, after which the mixture was filtered through Celite and the volatiles were removed from the filtrate *in vacuo*. The resulting solid was washed with 3 mL of hexanes and dried under high vacuum, yielding [^{Me}IPrCH(BH$_2$)$_2$(μ–H)] (**9**) as a white solid (0.0175 g, 61 %). ^{1}H NMR and ^{11}B NMR spectra match previously reported literature values (see Chapter 2).[29]

Synthesis of [(^{Me}IPrCHMes)B(THF)(OTf)H][OTf] (10). A solution of [Ph₃C]OTf (86.2 mg, 0.210 mmol) in 5 mL of toluene was added dropwise to solution of (^{Me}IPrCH)B(Mes)H (**7**) (59.0 mg, 0.105 mmol) in 3 mL of toluene. The reaction mixture was stirred for 1 h. The resulting white precipitate was collected via filtration and was then redissolved in 2 mL of THF. The resulting solution was concentrated under vacuum to a final volume of *ca.* 0.5 mL, then carefully layered with 0.3 mL of hexanes and stored at –5 °C for 3 days, resulting in the formation of X-ray quality crystals of [(^{Me}IPrCHMes)B(THF)(OTf)H][OTf] (**10**) (*ca.* 5 mg). Compound **10** could not be isolated in pure form as a bulk material.

Synthesis of [^{Me}IPrCH(AlⁱBu₂)₂(μ–H)] (11). Diisobutylaluminium hydride (0.422 mL, 1.0 M solution in hexanes, 0.42 mmol) was added dropwise to a stirring solution of (^{Me}IPrCH)₂Zn (**1**) (0.0931 g, 0.101 mmol) in 5 mL of toluene. The reaction mixture was allowed to stir for 14 h, after which the mixture was filtered through a pad of Celite and the volatiles were removed from the filtrate *in vacuo*. The resulting white solid was redissolved in 0.5 mL of toluene and the solution was stored at –35 °C, affording colorless X-ray quality crystals of **11** after 24 h. The supernatant was then removed/discarded, the crystals dissolved in 3 mL of toluene, and the resulting solution was filtered through a pad of Celite to remove a small amount of grey powder that appeared during crystallization. Removal of volatiles *in vacuo* resulted in [^{Me}IPrCH(AlⁱBu₂)₂(μ–H)] (**11**) as a white solid (53.6 mg, 78 %). ^{1}H NMR (700 MHz, C₆D₆): δ = 7.26 (t, 2H, $^3J_{HH}$ = 7.8 Hz, Ar*H*), 7.14 (d, 4H, $^3J_{HH}$ = 7.8 Hz, Ar*H*), 3.73 (s,

1H, C=C*H*), 2.75 (sept, 4H, $^3J_{HH}$ = 6.3 Hz, C*H*(CH$_3$)$_2$), 2.03-2.08 (m, 2H, AlCH$_2$C*H*(CH$_3$)$_2$), 1.90-1.96 (m, 2H, AlCH$_2$C*H*(CH$_3$)$_2$), 1.43 (d, 12H, $^3J_{HH}$ = 6.8 Hz, CH(C*H*$_3$)$_2$), 1.24 (s, 6H, NC-C*H*$_3$), 1.21 (d, 6H, $^3J_{HH}$ = 6.5 Hz, CH(C*H*$_3$)$_2$), 1.19 (d, 12H, $^3J_{HH}$ = 7.8 Hz, CH(C*H*$_3$)$_2$), 1.13 (d, 6H, $^3J_{HH}$ = 7.8 Hz, CH(C*H*$_3$)$_2$), 0.97 (d, 12H, $^3J_{HH}$ = 6.9 Hz, CH(C*H*$_3$)$_2$), 0.06 (d, 1H, $^3J_{HH}$ = 7.5 Hz, AlC*H*$_2$), 0.04 (d, 1H, $^3J_{HH}$ = 7.5 Hz, AlC*H*$_2$), -0.23 (d, 1H, $^3J_{HH}$ = 6.4 Hz, AlC*H*$_2$), -0.25 (d, 1H, $^3J_{HH}$ = 6.4 Hz, AlC*H*$_2$), -0.28 (d, 1H, $^3J_{HH}$ = 8.5 Hz, AlC*H*$_2$), -0.30 (d, 1H, $^3J_{HH}$ = 8.4 Hz, AlC*H*$_2$), -0.45 (d, 1H, $^3J_{HH}$ = 5.2 Hz, AlC*H*$_2$), -0.47 ppm (d, 1H, $^3J_{HH}$ = 5.3 Hz, AlC*H*$_2$); the Al-*H*-Al resonance could not be located; ^{13}C{^{1}H} NMR (175 MHz, C$_6$D$_6$): δ = 10.2 (NC-*C*H$_3$), 21.2 (Al-*C*H$_2$), 22.3 (Al-*C*H$_2$), 24.0 (CH(*C*H$_3$)$_2$), 24.2 (Al-*C*H$_2$), 24.7 (CH(*C*H$_3$)$_2$), 25.0 (Al-*C*H$_2$), 27.2 (CH(*C*H$_3$)$_2$), 27.3 (*C*H(CH$_3$)$_2$), 27.9 (*C*H(CH$_3$)$_2$), 28.5 (CH(*C*H$_3$)$_2$), 28.8 (CH(*C*H$_3$)$_2$), 29.1 (CH(*C*H$_3$)$_2$), 29.2 (CH(*C*H$_3$)$_2$), 125.4 (Ar*C*), 128.0 (Ar*C*), 128.4 (Ar*C*), 130.8 (Ar*C*), 146.8 (N*C*-CH$_3$), 164.0 ppm (N*C*N); element. anal.: calcd. for C$_{46}$H$_{78}$Al$_2$N$_2$: C, 77.37; H, 11.15; N, 3.92; found: C, 77.04; H, 10.95; N, 3.91 %; mp: 250 °C (dec.).

5.5. Crystallographic Data

Table 5.1. Crystallographic data for compounds **1**, **2**, and **3**.

Compound	1	2	3
formula	$C_{67}H_{90}N_4Zn$	$C_{81}H_{99.50}Cl_2F_{3.50}Ge$ N_4Zn	$C_{72}H_{106}Cl_4Ge_2N_4$ O_3Zn
formula weight	1016.79	1404.50	1427.95
crystal system	triclinic	triclinic	orthorhombic
Space Group	$P\bar{1}$	$P\bar{1}$	*Pbca*
a (Å)	11.9990(3)	13.0508(4)	25.8334(11)
b (Å)	12.4435(3)	23.2655(7)	20.7639(8)
c (Å)	12.7158(3)	25.1507(8)	27.4666(11)
α (deg)	76.5311(12)	91.857(2)	--
β (deg)	66.3582(13)	91.0760(18)	--
γ (deg)	61.3781(15)	97.9375(18)	--
V (Å^3)	1524.74(7)	7557.4(4)	14733.1(10)
Z	1	4	8
ρ_{calcd} (g cm^{-3})	1.107	1.234	1.288
Abs coeff (mm^{-1})	0.857	1.945	3.029
T (K)	173	173	173
$2\theta_{max}$ (°)	148.21	145.74	145.23
Total Data	5918	322143	666726
Unique data (R_{int})	5918 (0.0707)	28758 (0.1210)	14433 (0.0904)
Obs data [I>2(σ(I)]	5918	23168	12621
Params	335	1672	835
R_1 [I>2(σ(I)]^a	0.0431	0.0641	0.0505
wR$_2$ [all data]^a	0.1184	0.1871	0.1423
Max/min $\Delta\rho$ (e$^-$Å^{-3})	0.371/–0.284	1.268 /–0.812	1.191/–0.767

^{a} $R_1 = \Sigma||F_o| - |F_c||/\Sigma|F_o|$; $wR_2 = [\Sigma w(F_o^2 - F_c^2)^2/\Sigma w(F_o^4)]^{1/2}$

Table 5.2. Crystallographic data for compounds **4**, **6**, and **7**.

Compound	4	6	7
formula	$C_{150}H_{189}Cl_8F_5N_8Sn_4Zn_2$	$C_{43}H_{53}BN_2O_2$	$C_{39}H_{53}BN_2$
formula weight	3088.18	640.68	560.64
crystal system	triclinic	monoclinic	triclinic
Space Group	$P\bar{1}$	$P2_1/n$	$P\bar{1}$
a (Å)	19.6665(5)	14.2017(4)	10.7831(2)
b (Å)	21.1372(6)	19.6631(6)	11.9083(2)
c (Å)	23.9405(6)	14.4469(4)	15.1511(3)
α (deg)	108.6038(15)	--	79.9390(8)
β (deg)	96.4117(15)	108.4215(15)	74.5556(7)
γ (deg)	114.4712(16)	--	68.3866(8)
V (Å^3)	8234.6(4)	3827.56(19)	1737.04(6)
Z	2	4	2
ρ_{calcd} (g cm^{-3})	1.245	1.112	1.072
Abs coeff (mm^{-1})	6.664	0.512	0.452
T (K)	173	173	173
$2\theta_{max}$ (°)	145.02	144.72	148.13
Total Data	31021	135134	77538
Unique data (R_{int})	31021 (0.1210)	7563 (0.0588)	6762 (0.0288)
Obs data [I>2(σ(I)]	20456	6343	6266
Params	1564	564	388
R_1 [I>2(σ(I)][a]	0.0667	0.0475	0.0438
wR_2 [all data][a]	0.2003	0.1388	0.1222
Max/min $\Delta\rho$ (e$^-$Å^{-3})	2.288/–1.125	0.375 /–0.256	0.252/–0.213

[a] $R_1 = \Sigma||F_o| - |F_c||/\Sigma|F_o|$; $wR_2 = [\Sigma w(F_o^2 - F_c^2)^2/\Sigma w(F_o^4)]^{1/2}$

Table 5.3. Crystallographic data for compounds **8**, **10**, and **11**.

Compound	**8**	**10**	**11**
formula	$C_{45}H_{65}BN_2$	$C_{45}H_{61}BF_6N_2O_7S_2$	$C_{46}H_{78}Al_2N_2$
formula weight	644.80	930.88	713.06
crystal system	monoclinic	monoclinic	triclinic
Space Group	$P2_1/n$	$P2_1/n$	$P\bar{1}$
a (Å)	12.1730(3)	19.8311(5)	10.6829(3)
b (Å)	18.4268(4)	14.6751(3)	11.9351(3)
c (Å)	19.2075(4)	20.5531(5)	20.6326(5)
α (deg)	--	--	77.2635(10)
β (deg)	103.2431(11)	108.2896(13)	86.4989(11)
γ (deg)	--	--	64.9496(13)
V (Å^3)	4193.85(16)	5679.3(2)	2323.04(11)
Z	4	4	2
ρ_{calcd} (g cm^{-3})	1.021	1.089	1.019
Abs coeff (mm^{-1})	0427	1.375	0.772
T (K)	173	173	173
$2\theta_{max}$ (°)	144.98	144.86	148.35
Total Data	166151	181972	90572
Unique data (R_{int})	8284 (0.0461)	11219 (0.0933)	9049(0.0335)
Obs data [I>2(σ(I)]	7416	8448	8415
Params	440	577	557
R_1 [I>2(σ(I)][a]	0.0420	0.0693	0.0477
wR_2 [all data][a]	0.1156	0.2289	0.1369
Max/min Δρ (e$^-$Å^{-3})	2.262/–1.198	0.434 /–0.389	0.596/–0.650

[a] $R_1 = \Sigma||F_o| - |F_c||/\Sigma|F_o|$; $wR_2 = [\Sigma w(F_o^2 - F_c^2)^2/\Sigma w(F_o^4)]^{1/2}$

5.6 References

1. a) Frankland, E. *Q. J. Chem. Soc.* **1861**, *13*, 177-235. b) Seyferth, D. *Organometallics* **2001**, *20*, 2940-2955.

2. a) Martin, R.; Buchwald, S. L. *Acc. Chem. Res.* **2008**, *41*, 1461-1473. b) Suzuki, A. *Angew. Chem. Int. Ed.* **2011**, *50*, 6722-6737.

3. a) Haas, D.; Hammann, J. M.; Greiner, R.; Knochel, P. *ACS Catal.* **2016**, *6*, 1540-1552. b) Negishi, E.-i. *Angew. Chem. Int. Ed.* **2011**, *50*, 6738-6764.

4. Cordovilla, C.; Bartolomé, C.; Martínez-Ilarduya, J. M.; Espinet, P. *ACS Catal.* **2015**, *5*, 3040-3053.

5. a) Williams, V. C.; Piers, W. E.; Clegg, W.; Elsegood, M. R. J.; Collins, S.; Marder, T. B. *J. Am. Chem. Soc.* **1999**, *121*, 3244-3245. b) Sun, Y.; Piers, W. E.; Parvez, M. *Can. J. Chem.* **1998**, *76*, 513-517.

6. a) Overby, J. S.; Jayaratne, K. C.; Schoell, N. J.; Hanusa, T. P. *Organometallics* **1999**, *18*, 1663-1668. b) Esqueda, A. C.; Conejero, S.; Maya, C.; Carmona, E. *Organometallics* **2009**, *28*, 45-47. c) Lee, J.-D.; Han, W.-S.; Kim, T.-J.; Kim, S. H.; Kang, S. O. *Chem. Commun.* **2011**, *47*, 1018-1020. d) Gondzik, S.; Bläser, D.; Wölper, C.; Schulz, S. *Chem. Eur. J.* **2010**, *16*, 13599-13602. e) Freitag, K.; Gemel, C.; Jerabek, P.; Oppel, I. M.; Seidel, R. W.; Frenking, G.; Banh, H.; Dilchert, K.; Fischer, R. A. *Angew. Chem. Int. Ed.* **2015**, *54*, 4370-4374.

7. a) Wiegand, A.-K; Rit, A.; Okuda, J. *Coord. Chem Rev.* **2016**, *314*, 71-82. b) Lummis, P. A.; Momeni, M. R.; Lui, M. W.; McDonald, R.; Ferguson, M. J.; Miskolzie, M.; Brown, A.; Rivard, E. *Angew. Chem. Int. Ed.* **2014**, *53*, 9347-9351. c) Chambenahalli, R.; Andrews, A. P.; Ritter, F.; Okuda, J.; Venugopal, A. *Chem. Commun.* **2019**, *55*, 2054-2057.

8. a) For pioneering work in this field, see: Fagan, P. J.; Nugent, W. A.; Calabrese, J. C. *J. Am. Chem. Soc.* **1994**, *116*, 1880-1889. b) He, G.; Torres Delgado, W.; Shynkaruk, O.; Ferguson, M. J.; McDonald, R.; Rivard, E. *J. Am. Chem. Soc.* **2013**, *135*, 5360-5363. c) He, G.; Torres Delgado, W.; Schatz, D. J.; Merten, C.; Mohammadpour, A.; Mayr, L.; Ferguson, M. J.; McDonald, R.; Brown, A.; Shankar, K.; Rivard, E. *Angew. Chem. Int. Ed.* **2014**, *53*, 4587-4591. d) Parke, S. M.; Hupf, E.; Matharu, G. K.; de Aguiar, I.; Xu, L.; Yu, H.; Boone, M. P.; de Souza, G. L. C.; McDonald, R.; Ferguson, M. J.; He, G.; Brown, A.; Rivard, E. *Angew. Chem. Int. Ed.* **2018**, *57*, 14841-14846. e) Parke, S. M.; Tanaka, S.; Yu, H.; Hupf, E.; Ferguson, M. J.; Zhou, Y.; Naka, K.; Rivard, E. *Macromolecules* **2019**, *52*, 7477-7488. f) Rivard, E. *Chem. Rec.* **2020**, *20*, 640-648.

9. a) Roy, M. M. D.; Rivard, E. *Acc. Chem. Res.* **2017**, *50*, 2017-2025. For early examples of NHOs in coordination chemistry, see: b) Ponti, P. P.; Baldwin, J. C.; Kaska, W. C. *Inorg. Chem.* **1979**, *18*, 873-875. c) Kuhn, N.; Bohnen, H.; Kreutzberg, J.; Bläser, D.; Boese, R. *J. Chem. Soc., Chem. Commun.* **1993**, 1136-1137. d) Al-Rafia, S. M. I.; Malcolm, A. C.; Liew, S. K.; Ferguson, M. J.; McDonald, R.; Rivard, E. *Chem. Commun.* **2011**, *47*, 6987-6989. e) Huang, J.-S.; Lee, W.-H.; Shen, C.-T.;

Lin, Y.-F.; Liu, Y.-H.; Peng, S.-M.; Chiu, C.-W. *Inorg. Chem.* **2016**, *55*, 12427-12434. For the use of NHOs in organic chemistry, see: f) Naumann, S.; Thomas, A. W.; Dove, A. P. *Angew. Chem. Int. Ed.* **2015**, *54*, 9550-9554. g) Saptal, V. B.; Bhanage, B. M. *ChemSusChem* **2016**, *9*, 1980-1985. h) Kaya, U.; Tran, U. P. N.; Enders, D.; Ho, J.; Nguyen, T. V. *Org. Lett.* **2017**, *19*, 1398-1401. i) Schuldt, R.; Kästner, J.; Naumann, S. *J. Org. Chem.* **2019**, *84*, 2209-2218. j) Naumann, S. *Chem. Commun.* **2019**, *55*, 11658-11670. k) Eymann, L. Y. M.; Varava, P.; Shved, A. M.; Curchod, B. F. E.; Liu, Y. Z.; Planes, O. M.; Sienkiewicz, A.; Scopelliti, R.; Tirani, F. F.; Severin, K. *J. Am. Chem. Soc.* **2019**, *43*, 17112-17116.

10. Roy, M. M. D.; Baird, S. R.; Dornsiepen, E.; Paul, L. A.; Miao, L.; Ferguson, M. J.; Zhou, Y.; Siewert, I.; Rivard, E. *Chem. Eur. J.* **2021**, *27*, 8572-8579.

11. a) Kuhn, N.; Göhner, M.; Steimann, M. *Z. Anorg. Allg. Chem.* **2002**, *628*, 1108-1115. b) Al-Rafia, S. M. I.; Ferguson, M. J.; Rivard, E. *Inorg. Chem.* **2011**, *50*, 10543-10545. c) Ghadwal, R. S.; Reichmann, S. O.; Engelhardt, F.; Andrada, D. M.; Frenking, G. *Chem. Commun.* **2013**, *49*, 9440-9442. d) Hering-Junghans, C.; Andreiuk, P.; Ferguson, M. J.; McDonald, R.; Rivard, E. *Angew. Chem. Int. Ed.* **2017**, *56*, 6272-6275. e) Sharma, M. K.; Blomeyer, S.; Neumann, B.; Stammler, H.-G.; Ghadwal, R. S. *Chem. Eur. J.* **2019**, *25*, 8249-8253. f) Roy, M. M. D.; Ferguson, M. J.; McDonald, R.; Zhou, Y.; Rivard, E. *Chem. Sci.* **2019**, *10*, 6476-6481. g) Gupta, P.; Siewert, J.-E.; Wellnitz, T.; Fischer, M.; Baumann, W.; Beweries, T.; Hering-Junghans, C. *Dalton Trans.* **2021**, *50*, 1838-1844. For a backbone deprotonated

aNHO, see: h) Causero, A.; Elsen, H.; Pahl, J.; Harder, S. *Angew. Chem. Int. Ed.* **2017**, *56*, 6906-6910.

12. Chong, C. C.; Rao, B.; Ganguly, R.; Li, Y.; Kinjo, R. *Inorg. Chem.* **2017**, *56*, 8608-8614.

13. Powers, K.; Hering-Junghans, C.; McDonald, R.; Ferguson, M. J.; Rivard, E. *Polyhedron* **2016**, *108*, 8-14.

14. Singh, A. P.; Samuel, P. P.; Roesky, H. W.; Schwarzer, M. C.; Frenking, G.; Sidhu, N. S.; Dittrich, B. *J. Am. Chem. Soc.* **2013**, *135*, 7324-7329.

15. Bacsa, J.; Hanke, F.; Hindley, S.; Odedra, R.; Darling, G. R.; Jones, A. C.; Steiner, A. *Angew. Chem. Int. Ed.* **2011**, *50*, 11685-11687.

16. a) Sinhababu, S.; Yadav, D.; Karwasara, S.; Sharma, M. K.; Mukherjee, G.; Rajaraman, G.; Nagendran, S. *Angew. Chem. Int. Ed.* **2016**, *55*, 7742-7746. b) Sinhababu, S.; Sharma, M. K.; Mahawar, P.; Kaur, S.; Singh, V. K.; Paliwal, A.; Yadav, D.; Kashyap, H. K.; Nagendran, S. *Dalton Trans.* **2019**, *48*, 16366-16376. c) Rittinghaus, R. D.; Tremmel, J.; Růžička, A.; Conrads, C.; Albrecht, P.; Hoffmann, A.; Ksiazkiewicz, A. N.; Pich, A.; Jambor, R.; Herres-Pawlis, S. *Chem. Eur. J.* **2020**, *26*, 212-221. d) Yadav, S.; Kumar, R.; Raj, K. V.; Yadav, P.; Vanka, K.; Sen, S. S. *Chem. Asian. J.* **2020**, *15*, 3116-3121.

17. Erickson, J. D.; Riparetti, R. D.; Fettinger, J. C.; Power, P. P. *Organometallics* **2016**, *35*, 2124-2128.

18. Hupf, E.; Kaiser, F.; Lummis, P. A.; Roy, M. M. D.; McDonald, R.; Ferguson, M. J.; Kühn, F. E.; Rivard. E. *Inorg. Chem.* **2020**, *59*, 1592-1601.

19. Sita, L. R. *Acc. Chem. Res.* **1994**, *27*, 191-197.

20. a) Nied, D.; Breher, F. *Chem. Soc. Rev.* **2011**, *40*, 3455-3466. b) Nied, D.; Oña-Burgos, P.; Klopper. W.; Breher, F. *Organometallics* **2011**, *30*, 1419-1428.

21. Richards, A. F.; Brynda, M.; Power, P. P. *Organometallics* **2004**, *23*, 4009-4011.

22. Paisley, N. R.; Lui, M. W.; McDonald, R.; Ferguson, M.; Rivard, E. *Dalton Trans.* **2016**, *45*, 9860-9870.

23. The ability of anionic NHOs, such as the less hindered analogue [IPrCH]$^-$ to coordinate to two main group centers in a terminal fashion, *i.e.* to give [IPrCH(ER$_x$)$_2$] products, has been documented before in the Rivard Group: Lui, M. W.; Shynkaruk, O.; Oakley, M. S.; Sinelnikov, R.; McDonald, R.; Ferguson, M. J.; Meldrum, A.; Klobukowski, M.; Rivard, E. *Dalton Trans.* **2017**, *46*, 5946-5954.

24. Roy, M. M. D.; Omaña, A. A.; Wilson, A. S. S.; Hill, M. S.; Aldridge, S.; Rivard, E. *Chem. Rev.* **2021**, *121*, 12784-12965.

25. For selected examples of luminescence from "push-pull" boron-based compounds, see: a) He, J.; Rauch, F.; Friedrich, A.; Sieh, D.; Ribbeck, T.; Krummenacher, I.; Braunschweig, H.; Finze, M.; Marder, T. B. *Chem. Eur. J.* **2019**, *25*, 13777-13784. b) Chen, X.; Meng, G.; Liao, G.; Rauch, F.; He, J.; Friedrich, A.; Marder, T. B.; Wang, N.; Chen, P.; Wang, S.; Yin, X. *Chem. Eur. J.* **2021**, *27*, 6274-6282. c) Hudson, Z. M.;

Wang, S. *Acc. Chem. Res.* **2009**, *42*, 1584-1596. d) Baser-Kirazli, N.; Lalancette, R. A.; Jäkle, F. *Organometallics* **2021**, *40*, 520-528. e) Hatakeyama, T.; Shiren, K.; Nakajima, K.; Nomura, S.; Nakatsuka, S.; Kinoshita, K.; Ni, J.; Ono, Y.; Ikuta, T. *Adv. Mater.* **2016**, *28*, 2777-2781.

26. Zettler, F.; Hausen, H. D.; Hess, H. *J. Organomet. Chem.* **1974**, *72*, 157-162.

27. Klooster, W. T.; Koetzle, T. F.; Siegbahn, P. E. M.; Richardson, T. B.; Crabtree, R. H. *J. Am. Chem. Soc.* **1999**, *121*, 6337-6343.

28. Lui, M. W.; Paisley, N. R.; McDonald, R.; Ferguson, M. J.; Rivard, E. *Chem. Eur. J.* **2016**, *22*, 2134-2145.

29. Hering-Junghans, C.; Watson, I. C.; Ferguson, M. J.; McDonald, R.; Rivard, E. *Dalton Trans.* **2017**, *46*, 7150-7153.

30. a) Vedejs, E.; Nguyen, T.; Powell, D. R.; Schrimpf, M. R. *Chem. Commun.* **1996**, 2721-2722. b) Braunschweig, H.; Ganter, B. *J. Organomet. Chem.* **1997**, *545*, 163-167.

31. Watson, I. C.; Zhou, Y.; Ferguson, M. J.; Kränzlein, M.; Rieger, B.; Rivard, E. *Z. Anorg. Allg. Chem.* **2020**, *646*, 547-551.

32. Turley, J. W.; Rinn, H. W. *Inorg. Chem.* **1969**, *8*, 18-22.

33. Gavrilenko, V. V.; Chekulaeva, L. A.; Antonovich, V. A.; Zakharkin, L. I. *Bull. Acad. Sci. USSR, Div. Chem. Sci. (Engl. Transl.)*. **1981**, 505-508.

34. Pangborn, A. B.; Giardello, M. A.; Grubbs, R. A.; Rosen, R. K.; Timmers, F. J. *Organometallics* **1996**, *15*, 1518-1520.

35. Rheinboldt, H.; Luyken, A.; Schmittmann, H. *J. Prakt. Chem.* **1937**, *149*, 30-54.

36. Press, L. P.; McCulloch, B. J.; Gu, W.; Chen, C.-H.; Foxman, B. M.; Ozerov, O. V. *Chem. Commun.* **2015**, *51*, 14034-14037.

37. MacNeil, C. S.; Hsiang, S.-J.; Hayes, P. G. *Chem. Commun.* **2020**, *56*, 12323-12326.

38. Yuan, K.; Wang, X.; Wang, S. *Org. Lett.* **2018**, *20*, 1617-1620.

39. Blessing, R. H. *Acta. Cryst.* **1995**, *A51*, 33-38.

40. Sheldrick, G. M. *Acta. Cryst.* **2015**, *A71*, 3-8.

41. Sheldrick, G. M. *Acta. Cryst.* **2015**, *C71*, 3-8.

42. a) Becke, A. D. *J. Chem. Phys.* **1993**, *98*, 5648-5652. b) Lee, C.; Yang, W.; Parr, R. G. *Phys. Rev. B* **1988**, *37*, 785-789.

43. a) Weigend, F.; Ahlrichs, R. *Phys. Chem. Chem. Phys.* **2005**, *7*, 3297-3305. b) Schäfer, A.; Huber, C.; Ahlrichs, R. *J. Chem. Phys.* **1994**, *100*, 5829-5835. c) Schäfer, A.; Horn, H.; Ahlrichs, R. *J. Chem. Phys.* **1992**, *97*, 2571-2577.

44. Frisch, M. J.; Trucks, G. W.; Schlegel, H. B.; Scuseria, G. E.; Robb, M. A.; Cheeseman, J. R.; Scalmani, G.; Barone, V.; Petersson, G. A.; Nakatsuji, H.; Li, X.; Caricato, M.; Marenich, A. V.; Bloino, J.; Janesko, B. G.; Gomperts,

R.; Mennucci, B.; Hratchian, H. P.; Ortiz, J. V.; Izmaylov, A. F.; Sonnenberg, J. L.; Williams-Young, D.; Ding, F.; Lipparini, F.; Egidi, F.; Goings, J.; Peng, B.; Petrone, A.; Henderson, T.; Ranasinghe, D.; Zakrzewski, V. G.; Gao, J.; Rega, N.; Zheng, G.; Liang, W.; Hada, M.; Ehara, M.; Toyota, K.; Fukuda, R.; Hasegawa, J.; Ishida, M.; Nakajima, T.; Honda, Y.; Kitao, O.; Nakai, H.; Vreven, T.; Throssell, K.; Montgomery, J. A., Jr.; Peralta, J. E.; Ogliaro, F.; Bearpark, M. J.; Heyd, J. J.; Brothers, E. N.; Kudin, K. N.; Staroverov, V. N.; Keith, T. A.; Kobayashi, R.; Normand, J.; Raghavachari, K.; Rendell, A. P.; Burant, J. C.; Iyengar, S. S.; Tomasi, J.; Cossi, M.; Millam, J. M.; Klene, M.; Adamo, C.; Cammi, R.; Ochterski, J. W.; Martin, R. L.; Morokuma, K.; Farkas, O.; Foresman, J. B.; Fox, D. J. *Gaussian 16,* Revision A.03; Gaussian, Inc.: Wallingford, CT, **2016**.

45. Glendening, E. D.; Badenhoop, J. K.; Reed, A. E.; Carpenter, J. E.; Bohmann, J. A.; Morales, C. M.; Landis, C. R.; Weinhold, F. *NBO 6.0.;* Theoretical Chemistry Institute, University of Wisconsin, Madison, **2013**.

Chapter 6: Group 4 and 8 Transition Metal Complexes with Anionic *N*-Heterocyclic Olefin Ligands

6.1 Introduction

N-Heterocyclic olefins (NHOs) are a class of carbon-based ligand which feature an alkylidene unit (C=CR$_2$) appended to an *N*-heterocyclic carbene (NHC) frame. This alkylidene unit is highly ylidic, allowing NHOs to act as 2σ-electron donors.[1] Indeed, since the discovery of the first transition metal-NHO complex by Kaska and coworkers (**A**, Chart 6.1),[2] NHOs have been used as supporting ligands for transition metal-mediated catalysis.[3] Examples of NHO-transition metal complexes include those from the groups of Kuhn (**B**),[4] Ando and Ishizuka (**C**),[5] Rivard (**D**, also see Chapter 3),[3] and others.[6] While multiple examples of transition metal complexes supported by neutral NHO donors can be found in the literature, examples of metal complexes bearing deprotonated, anionic *N*-heterocyclic olefins (aNHOs) remain rare. The sole example of an aNHO-transition metal complex was reported by Rivard and coworkers, wherein two aNHO ligands are bound to a Zn(II) center to yield the linear, two-coordinate species **E** (Chart 6.1, see also Chapter 5).[7]
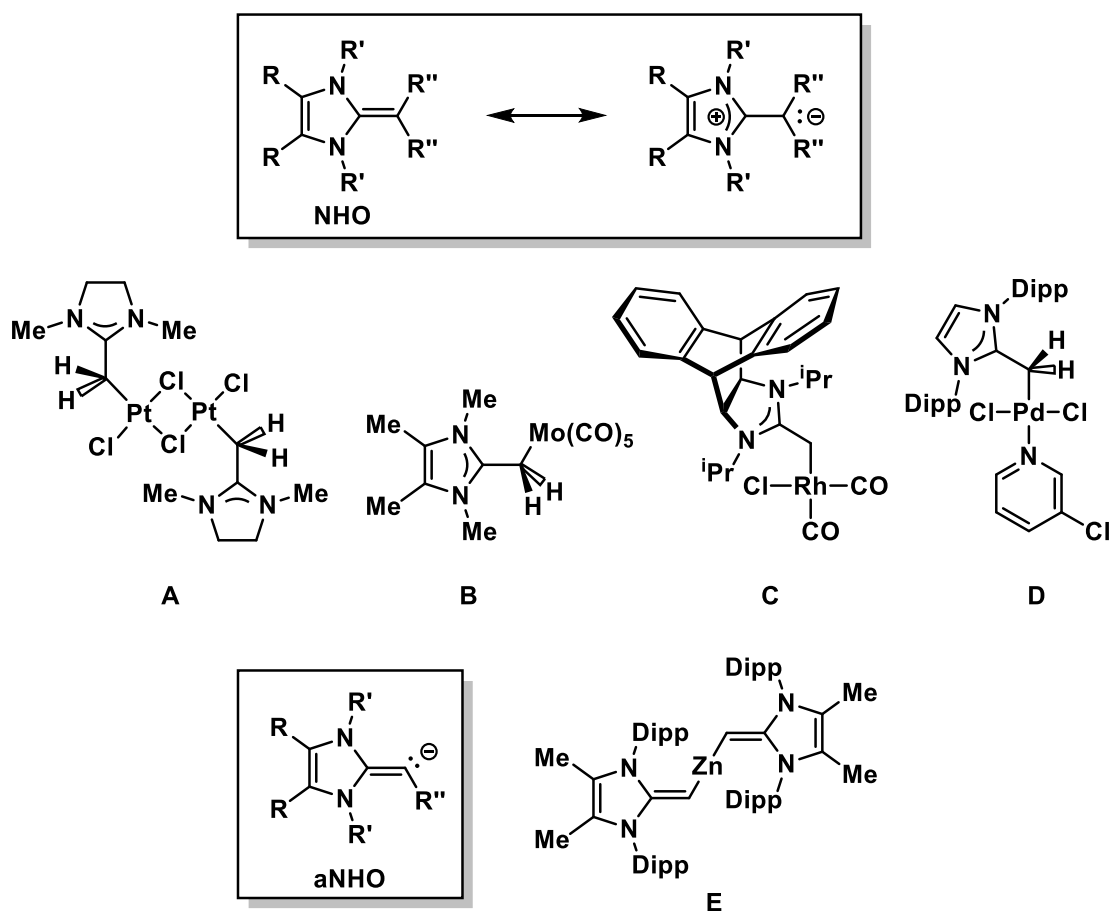
Chart 6.1. Canonical resonance forms of a general *N*-heterocyclic olefin (NHO) (top), selected examples of NHO-transition metal complexes (middle), a generic anionic *N*-heterocyclic olefin (aNHO), and an aNHO-bearing zinc complex **E** (bottom); Dipp = 2,6-^{i}Pr$_2$C$_6$H$_3$.

There is a longstanding interest in utilizing low valent Group 4 metal complexes as stoichiometric reagents and catalysts, as they are often very reactive owing to their low electronegativity, leading to polar (and reactive) metal-ligand bonds.[8] Examples of this reactivity include N$_2$ activation by reduced Group 4 metal centers,[9] reductive coupling reactions,[10] catalytic dehydrogenations,[11] and other

reactions.[12] These low valent complexes are often formed by reduction using alkali metals, gentler reducing metals (*e.g.,* Zn and Mg), or by β-hydride elimination processes.[8] These low valent Group 4 metal complexes are often not isolable upon generation, but can be stabilized upon combination with π-accepting ligands such as alkenes [*e.g.,* Negeshi's reagent $Cp_2Zr(\eta^2\text{-butene})$],[13] alkynes [*e.g.,* Rosenthal's reagent $Cp_2Zr(Me_3SiCCSiMe_3)(pyr)$; pyr = pyridine],[14] or arenes [*e.g.,* $(PNP)ZrCl(\eta^6\text{-}C_7H_8)$; PNP = 1,8-bis(phosphino)-3,6-di-*tert*-butyl-9*H*-carbazole].[15] These reagents can act as masked sources of M(II) (M = Ti and Zr), as loss of the π-accepting ligand leads to the regeneration of an active M(II) center.

Two-coordinate transition metal complexes that adopt a strictly linear geometry are still uncommon for Groups 4-9.[16] A notable consequence of a linear coordination geometry is that the resulting complexes are not susceptible to Jahn-Teller distortions. This results in a non-zero orbital angular moment when the degenerate orbitals (d_{xz}/d_{yz} or $d_{xy}/d_{x^2-y^2}$ are unsymmetrically filled (Figure 6.1).[17] This orbital angular moment leads to a large magnetic anisotropy, which is a key factor in a molecule's ability to act as a single molecule magnet.[18] Single molecule magnets that operate at room temperature are of technological interest as they would revolutionize computing by dramatically reducing the size of memory elements required to permanently store information.[19]
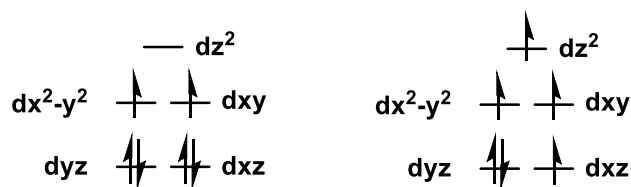
Figure 6.1. Low-spin and high-spin electron configurations for a linear, two-coordinate Fe^{2+} center.

Given the recent report of the lithiated NHO (^{Me}IPrCH)Li by Rivard and coworkers (^{Me}IPrCH = (MeCNDipp)$_2$CH; Dipp = 2,6-^{i}Pr$_2$C$_6$H$_3$), and its ability to form main group element complexes by salt metathesis[20] and to form a linear, two-coordinate zinc complex supported by aNHOs (**E**, Chart 6.1),[7] low-coordinate transition metal complexes supported by anionic *N*-heterocyclic olefins were selected as synthetic targets for this Chapter.

6.2 Results and Discussion

Given the highly electron-donating nature of anionic *N*-heterocyclic olefins (aNHOs), it was postulated that aNHOs would be effective at stabilizing low-coordinate early transition metal centers since these metals are known to be highly electrophilic. Group 4 metals precursors were targeted since they are diamagnetic in the +4 oxidation state (and therefore characterization is more straightforward); the observation of a tetrahedral geometry in the previously reported germane[21] (IPrCH)$_2$GeCl$_2$ [IPr = (HCNDipp)$_2$C:] suggested that two aNHO ligands could be sterically accommodated around the metal center in the (^{Me}IPrCH)$_2$MCl$_2$ complexes

targeted in this study. Two equivalents of the lithiated NHO (^{Me}IPrCH)Li was combined with (THF)$_2$TiCl$_4$ in toluene in the hope that salt metathesis would occur (Equation 6.1). Gratifyingly, a deep purple color was immediately observed and after removing the volatiles *in vacuo*, a new species was observed by ^{1}H NMR spectroscopy. Crystallization from a saturated hexanes solution at –35 °C yielded dark purple X-ray quality single-crystals and subsequent X-ray diffraction studies revealed (^{Me}IPrCH)$_2$TiCl$_2$ (**1**) had formed (Figure 6.2). Encouraged by this result, similar reactions were performed with (THF)$_2$ZrCl$_4$ and (THF)$_2$HfCl$_4$ yielding (^{Me}IPrCH)$_2$ZrCl$_2$ (**2**) and (^{Me}IPrCH)$_2$HfCl$_2$ (**3**) respectively (Equation 6.1, Figures 6.3 and 6.4).

(1)
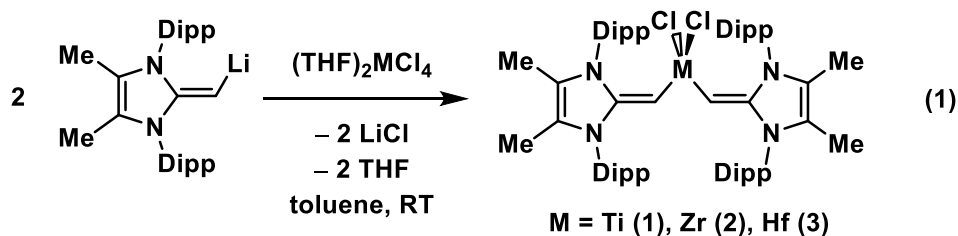
As expected, the Ti–C distances in **1** (1.991(3) Å) are shorter than the M–C distances in **2** and **3** (2.104(2) and 2.111(4) Å, respectively). The Ti–C bond length is notably longer than the Ti–N (1.788(2) Å) bonds in the structurally related bis-*N*-heterocyclic iminatotitanium (IV) complex (I^{t}Bu=N)$_2$TiCl$_2$ [I^{t}Bu = (HCN^{t}Bu)$_2$C] reported by Tamm, Eisen, and coworkers.[22] Each of the M–C distances in compounds **1-3** are greater than the Ge–C distances in the previously reported germanium bis(aNHO) analogue of these compound (IPrCH)$_2$GeCl$_2$ (1.874(4) Å).[21] The exocyclic C=C bonds of the aNHO ligands in these Group 4 complexes are the same length

within experimental error (1.381(4), 1.384(3), and 1.386(3) Å for **1**, **2**, and **3**, respectively) and show the retention of appreciable C=C π-character.
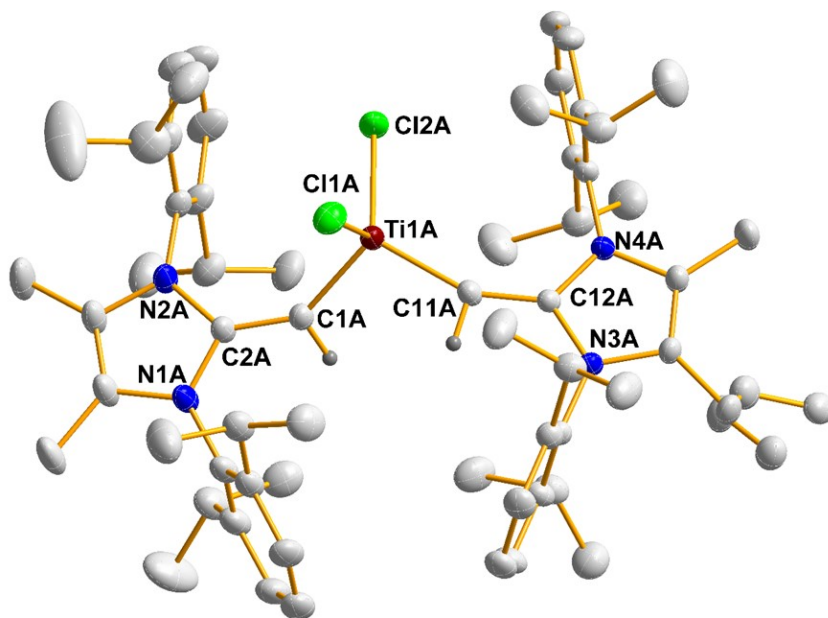
Figure 6.2. Molecular structure of (^{Me}IPrCH)$_2$TiCl$_2$ (**1**) with thermal ellipsoids plotted at 30 % probability. Hydrogen atoms, except for those on C1A and C11A, have been omitted for clarity. Selected bond lengths [Å] and angles [°] with values belonging to a second molecule in the asymmetric unit in square brackets: Ti1A–C1A 1.991(3) [1.988(4)], C1A–C2A 1.381(4) [1.385(5)], Ti1A–Cl1A 2.3315(11) [2.2867(14)], Ti1A–Cl2A 2.2466(10) [2.2350(15)]; C1A–Ti1A–C11A 103.27(13) [105.10(15)].
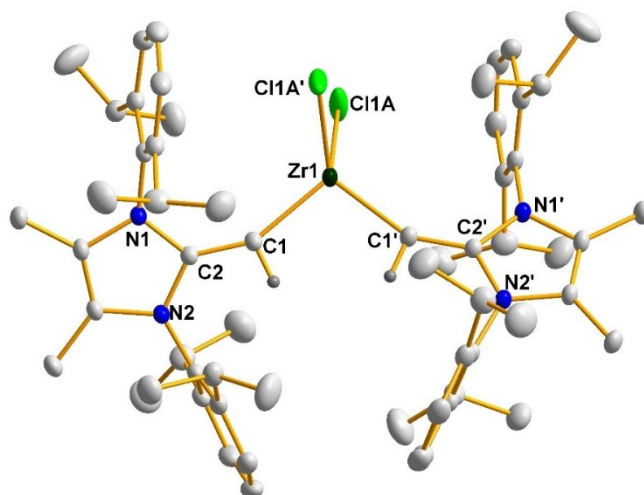
Figure 6.3. Molecular structure of (^{Me}IPrCH)$_2$ZrCl$_2$ (**2**) with ellipsoids plotted at a 30 % probability level. Hydrogen atoms, except for those on C1 and C1′, have been omitted for clarity. Primed atoms are related to unprimed atoms by a 2-fold rotational axis. Each Cl atoms is disordered over two positions, with values belonging to the second position in square brackets. Selected bond lengths [Å] and angles [°]: Zr1–C1 2.104(2), C1–C2 1.384(3), Zr1–Cl1A 2.335(9) [2.462(3)], Zr1–Cl2A 2.462(3) [2.462(3)]; C1–Zr1–C1' 102.23(12).
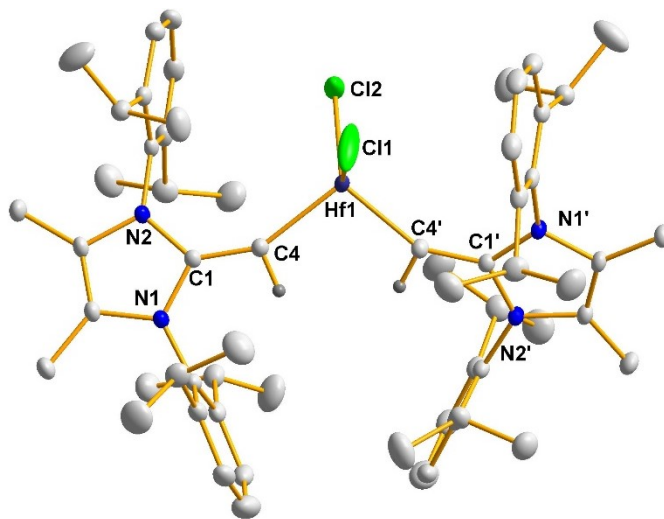
Figure 6.4. Molecular structure of (^{Me}IPrCH)$_2$HfCl$_2$ (**3**) with thermal ellipsoids plotted at a 30 % probability level. Hydrogen atoms, except for those on C4 and C4′, have been omitted for clarity. Primed atoms are related to unprimed atoms by a 2-fold rotation axis. Selected bond lengths [Å] and angles [°]: Hf1–C4 2.111(4), C1–C4 1.386(3), Hf1–Cl1 2.354(7), Hf–Cl2 2.369(7); C4–Hf1–C4′ 101.54(11).

The most notable feature in the ^{1}H NMR spectra of the (^{Me}IPrCH)$_2$MCl$_2$ complexes **1-3** is the variable chemical shift of the C=CH resonance among the three compounds. The C=CH resonance of the Ti congener **1** is found at 8.62 ppm, while the same resonances in the Zr and Hf complexes **2** and **3** can be found at 5.29 and 3.92 ppm respectively.

Inspired by the work of Fryzuk and coworkers, where reduction of a zirconium dichloride complexes under a nitrogen atmosphere led to the activation of N$_2$,[9a] (^{Me}IPrCH)$_2$ZrCl$_2$ (**2**) was combined with an excess of sodium metal in THF and was stirred for 3 h (Equation 6.2). The resulting brown solution was filtered through Celite, concentrated *in vacuo*, and stored at –35 °C for a week, resulting in the growth of dark-brown X-ray quality crystals. Surprisingly, N$_2$ activation was not observed, but instead, a 2,6-diisopropylphenyl (Dipp) group of one of the aNHO ligands was coordinated to the Zr center, resulting in the unsymmetric complex (^{Me}IPrCH)$_2$Zr (**4**) (Equation 6.2 and Figure 6.5).

(6.2)
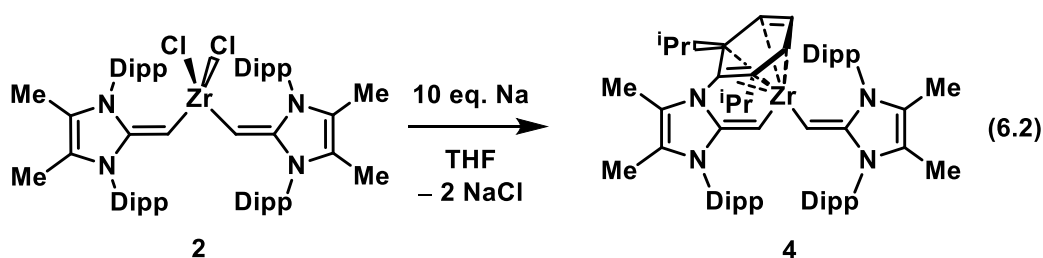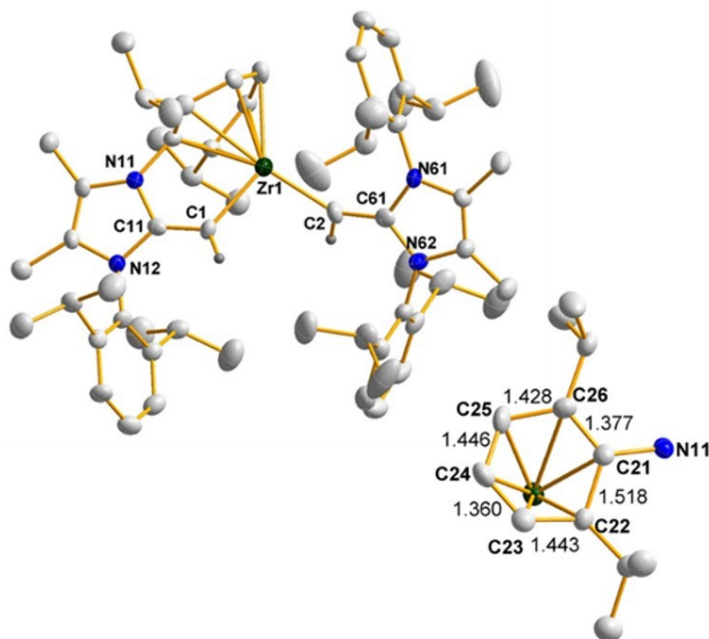
Figure 6.5. Molecular structure of (^{Me}IPrCH)$_2$Zr **4** with thermal ellipsoids plotted at a 30 % probability level and a top-down view of the Dipp group coordinated to the Zr center. Hydrogen atoms, except those on C1 and C2, have been omitted for clarity. Selected bond lengths [Å] and angles [°]: Zr1–C1 2.176(8), Zr1–C2 2.139(8), C1–C11 1.373(12), C2–C61 1.385(12), C21–C22 1.518(12), C22–C23 1.443(12), C23–C24 1.360(14), C24–C25 1.446(14), C25–C26 1.428(13), C21–C26 1.377(13); C1–Zr1–C2 99.5(2), C21–C22–C23 109.0(7), C24–C25–C26 115.4(8); torsion angle C2–Zr1–C1–C11 147.6(6). Note that crystals of **4** did not diffract at high angles, and as such, are not of publishable quality.

Compound **4** can be considered a "masked" Zr(II) species, but it is important to note the metal itself is still formally Zr(IV) due to oxidative addition of the masking arene ring. A loss of planarity of the coordinated Dipp group and distortion of the C–C bond lengths (*e.g.,* shortened C21–C26 and C23–C24 bond lengths relative to other bonds in the ring) indicates a formal 1,4-cyclohexadiene dianionic resonance form. The bond angles around the *ortho* and *meta* carbons (C22 and C25) of the capping arene have smaller bond angles (C21–C22–C23 109.0(7)°, C24–C25–C26 115.4(8)°)

than would be expected (120°) for a planar aromatic ring. The exocyclic C=C bonds of the ligands retain their olefinic character (1.373(12) and 1.385(12) Å) and are similar in length to those in the precursor **2**. It is worth noting that crystals of **4** did not diffract at high angles, and as such the crystal data collected is not of publishable quality.

Examples of this type of masked Group 4 metal are uncommon in the literature, with arene-capped titanium complexes reported by the groups of Stephan (**F**),[23] Power (**G**),[24] and Fortier (**H**)[11a,25] (Chart 6.2) and an example of an arene-masked zirconium complex from the Gade Group (**I**).[15] Notably, compound **H** reported by Fortier and coworkers has been shown to catalyze the transfer hydrogenation of alkenes.[11a]
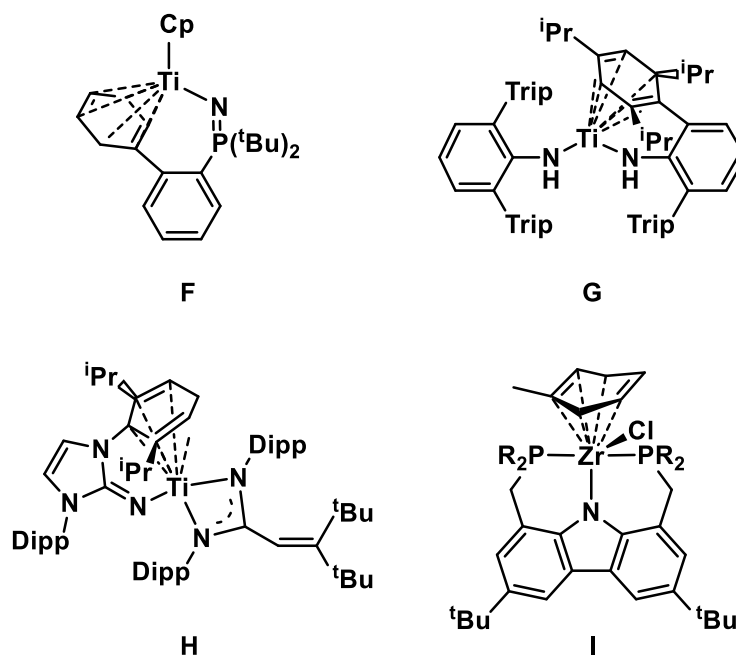
Chart 6.2. Examples of arene-capped titanium and zirconium complexes; Trip = 2,4,6-^{i}Pr$_3$C$_6$H$_2$.

261

Unfortunately, compound **4** proved exceedingly difficult to isolate in bulk. All attempts to synthesize **4** on a large scale resulted in the isolation of the (^{Me}IPrCH)$_2$ZrCl$_2$ (**2**) starting material and free ^{Me}IPr=CH$_2$. Reductants used in attempts to prepare/isolate **4** from **2** include: sodium metal, lithium metal, potassium metal, KC$_8$, and sodium naphthalenide. Attempts to access analogous arene-masked Ti or Hf complex via reduction of (^{Me}IPrCH)$_2$TiCl$_2$ (**1**) and (^{Me}IPrCH)$_2$HfCl$_2$ (**3**) respectively, likewise yielded a mixture of starting material and ^{Me}IPr=CH$_2$. Inspiration was also taken from the synthesis of Negishi's reagent, where Cp$_2$ZrCl$_2$ is combined with two equivalents of ^{n}BuLi to form a "Cp$_2$Zr" species *in situ*.[13] When **4** was combined two equivalents of ^{n}BuLi at –78 °C, a mixed of free ^{Me}IPr=CH$_2$ and three new products were observed by ^{1}H NMR analysis. However, attempts to separate these products by fractional crystallization failed.

To test the ability of (^{Me}IPrCH)Li to form complexes with other transition metals via salt metathesis, two equivalents of (^{Me}IPrCH)Li were combined with FeCl$_2$ (Equation 6.3). Gratifyingly, an immediate color change was observed as the solution became a dark-burgundy color. Filtration of the mixture, concentrating the resulting solution *in vacuo*, and storage at –35 °C for a week resulted in the growth of dark-burgundy X-ray quality crystal of (^{Me}IPrCH)$_2$Fe (**5**) (Figure 6.6).
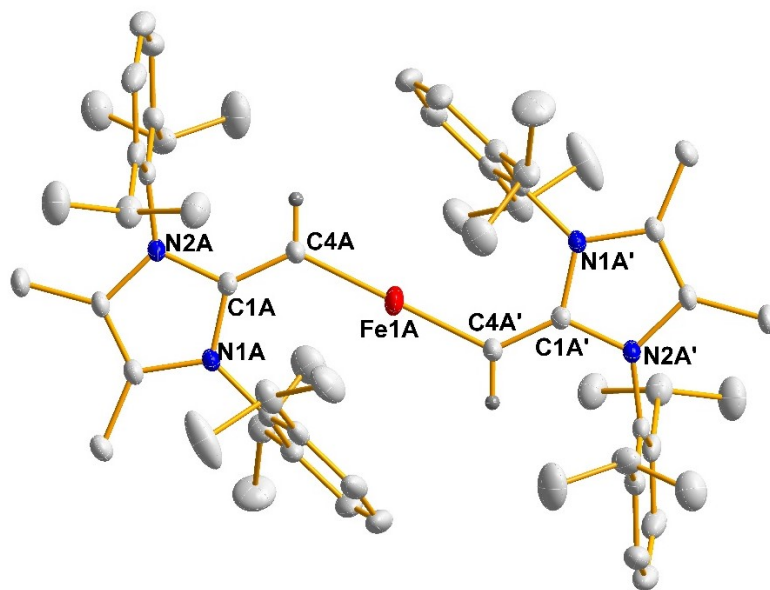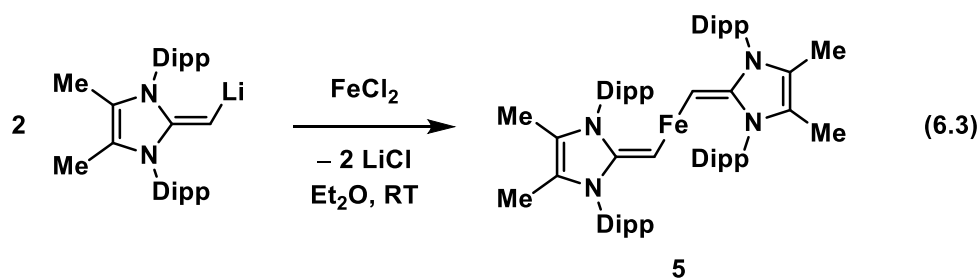
Figure 6.6. Molecular structure of (^{Me}IPrCH)$_2$Fe (5) with thermal ellipsoids plotted at a 30 % probability level. Hydrogen atoms, except those on C4A and C4A′, have been omitted for clarity. Primed atoms are related to unprimed ones by an inversion center. Selected bond lengths [Å] and angles [°] with values belonging to a second molecule in the asymmetric unit in square brackets: Fe1A–C4A 1.9699(18) [1.959(2)], C1A–C4A 1.354(3) [1.354(3)]; C4A–Fe1–C4A′ 180.0 [180.0].

Much like with (^{Me}IPrCH)$_2$Zn (as seen in Chapter 5),[7] the aNHO ligands in 5 enforce a linear geometry around the iron(II) center and the exocyclic C=C bond lengths of the aNHO ligands are consistent with a retention of multiple bond character [C1A–C4A 1.354(3) Å]. The Fe–C bonds in 5 are shorter than those in the linear iron(II) complex Fe[C(SiMe$_3$)]$_2$ (J, Chart 6.3) (1.9699(18) in 5 vs. 2.045(5) Å in J,

respectively). While aNHO-bearing Fe complexes have not been reported, an example of an *N*-heterocyclic iminatoiron(II) complex has been synthesized by the Tamm Group (**K**, Chart 6.3).[26] The Fe–N bond in **K** is shorter than the Fe–C bond in compound **5** (1.7885(13) *vs.* 1.9699(18) Å), which follows the trend of much shorter element-ligand bonds observed with *N*-heterocyclic imines compared to NHOs (see Chapter 4). As expected with an Fe(II) complex, **5** is paramagnetic and as such has a ^{1}H NMR spectrum that spans a large range (+116 to −122 ppm). Obtaining analytically pure (^{Me}IPrCH)$_2$Fe (**5**) has not been possible yet, as free ^{Me}IPrCH$_2$ is always detected (by ^{1}H NMR), despite multiple recrystallizations and washing the crystals with hexanes. While **5** shows promise as a single molecule magnet, these impurities prevented a detailed investigation of its magnetic properties as part of this Thesis.
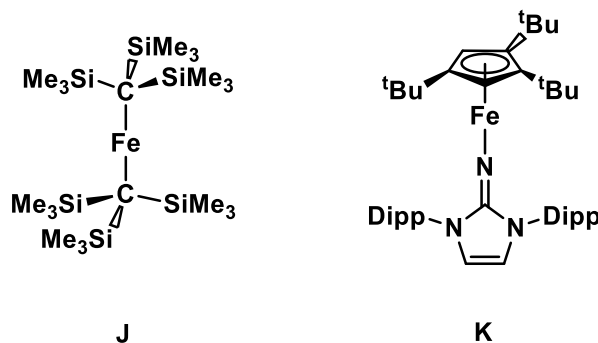
Chart 6.3. Selected examples of linear iron(II) complexes.

6.3. Conclusion

Using the lithiated NHO (^{Me}IPrCH)Li, it is possible to make new aNHO-transition metal complexes. Combination of Group 4 tetrahalides with two equivalents of (^{Me}IPrCH)Li resulted in the formation of (^{Me}IPrCH)$_2$MCl$_2$ complexes (M = Ti, Zr, Hf). It is possible to reduce (^{Me}IPrCH)$_2$ZrCl$_2$ using sodium metal to access an arene-masked zirconium complex (compound **4**), but this result has been difficult to reproduce. The linear iron(II) complex (^{Me}IPrCH)$_2$Fe (**5**) can be formed by combining two equivalents of (^{Me}IPrCH)Li with FeCl$_2$. The resulting iron(II) complex is paramagnetic and might hold promise as a single molecule magnet due to its linear geometry and expected high orbital angular momentum. Future work will involve isolation of **4** in bulk and evaluating the ability of this arene-masked zirconium species to perform C–H activation reactions, as well as purification of **5** and the subsequent evaluation of its efficacy as a single-molecule magnet. The (^{Me}IPrCH)$_2$MCl$_2$ complexes **1-3** could be methylated by reaction with MeLi to yield (^{Me}IPrCH)$_2$MMe$_2$ complexes, and following a methyl group abstraction from the metal center, a [(^{Me}IPrCH)$_2$MMe]$^+$ cationic complex could be formed. This cationic complex could then be used as an olefin polymerization catalyst.

6.4. Experimental Section

6.4.1. Materials and Instrumentation

All reactions were performed using standard Schlenk line techniques under an atmosphere of nitrogen or in an inert-atmosphere glovebox (MBruan Labmaster 100).

Solvents were dried using a Grubbs-type solvent-purification system manufactured by Innovative Technology, Inc. and stored under an atmosphere of nitrogen and over 4 Å molecular sieves prior to use. $(^{Me}IPrCH)Li,^{20}$ $(THF)_2TiCl_4,^{27}$ $(THF)_2ZrCl_4,^{27}$ and $(THF)_2HfCl_4^{27}$ were prepared according to literature procedures. $FeCl_2$, Na, and ^nBuLi (2.5 M in hexanes) were purchased from MilliporeSigma and used as received. ^1H and $^{13}C\{^1H\}$ NMR spectra were recorded on 400 MHz, 500 MHz or 700 MHz Varian Inova spectrometers and referenced externally to $SiMe_4$ (^1H, $^{13}C\{^1H\}$). Elemental analyses were performed by the Analytical and Instrumentation Laboratory at the University of Alberta. Melting points were measured in sealed glass capillaries under nitrogen using a MelTemp melting-point apparatus and are uncorrected.

6.4.2. X-ray Crystallography

Crystals of appropriate quality for single-crystal X-ray diffraction studies were removed from either a Schlenk flask under a stream of nitrogen, or from a vial (glove box) and immediately covered with a thin layer of hydrocarbon oil (Paratone-N). A suitable crystal was then selected, attached to a glass fiber, and quickly placed in a low-temperature stream of nitrogen. All data were collected using a Bruker APEX II CCD detector/D8 diffractometer using $Mo_{K\alpha}$ or $Cu_{K\alpha}$ radiation, with the crystal cooled to $-100\,°C$ or $-80\,°C$, respectively. The data were corrected for absorption through Gaussian integration from indexing of the crystal faces. Structures were solved using the direct methods programs SHELXT-2014,[28] and refinements were completed using the program SHELXL-2014.[29] Hydrogen atoms were assigned positions based on the

sp^2- or sp^3-hybridization geometries of their attached carbon atoms, and were given thermal parameters 20 % greater than those of their parent atoms.

6.4.3. Synthetic Procedures

Synthesis of (^{Me}IPrCH)$_2$TiCl$_2$ (1). A solution of ^{Me}IPrCHLi (0.0532 g, 0.129 mmol) in 2 mL of toluene was added dropwise to a solution of (THF)$_2$TiCl$_4$ (0.0203 g, 0.0608 mmol) in 2 mL of toluene. The resulting dark-purple solution was stirred for one hour, filtered through Celite, and the volatiles were removed *in vacuo* yielding (^{Me}IPrCH)$_2$TiCl$_2$ (0.0301 g, 48 %) as a dark-purple solid. Dark-purple X-ray quality crystals were obtained via recrystallization from hexanes at –30 °C for a period of one week. ^{1}H NMR (400 MHz, C$_6$D$_6$): δ = 8.62 (s, 2H, C=C*H*), 7.31 (t, 4H, $^3J_{HH}$ = 7.1 Hz, Ar*H*), 7.18 (d, 8H, $^3J_{HH}$ = 7.7 Hz, Ar*H*), 2.89 (sept, 8H, $^3J_{HH}$ = 6.9 Hz, C*H*(CH$_3$)$_2$), 1.40 (s, 12H, *H*$_3$C-CN), 1.37 (d, 24H, $^3J_{HH}$ = 6.8 Hz, CH(C*H*$_3$)$_2$, 1.11 ppm (d, 24H, $^3J_{HH}$ = 6.9 Hz, CH(C*H*$_3$)$_2$); ^{13}C{^{1}H} NMR (125 MHz, C$_6$D$_6$): δ = 9.1 (NC–*C*H$_3$), 23.5 (CH(*C*H$_3$)$_2$), 24.7 (CH(*C*H$_3$)$_2$), 28.6 (*C*H(CH$_3$)$_2$), 124.4 (Ar*C*), 129.5 (Ar*C*), 131.8 (Ar*C*), 147.1 (Ar*C*), 147.4 (Ar*C*), 148.7 (Ar*C*), 182.2 ppm (C=*C*H), the N*C*N and N*C*–CH$_3$ resonances could not be found; element. anal.: calcd for C$_{60}$H$_{82}$Cl$_2$N$_2$Ti: C, 73.68; H, 8.45; N, 5.73; found: C, 73.56; H, 8.46; N, 5.46 %; mp: 221 °C (dec.).

Synthesis of (^{Me}IPrCH)$_2$ZrCl$_2$ (2): To a suspension of ZrCl$_4$(THF)$_2$ (0.0216 g, 0.0573 mmol) in 4 mL of toluene was added a solution of ^{Me}IPrCHLi (0.0500 g, 0.115 mmol) in 4 mL of toluene. The resulting yellow mixture was stirred for one hour,

filtered through Celite, and the volatiles were removed from the filtrate *in vacuo*. The solid was triturated three times with 5 mL portions of petroleum ether and then dried under vacuum yielding (^{Me}IPrCH)$_2$ZrCl$_2$ (0.3539 g, 61 %) as a yellow solid. Yellow X-ray quality crystals were grown by layering (Me$_3$Si)$_2$O on top of a concentrated solution of (^{Me}IPrCH)$_2$ZrCl$_2$ in diethyl ether and storing at –35 °C for three days. ^{1}H NMR (400 MHz, C$_6$D$_6$): δ = 7.32 (t, 4H, $^3J_{HH}$= 7.2 Hz, Ar*H*), 7.19 (d, 8H, $^3J_{HH}$ = 7.7 Hz, Ar*H*), 5.29 (s, 2H, C=C*H*), 2.93 (br, 8H, C*H*(CH$_3$)$_2$), 1.42 (s, 12H, *H*$_3$C–CN), 1.38 (d, 24H, $^3J_{HH}$ = 6.9 Hz, CH(C*H*$_3$)$_2$), 1.12 ppm (d, 24H, $^3J_{HH}$ = 6.9 Hz, CH(C*H*$_3$)$_2$); ^{13}C{^{1}H} NMR (175 MHz, C$_6$D$_6$): δ = 9.4 (*H*$_3$C-CN), 23.5 (CH(*C*H$_3$)$_2$), 24.8 (CH(*C*H$_3$)$_2$), 28.8 (*C*H(CH$_3$)$_2$), 124.4 (Ar*C*), 124.8 (Ar*C*), 125.3 (Ar*C*), 128.2 (Ar*C*), 129.9 (Ar*C*), 130.0 (Ar*C*), 135.6 (C=*C*H), 149.6 (H$_3$C–*C*N), 152.6 ppm (N*C*N); elemental analysis was not performed due to the presence of *ca.* 2 % ^{Me}IPrCH$_2$ impurity; mp: 213 °C (dec.).

Synthesis of (^{Me}IPrCH)$_2$HfCl$_2$ (3): A solution of ^{Me}IPrCHLi (0.050 g, 0.12 mmol) in 4 mL of toluene was added dropwise to a solution of (THF)$_2$HfCl$_4$ (0.0278 g, 0.0598 mmol) in 4 mL of toluene. The resulting yellow mixture was stirred for one hour, filtered through Celite, and the volatiles were removed from the filtrate *in vacuo* yielding a yellow powder. The resulting crude product was triturated three times with 5 mL of petroleum ether and then dried under vacuum, yielding (^{Me}IPrCH)$_2$HfCl$_2$ (0.0354 g, 56 %) as a yellow solid. Yellow X-ray quality crystals were obtained via recrystallization from a saturated toluene solution at –35 °C for a period of one week.

^{1}H NMR (400 MHz, C$_6$D$_6$): δ = 7.27 (t, 4H, $^3J_{HH}$ = 8.3 Hz, ArH), 7.18 (d, 6H, $^3J_{HH}$ = 7.8 Hz, ArH), 3.92 (s, 2H, C=CH), 2.95 (br, 8H, CH(CH$_3$)$_2$), 1.43 (s, 12H, NC–CH_3), 1.34 (br, 24H, CH(CH_3)$_2$), 1.13 ppm (d, 24H, $^3J_{HH}$ = 6.9 Hz, CH(CH_3)$_2$); ^{13}C{^{1}H} NMR (175 MHz, C$_6$D$_6$): δ = 9.6 (H$_3$$C$–CN), 23.7 (CH($CH_3$)$_2$), 25.6 (CH($CH_3$)$_2$), 28.9 ($C$H(CH$_3$)$_2$), 124.6 (Ar$C$), 124.8 (Ar$C$), 125.6 (Ar$C$), 125.8 (Ar$C$), 128.2 (Ar$C$), 129.7 (Ar$C$), 124.5 ($C$=CH), 146.7 (H$_3$C–$C$N), 149.5 ppm (N$C$N); elemental analysis was not performed due to the presence of *ca.* 3 % ^{Me}IPrCH$_2$ impurity; mp: 218 °C (dec.).

Synthesis of (^{Me}IPrCH)₂Zr (4). A solution of (^{Me}IPrCH)$_2$ZrCl$_2$ (**3**) (0.0436 g, 0.00426 mmol) in 5 mL of toluene was added to freshly cut sodium metal (0.0098 g, 0.043 mmol). The resulting mixture was stirred for 2 h, then filtered through Celite, and the resulting filtrate was concentrated to a volume of 0.3 mL. A few dark-brown crystals were grown by storing this solution at –35 °C for one week. Despite repeated attempts, compound **4** was unable to be isolated in bulk.

Synthesis of (^{Me}IPrCH)₂Fe (5): ^{Me}IPrCHLi (0.1418 g, 0.3428 mmol) in 4 mL of Et$_2$O was added dropwise to a solution of anhydrous FeCl$_2$ (0.0206 g, 0.1624 mmol) in 6 mL of Et$_2$O and stirred for 4 h. The mixture was filtered through a pad of Celite and the volatiles were removed from the filtrate *in vacuo*. The resulting solid was washed with 3 × 1 mL of hexanes and then dried *in vacuo* yielding (^{Me}IPrCH)$_2$Fe as a purple-red solid (0.0658 g, 42 %). ^{1}H NMR (500 MHz, C$_6$D$_6$): δ = –168, –79.9, –34.2, –30.0,

25.2, 35.2, 37.2, 43.4, 51.5, 63.9, 118.6 ppm; element. anal.: calcd for $C_{60}H_{82}N_4Fe$: C, 59.47; H, 6.82; N, 4.62; found: C, 54.32; H, 6.38; N, 4.14; despite repeated attempts, analyses were consistently low in carbon content; mp: 167 °C (dec.).

6.5. Crystallography Data

Table 6.1. Crystallographic data for **1**, **2**, and **3**.

Compound	**1**	**2**	**3**
formula	$C_{60}H_{82}Cl_2N_4Ti$	$C_{60}H_{82}Cl_2N_4Zr$	$C_{60}H_{82}Cl_2HfN_4$
formula weight	978.09	1021.41	1108.68
crystal system	triclinic	monoclinic	monoclinic
Space Group	$P\bar{1}$	$C2/c$	$C2/c$
a (Å)	10.8291(2)	27.418(2)	27.3940(19)
b (Å)	23.0803(4)	11.6795(8)	11.6997(8)
c (Å)	23.7882(5)	19.8534(14)	19.8662(14)
α (deg)	101.2782(13)	--	--
β (deg)	97.7836(14)	115.244(4)	115.2170(11)
γ (deg)	92.5865(14)	--	--
V (Å^3)	5761.35(19)	5750.5(8)	5760.4(7)
Z	4	4	4
ρ_{calcd} (g cm^{-3})	1.128	1.180	1.278
Abs coeff (mm^{-1})	2.397	2.707	1.943
T (K)	173	173	173
$2\theta_{max}$ (°)	148.40	148.33	51.50
Total Data	181263	67011	21424
Unique data (R_{int})	22499 (0.1526)	5692 (0.0569)	5513 (0.0316)
Obs data [I>2(σ(I)]	15751	5165	5063
Params	1242	323	318
R_1 [I>2(σ(I)][a]	0.0742	0.0406	0.0227
wR_2 [all data][a]	0.2225	0.1095	0.0548
Max/min $\Delta\rho$ (e$^-$Å^{-3})	0.889/–0.756	0.758/–1.203	1.494 /–0.474

[a] $R_1 = \Sigma||F_o| - |F_c||/\Sigma|F_o|$; $wR_2 = [\Sigma w(F_o^2 - F_c^2)^2/\Sigma w(F_o^4)]^{1/2}$

Table 6.2. Crystallographic data for **4** and **5**.

Compound	**4**[b]	**5**
formula	$C_{60}H_{82}N_4Zr$	$C_{60}H_{82}FeN_4$
formula weight	950.51	915.14
crystal system	monoclinic	triclinic
Space Group	$P2_1/n$	$P\bar{1}$
a (Å)	10.7260(7)	11.4822(6)
b (Å)	36.864(2)	13.9697(7)
c (Å)	13.9857(10)	18.9402(10)
α (deg)	--	69.6290(9)
β (deg)	90.791(5)	76.5160(9)
γ (deg)	--	76.0852(9)
V (Å^3)	5529.5(6)	2726.9(2)
Z	4	2
ρ_{calcd} (g cm^{-3})	1.142	1.115
Abs coeff (mm^{-1})	1.913	0.316
T (K)	173	173
$2\theta_{max}$ (°)	106.32	53.50
Total Data	6237	23124
Unique data (R_{int})	22499 (0.1775)	11590 (0.0250)
Obs data [I>2(σ(I)]	15751	8231
Params	607	593
R_1 [I>2(σ(I)]^a	0.1507	0.0495
wR_2 [all data]^a	0.1859	0.1437
Max/min $\Delta\rho$ (e$^-$Å^{-3})	0.483 -0.445	0.497 /–0.559

^{a} $R_1 = \Sigma||F_o| - |F_c||/\Sigma|F_o|$; $wR_2 = [\Sigma w(F_o^2 - F_c^2)^2/\Sigma w(F_o^4)]$

^{b} Compound **4** did not diffract at high angles, and as such, the crystallographic data for this compound is not of publishable quality.

6.6 References

1. a) Roy, M. M. D.; Rivard, E. *Acc. Chem. Res.* **2017**, *50*, 2017-2025. b) Doddi, A.; Peters, M.; Tamm, M. *Chem. Rev.* **2019**, *119*, 6994-7112.

2. Ponti, P. P.; Baldwin, J. C.; Kaska, W. C. *Inorg. Chem.* **1979**, *18*, 873-875.

3. Watson, I. C.; Schumann, A.; Yu, H.; Davy, E. C.; McDonald, R.; Ferguson, M. J.; Hering-Junghans, C.; Rivard, E. *Chem. Eur. J.* **2019**, *25*, 9678-9690.

4. Kuhn, N.; Bohnen, H.; Bläser, D.; Boese, R. *Chem. Ber.* **1994**, *127*, 1405-1407.

5. Ando, S.; Ohara, A.; Ohwada, T.; Ishizuka, T. *Organometallics* **2021**, *40*, 3368-3367.

6. a) Iglesias, M.; Iturmendi, A.; Sanz Miguel, P. J.; Polo, V.; Pérez-Torrente, J. J; Oro, L. A. *Chem. Commun.* **2015**, *51*, 12431-12434. b) Iturmendi, A.; N. García, N.; Jaseer, E. A.; Munárriz, J.; Sanz Miguel, P. J.; Polo, V.; Iglesias, M.; Oro, L. A. *Dalton Trans.* **2016**, *45*, 12835-12845. c) Powers, K.; Hering-Junghans, C.; McDonald, R.; Ferguson, M. J.; Rivard, E. *Polyhedron* **2016**, *108*, 8-14. d) Fürstner, A.; Alcarazo, M.; Goddard, R.; Lehmann, C. W. *Angew. Chem. Int. Ed.* **2008**, *47*, 3210-3214. e) Kronig, S.; Jones, P. G.; Tamm, M. *Eur. J. Inorg. Chem.* **2013**, 2301-2314. f) Imbrich, D. A.; Frey, W.; Naumann, S.; Buchmeiser, M. R. *Chem. Commun.* **2016**, *52*, 6099-6102.

7. Watson, I. C.; Ferguson, M. J.; Rivard, E. *Inorg. Chem.* **2021**, *60*, 18347-18359.

8. Beaumier, E. P.; Pearce, A. J.; See, X. Y.; Tonks, I. A. *Nat. Rev. Chem.* **2019**, *3*, 15-34.

9. a) Fryzuk, M. D.; Haddad, T. S.; Rettig, S. J. *J. Am. Chem. Soc.* **1990**, *112*, 8185-8186. b) Sanner, R. D.; Manriquez, J. M.; Marsch, R. E.; Bercaw, J. E. *J. Am. Chem. Soc.* **1976**, *98*, 8351-8357. c) Mullins, S. M.; Duncan, A. P.; Bergman, R. G.; Arnold, J. *Inorg. Chem.* **2001**, *40*, 6952-6963. d) Chirik, P. J. *Dalton Trans.* **2007**, 16-25. e) Burford, R. J.; Yeo, A.; Fryzuk, M. D. *Coord. Chem. Rev.* **2017**, *334*, 84-99.

10. a) Valadez, T. N.; Norton, J. R.; Neary, M. *J. Am. Chem. Soc.* **2015**, *137*, 10152-10155. b) Rehbaum, F.; Thiele, K.-H.; Trojanov, S. I. *J. Organomet. Chem.* **1991**, *410*, 327-333. c) Okamoto, S. *Chem. Rec.* **2016**, *16*, 857-872.

11. a) Aguilar-Calderón, J. R.; Metta-Magaña, A. J.; Noll, B.; Fortier, S. *Angew. Chem. Int. Ed.* **2016**, *55*, 14101-14105. b) Clark, T. J.; Russell, C. A.; Manners, I. *J. Am. Chem. Soc.* **2006**, *128*, 9582-9583. c) Pun, D.; Lobkovsky, E.; Chirik, P. J. *Chem. Commun.* **2007**, 3297-3299. d) Solowey, D. P.; Mane, M. V.; Kurogi, T.; Carroll, P. J.; Manor, B. C.; Baik, M.-H.; Mindiola, D. J. *Nat. Chem.* **2017**, *9*, 1126-1132. e) Thomas, J.; Klahn, M.; Spannenberg, A.; Beweries, T. *Dalton Trans.* **2013**, *42*, 14668-14672. f) Lummis, P. A.; McDonald, R.; Ferguson, M. J.; Rivard, E. *Dalton Trans.* **2015**, *44*, 7009-7020.

12. a) Streuff, J.; Feurer, M.; Frey, G.; Steffani, A.; Kacprzak, S.; Weweler, J.; Leijendekker, L. H.; Kratzer, D.; Plattner, D. A. *J. Am. Chem. Soc.* **2015**, *137*, 14396-14405. b) Weweler, J.; Younas, S. L.; Streuff, J. *Angew. Chem. Int. Ed.* **2019**, *58*, 17700-17703. c) Gansäuer, A.; Hildebrandt, S.; Michelmann, A.; Dahmen, T.; von Laufenberg, D.; Kube, C.; Fianu, G. D.; Flowers II, R. A. *Angew. Chem. Int. Ed.*

2015, *54*, 7003-7006. d) Kern, C.; Selau, J.; Streuff, J. *Chem. Eur. J.* **2021**, *27*, 6178-6182.

13. Negishi, E.-i.; Cederbaum, F. E.; Takahashi, T. *Tetrahedron Lett.* **1986**, *27*, 2829-2832.

14. Rosenthal, U.; Ohff, A.; Baumann, W.; Tillack, A.; Görls, H.; Burlakov, V. V.; Shur, V. B. *Z. Anorg. Allg. Chem.* **1995**, *621*, 77-83.

15. Plundrich, G. T.; Wadepohl, H.; Clot, E.; Gade, L. H. *Chem. Eur. J.* **2016**, *22*, 9283-9292.

16. Power, P. P. *Chem. Rev.* **2012**, *112*, 3482-3507.

17. a) Bunting, P. C.; Atanasov, M.; Damgaard-Møller, E.; Perfetti, M.; Crassee, I.; Orlita, M.; Overgaard, J.; van Slageren, J.; Neese, F.; Long, J. R. *Science* **2018**, *362*, eaat7319. b) Thomsen, M. K.; Nyvang, A.; Walsh, J. P. S.; Bunting, P. C.; Long, J. R.; Neese, F.; Overgaard, J. *Inorg. Chem.* **2019**, *58*, 3211-3218.

18. Neese, F.; Pantazis, D. A. *Faraday Discuss.* **2011**, *148*, 229-238.

19. Christou, G.; Gatteschi, D.; Hendrickson, D. N.; Sessoli, R. *MRS Bulletin* **2000**, *25*, 66-71.

20. Roy, M. M. D.; Baird, S. R.; Dornsiepen, E.; Paul, L. A.; Miao, L.; Ferguson, M. J.; Zhou, Y.; Siewert, I.; Rivard, E. *Chem. Eur. J.* **2021**, *27*, 8572-8579.

21. Hering-Junghans, C.; Andreiuk, P.; Ferguson, M. J.; McDonald, R.; Rivard, E. *Angew. Chem. Int. Ed.* **2017**, *56*, 6272-6275.

22. Sharma, M.; Yameen, H. S.; Tumanskii, B.; Filimon, S.-A.; Tamm, M.; Eisen, M. S. *J. Am. Chem. Soc.* **2012**, *134*, 17234-17244.

23. Graham, T. W.; Kickham, J.; Courtenay, S.; Pingrong, W.; Stephan, D. W. *Organometallics* **2004**, *23*, 3309-3318.

24. Boynton, J. N.; Guo, J.-D.; Grandjean, F.; Fettinger, J. C.; Nagase, S.; Long, G. J.; Power, P. P. *Inorg. Chem.* **2013**, *52*, 14216-14223.

25. Aguilar-Calderón, J. R.; Murilo, J. Gomez-Torres, A.; Saucedo, C.; Jordan, A.; Metta-Magaña, A. J.; Pink, M.; Fortier, S. *Organometallics* **2020**, *39*, 295-311.

26. Peters, M.; Baabe, D.; Maekawa, M.; Bockfeld, D.; Zaretzke, M.-K.; Tamm, M.; Walter, M. D. *Inorg. Chem.* **2019**, *58*, 16475-16486.

27. Manzer, L. E.; Deaton, J.; Schrock, R. R. *Inorg. Synth.* **1982**, *21*, 135-140.

28. Sheldrick, G. M. *Acta. Crystallogr. Sect. A* **2015**, *71*, 3-8.

29. Sheldrick, G. M *Acta. Crystallogr. Sect. C* **2015**, *71*, 3-8.

Chapter 7: Summary and Future Directions

7.1. Summary and Future Work

Chapter 2 disclosed the synthesis of an anionic *N*-heterocyclic olefin (aNHO) supported $[B_2H_5]^+$ fragment and the serendipitous discovery that the parent *N*-heterocyclic olefin (NHO) acted as a catalyst for the hydroboration of ketones and aldehydes. It was noted that these reactions occurred more quickly when the ketone was electron-poor (*e.g.,* ketones with 4-ClC_6H_4 substituents reacted faster than C_6H_5 substituents), which facilitates nucleophilic attack by the NHO organocatalyst. As such, it is likely that using a more nucleophilic NHO would result in higher catalytic activity. It is important to note that while high nucleophilicity appears to facilitate these hydroboration reactions, it is likely that a very high Lewis basicity of the catalyst would be deleterious. For example, Lu showed that when $NHO\text{-}CO_2$ complexes are replaced by *N*-heterocyclic carbene-CO_2 adducts (NHCs) as organocatalysts in the carboxylative cyclization of propargyl alcohols, the NHC donor was bound too strongly to the product, preventing catalyst (NHC) regeneration. However, the weaker $NHO\text{-}CO_2$ interaction (*vs.* $NHC\text{-}CO_2$ complexation) allows for release of the product from the NHO.[1]

The Ji Group has evaluated the nucleophilicity of several different NHOs.[2] While the nucleophilicity of $IPrCH_2$ (the most thoroughly evaluated organocatalyst in Chapter 2) was not studied by Ji, a similar NHO, $IMesCH_2$ (IMes =

(HCNMes)$_2$C=CH$_2$; Mes = 2,4,6-Me$_3$C$_6$H$_2$) was. It was found that IMesCH$_2$ (**1**) was less nucleophilic than less sterically demanding NHOs, such as SImMe$_2$CH$_2$ (**2**) [SImMe$_2$ = (H$_2$CNMe)$_2$C:] and the benzimidazole-based NHO **3** (Chart 7.1). Since NHOs with greater nucleophilicity should act as more potent catalysts (*vide supra*), the use of NHOs **2** and **3** could result in a more effective catalyst system.

Chart 7.1. NHOs in ascending order of nucleophilicity as determined by Ji and coworkers.

Chapter 3 involved the synthesis of new NHOs and their use as ligands in Buchwald-Hartwig amination reactions. NHO-palladium complexes were synthesized and evaluated as pre-catalysts. It was found through a combination of poisoning, imaging, and kinetic experiments that it was not a molecular NHO-palladium complex that was the active catalyst, but colloidal palladium nanoparticles formed *in situ*. Further progress on this topic would focus mainly on the synthesis of new NHOs, with attention to functionalization of the backbone of the NHO and *N*-aryl groups of the imidazole ring. In the Organ Group's *N*-heterocyclic carbene-bearing PEPPSI pre-catalysts (PEPPSI = pyridine enhanced pre-catalyst preparation and stabilization), using palladium complexes featuring NHC ligands with chlorinated backbones resulted in increased catalyst effectiveness.[3] The synthesis of an NHO with a

chlorinated backbone (^{Cl}IPrCH$_2$) [^{Cl}IPr = (ClCNDipp)$_2$C:] would be possible by combining the known *N*-heterocyclic carbene ^{Cl}IPr[4] with KO^{t}Bu and MeI (Scheme 7.1). This NHO should be a poorer electron donor than ^{Me}IPrCH$_2$ [^{Me}IPr = (MeCNDipp)$_2$C:] (which was used extensively in Chapter 3). ^{Me}IPrCH$_2$ is highly σ-electron-donating with negligible π-electron-accepting ability. It is believed that the large amounts of electron density on the Pd^0 center result in catalyst decomposition, and formation of palladium metal. Using this chlorinated NHO in palladium-catalyzed Buchwald-Hartwig aminations may result in more effective stabilization of a molecular Pd^0 center when compared to ^{Me}IPrCH$_2$ ligands, as less electron density should be donated to the palladium center when ^{Cl}IPrCH$_2$ is used as a ligand, allowing for the access of a well-defined molecular NHO-Pd^0 catalyst.

Scheme 7.1. Proposed synthesis of ^{Cl}IPrCH$_2$.

The Organ Group has also modified the *N*-aryl groups of the NHCs used in PEPPSI pre-catalysts (*e.g.,* 2,6-isopentylphenyl or 2,6-isoheptylphenyl), finding that pre-catalysts formed with these bulky NHCs are more active in Buchwald-Hartwig cross-coupling.[5] Combination of the corresponding imidazolium salts with two

equivalents of KO^{t}Bu and one equivalent of MeI would form bulky NHOs (Scheme 7.2).

Scheme 7.2. Proposed synthesis of bulky NHOs.

^{Cl}IPrCH$_2$ would be valuable for chemists interested in using less electron-releasing NHOs as ligands in main group element or transition metal chemistry, especially when electron-rich elements are bound. Bulky NHOs featuring 2,6-isopentylphenyl or 2,6-isoheptylphenyl functionalized *N*-aryl groups could provide large amounts of steric protection to an NHO-Pd^0 catalyst. The long alkyl chains (2,6-isopentyl or 2,6-isoheptyl) provide flexible bulk, which can promote reductive elimination without dramatically hindering oxidative addition and amine binding in Buchwald-Hartwig amination.[6]

It is of great interest to use nickel-based catalysts to catalyze C–N bond forming reactions, due to the increase in price and rarity of palladium *vs.* nickel.[7] Thus, using NHOs as ligands in nickel-catalyzed cross-coupling reactions could provide a more economical method of forming C–N bonds when compared to that used in Chapter 3 (Equation 7.1).[8]

$$\text{R} \underset{}{\overset{}{\bigcirc}} \text{X} + \text{H}-\text{N} \underset{\text{R'}}{\overset{\text{R''}}{}} \xrightarrow[\text{THF, 80 °C, 1 h}]{\substack{\text{1.5 eq NaO}^t\text{Bu} \\ \text{5 mol. \% Ni[COD]}_2 \\ \text{5 mol. \% }^{\text{Me}}\text{IPrCH}_2}} \text{R} \underset{}{\overset{}{\bigcirc}} \text{N} \underset{\text{R'}}{\overset{\text{R''}}{}} \qquad (7.1)$$

NHO-trialkylaluminum adducts were used in Chapter 4 to polymerize Michael-type monomers. Three NHO-AlR$_3$ Lewis adducts were prepared by the combination of a free NHO with either AlMe$_3$ or AlEt$_3$. These adducts were proven to be potent catalysts for the polymerization of methylacrylate, 2-vinylpyridine, and dimethylacrylamide. ^{1}H NMR studies showed that NHO-AlR$_3$ adducts dissociate into free ligand and AlR$_3$, which suggests that Lewis pair polymerization (LPP) is the likely mechanism of monomer polymerization. This assertation is corroborated by the fact that neither NHOs nor trialkylaluminum species alone polymerize Michael-type monomers.

Work by Chen and coworkers have shown that using alanes with greater Lewis acidity (*e.g.,* Al(C$_6$F$_5$)$_3$) in LPP leads to greater catalyst activity.[9] As such, the synthesis of $^{\text{Me}}$IPrCH$_2$•Al(C$_6$F$_5$)$_3$ by mixing $^{\text{Me}}$IPrCH$_2$ and Al(C$_6$F$_5$)$_3$) could result in a

more effective polymerization catalyst (Chart 7.2). Chen and coworkers have also shown that functionalization of the exocyclic carbon of an NHO (*e.g.*, C=CR$_2$) with alkyl groups can supress premature chain termination in the LLP of methyl crotonate (a particularly challenging monomer).[10] As such, the synthesis and use of ImMe$_4$CMe$_2$•Al(C$_6$F$_5$)$_3$ as a polymerization catalyst could lead to higher molecular weight polymers of a more narrow polydispersity (Chart 7.2).

^{Me}IPrCH$_2$•Al(C$_6$F$_5$)$_3$ ImMe$_4$CH$_2$•Al(C$_6$F$_5$)$_3$

Chart 7.2. Proposed NHO-alane Lewis adducts for the polymerization of Michael-type monomers.

Chapter 5 featured the synthesis of (^{Me}IPrCH)$_2$Zn, which was then used to functionalize main group centers with aNHO ligands via transmetallation. (^{Me}IPrCH)$_2$Zn can be accessed by the combination of two equivalents of (^{Me}IPrCH)Li[11] with ZnCl$_2$, or in a one-pot procedure, where (^{Me}IPrCH)Li is generated *in situ* from (^{Me}IPr=CH)I.[11] The latter synthetic route has the advantage of bypassing the isolation of (^{Me}IPrCH)Li, which is thermally sensitive (decomposing over the course of 1 week in the solid state at –35 °C) and is unstable in polar solvents such as THF. This two-coordinate aNHO-zinc complex is also more thermally robust than (^{Me}IPrCH)Li (can be refluxed in toluene) and is stable in THF. Main group centers functionalized with aNHO ligands can be obtained by combining (^{Me}IPrCH)$_2$Zn with a

main group halide or hydride, which then undergo a transmetallation reaction, eliminating either $ZnCl_2$ or ZnH_2, respectively, as a side-product.

Currently, the number of aNHOs that can be installed onto main group or transition metal centers via pre-formed transfer reagents [*e.g.,* (^{Me}IPrCH)Li via salt metathesis or (^{Me}IPrCH)$_2$Zn via transmetallation] is limited to [^{Me}IPrCH]$^-$. As such there is an interest in discovering new aNHO transfer reagents. To this end, (SIPrCH)Li could be synthesized in a similar method as used to prepare (^{Me}IPrCH)Li:[11] by combination of SIPrCH$_2$ with I_2, followed by deprotonation to yield SIPr=CH(I) and lithiation with ^{n}BuLi (Scheme 7.3). This aNHO should be less strongly electron-donating than (^{Me}IPrCH)Li, and therefore should be helpful in stabilizing more electron-rich transition metal centers.

Scheme 7.3. Proposed synthesis of (SIPrCH)Li.

Unpublished attempts to stabilize Pd^{II} or Pt^{II} centers with [^{Me}IPrCH]$^-$ ligands resulted in the formation of palladium or platinum metal, presumably due to the large amount of electron density placed onto the metal center by the highly electron-releasing aNHO ligands. Using [SIPrCH]$^-$ to stabilize these Group 10 metal centers

may allow for two-coordinate Pd^{II} or Pt^{II} complexes to be isolated, which could then be reacted with alkyl or aryl halides (*e.g.,* MeI or Ph–Br) (Scheme 7.4). Should oxidative addition occur, this would prompt investigation into performing catalysis featuring a M(II)/M(IV) catalytic cycle.[12]

Scheme 7.4. The combination of two equivalents (^{Me}IPrCH)Li and a Group 10 metal dichloride resulting in the formation of metal and free ^{Me}IPr=CH$_2$ (top). The proposed synthesis of (SIPrCH)$_2$M and subsequent oxidative addition of an aryl or alkyl halide to the metal center (bottom); M = Pd or Pt.

The arylborane-aNHO complexes presented in Chapter 5 are not Lewis acidic enough (at boron) to allow frustrated Lewis pair (FLP) reactivity.[13] To this end, a transmetallation reaction involving (^{Me}IPrCH)$_2$Zn and two equivalents of Piers' borane [HB(C$_6$F$_5$)$_2$] could result in (^{Me}IPrCH)B(C$_6$F$_5$)$_2$ via elimination of ZnH$_2$ (Equation 7.2). This boron center should be more electron-deficient that those presented in Chapter 5, and therefore more likely to act as a Lewis acid, within an intramolecular FLP, to activate small molecules or to perform catalytic transfer hydrogenation reactions.[13,14]

$$\text{1/2} \quad [\text{Zn complex with Dipp, Me, N groups}] \xrightarrow[\;-\;1/2\;ZnH_2\;]{HB(C_6F_5)_2} [\text{boron complex}] \quad (7.2)$$
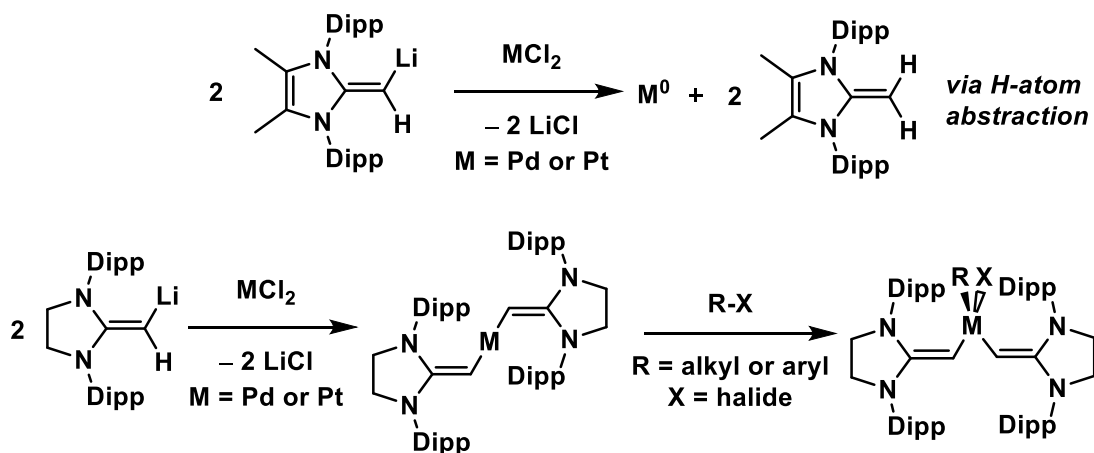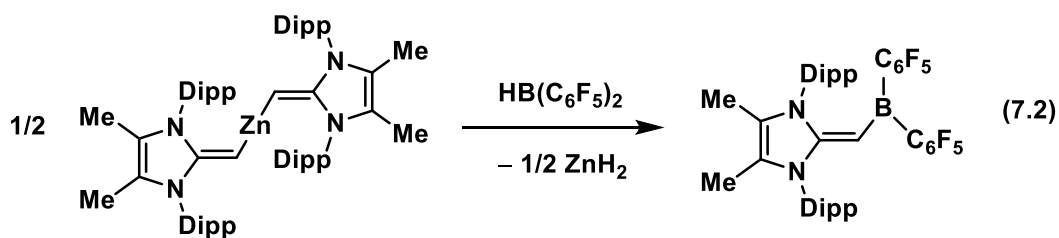
The focus of Chapter 6 was the synthesis of aNHO-supported Group 4 and Group 8 complexes. Using the previously reported ligand source (^{Me}IPrCH)Li, the syntheses of (^{Me}IPrCH)$_2$MCl$_2$ (M = Ti, Zr, and Hf) and the linear, two-coordinate (^{Me}IPrCH)$_2$Fe were completed by combining two equivalents of lithiated NHO with the respective metal halides. An interesting masked Zr(II) species was accessed by reduction of (^{Me}IPrCH)$_2$ZrCl$_2$ with sodium metal, but reproducing this result proved challenging, even when varying the reductant and reaction conditions. (^{Me}IPrCH)$_2$Fe is interesting as it is paramagnetic and has a linear geometry, which means it should have a high degree of orbital angular momentum, and thus, has the potential to act as a single molecule magnet.[15] Future work for this project will involve purification of (^{Me}IPrCH)$_2$Fe so that its magnetic properties can be evaluated in greater detail. Magnetic susceptibilities measurements in both solution (Evans method) and solid state (SQUID) should be made. To gain greater insight into the electronic structure of the iron center, Mössbauer and EPR spectroscopy experiments could also be performed.

Cationic Group 4 complexes are known to act as olefin polymerization catalysts (*e.g.,* [Cp$_2$ZrMe][MeB(C$_6$F$_5$)$_3$]).[16] A method that could be used to access

aNHO-supported Group 4 cationic complex could be to methylate $(^{Me}IPrCH)_2MCl_2$ with MeLi, followed by abstraction of a methyl group with $[Ph_3C][BAr^F_4]$ (Scheme 7.5). These cationic complexes could then be exposed to ethylene or propylene to form polyolefins. Studies by the groups of Tamm,[17] Hessen,[18] and Nomura[19] have indicated that a greater degree of π-donation from the ligand to the metal center can lead to an increase in catalyst activity. Therefore, due to the highly π-electron releasing nature of the $[^{Me}IPrCH]^-$ ligand, a $[(^{Me}IPrCH)_2MMe]^+$ cation could be an excellent olefin polymerization catalyst.
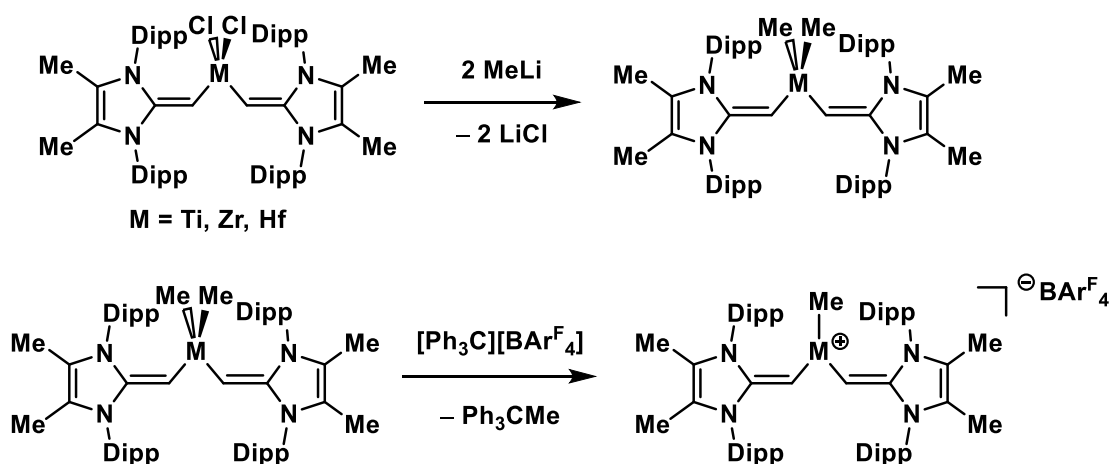
Scheme 7.5. Proposed methylation of $(^{Me}IPrCH)_2MCl_2$ followed by methyl group abstraction to generate an olefin polymerization catalyst; $Ar^F = 3,5\text{-}(F_3C)_2C_6H_3$.

7.2. References

1. Wang, Y.-B.; Wang, Y.-M.; Zhang, W.-Z.; Lu, X.-B. *J. Am. Chem. Soc.* **2013**, *135*, 11996-12003.

2. Li, Z.; Ji, P.; Cheng, J.-P. *J. Org. Chem.* **2021**, *86*, 2974-2985.

3. Pompeo, M.; Froese, R. D. J.; Hadei, N.; Organ, M. G. *Angew. Chem. Int. Ed.* **2012**, *51*, 11354-11357.

4. Arduengo III, A. J.; Krafczyk, R.; Schmutzler, R.; Craig, H. A.; Goerlich, J. R.; Marshall, W. J.; Unverzagt, M. *Tetrahedron* **1999**, *55*, 14523-14534.

5. a) Valente, C.; Çalimsiz, S.; Hoi, K. H.; Mallik, D.; Sayah, M.; Organ, M. G. *Angew. Chem. Int. Ed.* **2012**, *51*, 3314-3332. b) Atwater, B.; Chandrasoma, N.; Mitchell, D.; Rodriguez, M. J.; Organ, M. G. *Chem. Eur. J.* **2016**, *22*, 14531-14534.

6. a) Altenhoff, G.; Goddard, R.; Lehmann, C. W. Glorius, F. *Angew. Chem. Int. Ed.* **2003**, *42*, 3690-3693. b) Vanden Broeck, S. M. P.; Nahra, F.; Cazin, C. S. J. *Inorganics* **2019**, *7*, 78.

7. a) Bullock, R. M. *Catalysis Without Precious Metals*, Wiley-VCH, 2010. b) Hazari, N.; Melvin, P. R.; Beromi, M. *Nat. Rev. Chem.* **2017**, *1*, 0025.

8. a) Sinya, N.; Taisuke, M.; Yuji, K.; Kouki, M. *Chem. Lett.* **2011**, *40*, 1036-1038. b) Coman, S. M.; Parvulescu, V. I. *Org. Process Res. Dev.* **2015**, *19*, 1327-1355. c) Inatomi, T.; Fukahori, Y.; Yamada, Y.; Ishikawa, R.; Koga, Y.; Kouki, M. *Catal. Sci. Technol.* **2019**, *9*, 1784-1793.

9. Hong, M.; Chen, J.; Chen, E. Y.-X. *Chem. Rev.* **2018**, *118*, 10551-10616.

10. McGraw, M.; Chen, E. Y.-X. *ACS Catal.* **2018**, *8*, 9877-9887.

11. Roy, M. M. D.; Baird, S. R.; Dornsiepen, E; Paul, L. A.; Miao, L.; Ferguson, M. J.; Zhou, Y.; Siewert, I.; Rivard, E. *Chem. Eur. J.* **2021**, *27*, 8572-8579.

12. Xu, L.-M.; Li, B.-L.; Yang, Z.; Shi, Z.-J. *Chem. Soc. Rev.* **2010**, *39*, 712-733.

13. a) Stephan, D. W. *Science* **2016**, *354*, aaf7229. b) Légaré, M.-A.; Courtemanche, M.-A.; Rochette, É.; Fontaine, F.-G. *Science* **2015**, *349*, 513-516. c) Lui, M. W.; Paisley, N. R.; McDonald, R.; Ferguson, M. J.; Rivard, E. *Chem. Eur. J.* **2016**, *22*, 2134-2145.

14. a) Wang, D.; Astruc, D. *Chem. Rev.* **2015**, *115*, 6621-6686. b) Khan, I.; Reed-Berendt, B. G.; Melen, R. L.; Morrill, L. C. *Angew. Chem. Int. Ed.* **2018**, *57*, 12356-12359. c) Li, S.; Li, G.; Meng, W.; Du, H. *J. Am. Chem. Soc.* **2016**, *138*, 12956-12962.

15. Christou, G.; Gatteschi, D.; Hendrickson, D. N.; Sessoli, R. *MRS Bulletin* **2000**, *25*, 66-71.

16. a) Yang, X.; Stern, C. L.; Marks, T. J. *J. Am. Chem. Soc.* **1994**, *116*, 10015-10031. b) Chen, E. Y.-X.; Marks, T. J. *Chem. Rev.* **2000**, *100*, 1391-1434. c) Collins, R. A.; Russell, A. F.; Mountford, P. *Appl. Petrochem. Res.* **2015**, *5*, 135-171.

17. Sharma, M.; Yameen, H. S.; Tumanskii, B.; Filimon, S.-A.; Tamm, M.; Eisen, M. S. *J. Am. Chem. Soc.* **2012**, *134*, 17234-17244.

18. Kretschmer, W. P.; Dijkhuis, C.; Meetsma, M.; Hessen, B.; Teuben, J. H. *Chem. Commun.* **2002**, 608-609.

19. Nomura, K.; Fukada, H.; Katao, S.; Fujiki, M.; Kim, H. J.; Kim, D.-H.; Zhang, S. *Dalton Trans.* **2011**, *40*, 7842-7849.

Complete Bibliography

Chapter 1

1. Hopkinson, M. N.; Richter, C.; Schedler, M.; Glorious, F. *Nature* **2014**, *510*, 485-496.

2. Nelson, D. J.; Nolan, S. P. *N*-Heterocyclic Carbenes. In *N-Heterocyclic Carbenes: Effective Tools for Organometallic Synthesis*, 1st ed.; Wiley-VCH Verlag GmbH & Co. KGaA, 2014; pp 1-24.

3. Wanzlick, H. W. *Angew. Chem. Int. Ed. Engl.* **1962**, *1*, 75-80.

4. Hermann, W. A.; Köcher, C. *Angew. Chem. Int. Ed. Engl.* **1997**, *36*, 2162-2187.

5. Denk, M. K.; Hatano, K.; Ma, M. *Tetrahedron Lett.* **1999**, *40*, 2057-2060.

6. a) Wanzlick, H. W.; Schönherr, H. J. *Angew. Chem. Int. Ed. Engl.* **1968**, *7*, 141-142. b) Öfele, K. *J. Organometal. Chem.* **1968**, *12*, 42-43.

7. Sinclair, J.; Dai, G.; McDonald, R.; Ferguson, M. J.; Brown, A.; Rivard, E. *Inorg. Chem.* **2020**, *59*, 10996-11008.

8. Lappert, M. F.; Pye, P. L. *J. Chem. Soc., Dalton Trans.* **1978**, 837-844 and references therein.

9. Igau, A.; Grützmacher, H.; Baceiredo, A.; Bertrand, G. *J. Am. Chem. Soc.* **1988**, *110*, 6463-6466.

10. Arduengo III, A. J.; Harlow, R. L.; Kline, M. *J. Am. Chem. Soc.* **1991**, *113*, 363-365.

11. a) Crudden, C. M.; Allen, D. P. *Coord. Chem. Rev.* **2004**, *248*, 2247-2273. b) Nesterov, V.; Reiter, D.; Bag, P.; Frisch, P.; Holzner, R.; Porzelt, A.; Inoue, S. *Chem. Rev.* **2018**, *118*, 9678-9842.

12. a) Cazin, C. S. J. *N-Heterocyclic Carbenes in Transition Metal Catalysis and Organocatalysis*; Springer, Dordrecht, 2011. b) Peris, E. *Chem. Rev.* **2018**, *118*, 9988-10031.

13. Smith, C. A.; Narouz, M. R.; Lummis, P. A.; Singh, I.; Nazemi, A.; Li, C.-H.; Crudden, C. M. *Chem. Rev.* **2019**, *119*, 4986-5056.

14. Flanigan, D. M.; Romanov-Michailidis, F.; White, N. A.; Rovis, T. *Chem. Rev.* **2015**, *115*, 9307-9387.

15. Tulloch, A. A. D.; Danopoulos, A. A.; Kleinhenz, S.; Light, M. E.; Hursthouse, M. B.; Eastman, G. *Organometallics* **2001**, *20*, 2027-2031.

16. Hu, X.; Tang, Y.; Gantzel, P.; Meyer, K. *Organometallics* **2003**, *22*, 612-614.

17. Nemcsok, D.; Wichmann, K.; Frenking, G. *Organometallics* **2004**, *23*, 3640-3646.

18. a) Lavallo, V.; Canac, Y.; Präsang, C.; Donnadieu, B.; Bertrand, G. *Angew. Chem. Int. Ed.* **2005**, *44*, 5705-5709. b) Melaimi, M.; Jaszzar, R.; Soleilhavoup, M.; Bertrand, G. *Angew. Chem. Int. Ed.* **2017**, *56*, 10046-10068.

19. a) Frey, G. D.; Lavallo, V.; Donnadieu, B.; Schoeller, W. W.; Bertrand, G. *Science* **2007**, *316*, 439-441. b) Lavallo, V.; Canac, Y.; Donnadieu, B.; Schoeller, W. W.; Bertrand, G. *Angew. Chem. Int. Ed.* **2006**, *45*, 3488-3491.

20. Soleilhavoup, M.; Bertrand, G. *Acc. Chem. Res.* **2015**, *48*, 256-266.

21. Crabtree, R. H. *Coord. Chem. Rev.* **2013**, *257*, 755-766.

22. Araki, S.; Wanibe, Y.; Uno, F.; Morikawa, A.; Yamamoto, K.; Chiba, K.; Butsugan, Y. *Chem. Ber.* **1993**, *126*, 1149-1155.

23. Gründemann, S.; Kovacevic, A.; Albrecht, M.; Robert, J. W. F.; Crabtree, R. H. *Chem. Commun.* **2001**, 2274-2275.

24. a) Aldeco-Perez, E.; Rosenthal, A. J.; Parameswaran, P.; Frenking, G.; Bertrand, G. *Science* **2009**, *326*, 556-559. b) Guisado-Barrios, G.; Bouffard, J.; Donnadieu, B.; Bertrand, G. *Angew. Chem. Int. Ed.* **2010**, *49*, 4759-4762.

25. Gusev, D. G. *Organometallics* **2009**, *28*, 6458-6461.

26. Magill, A. M.; Yates, B. F. *Aust. J. Chem.* **2004**, *57*, 1205-1210.

27. a) Roy, M. M. D.; Rivard, E. *Acc. Chem. Res.* **2017**, *50*, 2017-2025. b) Doddi, A.; Peters, M.; Tamm, M. *Chem. Rev.* **2019**, *119*, 6994-7112.

28. a) Tolman, C. A. *Chem. Rev.* **1977**, *77*, 313-336. b) Chianese, A. R.; Li, X.; Janzen, M. C.; Faller, J. W.; Crabtree, R. H. *Organometallics* **2003**, *22*, 1663-1667. c) Kelly III, R. A.; Clavier, H.; Giudice, S.; Scott, N. M.; Stevens, E. D.; Bordner, J.; Samardijev, I.; Hoff, C. D.; Cavallo, L.; Nolan, S. P. *Organomettalics* **2008**, *27*, 202-210. d) Wolf, S.; Plenio, H. *J. Organomet. Chem.* **2009**, *694*, 1487-1492.

29. Powers, K.; Hering-Junghans, C.; McDonald, R.; Ferguson, M. J.; Rivard, E. *Polyhedron* **2016**, *108*, 8-14.

30. Fürstner, A.; Alcarazo, M.; Goddard, R.; Lehmann, C. W. *Angew. Chem. Int. Ed.* **2008**, *47*, 3210-3214.

31. Hillier, A. C.; Sommer, W. J.; Yong, B. S.; Petersen, J. L.; Cavallo, L.; Nolan, S. P. *Organometallics* **2003**, *22*, 4322-4326.

32. Clavier, H.; Nolan, S. P. *Chem. Commun.* **2010**, *46*, 841-861.

33. Poater, A.; Cosenza, B.; Correa, A.; Giudice, S.; Ragone, F.; Scarano, V.; Cavallo, L. *Eur. J. Inorg. Chem.* **2009**, 1759-1766.

34. Falivene, L.; Cao, Z.; Petta, A.; Serra, L.; Poater, A.; Oliva, R.; Scarano, V.; Cavallo, L. *Nat. Chem.* **2019**, *11*, 872-879.

35. El-Hellani, A.; Monot, J.; Guillot, R.; Bour, C.; Gandon, V. *Inorg. Chem.* **2013**, *52*, 506-514.

36. Powers, K. *N-Heterocyclic Olefins: An Investigation into a Developing Class of Ligands.* M.Sc. Dissertation, University of Alberta, Edmonton, AB, 2016.

37. Schuldt, R.; Kästner, J.; Naumann, S. *J. Org. Chem.* **2019**, *84*, 2209-2218.

38. Raczyńska, E. D.; Decouzon, M.; Gal, J.-F.; Maria, P.-C.; Woźniak, K.; Kurg R.; Carins, S. N. *Trends Org. Chem.* **1998**, *7*, 996-103.

39. Chen, H.; Justes, D. R.; Cooks, R. G. *Org. Lett.* **2005**, *7*, 3949-3952.

40. Wang, Z.; Niu, Q.-H.; Xue, X.-S.; Ji, P. *J. Org. Chem.* **2020**, *85*, 13204-13210.

41. Gruseck, U.; Heuschmann, M. *Chem. Ber.* **1987**, *120*, 2053-2064.

42. Li, Z.; Ji, P.; Cheng, J.-P. *J. Org. Chem.* **2021**, *86*, 2974-2985.

43. a) Mayr, H.; Patz, M. *Angew. Chem. Int. Ed. Engl.* **1994**, *33*, 938-957. b) Maji, B.; Breugst, M.; Mayr, H. *Angew. Chem. Int. Ed.* **2011**, *50*, 6915-6919. c) Levens, A.; An, F.; Breugst, M.; Mayr, H. *Org. Lett.* **2016**, *18*, 3566-3569.

44. Ponti, P. P.; Baldwin, J. C.; Kaska, W. C. *Inorg. Chem.* **1979**, *18*, 873-875.

45. a) Kuhn, N.; Bohnen, H.; Bläser, D.; Boese, R. *Chem. Ber*. **1994**, *127*, 1405-1407.

b) Kuhn, N.; Bohnen, H.; Kreutzberg, J.; Bläser, D.; Boese, R. *J. Chem. Soc., Chem. Commun*. **1993**, 1136-1137.

46. Schumann, H.; Glanz, M.; Winterfeld, J.; Hemling, H.; Kuhn, N.; Bohnen, H.; Blaser, D.; Boese, R. *J. Organomet. Chem.* **1995**, *493*, C14-C18.

47. Dumrath, A.; Wu, X.-F.; Neumann, H.; Spannenberg, A.; Jackstell, R.; Beller, M. *Angew. Chem. Int. Ed.* **2010**, *49*, 8988-8992.

48. Al-Rafia, S. M. I.; Malcolm, A. C.; Liew, S. K.; Ferguson, M. J.; McDonald, R.; Rivard, E. *Chem. Commun.* **2011**, *47*, 6987-6989.

49. Al-Rafia, S. M. I.; Momeni, M. R.; Ferguson, M. J.; McDonald, R.; Brown, A.; Rivard, E. *Organometallics* **2013**, *32*, 6658-6665.

50. Ghadwal, R. S.; Schürmann, C. J.; Andrada, D. M.; Frenking, G. *Dalton Trans.* **2015**, *44*, 14359-14367.

51. Kronig, S.; Jones, P. G.; Tamm, M. *Eur. J. Inorg. Chem.* **2013**, 2301-2314.

52. Imbrich, D. A.; Frey, W.; Naumann, S.; Buchmeiser, M. R. *Chem. Commun.* **2016**, *52*, 6099-6102.

53. Rufh, S. A.; Goudreault, A. Y.; Foscato, M.; Jensen, V. R.; Fogg, D. E. *ACS Catal.* **2018**, *8*, 11822-11826.

54. Wang, Y. W.; Abraham, M. Y.; Gilliard Jr. R. J.; Sexton, D. R.; Wei, P.; Robinson, G. H. *Organometallics* **2013**, *32*, 6639-6642.

55. Enders, D.; Breuer, K.; Raabe, G.; Runsink, J.; Teles, H.; Melder, J.-P.; Ebel, K.; Brode, S. *Angew. Chem. Int. Ed. Engl.* **1995**, *34*, 1021-1023.

56. Matsuoka, S.; Tochiji, Y.; Takagi, K.; Suzuki, M. *Tetrahedron* **2012**, *68*, 9836-9841.

57. Hansmann, M. M.; Antoni, P. W.; Pesch, H. *Angew. Chem. Int. Ed.* **2020**, *59*, 5782-5787.

58. Clendenning, S. B.; Hitchcock, P. B.; Nixon, J. F.; Nyulászi, L. *Chem. Commun.* **2000**, 1305-1306.

59. Hahn, F. E.; Wittenbecher, L.; Van, D. L.; Frölich, R.; Wibbeling, B. *Angew. Chem. Int. Ed.* **2000**, *39*, 2307-2310.

60. Kuhn, N.; Göhner, M.; Steimann, M. *Z. Anorg. Allg. Chem.* **2002**, *628*, 1108-1115.

61. Al-Rafia, S. M. I.; Ferguson, M. J.; Rivard, E. *Inorg. Chem.* **2011**, *50*, 10543-10545.

62. Paisley, N. R.; Lui, M. W.; McDonald, R.; Ferguson, M. J.; Rivard, E. *Dalton Trans.* **2016**, *45*, 9860-9870.

63. Lui, M. W.; Shynkaruk, O.; Oakley, M. S.; Sinelnikov, R.; McDonald, R.; Ferguson, M. J.; Meldrum, A.; Klobukowski, M.; Rivard, E. *Dalton Trans*. **2017**, *46*, 5946-5954.

64. Hering-Junghans, C.; Andreiuk, P.; Ferguson, M. J.; McDonald, R.; Rivard, E. *Angew. Chem. Int. Ed*. **2017**, *56*, 6272-6275.

65. Eymann, L. Y. M.; Varava, P.; Shved, A. M.; Curchod, B. F. E.; Liu, Y.; Planes, O. M.; Sienkiewicz, A.; Scopelliti, R.; Tirani, F. F.; Severin, K. *J. Am. Chem. Soc.* **2019**, *141*, 17112-17116.

66. Roy, M. M. D.; Baird, S. R.; Dornsiepen, E; Paul, L. A.; Miao, L.; Ferguson, M. J.; Zhou, Y.; Siewert, I.; Rivard, E. *Chem. Eur. J.* **2021**, *27*, 8572-8579.

67. Gentner, T. X.; Ballmann, G.; Pahl, J.; Elsen, H.; Harder, S. *Organometallics* **2018**, *37*, 4473-4480.

68. a) Crocker, R. D.; Nguyen, T. V. *Chem. Eur. J.* **2016**, *22*, 2208-2213. b) Neumann, S. *Chem. Commun.* **2019**, *55*, 11658-11670.

69. Breslow, R. *J. Am. Chem. Soc.* **1958**, *80*, 3719-3726.

70. Paul. M.; Sudkaow, P.; Wessels, A.; Schlörer, N. E.; Neudörfl, J.-M.; Berkessel, A. *Angew. Chem. Int. Ed.* **2018**, *57*, 8310-8315.

71. Wang, Y.-B.; Wang, Y.-M.; Zhang, W.-Z.; Lu, X.-B. *J. Am. Chem. Soc.* **2013**, *135*, 11996-12003.

72. Saptal, V. B.; Bhanage, B. M. *ChemSusChem* **2016**, *9*, 1980-1985.

73. Kaya, U.; Tran, U. P. N.; Enders, D.; Ho, J.; Nguyen, T. V. *Org. Lett.* **2017**, *19*, 1398-1401.

74. Blümel, M.; Noy, J.-M.; Enders, D.; Stenzel, M. H.; Nguyen, T. V. *Org. Lett.* **2016**, *18*, 2208-2211.

75. Peixoto, D.; Malta, G.; Cruz, H.; Barroso, S.; Carvalho, A. L.; Ferreira, L. M.; Branco, P. S. *J. Org. Chem.* **2019**, *84*, 3793-3800.

76. a) Zhang, Y.; Miyake, G. M.; Chen, E. Y.-X. *Angew. Chem. Int. Ed.* **2010**, *49*, 10158-10162. b) Hong, M.; Chen, J.; Chen, E. Y.-X. *Chem. Rev.* **2018**, *118*, 10551-10616.

77. McGraw, M. L.; Chen, E. Y.-X. *Macromolecules* **2020,** *53*, 6102-6122.

78. Jia, Y.-B.; Wang, Y.-B.; Ren, W.-M.; Xu. T.; Wang, J.; Lu, X.-B. *Macromolecules* **2014**, *47*, 1966-1972.

79. Wang, Q.; Zhao, W.; Zhang, S.; He, J.; Zhang, Y.; Chen, E. Y.-X. *ACS Catal.* **2018**, *8*, 3571-3578.

80. McGraw, M.; Chen, E. Y.-X. *ACS Catal.* **2018**, *8*, 9877-9887.

81. Walther, P.; Krauß, A.; Naumann, S. *Angew. Chem. Int. Ed.* **2019**, *58*, 10737-10741.

82. Naumann, S.; Thomas, A. W.; Dove, A. P. *Angew. Chem. Int. Ed.* **2015**, *54*, 9550-9554.

83. Balint, A.; Papendick, M.; Clauss, M.; Müller, C.; Giesselmann, F.; Naumann, S. *Chem. Commun.* **2017**, *54*, 2220-2223.

84. Naumann, S.; Thomas, A. W.; Dove, A. P. *ACS Macro Lett.* **2016**, *5*, 134-138.

85. Naumann, S.; Mundsinger, K.; Cavallo, L.; Falivene, L. *Polym. Chem.* **2017**, *8*, 5803-5812.

86. Frankland, E. *Justus Liebigs Ann. Chem.* **1849**, *71*, 171-213.

87. Frankland, E. *Q. J. Chem. Soc.* **1861**, *13*, 177-235.

88. Frankland, E.; Duppa, B. F. *J. Chem. Soc.* **1864**, *17*, 29-36.

89. Rasmussen, S. C. *ChemTexts* **2021**, *7*, DOI:10.1007/s40828-020-00124-9.

90. Pearson, R. G. *J. Am. Chem. Soc.* **1963**, *85*, 3533-3539.

91. Yimin, S.; Piers, W. E.; Parvez, M. *Can. J. Chem*. **1998**, *76*, 513-517.

92. Williams, V. C.; Piers, W. E.; Clegg, W.; Elsegood, M. R. J.; Collins, S.; Marder, T. B. *J. Am. Chem. Soc.* **1999**, *121*, 3244-3245.

93. a) Esqueda, A. C.; Conejero, S.; Maya, C.; Carmona, E. *Organometallics* **2009**, *28*, 45-47. b) Lee, J.-D.; Han, W.-S.; Kim, T.-J.; Kim, S. H.; Kang, S. O. *Chem. Commun.* **2011**, *47*, 1018-1020. c) Oversby, J. S.; Jayaratne, K. C.; Schoell, N. J.; Hanusa, T. P. *Organometallics* **1999**, *18*, 1663-1668.

94. Fagan, P. J.; Nugent, W. A. *J. Am. Chem. Soc.* **1998**, *110*, 2310-2312.

95. Yan, X.; Xi. C. *Coord. Chem. Rev.* **2017**, *350*, 275-284.

96. Rivard, E. *Chem. Rec.* **2020**, *20*, 640-648.

97. a) He, G.; Kang, L.; Torres Delgado, W.; Shynkaruk, O.; Ferguson, M. J.; McDonald, R.; Rivard, E. *J. Am. Chem. Soc.* **2013**, *135*, 5360-5363. b) Parke, S. M.; Hupf, E.; Matharu, G. K.; de Aguiar, I.; Xu, L.; Yu, H.; Boone, M. P.; de Souza, G. L. C.; McDonald, R.; Ferguson, M. J.; He, G.; Brown, A.; Rivard, E. *Angew. Chem. Int. Ed.* **2018**, *57*, 14841-14846.

98. Johansson, C. C. C.; Kitching, M. O.; Colacot, T. J.; Snieckus, V. *Angew. Chem. Int. Ed.* **2012**, *51*, 5062-5085.

99. Miyaura, N.; Suzuki, A. *Chem. Rev.* **1995**, *95*, 2457-2483.

100. Amatore, C.; Jutland, A.; Le Duc, G. *Chem. Eur. J.* **2011**, *17*, 2492-2503.

101. Thomas, A. A.; Denmark, S. E. *Science* **2016**, *352*, 329-332.

102. a) Liu, Q.; Lan, Y.; Liu, J.; Wu, Y.-D.; Lei, A. *J. Am. Chem. Soc.* **2009**, *131*, 10201-10210. b) Jin. L.; Lei, A. *Org. Biomol. Chem.* **2012**, *10*, 6817-6825.

103. a) Ruiz-Castillo, P.; Buchwald, S. L. *Chem. Rev.* **2016**, *116*, 12564-12649. b) Kawaguchi, K.; Nakano, K.; Nozaki, K. *Org. Lett.* **2008**, *10*, 119-1202. c) Tan, Y.;

Liang, M.; Lu, Z.; Zheng, Y.; Tong, X.; Sun, Z.; Xue, S. *Org. Lett.* **2014**, *16*, 3978-3981.

145. Dorel, R.; Grugel, C. P.; Haydl, A. M. *Angew. Chem. Int. Ed.* **2019**, *58*, 17118-17129.

104. Sample, H. C.; Senge, M. O. *Eur. J. Org. Chem.* **2021**, 7-42.

105. a) Sambiago, C.; Marsden, S. P.; Blacker, A. J.; McGowan, P. C. *Chem. Soc. Rev.* **2014**, *43*, 3525-3550. b) Lin, H.; Sun, D. *Org. Prep. Proced. Int.* **2013**, *45*, 341-394.

106. Kosugi, M.; Kameyama, M.; Migita, T. *Chem. Lett.* **1983**, *12*, 927-928.

107. Boger, L. D.; Panek, J. S. *Tetrahedron Lett.* **1984,** *25*, 3175-3178.

108. Sunesson, Y.; Limé, E.; Nilsson Lill, S. O.; Meadows, R. E.; Norrby, P.-O. *J. Org. Chem.* **2014**, *79*, 11961-19969.

109. Guram, A. S.; Rennels, R. A.; Buchwald, S. L. *Angew. Chem. Int. Ed. Engl.* **1995**, *34*, 1348-1350.

110. Louie, J.; Hartwig, J. F. *Tetrahedron Lett.* **1995**, *36*, 3609-3612.

111. Muci, A. R.; Buchwald, S. L. *Practical Palladium Catalysts for C-N and C-O Bond Formation*. In Cross-Coupling Reactions; Topics in Current Chemistry; vol 219. Springer, Berlin, Heidelberg; pp 131-209.

112. a) Alcazar-Roman, L. M.; Hartwig, J. F.; Rheingold, A. L.; Liable-Sands, L. M.; Guzei, I. A. *J. Am. Chem. Soc.* **2000**, *122*, 4618-4630. b) Alcazar-Roman, L. M.; Hartwig, J. F. *J. Am. Chem. Soc.* **2001**, *123*, 12905-12906. c) Singh, U. K.; Strieter, E. R.; Blackmond, D. G.; Buchwald, S. L. *J. Am. Chem. Soc.* **2002**, *124*, 14104-14114.

d) Shekhar, S.; Ryberg, P.; Hartwig, J. F.; Mathew, J. S.; Blackmond, D. G. *J. Am. Chem. Soc.* **2006**, *128*, 3584-3591.

113. Louie, J.; Paul, F.; Hartwig, J. F. *Organometallics* **1996**, *15*, 2794-2805.

114. Thomas, G. T.; Janusson, E.; Zijlstra, H. S.; McIndoe, J. S. *Chem. Commun.* **2019**, *55*, 11727-11730.

115. Wambua, V.; Hirschi, J. S.; Vetticatt, M. J. *ACS Catal.* **2021**, *11*, 60-67.

116. Tian, J.; Wang, G.; Qi, Z.-H.; Ma, J. *ACS Omega* **2020**, *5*, 21385-21391.

117. Wolfe, J. P.; Wagaw, S.; Buchwald, S. L. *J. Am. Chem. Soc.* **1996**, *118*, 7215-7216.

118. a) Mann, G.; Hartwig, J. F.; Driver, M. S.; Fernández-Rivas, C. *J. Am. Chem. Soc.* **1998**, *120*, 827-828. b) Wolfe, J. P.; Ahman, J.; Sadigui, J. P.; Singer, R. A.; Buchwald, S. L. *Tetrahedron Lett.* **1997**, *38*, 6367-6370. c) Shakespeare, W. C. *Tetrahedron Lett.* **1999**, *40*, 2035-2038. d) Bolm, C.; Hildebrand, J. P. *Tetrahedron Lett.* **1998**, *39*, 5731-5734.

119. Mole, L.; Spencer, J. L.; Carr, N.; Orpen, A. G. *Organometallics* **1991**, *10*, 49-52.

120. Marcone, J. E.; Moloy, K. G. *J. Am. Chem. Soc.* **1998**, *120*, 8527-8528.

121. Fujita, K.-I.; Yamashita, M.; Puschmann, F.; Alvarez-Falcon, M. M.; Incarvito, C. D.; Hartwig, J. F. *J. Am. Chem. Soc.* **2006**, *128*, 9044-9045.

122. Surry, D. S.; Buchwald, S. L. *Angew. Chem. Int. Ed.* **2008**, *47*, 6338-6361.

123. Barder, T. E.; Buchwald, S. L. *J. Am. Chem. Soc.* **2007**, *129*, 5096-5101.

124. a) Lundgren, R. J.; Peters, B. D.; Alsabeh, P. G.; Stradiotto, M. *Angew. Chem. Int. Ed.* **2010**, 4071-4074. b) Lundgren, R. J.; Stradiotto, M. *Angew. Chem. Int. Ed.* **2010**, *49*, 8686-8690.

125. Lavoie, C. M.; MacQueen, P. M.; Rotta-Loria, N. L.; Sawatzky, R. S.; Borzenko, A.; Chisholm, A. J.; Hargreaves, B. K. V.; McDonald, R.; Ferguson, M. J.; Stradiotto, M. *Nat. Commun.* **2016**, *7*, 11073.

126. Fors, B. P.; Davis, N. D.; Buchwald, S. L. *J. Am. Chem. Soc.* **2009**, *131*, 5766-5768.

127. Surry, D. S.; Buchwald, S. L.; *Chem. Sci.* **2011**, *2*, 27-50.

128. Maiti, D.; Fors, B. P.; Henderson, J. L.; Nakamura, Y.; Buchwald, S. L. *Chem. Sci.* **2011**, *2*, 57-68.

129. Düfert, M. A.; Billingsley, K. L.; Buchwald, S. L. *J. Am. Chem. Soc.* **2013**, *135*, 12877-12885.

130. Ueling, M. R.; King, R. P.; Krska, S. W.; Cernak, T.; Buchwald, S. L. *Science* **2019**, *363*, 405-408.

131. Huang, J.; Grasa, G.; Nolan, S. P. *Org. Lett.* **1999**, *1*, 1307-1309.

132. Stauffer, S. R.; Lee, S. Stambuli, J. P.; Hauck, S. I.; Hartwig, J. F. *Org. Lett.* **2000**, *2*, 1423-1426.

133. Viciu, M. S.; Germaneau, R. F.; Navarro-Fernandez, O.; Stevens, E. D.; Nolan, S. P. *Organometallics* **2002**, *21*, 5470-5472.

134. Marion, N.; Navarro, O.; Mei, J.; Stevens, E. D.; Scott, N. M.; Nolan, S. P. *J. Am. Chem. Soc.* **2006**, *128*, 4101-4111.

135. Marion, N.; Ecarnot, E. C.; Navarro, O.; Amoroso, D.; Bell, A.; Nolan, S. P. *J. Org. Chem.* **2006**, *71*, 3816-3821.

136. a) O'Brien, C. J.; Kantchev, E. A. B.; Valente, C.; Hadei, N.; Chass, G. A.; Lough, A. J.; Hopkinson, A. C.; Organ, M. G. *Chem. Eur. J.* **2006**, *12*, 4743-4748. b) Organ, M. G.; Abdel-Hadi, M.; Avola, S.; Dubovyk, I.; Hadei, N.; Kantchev, E. A. B.; O'Brien, C. J.; Sayah, M.; Valente, C. *Chem. Eur. J.* **2008**, *14*, 2443-2452.

137. Valente, C.; Çalimsiz, S.; Hoi, K. H.; Mallik, D.; Sayah, M.; Organ, M. G. *Angew. Chem. Int. Ed.* **2012**, *51*, 3314-3332.

138. Guillet, S.G.; Voloshkin, V. A.; Saab, M.; Beliš, M.; Van Hecke, K.; Nahra, F.; Nolan, S. P. *Chem. Commun.* **2020**, *56*, 5953-5956.

139. Sayah, M.; Organ, M. G. *Chem. Eur. J.* **2013**, *19*, 16196-16199.

140. Pompeo, M.; Farmer, J. L.; Froese, R. D. J.; Organ, M. G. *Angew. Chem. Int. Ed.* **2014**, *53*, 3223-3226.

141. Fantasia, J.; Petersen, J. L.; Jacobsen, H.; Cavallo, L.; Nolan, S. P. *Organometallics* **2007**, *26*, 5880-5889.

146. Organ, M. G.; Çalimsiz, S.; Sayah, M.; Hoi, K. H.; Lough, A. J. *Angew. Chem. Int. Ed.* **2009**, *48*, 2383-2387.

147. a) Hoi, K. H.; Coggan, J. A.; Organ, M. G. *Chem. Eur. J.* **2012**, *19*, 843-845. b) Atwater, B.; Chandrasoma, N.; Mitchell, D.; Rodriguez, M. J.; Organ, M. G. *Chem. Eur. J.* **2016**, *22*, 14531-14534.

Chapter 2

1. a) Brown, H. C.; Rao, B. C. S. *J. Am. Chem. Soc.* **1956**, *78*, 5694-5695. b) Köster, R. *Liebigs Ann. Chem.* **1958**, *618*, 31-43.

2. a) Magano, J.; Dunetz, J. R. *Org. Process Res. Dev.* **2012**, *16*, 1156-1184. b) Clarke, M. L.; Roff, G. J. *The Handbook of Homogeneous Hydrogenation*, Wiley-VCH Verlag GmbH, 2008, pp. 413-454.

3. a) Suzuki, A. *J. Organomet. Chem.* **1999**, *576*, 147-168. b) Lennox, A. J. J.; Lloyd-Jones, G. C. *Chem. Soc. Rev.* **2014**, *43*, 412-443.

4. Hadlington, T. J.; Hermann, M.; Frenking, G.; Jones, C. *J. Am. Chem. Soc.* **2014**, *136*, 3028-3031.

5. Schneider, J.; Sindlinger, C. P.; Freitag, S. M.; Schubert, H.; Wesemann, L. *Angew. Chem. Int. Ed.* **2017**, *56*, 333-337.

6. a) Arrowsmith, M.; Hadlington, T. J.; Hill, M. S.; Kociok-Köhn, G. *Chem. Commun.* **2012**, *48*, 4567-4569. b) Fohlmeister, L.; Stasch, A. *Chem. Eur. J.* **2016**, *22*, 10235-10246.

7. a) Gudat, D. *Acc. Chem. Res.* **2010**, *43*, 1307-1316. b) Chong, C. C.; Kinjo, R. *ACS Catal.* **2015**, *5*, 3238-3259.

8. a) Mukherjee, D.; Osseili, H.; Spaniol, T. P.; Okuda, J. *J. Am. Chem. Soc.* **2016**, *138*, 10790-107930. b) Jakhar, V. K.; Barman, M. K.; Nembenna, S. *Org. Lett.* **2016**, *18*, 4710-4713. c) Bismuto, A.; Thomas, S. P.; Cowley, M. J. *Angew. Chem. Int. Ed.* **2016**, *55*, 15356-15359. d) Blake, A. J.; Cunningham, A.; Ford, A.; Teat, S. J.; Woodward, S. *Chem. Eur. J.* **2000**, *6*, 3586-3594.

9. a) Lummis, P. A.; Momeni, M. R.; Lui, M. W.; McDonald, R.; Ferguson, M. J.; Miskolzie, M.; Brown, A.; Rivard, E. *Angew. Chem. Int. Ed.* **2014**, *53*, 9347-9351. For reviews on zinc hydrides and main group element hydrides, see: b) Wiegand, A.-K.; Rit, A.; Okuda, J. *Coord. Chem. Rev.* **2016**, *314*, 71-82. c) Roy, M. M. D.; Omaña, A. A.; Wilson, A. S. S.; Hill, M. S.; Aldridge, S.; Rivard, E. *Chem. Rev.* **2021**, *121*, 12784-12965.

10. Roy, M. M. D.; Ferguson, M. J.; McDonald, R.; Rivard, E. *Chem. Eur. J.* **2016**, *22*, 18236-18246.

11. a) Hering-Junghans, C.; Andreiuk, P.; Ferguson, M. J.; McDonald, R; Rivard, E. *Angew. Chem. Int. Ed.* **2017**, *56*, 6272-6275. b) Roy, M. M. D.; Baird, S. R.; Dornsiepen, E.; Paul, L. A.; Miao, L.; Ferguson, M. J.; Zhou, Y.; Siewert, I.; Rivard, E. *Chem. Eur. J.* **2021**, *27*, 8572-8579.

12. Stephan, D. W. *Science* **2016**, *354*, aaf7229.

13. Légaré, M.-A.; Courtemanche, M.-A.; Rochette, É.; Fontaine, F.-G. *Science* **2015**, *349*, 513-516.

14. Lui, M. W.; Paisley, N. R.; McDonald, R.; Ferguson, M. J.; Rivard, E. *Chem. Eur. J.* **2016**, *22*, 2134-2145.

15. a) Kuhn, N.; Bohnen, H.; Kreutzberg, J.; Bläser, D.; Boese, R. *J. Chem. Soc., Chem. Commun.* **1993**, 1136-1137. b) Knappke, C. E. I.; Arduengo III, A. J.; Jiao, H.; Neudörfl, J.-M.; von Wangelin, A. J. *Synthesis* **2011**, 3784-3795. c) Al-Rafia, S. M. I.; Malcolm, A. C.; Liew, S. K.; Ferguson, M. J.; McDonald, R.; Rivard, E. *Chem.*

Commun. **2011**, *47*, 6987-6989. d) Powers, K.; Hering-Junghans, C.; McDonald, R.; Ferguson, M. J.; Rivard, E. *Polyhedron* **2016**, *108*, 8-14.

16. For recent review articles see: a) Roy, M. M. D.; Rivard, E. *Acc. Chem. Res.* **2017**, *50*, 2017-2025. b) Crocker, R. D.; Nguyen, T. V. *Chem. Eur. J.* **2016**, *22*, 2208-2213. c) Saptal, V. B.; Bhanage, B. M. *ChemSusChem* **2016**, *9*, 1980-1985. d) Ghadwal, R. S. *Dalton Trans.* **2016**, *45*, 16081-16095. See also: e) Wang, Q.; Zhao, W.; He, J.; Zhang, Y.; Chen, E. Y.-X. *Macromolecules* **2017**, *50*, 123-136. f) Wang, Y.-B.; Wang, Y.-M.; Zhang, W.-Z.; Lu, X.-B. *J. Am. Chem. Soc.* **2013**, *135*, 11996-12003. g) Blümel, M.; Noy, J.-M.; Enders, D.; Stenzel, M. H.; Nguyen, T. V. *Org. Lett.* **2016**, *18*, 2208-2211. h) Naumann, S.; Thomas, A. W.; Dove, A. P. *Angew. Chem. Int. Ed.* **2015**, *54*, 9550-9554.

17. For a related silylated NHO, see: Ghadwal, R. S.; Reichmann, S. O.; Englehardt, F.; Andrada, D. M.; Frenking, G. *Chem. Commun.* **2013**, *49*, 9440-9442.

18. Despite the low quality of the X-ray data, atom connectivity in **3a** was confirmed. Closer inspection of the difference map revealed a minor germanium containing component, IPrCH–GeH, which was allowed to refine freely with an occupancy of 4.5 %; the bulk sample of **3b** for which yield and analytical data was obtained did not have the Ge impurity.

19. Ghadwal, R. S.; Schürmann, C. J.; Andrada, D. M.; Frenking, G. *Dalton Trans.* **2015**, *44*, 14359-14367.

20. Petz, W.; Öxler, F.; Neumüller, B.; Tonner, R.; Frenking, G. *Eur. J. Inorg. Chem.* **2009**, 4507-4517.

21. Lafage, M.; Pujol, A.; Saffon-Merceron, N.; Mézailles, N. *ACS Catal.* **2016**, *6*, 3030-3035.

22. For recent work involving hybrid *N*-heterocyclic olefin-phosphine (NHOP) ligands as four-electron donors, see: a) Paisley, N. R.; Lui, M. W.; McDonald, R.; Rivard, E. *Dalton Trans.* **2016**, *45*, 9860-9870. b) Lui, M. W.; Shynkaruk, O.; Oakley, M. S.; Sinelnikov, R.; McDonald, R.; Ferguson, M. J.; Klobukowski, M.; Rivard, E. *Dalton Trans.* **2017**, *46*, 5946-5954.

23. Weigend, F.; Ahlrichs, R. *Phys. Chem. Chem. Phys.* **2005**, 7, 3297-3305.

24. Courtemanche, M.-A.; Légaré, M.-A.; Maron, L.; Fontaine, F.-G. *J. Am. Chem. Soc.* **2013**, *135*, 9326-9329.

25. Chong, C. C.; Hirao, H.; Kinjo, R. *Angew. Chem. Int. Ed.* **2014**, *54*, 190-194.

26. Sheldrick, G. M. *Acta. Crystallogr. Sect. A* **2015**, *A71*, 3-8.

27. Sheldrake, G. M. *Acta. Crystallogr. Sect. C* **2015**, *C71*, 3-8.

28. Frisch, M. J.; Trucks, G. W.; Schlegel, H. B.; Scuseria, G. E.; Robb, M. A.; Cheeseman, J. R.; Scalmani, G.; Barone, V.; Petersson, G. A.; Nakatsuji, H.; Li, X.; Caricato, M.; Marenich, A. V.; Bloino, J.; Janesko, B. G.; Gomperts, R.; Mennucci, B.; Hratchian, H. P.; Ortiz, J. V.; Izmaylov, A. F.; Sonnenberg, J. L.; Williams-Young, D.; Ding, F.; Lipparini, F.; Egidi, F.; Goings, J.; Peng, B.; Petrone, A.; Henderson, T.; Ranasinghe, D.; Zakrzewski, V. G.; Gao, J.; Rega, N.; Zheng, G.; Liang, W.; Hada, M.; Ehara, M.; Toyota, K.; Fukuda, R.; Hasegawa, J.; Ishida, M.; Nakajima, T.; Honda, Y.; Kitao, O.; Nakai, H.; Vreven, T.; Throssell, K.; Montgomery, J. A., Jr.; Peralta, J. E.; Ogliaro, F.; Bearpark, M. J.; Heyd, J. J.;

Brothers, E. N.; Kudin, K. N.; Staroverov, V. N.; Keith, T. A.; Kobayashi, R.; Normand, J.; Raghavachari, K.; Rendell, A. P.; Burant, J. C.; Iyengar, S. S.; Tomasi, J.; Cossi, M.; Millam, J. M.; Klene, M.; Adamo, C.; Cammi, R.; Ochterski, J. W.; Martin, R. L.; Morokuma, K.; Farkas, O.; Foresman, J. B.; Fox, D. J. Gaussian 16, Revision A.03; Gaussian, Inc.: Wallingford, CT, **2016**.

29. Becke, A. D. *Phys. Rev. A* **1988**, *38*, 3098-3100.

30. a) Glendening, E. D.; Weinhold, F. *J. Comput. Chem.* **1998**, *19*, 593-609. b) Glendening, E. D.; Weinhold, F. *J. Comput. Chem.* **1998**, *19*, 610-627.

31. a) Hadlington, T. J.; Hermann, M.; Frenking, G.; Jones, C. J. Am. Chem. Soc. 2014, 136, 3028-3031. b) Arrowsmith, M.; Hadlington, T. J.; Hill, M. S.; Kociok-Köhn, G. Chem. Commun. 2012, 48, 4567-4569/

32. Chong, C. C.; Hirao, H.; Kinjo, R. Angew. Chem. Int. Ed. 2015, 54, 190-195.

Chapter 3

1. Arduengo, A. J.; Harlow, R. L.; Kline, M. *J. Am. Chem. Soc.* **1991**, *113*, 361-363.

2. Nolan, S. P.; Cazin, C. S. J. *Science of Synthesis: N-Heterocyclic Carbenes in Catalytic Organic Synthesis, Vol. 1* (Eds.: S. P. Nolan, C. S. J. Cazin), Thieme, Stuttgart, 2017, pp. 161-182.

3. a) Grendemann, S.; Kovacevic, A.; Albrecht, M.; Faller, J. W.; Crabtree, R. H. *J. Am. Chem. Soc.* **2002**, *124*, 10473-10481. b) Lebel, H.; Janes, M. K.; Charette, A. B.;

Nolan, S. P. *J. Am. Chem. Soc.* **2004**, *126*, 5046-5047. c) Schuster, O.; Yang, L.; Raubenheimer, H. G.; Albrecht, M. *Chem. Rev.* **2009**, *109*, 3445-3478.

4. Melaimi, M.; Jazzar, R.; Soleilhavoup, M.; Bertrand, G. *Angew. Chem. Int. Ed.* **2017**, *56*, 10046-10068.

5. a) Dröge, T.; Glorius, F. *Angew. Chem. Int. Ed.* **2010**, *49*, 6940-6952. b) Hopkinson, M. N.; Richter, C.; Schedler, M.; Glorius, F. *Nature* **2014**, *510*, 485-496.

6. Fortman, G. C.; Nolan, S. P. *Chem. Soc. Rev.* **2011**, *40*, 5151-5169.

7. Viciu, M. S.; Kissling, R. M.; Stevens, E. D.; Nolan, S. P. *Org. Lett.* **2002**, *4*, 2229-2231.

8. a) Viciu, M. S.; Germaneau, R. F.; Navarro-Fernandez, O.; Stevens, E. D.; Nolan, S. P. *Organometallics* **2002**, *21*, 5470-5472. b) Marion, N.; Navarro-Fernandez, O.; Mei, J.; Stevens, E. D.; Scott, N. M.; Nolan, S. P. *J. Am. Chem. Soc.* **2006**, *128*, 4101-4111.

9. a) O'Brien, C. J.; Kantchev, E. A. B.; Valente, C.; Hadei, N.; Chass, G. A.; Lough, A. J.; Hopkinson, A. C.; Organ, M. G. *Chem. Eur. J.* **2006**, *12*, 4743-4748. b) Organ, M. G.; Abdel-Hadi, M.; Avola, S.; Dubovyk, I.; Hadei, N.; Kantchev, E. A. B.; O'Brien, C. J.; Sayah, M.; Valente, C. *Chem. Eur. J.* **2008**, *14*, 2443-2452. c) Tu, T.; Fang, W.; Jiang, J. *Chem. Commun.* **2011**, *47*, 12358-12360.

10. a) Kuhn, N.; Bohnen, H.; Kreutzberg, J.; Bläser, D.; Boese, R. *J. Chem. Soc. Chem. Commun.* **1993**, 1136-1137. b) Kuhn, N.; Bohnen, H.; Bläser, D.; Boese, R.;

Chem. Ber. **1994**, *127*, 1405-1407. c) Ponti, P. P.; Baldwin, J. C.; Kaska, W. C. *Inorg. Chem.* **1979**, *18*, 873-875. d) For a related study on triazolylidene-based NHOs, see: Enders, D.; Breuer, K.; Raabe, G.; Runsink, J.; Teles, J. H.; Melder, J.-P.; Ebel, K.; Brode, S. *Angew. Chem. Int. Ed. Engl.* **1995**, *34*, 1021-1023.

11. Roy, M. M. D.; Rivard, E. *Acc. Chem. Res.* **2017**, *50*, 2017-2025.

12. a) Fürstner, A.; Alcarazo, M.; Goddard, R.; Lehmann, C. W. *Angew. Chem. Int. Ed.* **2008**, *47*, 3210-3214. b) Al-Rafia, S. M. I.; Malcolm, A. C.; Liew, S. K.; Ferguson, M. J.; McDonald, R.; Rivard, E. *Chem. Commun.* **2011**, *47*, 6987-6989. c) Knappke, C. E. I.; Arduengo III, A. J.; Jiao, H.; Neudörfl, J. M.; von Wangelin, A. J. *Synthesis* **2011**, 3784-3795.

13. Powers, K.; Hering-Junghans, C.; McDonald, R.; Ferguson, M. J.; Rivard, E. *Polyhedron* **2016**, *108*, 8-14.

14. Kronig, S.; Jones, P. G.; Tamm, M. *Eur. J. Inorg. Chem.* **2013**, 2301-2314.

15. a) Iglesias, M.; Iturmendi, A.; Sanz Miguel, P. J.; Polo, V.; Pérez-Torrente, J. J; Oro, L. A. *Chem. Commun.* **2015**, *51*, 12431-12434. b) Iturmendi, A.; García, N.; Jaseer, E. A.; Munárriz, J.; Sanz Miguel, P. J.; Polo, V.; Iglesias, M.; Oro, L. A. *Dalton Trans.* **2016**, *45*, 12835-12845.

16. Al-Rafia, S. M. I.; Ferguson, M. J.; Rivard, E. *Inorg. Chem.* **2011**, *50*, 10543-10545. b) Al-Rafia, S. M. I.; Momeni, M. R.; Ferguson, M. J; McDonald, R.; Brown, A.; Rivard, E. *Organometallics* **2013**, *32*, 6658-6665. c) Wang, Y.; Abraham, M. Y.; Gilliard, Jr., R. J.; Sexton, D. R.; Wei, P.; Robinson, G. H. *Organometallics* **2013**, *32*,

6639-6642. d) Berger, C. J.; He, G.; Merten, C.; McDonald, R.; Ferguson, M. J.; Rivard, E. *Inorg. Chem.* **2014**, *53*, 1475-1486. e) Ghadwal, R. S.; Schermann, C. J.; Engelhardt, F.; Steinmetzger, C. *Eur. J. Inorg. Chem.* **2014**, 4921-4926. f) Lee, W.-H.; Lin, Y.-F.; Lee, G.-H.; Peng, S.-M.; Chiu, C.-W. *Dalton Trans.* **2016**, *45*, 5937-5940. g) Hering-Junghans, C.; Andreiuk, P.; Ferguson, M. J.; McDonald, R.; Rivard, E. *Angew. Chem. Int. Ed.* **2017**, *56*, 6272-6275. h) Causero, A.; Elsen, H.; Pahl, J.; Harder, S. *Angew. Chem. Int. Ed.* **2017**, *56*, 6906-6910. i) Roy, M. M. D.; Ferguson, M. J.; McDonald, R.; Zhou, Y.; Rivard, E. *Chem. Sci.* **2019**, *10*, 6476-6481.

17. For recent examples, see: a) Wang, Q.; Zhao, W.; Zhang, S.; He, J.; Zhang, S.; Chen, E. Y.-X. *ACS Catal.* **2018**, *8*, 3571-3578. b) Walther, P.; Naumann, S. *Macromolecules* **2017**, *50*, 8406-8416. c) Hering-Junghans, C.; Watson, I. C.; Ferguson, M. J.; McDonald, R.; Rivard, E. *Dalton Trans.* **2017**, *46*, 7150-7153. d) Kaya, U.; Tran, U. P. N.; Enders, D.; Ho, J.; Nguyen, T. V. *Org. Lett.* **2017**, *19*, 1398-1401.

18. Crocker, R. D.; Nguyen, T. V. *Chem. Eur. J.* **2016**, *22*, 2208-2213.

19. Knappke, C. E. I.; Neudörfl, J. M.; von Wangelin, A. J. *Org. Biomol. Chem.* **2010**, *8*, 1695-1705.

20. For related fulvalene-type NHOs, see: Kunz, D.; Johnsen, E. Ø.; Monsler, B.; Rominger, F. *Chem. Eur. J.* **2008**, *14*, 10909-10914.

21. Schumann, A.; Hering-Junghans, C. *Eur. J. Inorg. Chem.* **2018**, 2584-2588.

22. CCDC 1903754, 1903755, 1903756, 1903757, 1903758, 1903759, 1903760, 1903761, 1903762, 1903763, 1903764 contain the supplementary crystallographic data for this Chapter. These data are provided free of charge by The Cambridge Crystallographic Data Centre.

23. Gasperini, M.; Ragaini, F.; Cenini, S. *Organometallics* **2002**, *21*, 2950-2957.

24. Ghadwal, R. S.; Reichmann, S. O.; Engelhardt, F.; Andrada, D. M.; Frenking, G. *Chem. Commun.* **2013**, *49*, 9440-9442.

25. a) Schuldt, R.; Kästner, J.; Naumann, S. *J. Org. Chem.* **2019**, *84*, 2209-2218. b) Raczyńska, E. D.; Decouzon, M.; Gal, J.-F.; Maria, P.-C.; Woźniak, K.; Kurg R.; Carins, S. N. *Trends Org. Chem.* **1998**, *7*, 996-103.

26. Lesieur, M.; Slawin, A. M. Z.; Cazin, C. S. *Org. Biomol. Chem.* **2014**, *12*, 5586-5589.

27. a) Hoi, K. H.; Coggan, J. A.; Organ, M. G. *Chem. Eur. J.* **2013**, *19*, 843-845. b) Pompeo, M.; Farmer, J. L.; Froese, R. D. J.; Organ, M. G. *Angew. Chem. Int. Ed.* **2014**, *53*, 3223-3226. c) Sharif, S.; Rucker, R. P; Chandrasoma, N.; Mitchell, D.; Rodriquez, M. J.; Froese, R. D. J.; Organ, M. G. *Angew. Chem. Int. Ed.* **2015**, *54*, 9507-9511.

28. Surry, D. S.; Buchwald, S. L. *Chem. Sci.* **2011**, *2*, 27-50.

29. Crabtree, R. H. *Chem. Rev.* **2012**, *112*, 1536-1554.

30. Higman, C. S.; Lanterna, A. E.; Marin, M. L.; Scaiano, J. C.; Fogg, D. E. *ChemCatChem* **2016**, *8*, 2446-2449.

31. Gorunova, O. N.; Novitskiy, I. M.; Grishin, Y. K.; Gloriozov, I. P.; Roznyatovsky, V. A.; Khrustalev, V. N.; Kochetkov, K. A.; Dunina, V. V. *Organometallics* **2018**, *37*, 2842-2858.

32. Watzky, M. A.; Finke, R. G. *J. Am. Chem. Soc.* **1997**, *119*, 10382-10400.

33. McGuinness, D. S.; Saendig, N.; Yates, B. F.; Cavell, K. J. *J. Am. Chem. Soc.* **2001**, *123*, 4029-4040.

34. Sable, V.; Maindan, K.; Kapdi, A. R.; Shejwalker, P. S.; Hara, K. *ACS Omega* **2017**, *2*, 204-217.

35. Navaladian, S.; Viswanathan, B.; Varadarajan, T. K.; Viswanath, R. P. *Nanoscale Res. Lett.* **2009**, *4*, 181-186.

36. Arduengo III, A. J.; Krafczyk, R.; Schmutzler, R.; Craig, H. A.; Goerlich, J. R.; Marshall, W. J.; Unverzagt, M. *Tetrahedron* **1999**, *55*, 14523-14534.

37. Gaillard, S.; Bantreil, X.; Slawin, A. M. Z.; Nolan, S. P. *Dalton Trans.* **2009**, 6967-6971.

38. Vasudevan, K. V.; Butorac, R. R.; Abernathy, C. D.; Cowley, A. H. *Dalton Trans.* **2010**, *39*, 7401-7408.

39. Bantreil, X.; Nolan, S. P. *Nat. Protoc.* **2011**, *6*, 69-77.

40. Ryan, S. J; Schimler, S. D.; Bland, D. C.; Sanford, M. S. *Org. Lett.* **2015**, *17*, 1866-1869.

41. Sheldrick, G. M. *Acta. Crystallogr. Sect. A* **2015**, *71*, 3-8.

42. Sheldrick, G. M *Acta. Crystallogr. Sect. C* **2015**, *71*, 3-8.

43. Frisch, M. J.; Trucks, G. W.; Schlegel, H. B.; Scuseria, G. E.; Robb, M. A.; Cheeseman, J. R.; Scalmani, G.; Barone, V.; Mennucci, B.; Petersson, G. A.; Nakatsuji, H.; Caricato, M.; Li, X.; Hratchian, H. P,; Izmaylov, A. F.; Bloino, J.; Zheng, G.; Sonnenberg, J. L.; Hada, M.; Ehara, M.; Toyota, K.; Fukuda, R.; Hasegawa, J.; Ishida, M.; Nakajima, T.; Honda, Y.; Kitao, O.; Nakai, H.; Vreven, T.; Montgomery, Jr., J. A.; Peralta, J. E.; Ogliaro, F.; Bearpark, M.; Heyd, J. J.; Brothers, E.; Kudin, K. N.; Staroverov, V. N.; Kobayashi, R.; Normand, J.; Raghavachari, K.; Rendell, A.; Burant, J. C.; Iyengar, S. S.; Tomasi, J.; Cossi, M.; Rega, N.; Millam, J. M.; Klene, M.; Knox, J. E.; Cross, J. B.; Bakken, V.; Adamo, C.; Jaramillo, J.; Gomperts, R.; Stratmann, R. E.; Yazyev, O.; Austin, A. J.; Cammi, R.; Pomelli, C.; Ochterski, J. W.;. Martin, R. L.; Morokuma, K.; Zakrzewski, V. G.; Voth, G. A.; Salvador, P.; Dannenberg, J. J.; Dapprich, S.; Daniels, A. D.; Farkas, Ö.; Foresman, J. B.; Ortiz, J. V.; Cioslowski, J.; Fox, D. J. Gaussian 09, Revision E.01, Gaussian, Inc., Wallingford CT, **2009**.

44. Becke, A. D. *J. Chem. Phys.* **1993**, *98*, 5648-5652.

45. a) Petersson, G. A.; Bennett, A.; Tensfeldt, T. G.; Al-Laham, M. A.; Shirley, W. A.; Mantzaris, J. *J. Chem. Phys.* **1988**, *89*, 2193-2218. b) Petersson, G. A.; Al-Laham, M. A. *J. Chem. Phys*. **1991**, *94*, 6081-6090.

46. a) Glendening, E. D.; Badenhoop, J. K.; Reed, A. E.; Carpenter, J. E.; Bohmann, J. A.; Morales, C. M.; Landis, C. R.; Weinhold, F. *NBO* 6.0, Theoretical Chemistry Institute, University of Wisconsin, Madison, 2013. b) Carpenter, J. E.; Weinhold, F. J. *Mol. Struct.* **1988**, *169*, 41-62. c) Weinhold, F.; Carpenter, J. E. *The Structure of Small Molecules and Ions*, Plenum, New York, 1988. d) Weinhold, F.; Landis, C. R. *Valency and Bonding. A Natural Bond Orbital Donor-Acceptor Perspective*, Cambridge University Press, Cambridge, 2005.

47. Tian, X.; Lin, J.; Zuo, S.; Lv, J.; Huang, Q.; Zhu, J.; Huang, S.; Wang, Q. *J. Organomet. Chem.* **2018**, *861*, 125-130.

48. Kim, M.; Shin, T.; Lee, A.; Kim, H. *Organometallics* **2018**, *19*, 3253-3258.

49. Sugahara, T.; Murakami, K.; Yorimitsu, H.; Osuka, A. *Angew. Chem. Int. Ed.* **2014**, *53*, 9329-9333.

50. Sai, M. *Adv. Synth. Catal.* **2021,** *363*, 5422-5428.

51. Cui, X.; Dai, X.; Deng, Y.; Shi, F. *Chem. Eur. J.* **2013**, *19*, 3665-3675.

Chapter 4

1. a) Ponti, P. P.; Baldwin, J. C.; Kaska, W. C. *Inorg. Chem.* **1979**, *18*, 873-875. b) Kuhn, N.; Bohnen, H.; Kreutzberg, J.; Bläser, D.; Boese, R. *J. Chem. Soc., Chem. Commun.* **1993**, 1136-1137. c) Kuhn, N.; Bohnen, H.: Bläser, D.; Boese, R. *Chem. Ber.* **1994**, *127*, 1405-1407.

2. a) Roy, M. M. D.; Rivard, E. *Acc. Chem. Res.* **2017**, *50*, 2017-2025. b) Al-Rafia, S. M. I.; Malcolm, A. C.; Liew, S. K.; Ferguson, M. J.; McDonald, R.; Rivard, E. *Chem. Commun.* **2011**, *47*, 6987-6989. c) Wang, Y. W.; Abraham, M. Y.; Gilliard Jr., R. J.; Sexton, D. R.; Wei, P.; Robinson, G. H. *Organometallics* **2013**, *32*, 6639-6642. d) Al-Rafia, S. M. I.; Momeni, M. R.; Ferguson, M. J.; McDonald, R.; Brown, A.; Rivard, E. *Organometallics* **2013**, *32*, 6658-6665. e) Ghadwal, R. S.; Schürmann, C. J.; Andrada, D. M.; Frenking, G. *Dalton Trans*. **2015**, *44*, 14359-14367. f) Ghadwal, R. S. *Dalton Trans.* **2016**, *45*, 16081-16095. g) Lee, W.-H.; Lin, Y.-F.; Lee, G.-H.; Peng, S.-M.; Chiu, C.-W. *Dalton Trans.* **2016**, *45*, 5937-5940. h) Eymann, L. Y. M.; Varava, R.; Shved, A. M.; Curchod, B. F. E.; Liu, Y.; Planes, O. M.; Sienkiewicz, A.; Scopelliti, R.; Tirani, F. F.; Severin, K. *J. Am. Chem. Soc.* **2019**, *141*, 17112-17116.

3. Powers, K.; Hering-Junghans, C.; McDonald, R.; Ferguson, M. J.; Rivard, E. *Polyhedron* **2016**, *108*, 8-14.

4. For selected reviews and articles, see: a) Naumann, S. *Chem. Commun.* **2019**, *55*, 11658-11670. b) Crocker, R. D.; Nguyen, T. V. *Chem. Eur. J.* **2016**, *22*, 2208-2213. c) Naumann, S.; Mudsinger, K.; Cavallo, L.; Falivene, L. *Polym. Chem.* **2017**, *8*, 5803-5812. d) Hering-Junghans, C.; Watson, I. C.; Ferguson, M. J.; McDonald, R.; Rivard, E.

Dalton Trans. **2017**, *46*, 7150-7153. e) Walther, P.; Krauβ, A.; Naumann, S. *Angew. Chem. Int. Ed.* **2019**, *58*, 10737-10741.

5. McGraw, M.; Chen, E. Y.-X. *ACS Catal.* **2018**, *8*, 9877-9887.

6. Jia, Y.-B.; Wang, Y.-B.; Ren, W.-M.; Xu, T.; Wang, J.; Lu, X.-B. *Macromolecules* **2014**, *47*,1966-1972.

7. Zhang, Y.; Miyake, G. M.; Chen, E. Y.-X. *Angew. Chem. Int. Ed.* **2010**, *49*, 10158-10162.

8. a) Li, X.-W.; Su, J.; Robinson, G. *Chem. Commun.* **1996**, 2683-2684. b) Todd, A. D. K.; McClennan, W. L.; Masuda, J. D. *RSC Adv.* **2016**, *6*, 69270-69276.

9. a) Hering-Junghans, C.; Andreiuk, P.; Ferguson, M. J.; McDonald, R.; Rivard, E. *Angew. Chem. Int. Ed.* **2017**, *56*, 6272-6275. b) Lui, M.; Merten, C.; Ferguson, M. J.; McDonald, R.; Xu, Y.; Rivard, E. *Inorg. Chem.* **2015**, *54*, 2040-2049. For a review on NHI complexes, see: c) Ochiai, T.; Franz, D.; Inoue, S. *Chem. Soc. Rev.* **2016**, *45*, 6327-6344.

10. Schnee, G.; Bolley, A.; Hild, F.; Specklin, D.; Dagorne, S. *Catal. Today* **2017**, *289*, 204-210.

11. Watson, I. C.; Schumann, A.; Yu, H.; Davy, E. C.; McDonald, R.; Ferguson, M. J.; Hering-Junghans, C.; Rivard, E. *Chem. Eur. J.* **2019**, *25*, 9678-9690.

12. Weger, M.; Grötsch, R. K.; Knaus, M. G.; Giuman, M. M.; Mayer, D. C.; Altmann, P. J.; Mossou, E., Dittrich, B.; Pöthig, A.; Rieger, B. *Angew. Chem. Int. Ed.* **2019**, 58, 9797-9801.

13. a) Zhao, Z.; Wang, Q.; He, J.; Zhang, Y. *Polym. Chem.* **2019**, *10*, 4328-4335. b) Xu, T.; Chen, E. Y.-X. *J. Am. Chem. Soc.* **2014**, *136*, 1774-1777.

14. Wang, Q.; Zhao, W.; Zhang, S.; He, J.; Zhang, Y.; Chen, E. Y.-X. *ACS Catal.* **2018**, *8*, 3571-3578.

15. For the polymerization of DEVP, see: Weger, M.; Pahl, P.; Schmidt, F.; Soller, B. S.; Altmann, P. J.; Pöthig, A.; Gemmecker, G.; Eisenreich, W.; Rieger, B. *Macromolecules* **2019**, *24*, 7073-7080 and references therein.

16. He, J.; Zhang, Y.; Chen, E. Y.-X. *Synlett* **2014**, *25*, 1534-1538.

17. Takada, K.; Fuchise, K.; Chen, Y.; Satoh, T.; Kakuchi, T. *J. Polym. Sci., Part A: Polym. Chem.* **2012**, *50*, 3560-3566.

18. a) Radical Polymerization in Industry, *Encyclopedia of Radicals in Chemistry, Biology and Materials* [Online]; John Wiley & Sons, Posted March 15, 2012. https://onlinelibrary.wiley.com/doi/full/10.1002/9781119953678.rad080 (accessed December 12, 2019). b) Kennemur, J. G. *Macromolecules* **2019**, 52, 1354-1370. c) Rudin, A.; Choi, P. *The Element of Polymer Science & Engineering, 3rd* ed.; Academic Press: Waltham, MA, USA, **2013**; pg. 380.

19. For work on complexes supported by anionic NHO ligands, see: a) Al-Rafia, S. M. I.; Ferguson, M. J.; Rivard, E. *Inorg. Chem.* **2011**, *50*, 10543-10545. b) Ghadwal, R. S.; Reichmann, S. O.; Engelhardt, F.; Andrada, D. M.; Frenking, G. *Chem. Commun.* **2013**, *49*, 9440-9442. c) Paisley, N. R., Lui, M. W.; McDonald, R.; Ferguson, M. J.; Rivard, E. *Dalton Trans.* **2016**, *45*, 9860-9870. d) Chong, C. C.; Rao, B.; Ganguly, R.; Li, Y.; Kinjo, R. *Inorg. Chem.* **2017**, *56*, 8608-8614. e) Roy, M. M. D.; Ferguson, M. J.;

McDonald, R.; Zhou, Y.; Rivard, E. *Chem. Sci.* **2019**, *10*, 6476-6481. f) Sharma, M. K.; Blomeyer, S.; Neumann, B.; Stammler, H.-G.; van Gastel, M.; Hinz, A.; Ghadwal, R. S. *Angew. Chem. Int. Ed.* **2019**, *58*, 17599-17603. g) Hupf, E.; Kaiser, F.; Lummis, P. A.; Roy, M. M. D.; McDonald, R.; Ferguson, M. J.; Kühn, F.; Rivard, E. *Inorg. Chem.* **2020**, *59*, 1592-1601. h) Sharma, M. K.; Neumann, B.; Stammler, H.-G.; Andrada, D. M.; Ghadwal, R. S. *Chem. Commun.* **2019**, *55*, 14669-14672. i) Roy, M. M. D.; Baird, S. R.; Dornsiepen, E.; Paul, L. A.; Miao, L.; Ferguson, M. J.; Zhou, Y.; Siewert, I.; Rivard, E. *Chem. Eur. J.* **2021**, *27*, 8572-8579.

20. Sheldrick, G. M. *Acta. Crystallogr. Sect. A* **2015**, *71*, 3-8.

21. Sheldrick, G. M. *Acta. Crystallogr. Sect. C* **2015**, *71*, 3-8.

Chapter 5

1. a) Frankland, E. *Q. J. Chem. Soc.* **1861**, *13*, 177-235. b) Seyferth, D. *Organometallics* **2001**, *20*, 2940-2955.

2. a) Martin, R.; Buchwald, S. L. *Acc. Chem. Res.* **2008**, *41*, 1461-1473. b) Suzuki, A. *Angew. Chem. Int. Ed.* **2011**, *50*, 6722-6737.

3. a) Haas, D.; Hammann, J. M.; Greiner, R.; Knochel, P. *ACS Catal.* **2016**, *6*, 1540-1552. b) Negishi, E.-i. *Angew. Chem. Int. Ed.* **2011**, *50*, 6738-6764.

4. Cordovilla, C.; Bartolomé, C.; Martínez-Ilarduya, J. M.; Espinet, P. *ACS Catal.* **2015**, *5*, 3040-3053.

5. a) Williams, V. C.; Piers, W. E.; Clegg, W.; Elsegood, M. R. J.; Collins, S.; Marder, T. B. *J. Am. Chem. Soc.* **1999**, *121*, 3244-3245. b) Sun, Y.; Piers, W. E.; Parvez, M. *Can. J. Chem.* **1998**, *76*, 513-517.

6. a) Overby, J. S.; Jayaratne, K. C.; Schoell, N. J.; Hanusa, T. P. *Organometallics* **1999**, *18*, 1663-1668. b) Esqueda, A. C.; Conejero, S.; Maya, C.; Carmona, E. *Organometallics* **2009**, *28*, 45-47. c) Lee, J.-D.; Han, W.-S.; Kim, T.-J.; Kim, S. H.; Kang, S. O. *Chem. Commun.* **2011**, *47*, 1018-1020. d) Gondzik, S.; Bläser, D.; Wölper, C.; Schulz, S. *Chem. Eur. J.* **2010**, *16*, 13599-13602. e) Freitag, K.; Gemel, C.; Jerabek, P.; Oppel, I. M.; Seidel, R. W.; Frenking, G.; Banh, H.; Dilchert, K.; Fischer, R. A. *Angew. Chem. Int. Ed.* **2015**, *54*, 4370-4374.

7. a) Wiegand, A.-K; Rit, A.; Okuda, J. *Coord. Chem Rev.* **2016**, *314*, 71-82. b) Lummis, P. A.; Momeni, M. R.; Lui, M. W.; McDonald, R.; Ferguson, M. J.; Miskolzie, M.; Brown, A.; Rivard, E. *Angew. Chem. Int. Ed.* **2014**, *53*, 9347-9351. c) Chambenahalli, R.; Andrews, A. P.; Ritter, F.; Okuda, J.; Venugopal, A. *Chem. Commun.* **2019**, *55*, 2054-2057.

8. a) For pioneering work in this field, see: Fagan, P. J.; Nugent, W. A.; Calabrese, J. C. *J. Am. Chem. Soc.* **1994**, *116*, 1880-1889. b) He, G.; Torres Delgado, W.; Shynkaruk, O.; Ferguson, M. J.; McDonald, R.; Rivard, E. *J. Am. Chem. Soc.* **2013**, *135*, 5360-5363. c) He, G.; Torres Delgado, W.; Schatz, D. J.; Merten, C.; Mohammadpour, A.; Mayr, L.; Ferguson, M. J.; McDonald, R.; Brown, A.; Shankar, K.; Rivard, E. *Angew. Chem. Int. Ed.* **2014**, *53*, 4587-4591. d) Parke, S. M.; Hupf, E.;

Matharu, G. K.; de Aguiar, I.; Xu, L.; Yu, H.; Boone, M. P.; de Souza, G. L. C.; McDonald, R.; Ferguson, M. J.; He, G.; Brown, A.; Rivard, E. *Angew. Chem. Int. Ed.* **2018**, *57*, 14841-14846. e) Parke, S. M.; Tanaka, S.; Yu, H.; Hupf, E.; Ferguson, M. J.; Zhou, Y.; Naka, K.; Rivard, E. *Macromolecules* **2019**, *52*, 7477-7488. f) Rivard, E. *Chem. Rec.* **2020**, *20*, 640-648.

9. a) Roy, M. M. D.; Rivard, E. *Acc. Chem. Res.* **2017**, *50*, 2017-2025. For early examples of NHOs in coordination chemistry, see: b) Ponti, P. P.; Baldwin, J. C.; Kaska, W. C. *Inorg. Chem.* **1979**, *18*, 873-875. c) Kuhn, N.; Bohnen, H.; Kreutzberg, J.; Bläser, D.; Boese, R. *J. Chem. Soc., Chem. Commun.* **1993**, 1136-1137. d) Al-Rafia, S. M. I.; Malcolm, A. C.; Liew, S. K.; Ferguson, M. J.; McDonald, R.; Rivard, E. *Chem. Commun.* **2011**, *47*, 6987-6989. e) Huang, J.-S.; Lee, W.-H.; Shen, C.-T.; Lin, Y.-F.; Liu, Y.-H.; Peng, S.-M.; Chiu, C.-W. *Inorg. Chem.* **2016**, *55*, 12427-12434. For the use of NHOs in organic chemistry, see: f) Naumann, S.; Thomas, A. W.; Dove, A. P. *Angew. Chem. Int. Ed.* **2015**, *54*, 9550-9554. g) Saptal, V. B.; Bhanage, B. M. *ChemSusChem.* **2016**, *9*, 1980-1985. h) Kaya, U.; Tran, U. P. N.; Enders, D.; Ho, J.; Nguyen, T. V. *Org. Lett.* **2017**, *19*, 1398-1401. i) Schuldt, R.; Kästner, J.; Naumann, S. *J. Org. Chem.* **2019**, *84*, 2209-2218. j) Naumann, S. *Chem. Commun.* **2019**, *55*, 11658-11670. k) Eymann, L. Y. M.; Varava, P.; Shved, A. M.; Curchod, B. F. E.; Liu, Y. Z.; Planes, O. M.; Sienkiewicz, A.; Scopelliti, R.; Tirani, F. F.; Severin, K. *J. Am. Chem. Soc.* **2019**, *43*, 17112-17116.

10. Roy, M. M. D.; Baird, S. R.; Dornsiepen, E.; Paul, L. A.; Miao, L.; Ferguson, M. J.; Zhou, Y.; Siewert, I.; Rivard, E. *Chem. Eur. J.* **2021**, *27*, 8572-8579.

11. a) Kuhn, N.; Göhner, M.; Steimann, M. *Z. Anorg. Allg. Chem.* **2002**, *628*, 1108-1115. b) Al-Rafia, S. M. I.; Ferguson, M. J.; Rivard, E. *Inorg. Chem.* **2011**, *50*, 10543-10545. c) Ghadwal, R. S.; Reichmann, S. O.; Engelhardt, F.; Andrada, D. M.; Frenking, G. *Chem. Commun.* **2013**, *49*, 9440-9442. d) Hering-Junghans, C.; Andreiuk, P.; Ferguson, M. J.; McDonald, R.; Rivard, E. *Angew. Chem. Int. Ed.* **2017**, *56*, 6272-6275. e) Sharma, M. K.; Blomeyer, S.; Neumann, B.; Stammler, H.-G.; Ghadwal, R. S. *Chem. Eur. J.* **2019**, *25*, 8249-8253. f) Roy, M. M. D.; Ferguson, M. J.; McDonald, R.; Zhou, Y.; Rivard, E. *Chem. Sci.* **2019**, *10*, 6476-6481. g) Gupta, P.; Siewert, J.-E.; Wellnitz, T.; Fischer, M.; Baumann, W.; Beweries, T.; Hering-Junghans, C. *Dalton Trans.* **2021**, *50*, 1838-1844. For a backbone deprotonated aNHO, see: h) Causero, A.; Elsen, H.; Pahl, J.; Harder, S. *Angew. Chem. Int. Ed.* **2017**, *56*, 6906-6910.

12. Chong, C. C.; Rao, B.; Ganguly, R.; Li, Y.; Kinjo, R. *Inorg. Chem.* **2017**, *56*, 8608-8614.

13. Powers, K.; Hering-Junghans, C.; McDonald, R.; Ferguson, M. J.; Rivard, E. *Polyhedron* **2016**, *108*, 8-14.

14. Singh, A. P.; Samuel, P. P.; Roesky, H. W.; Schwarzer, M. C.; Frenking, G.; Sidhu, N. S.; Dittrich, B. *J. Am. Chem. Soc.* **2013**, *135*, 7324-7329.

15. Bacsa, J.; Hanke, F.; Hindley, S.; Odedra, R.; Darling, G. R.; Jones, A. C.; Steiner, A. *Angew. Chem. Int. Ed.* **2011**, *50*, 11685-11687.

16. a) Sinhababu, S.; Yadav, D.; Karwasara, S.; Sharma, M. K.; Mukherjee, G.; Rajaraman, G.; Nagendran, S. *Angew. Chem. Int. Ed.* **2016**, *55*, 7742-7746. b) Sinhababu, S.; Sharma, M. K.; Mahawar, P.; Kaur, S.; Singh, V. K.; Paliwal, A.; Yadav, D.; Kashyap, H. K.; Nagendran, S. *Dalton Trans.* **2019**, *48*, 16366-16376. c) Rittinghaus, R. D.; Tremmel, J.; Růžička, A.; Conrads, C.; Albrecht, P.; Hoffmann, A.; Ksiazkiewicz, A. N.; Pich, A.; Jambor, R.; Herres-Pawlis, S. *Chem. Eur. J.* **2020**, *26*, 212-221. d) Yadav, S.; Kumar, R.; Raj, K. V.; Yadav, P.; Vanka, K.; Sen, S. S. *Chem. Asian. J.* **2020**, *15*, 3116-3121.

17. Erickson, J. D.; Riparetti, R. D.; Fettinger, J. C.; Power, P. P. *Organometallics* **2016**, *35*, 2124-2128.

18. Hupf, E.; Kaiser, F.; Lummis, P. A.; Roy, M. M. D.; McDonald, R.; Ferguson, M. J.; Kühn, F. E.; Rivard. E. *Inorg. Chem.* **2020**, *59*, 1592-1601.

19. Sita, L. R. *Acc. Chem. Res.* **1994**, *27*, 191-197.

20. a) Nied, D.; Breher, F. *Chem. Soc. Rev.* **2011**, *40*, 3455-3466. b) Nied, D.; Oña-Burgos, P.; Klopper. W.; Breher, F. *Organometallics* **2011**, *30*, 1419-1428.

21. Richards, A. F.; Brynda, M.; Power, P. P. *Organometallics* **2004**, *23*, 4009-4011.

22. Paisley, N. R.; Lui, M. W.; McDonald, R.; Ferguson, M.; Rivard, E. *Dalton Trans.* **2016**, *45*, 9860-9870.

23. The ability of anionic NHOs, such as the less hindered analogue [IPrCH]$^-$ to coordinate to two main group centers in a terminal fashion, *i.e.* to give [IPrCH(ER$_x$)$_2$]

products, has been documented before in the Rivard group: Lui, M. W.; Shynkaruk, O.; Oakley, M. S.; Sinelnikov, R.; McDonald, R.; Ferguson, M. J.; Meldrum, A.; Klobukowski, M.; Rivard, E. *Dalton Trans.* **2017**, *46*, 5946-5954.

24. Roy, M. M. D.; Omaña, A. A.; Wilson, A. S. S.; Hill, M. S.; Aldridge, S.; Rivard, E. *Chem. Rev.* **2021**, *121*, 12784-12965.

25. For selected examples of luminescence from "push-pull" boron-based compounds, see: a) He, J.; Rauch, F.; Friedrich, A.; Sieh, D.; Ribbeck, T.; Krummenacher, I.; Braunschweig, H.; Finze, M.; Marder, T. B. *Chem. Eur. J.* **2019**, *25*, 13777-13784. b) Chen, X.; Meng, G.; Liao, G.; Rauch, F.; He, J.; Friedrich, A.; Marder, T. B.; Wang, N.; Chen, P.; Wang, S.; Yin, X. *Chem. Eur. J.* **2021**, *27*, 6274-6282. c) Hudson, Z. M.; Wang, S. *Acc. Chem. Res.* **2009**, *42*, 1584-1596. d) Baser-Kirazli, N.; Lalancette, R. A.; Jäkle, F. *Organometallics* **2021**, *40*, 520-528. e) Hatakeyama, T.; Shiren, K.; Nakajima, K.; Nomura, S.; Nakatsuka, S.; Kinoshita, K.; Ni, J.; Ono, Y.; Ikuta, T. *Adv. Mater.* **2016**, *28*, 2777-2781.

26. Zettler, F.; Hausen, H. D.; Hess, H. *J. Organomet. Chem.* **1974**, *72*, 157-162.

27. Klooster, W. T.; Koetzle, T. F.; Siegbahn, P. E. M.; Richardson, T. B.; Crabtree, R. H. *J. Am. Chem. Soc.* **1999**, *121*, 6337-6343.

28. Lui, M. W.; Paisley, N. R.; McDonald, R.; Ferguson, M. J.; Rivard, E. *Chem. Eur. J.* **2016**, *22*, 2134-2145.

29. Hering-Junghans, C.; Watson, I. C.; Ferguson, M. J.; McDonald, R.; Rivard, E. *Dalton Trans.* **2017**, *46*, 7150-7153.

30. a) Vedejs, E.; Nguyen, T.; Powell, D. R.; Schrimpf, M. R. *Chem. Commun.* **1996**, 2721-2722. b) Braunschweig, H.; Ganter, B. *J. Organomet. Chem.* **1997**, *545*, 163-167.

31. Watson, I. C.; Zhou, Y.; Ferguson, M. J.; Kränzlein, M.; Rieger, B.; Rivard, E. *Z. Anorg. Allg. Chem.* **2020**, *646*, 547-551.

32. Turley, J. W.; Rinn, H. W. *Inorg. Chem.* **1969**, *8*, 18-22.

33. Gavrilenko, V. V.; Chekulaeva, L. A.; Antonovich, V. A.; Zakharkin, L. I. *Bull. Acad. Sci. USSR, Div. Chem. Sci. (Engl. Transl.)*. **1981**, 505-508.

34. Pangborn, A. B.; Giardello, M. A.; Grubbs, R. A.; Rosen, R. K.; Timmers, F. J. *Organometallics* **1996**, *15*, 1518-1520.

35. Rheinboldt, H.; Luyken, A.; Schmittmann, H. *J. Prakt. Chem.* **1937**, *149*, 30-54.

36. Press, L. P.; McCulloch, B. J.; Gu, W.; Chen, C.-H.; Foxman, B. M.; Ozerov, O. V. *Chem. Commun.* **2015**, *51*, 14034-14037.

37. MacNeil, C. S.; Hsiang, S.-J.; Hayes, P. G. *Chem. Commun.* **2020**, *56*, 12323-12326.

38. Yuan, K.; Wang, X.; Wang, S. *Org. Lett.* **2018**, *20*, 1617-1620.

39. Blessing, R. H. *Acta. Cryst.* **1995**, *A51*, 33-38.

40. Sheldrick, G. M. *Acta. Cryst.* **2015**, *A71*, 3-8.

41. Sheldrick, G. M. *Acta. Cryst.* **2015**, *C71*, 3-8.

42. a) Becke, A. D. *J. Chem. Phys.* **1993**, *98*, 5648-5652. b) Lee, C.; Yang, W.; Parr, R. G. *Phys. Rev. B* **1988**, *37*, 785-789.

43. a) Weigend, F.; Ahlrichs, R. *Phys. Chem. Chem. Phys.* **2005**, *7*, 3297-3305. b) Schäfer, A.; Huber, C.; Ahlrichs, R. *J. Chem. Phys.* **1994**, *100*, 5829-5835. c) Schäfer, A.; Horn, H.; Ahlrichs, R. *J. Chem. Phys*. **1992**, *97*, 2571-2577.

44. Frisch, M. J.; Trucks, G. W.; Schlegel, H. B.; Scuseria, G. E.; Robb, M. A.; Cheeseman, J. R.; Scalmani, G.; Barone, V.; Petersson, G. A.; Nakatsuji, H.; Li, X.; Caricato, M.; Marenich, A. V.; Bloino, J.; Janesko, B. G.; Gomperts, R.; Mennucci, B.; Hratchian, H. P.; Ortiz, J. V.; Izmaylov, A. F.; Sonnenberg, J. L.; Williams-Young, D.; Ding, F.; Lipparini, F.; Egidi, F.; Goings, J.; Peng, B.; Petrone, A.; Henderson, T.; Ranasinghe, D.; Zakrzewski, V. G.; Gao, J.; Rega, N.; Zheng, G.; Liang, W.; Hada, M.; Ehara, M.; Toyota, K.; Fukuda, R.; Hasegawa, J.; Ishida, M.; Nakajima, T.; Honda, Y.; Kitao, O.; Nakai, H.; Vreven, T.; Throssell, K.; Montgomery, J. A., Jr.; Peralta, J. E.; Ogliaro, F.; Bearpark, M. J.; Heyd, J. J.; Brothers, E. N.; Kudin, K. N.; Staroverov, V. N.; Keith, T. A.; Kobayashi, R.; Normand, J.; Raghavachari, K.; Rendell, A. P.; Burant, J. C.; Iyengar, S. S.; Tomasi, J.; Cossi, M.; Millam, J. M.; Klene, M.; Adamo, C.; Cammi, R.; Ochterski, J. W.; Martin, R. L.; Morokuma, K.; Farkas, O.; Foresman, J. B.; Fox, D. J. *Gaussian 16,* Revision A.03; Gaussian, Inc.: Wallingford, CT, **2016**.

45. Glendening, E. D.; Badenhoop, J. K.; Reed, A. E.; Carpenter, J. E.; Bohmann, J. A.; Morales, C. M.; Landis, C. R.; Weinhold, F. *NBO 6.0.;* Theoretical Chemistry Institute, University of Wisconsin, Madison, **2013**.

Chapter 6

1. a) Roy, M. M. D.; Rivard, E. *Acc. Chem. Res.* **2017**, *50*, 2017-2025. b) Doddi, A.; Peters, M.; Tamm, M. *Chem. Rev.* **2019**, *119*, 6994-7112.

2. Ponti, P. P.; Baldwin, J. C.; Kaska, W. C. *Inorg. Chem.* **1979**, *18*, 873-875.

3. Watson, I. C.; Schumann, A.; Yu, H.; Davy, E. C.; McDonald, R.; Ferguson, M. J.; Hering-Junghans, C.; Rivard, E. *Chem. Eur. J.* **2019**, *25*, 9678-9690.

4. Kuhn, N.; Bohnen, H.; Bläser, D.; Boese, R. *Chem. Ber.* **1994**, *127*, 1405-1407.

5. Ando, S.; Ohara, A.; Ohwada, T.; Ishizuka, T. *Organometallics* **2021**, *40*, 3368-3367.

6. a) Iglesias, M.; Iturmendi, A.; Sanz Miguel, P. J.; Polo, V.; Pérez-Torrente, J. J; Oro, L. A. *Chem. Commun.* **2015**, *51*, 12431-12434. b) Iturmendi, A.; N. García, N.; Jaseer, E. A.; Munárriz, J.; Sanz Miguel, P. J.; Polo, V.; Iglesias, M.; Oro, L. A. *Dalton Trans.* **2016**, *45*, 12835-12845. c) Powers, K.; Hering-Junghans, C.; McDonald, R.; Ferguson, M. J.; Rivard, E. *Polyhedron* **2016**, *108*, 8-14. d) Fürstner, A.; Alcarazo, M.; Goddard, R.; Lehmann, C. W. *Angew. Chem. Int. Ed.* **2008**, *47*, 3210-3214. e) Kronig, S.; Jones, P. G.; Tamm, M. *Eur. J. Inorg. Chem.* **2013**, 2301-2314. f) Imbrich, D. A.; Frey, W.; Naumann, S.; Buchmeiser, M. R. *Chem. Commun.* **2016**, *52*, 6099-6102.

7. Watson, I. C.; Ferguson, M. J.; Rivard, E. *Inorg. Chem.* **2021**, *60*, 18347-18359.

8. Beaumier, E. P.; Pearce, A. J.; See, X. Y.; Tonks, I. A. *Nat. Rev. Chem.* **2019**, *3*, 15-34.

9. a) Fryzuk, M. D.; Haddad, T. S.; Rettig, S. J. *J. Am. Chem. Soc.* **1990**, *112*, 8185-8186. b) Sanner, R. D.; Manriquez, J. M.; Marsch, R. E.; Bercaw, J. E. *J. Am. Chem. Soc.* **1976**, *98*, 8351-8357. c) Mullins, S. M.; Duncan, A. P.; Bergman, R. G.; Arnold, J. *Inorg. Chem.* **2001**, *40*, 6952-6963. d) Chirik, P. J. *Dalton Trans.* **2007**, 16-25. e) Burford, R. J.; Yeo, A.; Fryzuk, M. D. *Coord. Chem. Rev.* **2017**, *334*, 84-99.

10. a) Valadez, T. N.; Norton, J. R.; Neary, M. *J. Am. Chem. Soc.* **2015**, *137*, 10152-10155. b) Rehbaum, F.; Thiele, K.-H.; Trojanov, S. I. *J. Organomet. Chem.* **1991**, *410*, 327-333. c) Okamoto, S. *Chem. Rec.* **2016**, *16*, 857-872.

11. a) Aguilar-Calderón, J. R.; Metta-Magaña, A. J.; Noll, B.; Fortier, S. *Angew. Chem. Int. Ed.* **2016**, *55*, 14101-14105. b) Clark, T. J.; Russell, C. A.; Manners, I. *J. Am. Chem. Soc.* **2006**, *128*, 9582-9583. c) Pun, D.; Lobkovsky, E.; Chirik, P. J. *Chem. Commun.* **2007**, 3297-3299. d) Solowey, D. P.; Mane, M. V.; Kurogi, T.; Carroll, P. J.; Manor, B. C.; Baik, M.-H.; Mindiola, D. J. *Nat. Chem.* **2017**, *9*, 1126-1132. e) Thomas, J.; Klahn, M.; Spannenberg, A.; Beweries, T. *Dalton Trans.* **2013**, *42*, 14668-14672. f) Lummis, P. A.; McDonald, R.; Ferguson, M. J.; Rivard, E. *Dalton Trans.* **2015**, *44*, 7009-7020.

12. a) Streuff, J.; Feurer, M.; Frey, G.; Steffani, A.; Kacprzak, S.; Weweler, J.; Leijendekker, L. H.; Kratzer, D.; Plattner, D. A. *J. Am. Chem. Soc.* **2015**, *137*, 14396-14405. b) Weweler, J.; Younas, S. L.; Streuff, J. *Angew. Chem. Int. Ed.* **2019**, *58*, 17700-17703. c) Gansäuer, A.; Hildebrandt, S.; Michelmann, A.; Dahmen, T.; von

Laufenberg, D.; Kube, C.; Fianu, G. D.; Flowers II, R. A. *Angew. Chem. Int. Ed.* **2015**, *54*, 7003-7006. d) Kern, C.; Selau, J.; Streuff, J. *Chem. Eur. J.* **2021**, *27*, 6178-6182.

13. Negishi, E.-i.; Cederbaum, F. E.; Takahashi, T. *Tetrahedron Lett.* **1986**, *27*, 2829-2832.

14. Rosenthal, U.; Ohff, A.; Baumann, W.; Tillack, A.; Görls, H.; Burlakov, V. V.; Shur, V. B. *Z. Anorg. Allg. Chem.* **1995**, *621*, 77-83.

15. Plundrich, G. T.; Wadepohl, H.; Clot, E.; Gade, L. H. *Chem. Eur. J.* **2016**, *22*, 9283-9292.

16. Power, P. P. *Chem. Rev.* **2012**, *112*, 3482-3507.

17. a) Bunting, P. C.; Atanasov, M.; Damgaard-Møller, E.; Perfetti, M.; Crassee, I.; Orlita, M.; Overgaard, J.; van Slageren, J.; Neese, F.; Long, J. R. *Science* **2018**, *362*, eaat7319. b) Thomsen, M. K.; Nyvang, A.; Walsh, J. P. S.; Bunting, P. C.; Long, J. R.; Neese, F.; Overgaard, J. *Inorg. Chem.* **2019**, *58*, 3211-3218.

18. Neese, F.; Pantazis, D. A. *Faraday Discuss.* **2011**, *148*, 229-238.

19. Christou, G.; Gatteschi, D.; Hendrickson, D. N.; Sessoli, R. *MRS Bulletin* **2000**, *25*, 66-71.

20. Roy, M. M. D.; Baird, S. R.; Dornsiepen, E.; Paul, L. A.; Miao, L.; Ferguson, M. J.; Zhou, Y.; Siewert, I.; Rivard, E. *Chem. Eur. J.* **2021**, *27*, 8572-8579.

21. Hering-Junghans, C.; Andreiuk, P.; Ferguson, M. J.; McDonald, R.; Rivard, E. *Angew. Chem. Int. Ed.* **2017**, *56*, 6272-6275.

22. Sharma, M.; Yameen, H. S.; Tumanskii, B.; Filimon, S.-A.; Tamm, M.; Eisen, M. S. *J. Am. Chem. Soc.* **2012**, *134*, 17234-17244.

23. Graham, T. W.; Kickham, J.; Courtenay, S.; Pingrong, W.; Stephan, D. W. *Organometallics* **2004**, *23*, 3309-3318.

24. Boynton, J. N.; Guo, J.-D.; Grandjean, F.; Fettinger, J. C.; Nagase, S.; Long, G. J.; Power, P. P. *Inorg. Chem.* **2013**, *52*, 14216-14223.

25. Aguilar-Calderón, J. R.; Murilo, J. Gomez-Torres, A.; Saucedo, C.; Jordan, A.; Metta-Magaña, A. J.; Pink, M.; Fortier, S. *Organometallics* **2020**, *39*, 295-311.

26. Peters, M.; Baabe, D.; Maekawa, M.; Bockfeld, D.; Zaretzke, M.-K.; Tamm, M.; Walter, M. D. *Inorg. Chem.* **2019**, *58*, 16475-16486.

27. Manzer, L. E.; Deaton, J.; Schrock, R. R. *Inorg. Synth.* **1982**, *21*, 135-140.

28. Sheldrick, G. M. *Acta. Crystallogr. Sect. A* **2015**, *71*, 3-8.

29. Sheldrick, G. M *Acta. Crystallogr. Sect. C* **2015**, *71*, 3-8.

Chapter 7

1. Wang, Y.-B.; Wang, Y.-M.; Zhang, W.-Z.; Lu, X.-B. *J. Am. Chem. Soc.* **2013**, *135*, 11996-12003.

2. Li, Z.; Ji, P.; Cheng, J.-P. *J. Org. Chem.* **2021**, *86*, 2974-2985.

3. Pompeo, M.; Froese, R. D. J.; Hadei, N.; Organ, M. G. *Angew. Chem. Int. Ed.* **2012**, *51*, 11354-11357.

4. Arduengo III, A. J.; Krafczyk, R.; Schmutzler, R.; Craig, H. A.; Goerlich, J. R.; Marshall, W. J.; Unverzagt, M. *Tetrahedron* **1999**, *55*, 14523-14534.

5. a) Valente, C.; Çalimsiz, S.; Hoi, K. H.; Mallik, D.; Sayah, M.; Organ, M. G. *Angew. Chem. Int. Ed.* **2012**, *51*, 3314-3332. b) Atwater, B.; Chandrasoma, N.; Mitchell, D.; Rodriguez, M. J.; Organ, M. G. *Chem. Eur. J.* **2016**, *22*, 14531-14534.

6. a) Altenhoff, G.; Goddard, R.; Lehmann, C. W. Glorius, F. *Angew. Chem. Int. Ed.* **2003**, *42*, 3690-3693. b) Vanden Broeck, S. M. P.; Nahra, F.; Cazin, C. S. J. *Inorganics* **2019**, *7*, 78.

7. a) Bullock, R. M. *Catalysis Without Precious Metals*, Wiley-VCH, 2010. b) Hazari, N.; Melvin, P. R.; Beromi, M. *Nat. Rev. Chem.* **2017**, *1*, 0025.

8. a) Sinya, N.; Taisuke, M.; Yuji, K.; Kouki, M. *Chem. Lett.* **2011**, *40*, 1036-1038. b) Coman, S. M.; Parvulescu, V. I. *Org. Process Res. Dev.* **2015**, *19*, 1327-1355. c) Inatomi, T.; Fukahori, Y.; Yamada, Y.; Ishikawa, R.; Koga, Y.; Kouki, M. *Catal. Sci. Technol.* **2019**, *9*, 1784-1793.

9. Hong, M.; Chen, J.; Chen, E. Y.-X. *Chem. Rev.* **2018**, *118*, 10551-10616.

10. McGraw, M.; Chen, E. Y.-X. *ACS Catal.* **2018**, *8*, 9877-9887.

11. Roy, M. M. D.; Baird, S. R.; Dornsiepen, E; Paul, L. A.; Miao, L.; Ferguson, M. J.; Zhou, Y.; Siewert, I.; Rivard, E. *Chem. Eur. J.* **2021**, *27*, 8572-8579.

12. Xu, L.-M.; Li, B.-L.; Yang, Z.; Shi, Z.-J. *Chem. Soc. Rev.* **2010**, *39*, 712-733.

13. a) Stephan, D. W. *Science* **2016**, *354*, aaf7229. b) Légaré, M.-A.; Courtemanche, M.-A.; Rochette, É.; Fontaine, F.-G. *Science* **2015**, *349*, 513-516. c) Lui, M. W.; Paisley, N. R.; McDonald, R.; Ferguson, M. J.; Rivard, E. *Chem. Eur. J.* **2016**, *22*, 2134-2145.

14. a) Wang, D.; Astruc, D. *Chem. Rev.* **2015**, *115*, 6621-6686. b) Khan, I.; Reed-Berendt, B. G.; Melen, R. L.; Morrill, L. C. *Angew. Chem. Int. Ed.* **2018**, *57*, 12356-12359. c) Li, S.; Li, G.; Meng, W.; Du, H. *J. Am. Chem. Soc.* **2016**, *138*, 12956-12962.

15. Christou, G.; Gatteschi, D.; Hendrickson, D. N.; Sessoli, R. *MRS Bulletin* **2000**, *25*, 66-71.

16. a) Yang, X.; Stern, C. L.; Marks, T. J. *J. Am. Chem. Soc.* **1994**, *116*, 10015-10031. b) Chen, E. Y.-X.; Marks, T. J. *Chem. Rev.* **2000**, *100*, 1391-1434. c) Collins, R. A.; Russell, A. F.; Mountford, P. *Appl. Petrochem. Res.* **2015**, *5*, 135-171.

17. Sharma, M.; Yameen, H. S.; Tumanskii, B.; Filimon, S.-A.; Tamm, M.; Eisen, M. S. *J. Am. Chem. Soc.* **2012**, *134*, 17234-17244.

18. Kretschmer, W. P.; Dijkhuis, C.; Meetsma, M.; Hessen, B.; Teuben, J. H. *Chem. Commun.* **2002**, 608-609.

19. Nomura, K.; Fukada, H.; Katao, S.; Fujiki, M.; Kim, H. J.; Kim, D.-H.; Zhang, S. *Dalton Trans.* **2011**, *40*, 7842-7849.